

**Santa Clara University
Scholar Commons**

Mechanical Engineering Senior Theses

Engineering Senior Theses

6-15-2013

Design, fabrication, and analysis of a 3U CubeSat platform

Todd Chun-Van Osdol
Santa Clara University

Charles Dorsey
Santa Clara University

Jake Hedlund
Santa Clara University

Thomas Hoye
Santa Clara University

Owen Jacobs
Santa Clara University

See next page for additional authors

Follow this and additional works at: http://scholarcommons.scu.edu/mech_senior



Part of the [Mechanical Engineering Commons](#)

Recommended Citation

Osdol, Todd Chun-Van; Dorsey, Charles; Hedlund, Jake; Hoye, Thomas; Jacobs, Owen; Klarreich-Giglio, Kadja; Martin, Elliott; Ruiz, Michael; Schlesselmann, Michael; and Singh, Zachary, "Design, fabrication, and analysis of a 3U CubeSat platform" (2013).
Mechanical Engineering Senior Theses. Paper 13.

Author

Todd Chun-Van Osdol, Charles Dorsey, Jake Hedlund, Thomas Hoye, Owen Jacobs, Kadja Klarreich-Giglio, Elliott Martin, Michael Ruiz, Michael Schlesselmann, and Zachary Singh

SANTA CLARA UNIVERSITY

School of Engineering

Date: June 15, 2013

I HEREBY RECOMMEND THAT THE THESIS PREPARED UNDER MY
SUPERVISION BY

Todd Chun-Van Osdol, Charles Dorsey, Jake Hedlund, Thomas Hoye,
Owen Jacobs, Kadja Klarreich-Giglio, Elliott Martin, Michael Ruiz,
Michael Schlesselmann, and Zachary Singh

ENTITLED

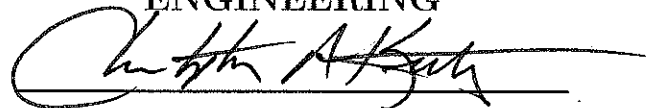
Design, Fabrication, and Analysis of a 3U CubeSat Platform

BE ACCEPTED IN PARTIAL FULFILLMENT OF THE REQUIREMENTS FOR
THE DEGREE OF

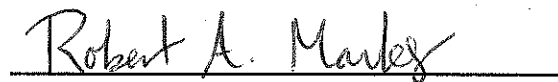
BACHELOR OF SCIENCE

IN

ENGINEERING



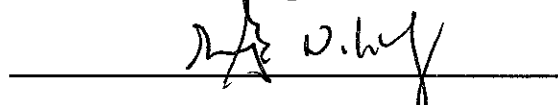
Dr. Christopher A. Kitts - Thesis Advisor



Dr. Robert A. Marks - Thesis Advisor



Dr. Drazen Fabris - Chairman of Department of Mechanical Engineering



Dr. Nam Ling - Chairman of Department of Computer Engineering

Design, Fabrication, and Analysis of a 3U CubeSat Platform

BY

Todd Chun-Van Osdol, Charles Dorsey, Jake Hedlund, Thomas Hoye,
Owen Jacobs, Kadja Klarreich-Giglio, Elliott Martin, Michael Ruiz,
Michael Schlesselmann, and Zachary Singh

THESIS

Submitted in Partial Fulfillment of the Requirements for the
Bachelor of Science Degrees in
Mechanical Engineering and Computer Engineering in the School of
Engineering

Santa Clara University, 2013

Santa Clara, California

Design, Fabrication, and Analysis of a 3U CubeSat Platform

Todd Chun-Van Osdol, Charles Dorsey, Jake Hedlund, Thomas Hoye,
Owen Jacobs, Kadja Klarreich-Giglio, Elliott Martin, Michael Ruiz,
Michael Schlesselmann, and Zachary Singh

Department of Mechanical Engineering

Department of Computer Engineering

Santa Clara University

Santa Clara, California

2013

Abstract

The goal of this project is to develop a 3U CubeSat nanosatellite bus capable of short duration technology verification experiments while providing compelling hands-on student education opportunities. This 3U CubeSat platform has been prototyped by the design team in order to demonstrate its capabilities. This spacecraft, the Unspecified Payload Active Attitude Control Nanosatellite (UPAACN), is designed to perform a 3-6 month technology verification experiment for a NASA test component and an SCU single-axis attitude control system (AACS) in Low Earth Orbit (LEO). This project builds upon the flight heritage of SCU's Robotic Systems Laboratory (RSL) and improves its satellite development capabilities. The 3U CubeSat platform is designed to support any payload that meets basic constraints. This design can be manufactured and assembled entirely at the university level. It allows for a faster design cycle, lower project risk and cost, and the opportunity to launch university payloads.

Acknowledgment

The team would like to thank our project adviser, Dr. Christopher A. Kitts, for all the help he has provided. He has given us access to NASA resources and professionals who have greatly helped our project. Without him the project would never have come together. We thank him for his interest, his time, and above all, his patience.

We would also like to thank our other project adviser, Dr. Robert A. Marks, for his help and guidance. His assistance on day-to-day project management and engineering processes has proven invaluable. He also gave us access to important testing equipment that helped us develop the testing capabilities of the RSL, for which we are very thankful.

The team would like to thank Don MacCubbin for his help with the machining process. Our project required a large amount of detailed machining, and Don's patience and insight were much appreciated.

Finally, the team would like to thank the previous nanosatellite design team. Their work was the foundation for our success. We would specifically like to thank Victor Zapien for helping us understand the SatTherm MATLAB package.

Contents

1	Introduction	1
1.1	Background	1
1.2	Review of Field and Literature	2
1.3	SCU Satellite Heritage	3
1.4	Project Objectives	4
1.5	Design Team Composition	5
1.6	Reader's Guide	5
2	System Overview	6
2.1	CubeSat Design Specifications	6
2.2	RSL Requirements	7
2.3	Customer Needs	7
2.4	Subsystem Summary	8
2.5	Payload Support	10
3	Systems Engineering (SYST)	12
3.1	Project Challenges and Constraints	12
3.2	Project Organization	12
3.3	Budgeting	13
3.4	Timeline	13
3.5	Design Process	14
3.6	Risk Mitigation	15
4	Structural Engineering (STRUC)	16
4.1	Background	16
4.2	Requirements	17
4.3	Inherited Design	18
4.4	Design Updates	18
4.5	Challenges	20
4.6	Analysis	20
5	Thermal Design and Analysis (THERM)	22
5.1	Satellite Thermal Background	22
5.2	Modes of Heat Transfer	23
5.2.1	Conduction	23
5.2.2	Radiation	24
5.3	SatTherm	24
5.4	Active and Passive Thermal Solutions	26
5.5	SatTherm Updates	27
5.6	Work Summary	28
5.7	Challenges	28
5.8	Results	28
5.9	Future Work	31

6 Distributed Command and Data Handling (dCDH) and Communications (COMM)	32
6.1 Introduction	32
6.2 Requirements	32
6.3 System Architecture	33
6.3.1 Conceptual Model	33
6.3.2 Final Model	33
6.4 Use Cases	35
6.4.1 Sending Commands <i>via</i> the Transmitter	35
6.4.2 Sending Beacon Packets	35
6.4.3 System Power On	36
6.4.4 System Power Off	36
6.4.5 AACS Motor Control	36
6.5 Activity Diagrams	37
6.6 Technologies Implemented	37
6.6.1 Software	37
6.6.2 Hardware	37
6.7 Design Rationale	37
6.8 Project Risks	38
7 Electronic Power System (EPS)	39
7.1 Background	39
7.2 System Architecture	39
7.3 Solar Array Design and Assembly	41
7.4 Battery and Support Circuitry	43
7.5 Peak Power Tracker	43
7.6 Power Board Design Updates	44
8 Active Attitude Control System (AACS)	47
8.1 Purpose	47
8.2 Requirements	47
8.3 System Architecture	48
8.4 Control System Design	48
8.5 Flywheel Mechanism Design	52
8.6 Passive Control	56
8.7 Future Work	57
9 Subsystem Functionality Verification and Testing (TEST)	60
9.1 Introduction	60
9.2 Requirements	60
9.3 Methodology	60
9.4 Shock and Vibration Testing	61
9.5 Thermal Cycling	63
9.6 Acoustic Testing	64
9.7 Vacuum Testing	64

9.8	Subsystem Verification of Functionality	67
9.8.1	Active Attitude Control System	67
9.8.2	Distributed Command and Data Handling (dCDH) and Communications (COMM)	74
9.8.3	Electronic Power System (EPS)	76
10	Business Plan and Cost Analysis	78
10.1	Introduction	78
10.2	Goals and Objectives	78
10.3	Product Description	78
10.4	Potential Market	79
10.5	Manufacturing	80
10.6	Cost Analysis	80
10.7	Financial Outlook	80
11	Engineering Standards and Constraints	81
11.1	Sustainability	81
11.2	Economics	81
11.3	Manufacturability	82
11.4	Ethics	82
11.5	Political	83
12	Conclusion	84
12.1	Summary	84
12.2	Lessons Learned	84
12.3	Future Work	85
	Bibliography	86
A	Build Book	89
A.1	Top and Bottom Faces and Fixtures	89
A.1.1	Bottom Fixture	89
A.1.2	Top Fixture	90
A.1.3	Top and Bottom Faces	90
A.2	Side Faces and Fixtures	91
A.2.1	Bottom Fixture	91
A.2.2	Top Fixture	91
A.2.3	Side Faces	93
A.3	Corner Brackets and Fixture	95
A.3.1	Fixture	95
A.3.2	Corner Brackets	95
A.4	Assembly Tools	98
A.5	AACS Fixtures	98
A.5.1	Soft Jaws	98
A.5.2	Soft Collet	99

A.6	AACS Parts	99
A.6.1	Can Body	99
A.6.2	Top Can Lid	100
A.6.3	Bottom Can Lid	101
A.6.4	Flywheel	101
A.6.5	Motor Spacer	103
A.6.6	Motor Mounting Bracket	103
A.6.7	Assembly	103
A.7	System Integration	104
B	Drawings	106
C	Detailed Calculations	138
C.1	SatTherm Code	138
C.2	AACS Code and Calculations	138
C.2.1	Control Code	138
C.2.2	Controller	143
C.2.3	Steady State Motor Analysis MATLAB Script	144
C.2.4	Reaction Wheel Sizing MATLAB Script	145
C.2.5	Bump Test Arduino Sketch	147
C.3	dCDH and COMM Code	149
D	Requirements Flowdown	150
E	Timeline	156
F	Budgets and Spreadsheets	159
F.1	Operating Modes	159
F.1.1	Purpose	159
F.1.2	Relevant Subsystems	159
F.1.3	Operating Modes	159
F.1.4	Operating Schedule	160
F.2	Activity Diagrams	162
F.3	Success Criteria	166
F.3.1	Mission Statement	166
F.3.2	Primary Mission Success Criteria	166
F.4	Mass Budget	167
F.5	Monetary Budget	168
G	Senior Design Conference Presentations	170
G.1	Nanosatellite - Design, Fabrication, and Systems	170
G.2	Active Attitude Determination and Control Subsystem	170
G.3	Nanosatellite - Communications and Data Handling	170
H	Parts List	186

List of Figures

1.1	Sapphire microsatellite before launch.	3
1.2	PharmaSat spacecraft before launch.	4
2.1	System architecture with labeled subsystems.	9
2.2	System architecture interfaced with RSL ground station.	9
4.1	Bus structure from 2012 design team.	18
4.2	Updated bus structure design.	19
4.3	Six modes of vibration of the bus structure.	21
5.1	Energy balance of a satellite in LEO.	23
5.2	Hot case simulation over six hour period with aluminum 6061 as a surface finish on the top and bottom faces.	29
5.3	Cold case simulation over six hour period with aluminum 6061 as a surface finish on the top and bottom faces.	29
5.4	Hot case simulation over six hour period with Chemglaze Z306 Black Paint as a surface finish on the top and bottom faces.	30
5.5	Cold case simulation over six hour period with Chemglaze Z306 Black Paint as a surface finish on the top and bottom faces.	31
6.1	Clockwise from top left: two AVR-SAT boards, beacon board, lab power board, MHX2420 OEM Radio Transmitter board.	33
6.2	Conceptual architectural model of dCDH and COMM.	34
6.3	Final architectural model for dCDH and COMM.	34
7.1	IV curve for Triangular Advanced Solar Cell.	39
7.2	EPS block diagram.	40
7.3	IV curve for a solar cell and maximum power point (MPP).	42
7.4	Solar panel PCB layout showing top traces in red and bottom traces in blue.	42
7.5	Start-up comparator circuit design.	43
7.6	LT3652 PPT circuit design.	44
7.7	Buck converter circuitry schematic.	45
7.8	Boost converter circuitry schematic.	45
8.1	AACS architectural diagram.	48
8.2	Torque and angular speed relationship for Faulhaber DC motor.	50
8.3	Flywheel diameter plotted against operating speeds for Faulhaber DC motor.	51
8.4	SolidWorks model of Faulhaber DC motor showing boss in red.	54
8.5	SolidWorks model of AACS bracket, DC motor, and can lid.	55
8.6	Effects of distance between motor and lid on system performance.	56
8.7	Effects of distance between motor and lid on system current draw.	57
9.1	Accelerometer response to impact testing.	62
9.2	Set-up for baseline vibration table testing.	62
9.3	Thermal cycling experimental setup.	63
9.4	Oven used for thermal cycling.	64
9.5	Bump test results of AACS mechanism in between thermal cycles.	66
9.6	Bump test of AACS motor.	67

9.7	Angular speed response of UPAACN for three tests.	69
9.8	Response of AACS from PI control.	70
9.9	Response of AACS from PI control with lowered proportional gain. .	71
9.10	Response of AACS from PI control with lowered integral gain. . .	71
9.11	Response of AACS with PID control.	72
9.12	Response of AACS from different integral gains; 0.1 is in blue and 0.001 is in red.	73
9.13	Response for proportional gains of 1 in blue and 0.8 in red.	74
10.1	Assembled bus structure for 3U CubeSat platform.	79
A.1	Bottom fixture for top and bottom faces.	89
A.2	Top fixture for top and bottom faces.	90
A.3	Top/bottom face.	91
A.4	Top/bottom face fixture assembly.	92
A.5	Bottom fixture for side faces.	92
A.6	Top fixture for side faces.	93
A.7	Side faces.	94
A.8	Side faces fixture assembly.	95
A.9	Fixture for corner brackets.	96
A.10	Corner bracket.	97
A.11	Corner bracket fixture assembly.	97
A.12	Assembly tool.	98
A.13	Soft jaws.	99
A.14	Soft collet.	99
A.15	Can body.	100
A.16	Top can lid.	101
A.17	Bottom can lid.	102
A.18	Flywheel.	102
A.19	Motor spacer.	103
A.20	Motor bracket.	104
A.21	AACS assembly.	105
C.1	Open loop Simulink model.	143
C.2	Closed loop Simulink model.	144
F.1	Activity diagram for Dallas-Master.	162
F.2	Activity diagram for Expert.	163
F.3	Activity diagram for Scheduler.	164
F.4	Activity diagram for COMM.	165
F.5	Activity diagram for Beacon.	166

List of Tables

3.1	UPAACN mass budget.	13
4.1	Natural frequencies for different modes of vibration.	21
5.1	Thermal properties of surface finishes.	28
5.2	Temperature ranges for hot and cold cases with and without Chemglaze Z306 Black Paint on the top and bottom faces.	30
6.1	Risk analysis chart for dCDH and COMM subsystems.	38
8.1	Summary of AACS requirements.	47
9.1	Thermal cycling temperature results on AACS mechanism.	65
F.1	Mass budget for UPAACN.	167

Nomenclature

AACS	Active Attitude Control System
ATC	Active Thermal Control
[atm]	Atmosphere
BCN	Beacon
BoM	Bill of Materials
CAD	Computer Aided Design
CalPoly	California Polytechnic State University
[cm]	Centimeters
COMM	Communications
CVCM	Collected Volatile Condensable Material
dCDH	Distributed Command and Data Handling
DMS	Dallas-Master
EPS	Electronic Power System
EXP	Expert
FEA	Finite Element Analysis
[Hz]	Hertz
ISS	International Space Station
[kbps]	Kilobits per Second
[kg]	Kilograms
[kΩ]	Kilo Ohm
LEO	Low Earth Orbit
[mA]	Milliamp
MATLAB	Matrix Laboratory
MEMS	Microelectromechanical Systems
MLI	Multi-Layer Insulation
[mm]	Millimeter

[mNm]	Millinewton Meter
MPP	Maximum Power Point
[ms]	Millisecond
[mV]	Millivolt
NASA	National Aeronautics and Space Administration
O/OREOS	Organism/Organic Exposure to Orbital Stresses
OPAL	Orbiting Picosat Automatic Launcher
PCB	Printed Circuit Board
P-POD	Poly Picosatellite Orbital Deployer
PPT	Peak Power Tracker
PTC	Passive Thermal Control
[rpm]	Revolutions per Minute
RSL	Robotic Systems Laboratory
SCH	Scheduler
SCU	Santa Clara University
SJSU	San Jose State University
STRUC	Structural Subsystem
SYST	Systems Engineering
TEST	Subsystem Functionality Testing and Verification
THERM	Thermal Design and Analysis
TML	Total Mass Loss
U	10 x 10 x 11.35 [cm]
UPAACN	Unspecified Payload Active Attitude Control Nanosatellite
[V]	Volt
[W]	Watt
[W/m ²]	Watts per Meter Squared
[W/mK]	Watts per Meter Kelvin

1 Introduction

1.1 Background

Over the past few decades, satellites have grown in size, cost, and complexity. This trend has greatly increased the capabilities of satellites, but technological advancement is still limited by the risky, high-cost nature of space missions. Large projects tend to rely on older technology with proven flight histories. However, as the demand for more advanced spacecraft increases, a need for cheap low-risk on-orbit testbeds has risen. Smaller satellites have become increasingly popular in the aerospace industry and have allowed non-governmental organizations to develop space technologies.

Nanosatellites, a type of small satellite weighing between 1 and 10 [kg], are a popular low-cost platform for academic and some government missions. This is due in part to the CubeSat program, developed by California Polytechnic State University in 1999, as well as to the many new private spaceflight startups.¹ Using standardized design parameters, CubeSats can be launched from a common mechanism, called a P-POD (Poly Picosatellite Orbital Deployer). The P-POD is mounted in the fairing of a launch vehicle, usually sharing a launch with a much larger spacecraft. The size of these spacecraft are measured in "U's", a unit of volume measuring 10x10x11.35 [cm]. CubeSats can support a variety of mission types, including biological research, communications, deep space observation, or technology testing and characterization. These spacecraft have high educational potential. Santa Clara University (SCU) has launched and operated nanosatellites in the past, including the NASA PharmaSat and NASA O/OREOS spacecraft.²

In addition to the uses already mentioned, nanosatellites and CubeSats have several important capabilities. For instance, using multiple nanosatellites in a constellation or “satellite swarm” is being explored for its communications and defense potential.³ Nanosatellites are also beginning to replace much older and larger satellites due to their versatility and lower cost. One example of this is using 6U CubeSats to replace the RapidEye Earth-imaging satellite constellation.⁴ These planned spacecraft will be faster than the old system and will be more accessible to developing nations interested in geoimaging.

Despite the increased accessibility of nanosatellites, the overall cost and development time of these spacecraft is still high. The CubeSat program has improved the situation, but these spacecraft still require a high level of technology development. There are several third-party solutions, including companies that manufacture flight-ready CubeSat buses and support circuitry, but these products can cost tens of thousands of dollars, essentially excluding small companies and educational institutions from being competitive in today’s industry. If this process were streamlined and made cheaper, nanosatellites could be more easily produced, thus growing the industry and accelerating technological progress.

1.2 Review of Field and Literature

As previously mentioned, there are several companies producing flight-ready nanosatellite components. Pumpkin Inc., based in San Francisco, has been prominent in the small satellite community for producing flight processors and bus structures for CubeSats.⁵ Pumpkin's products successfully streamline the design process, but their high cost limits their use to larger projects at institutions already well-established in the industry.

Several publications were consulted regarding the CubeSat standard, most notably "CubeSat: Developing a Standard Bus for Picosatellites."⁶ Their publication was authored by the founders of the CubeSat program, several of whom were originally professors from Stanford University. This paper describes the need for the standard as well as the services it can offer. Furthermore, it outlines some of the most important design specifications which were later organized into an explicit design document still used today.

Once the CubeSat program was formally established at Cal Poly, several papers were published further developing on the capabilities of the platform, including "CubeSats as Responsive Satellites."⁷ This paper describes the CubeSat platform as inexpensive, cost effective, reliable, and capable of creating launch opportunities for universities.

The current design team relies heavily on the work completed by the 2011-12 undergraduate design team here at SCU. Their thesis, "Nanosatellite Fabrication and Analysis", outlines the design, analysis, and manufacturing processes of a 3U CubeSat (also termed a triple CubeSat), entirely relying upon existing university resources, at a fraction of the cost of a Pumpkin bus structure.⁸ The team completed finite element analysis of the structure to predict its natural frequency and failure modes. This thesis also includes a buildbook giving instructions on how to fabricate a similar structure from scratch.

The thermal analysis of this project uses the SatTherm MATLAB package developed by Cassandra Belle VanOutryve of San Jose State University (SJSU) as part of her thesis "A Thermal Analysis and Design Tool for Small Spacecraft."⁹ Completed in 2008, the package models the orbit and incoming heat flux for a small satellite on-orbit. SatTherm is simple and accessible compared to the industry standard, Thermal Desktop.¹⁰ The latter is expensive and has a steep learning curve, making it difficult to implement at the university level.

All design work completed by the design team is in accordance with the CubeSat Design Specification document published by the CubeSat Program at California Polytechnic State University.¹¹

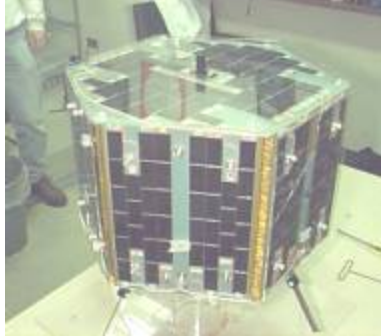


Figure 1.1: Sapphire microsatellite before launch.

1.3 SCU Satellite Heritage

Santa Clara University (SCU) has launched and operated several nanosatellites in the past.¹² This section will give a brief overview of some of these projects and the extent to which the RSL contributed.

One of the first satellite projects at SCU was the Artemis picosatellite.¹³ This was one of the picosatellites provided to Stanford's Orbiting Picosat Automatic Launcher (OPAL). The goal of the project was to use a quick, low-cost prototype process in order to explore the limitations of picosatellites. Artemis was launched in 2000.

The RSL operated the Sapphire microsatellite, launched in September 2001.¹⁴ In addition, several lab members served on the Sapphire design team at Stanford in the mid 1990s. This satellite was capable of digital Earth photography, FM digital voice broadcasts, and MEMS sensor characterization. The RSL also used Sapphire to experimentally demonstrate a model-based reasoning anomaly management system. Sapphire is shown in Figure 1.1.

Working with NASA Ames Research Center, the RSL operated the GeneSat-1 nanosatellite.¹⁵ GeneSat-1 contained a life support system that monitored the effects of spaceflight on bacteria. The RSL currently operates several satellites, including two FASTRAC nanosatellites, the NASA PharmaSat spacecraft (shown in Figure), and the O/OREOS spacecraft.¹⁶

In addition to helping design, launch, and operate several NASA spacecraft, there are several research projects into satellite technologies within the RSL. For example, the current project team has built upon the active attitude control flywheel mechanism used in previous projects. The RSL has also designed a distributed flight computing system which has been used in several satellite projects, some of which have been launched.

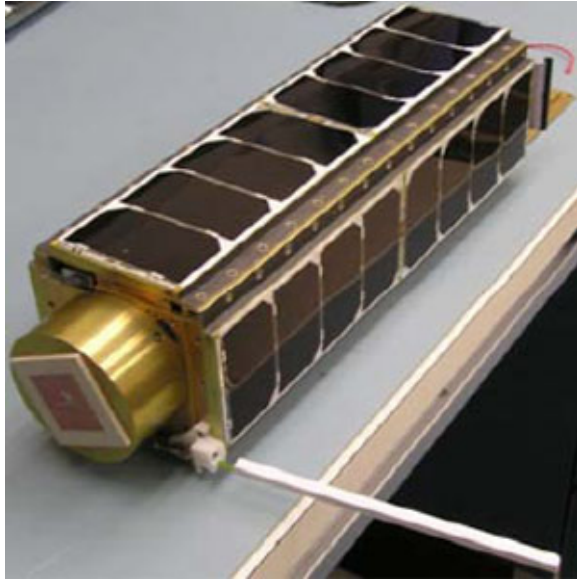


Figure 1.2: PharmaSat spacecraft before launch.

1.4 Project Objectives

The goal of this project is to develop a 3U CubeSat nanosatellite bus capable of supporting short duration technology verification experiments in Low Earth Orbit (LEO) while providing compelling hands-on student educational opportunities. The project makes use of past work and existing technology within the Robotic Systems Laboratory (RSL) here at SCU. Building on the goals of previous design teams, this project has produced a design methodology for future CubeSat projects that allows for easy customization and minimizes cost and design time. This spacecraft can be manufactured at the university level and can act as a testbed for student projects.

Furthermore, the team has built and tested a 3U CubeSat making use of this method. The bus structure was updated and assembled based on the buildbook included in the aforementioned 2011-12 thesis. This satellite includes the Active Attitude Control System (ACCS), a student project. The flight computing is handled by the RSL Distributed Command and Data Handling (dCDH) and Communications (COMM) systems. The Electronic Power System (EPS) relies on an updated RSL power board design, a student designed Peak Power Tracker (PPT), and a student designed solar array. Thermal analysis was completed using an updated SatTherm MATLAB package. Once again, Finite Element Analysis (FEA) was used to predict the natural frequency and potential failure modes of the final spacecraft. Sensitive components as well as the assembled satellite were subjected to vibration, thermal cycling, and vacuum testing. This spacecraft is called the Unspecified Payload Active Attitude Control Nanosatellite (UPAACN).

1.5 Design Team Composition

The current project team has ten primary engineers. There are seven mechanical engineers and three computer engineers, all seniors within the School of Engineering. These members have been further divided into subsystem design teams, to be described in Chapter 3. At the SCU School of Engineering 43rd Annual Senior Design Conference, this design team made three separate presentations. These included “Design, Fabrication, and Systems,” which described the 3U CubeSat platform from a chiefly mechanical perspective; “Active Attitude Determination and Control,” which described the mechanical attitude control system; and “Communications and Data Handling,” which described the flight computing system.

In addition to the primary design team, a group of four Junior electrical engineering students designed the electrical power system (EPS) for the 3U CubeSat platform. Although their work was not presented at the Senior Design Conference, it is summarized in Chapter 7.

1.6 Reader’s Guide

This thesis has been prepared to accomplish three goals. These are to describe the services offered by the 3U CubeSat platform within the RSL, to showcase the work completed by the design team, and to instruct future users on use and replication of the CubeSat.

The thesis is broken down into subsystem chapters along with supporting documentation. Each chapter describes the background of the system, its purpose, and how it was implemented in the UPAACN. A buildbook is included in Appendix A. This comprehensive guide will help future users reproduce and update the current designs. These instructions focus on machining the structure and the testing procedures, but will also touch on programming the flight computers and completing the thermal analysis. Also included is a bill of materials, a copy of the SatTherm package, and controller code for AACs.

2 System Overview

The 3U CubeSat design team must meet a variety of requirements from different sources. These requirements come from the CubeSat Design Specifications, internal RSL goals, and a customer needs survey. The following sections describe these in detail.

2.1 CubeSat Design Specifications

The purpose of the CubeSat Program is to “provide a standard for design of picosatellites to reduce cost and development time, increase accessibility to space, and sustain frequent launches.”¹⁷ The CubeSat Design Specification is a document that explicitly states all requirements needed for CubeSats to be designated acceptable for launch as well as integration into the P-POD. It includes mechanical, electrical, operational, and testing requirements.

There are several major general satellite requirements. The most significant are as follows:

- 2.1.4 No pressure vessels over 1.2 standard atmosphere shall be permitted.
- 2.1.7.1 Total Mass Loss (TML) shall be $\leq 1.0\%$
- 2.1.7.2 Collected Volatile Condensable Material (CVCM) shall be $\leq 0.1\%$

In addition, there are important mechanical requirements. The most important are listed here:

- 2.2.4 The CubeSat shall be 100.0 ± 0.1 [mm] wide.
- 2.2.5.1 A Triple CubeSat shall be 340.5 ± 0.3 [mm] tall.
- 2.2.6 All components shall not exceed 6.5 [mm] normal to the surface of the 100.0 [mm] cube.
- 2.2.16 Each triple CubeSat shall not exceed 4.0 [kg] mass.
- 2.2.19 Aluminum 7075 or 6061 shall be used for both the main CubeSat structure and rails.

The important electrical requirements affect the design of the EPS. They are:

- 2.3.1 No electronics shall be active during launch to prevent any electrical or RF interference with the launch vehicle and primary payloads. CubeSats with batteries shall be fully deactivated during launch or launch with discharged batteries.
- 2.3.2 The CubeSat shall include at least one deployment switch on the designated rail standoff to completely turn off satellite power once actuated.

Testing requirements for CubeSats are derived from specific launch vehicles. However, if the launch vehicle environment is unknown, generalized NASA standards are used, given in GSFC-STD-7000.¹⁸

The above requirements can be found in their entirety in the CubeSat Design Specification document.¹⁹

2.2 RSL Requirements

There are several project goals set by Dr. Christopher Kitts, the head of the RSL. His goal is to use this project as a platform for future satellite development at SCU. While the RSL has helped develop and operate several spacecraft in the past, the UPAACN will be the first CubeSat developed entirely by the RSL. This platform will be used to attract potential users at NASA Ames which may lead to future flight opportunities. The 3U CubeSat platform is required to support payloads that meet some basic mechanical, electrical, and data constraints; these are specified in section 2.9. Finally, all mechanical work is required to be completed by students in the SCU machine shop.

In addition to developing the 3U CubeSat platform, the design team is required to perform all thermal analysis using the SatTherm MATLAB package. This program was used by the 2011-2012 design team and has been improved by the current design team.

To increase the likelihood of future launches, Professor Kitts has required that the design team work to improve the baseline testing capabilities of the RSL. This includes basic environmental testing as well as interfacing with the existing ground station. He has also required that the team assemble the spacecraft in a low-grade cleanroom located in the RSL space at NASA Ames. The testing developments are further described in sections 2.8 and 3.9.

Overall, the RSL requires that all designs be reproducible by future SCU students. The system architecture is designed such that future students will be able to quickly and easily customize the project for future missions.

2.3 Customer Needs

In addition to the specific requirements stated by the CubeSat Design Specification, the project team has completed a customer needs survey. This information has helped the design team tailor the CubeSat platform to the needs of potential users outside of the RSL. These users are space industry professionals, university professors, and university students. The survey gathered feedback from these potential customers based on the design capabilities of SCU and the RSL, specifically related to payload constraints.

First of all, the industry professionals agreed that when working with a university group, proper project management techniques must be implemented. This includes proper documentation and adherence to engineering standards. The project team takes this customer need very seriously. The need for proper documentation is exacerbated by the fact that the team is working with government agencies. The systems engineering component of the project is dedicated to meeting this customer need. It is further described in Chapter 3.

The industry professionals surveyed unanimously stressed the importance of proper testing. This includes functional testing of all subsystems as well as environmental testing of the final launch-ready spacecraft.

The potential customers collectively indicated that additional attitude control capabilities would be required for the 3U CubeSat platform. Currently, the UPAACN will include the AACS flywheel mechanism, which is able to control the spacecraft's z-axis angular position and rotation. This is a single degree of freedom system. Future iterations could include a three degree of freedom attitude control system, but this would likely occupy more space in the 3U CubeSat. The design team is comfortable with the current configuration as it is being used as a technology demonstration. Future work on this system could improve the pointing capabilities of the spacecraft.

The customer needs survey questions and responses can be found in their entirety in Appendix I.

2.4 Subsystem Summary

The system architecture has been designed such that each subsystem can have dedicated team members with minimal overlap. Each subsystem team is managed by the systems engineering (SYST) component. SYST manages the project documentation, scheduling, and trade-off analysis. These functions are further described in Chapter 3.

The major mechanical subsystems are Structures (STRUC), Thermal Design and Analysis (THERM), and Testing (TEST). The two software-based subsystems are Distributed Command and Data Handling (dCDH) and Communications (COMM). Finally, the Electronic Power System (EPS) is handled by the Junior level electrical engineering students. The specific functions of each subsystem and their roles within the UPAACN will be further explained in the following chapters.

A baseline configuration of the 3U CubeSat platform is shown in Figure 2.1. It is color-coded to indicate each subsystem. The system architecture is shown in Figure 2.2. This block diagram indicates inter-subsystem interfacing as well as the connection to the RSL ground station.

- **(STRUC)** Structural Engineering
- **(EPS)** Electronic Power System
- **(dCDH)** Distributed Command and Data Handling/Communications
- **(AACS)** Active Attitude Control System – RSL payload

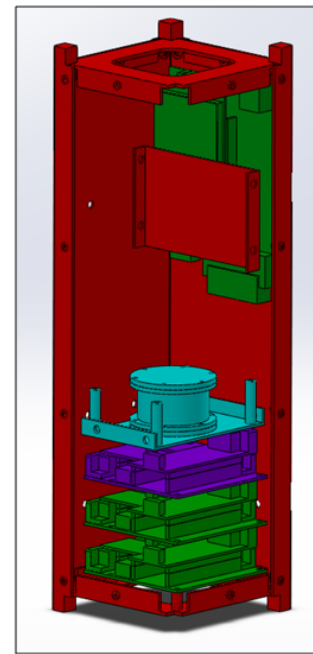


Figure 2.1: System architecture with labeled subsystems.

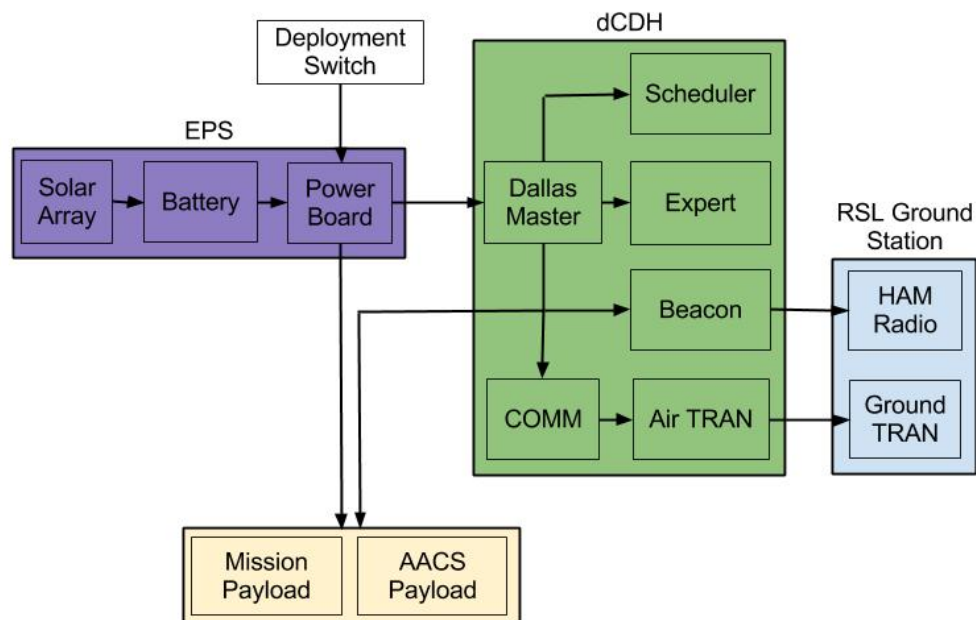


Figure 2.2: System architecture interfaced with RSL ground station.

2.5 Payload Support

The 3U CubeSat platform is capable of supporting any payload that meets some basic constraints. In general, the payload is the cargo of the satellite, and defines the mission. All bus components are tailored to the payload, which have mission specific requirements. In nanosatellite projects, especially in an academic environment, payloads are often scientific instruments or experiments used for research purposes. Another common payload type is on-orbit technology characterization.

There are obvious limitations to designing a satellite that does not already have a payload, but the design team hopes to overcome these *via* a semi-modular design. The characteristics of the bus components and subsystems will be described in later chapters.

Based on the technical capabilities of the RSL and SCU, the CubeSat Design Specifications, and the customer needs survey, the 3U CubeSat platform has been designed to support payloads that meet the following requirements:

- Volume
 - 0.5-1U
 - 7 x 8 x 8 [cm] without a sealed container
 - 6 x 7 x 7 [cm] if a sealed container is needed
- Fixturing
 - Must be mountable using standard ISO sized screw holes
 - Must have sufficient mounting points to ensure stability during launch
- Weight
 - < 1 [kg]
- Power
 - Must accept 3.3, 5, or 12 [V] input
 - Must accept 50 or 150 [mA] input
- Data
 - S-Band - 115 [kbps]
 - Beacon (HAM radio) - 9.6 [kbps]
- Thermal

- Passive thermal control (PTC) - payload must be able to function at ambient satellite temperature
- Active thermal control (ATC) - heating element can be incorporated via simple circuitry in order to maintain the operational temperature range, however this may cut into available volume, weight, and power

- Attitude Control

- Passive stabilization via magnets and hysteresis rods
- Angular position and rotation control about Z-axis
- De-spin in \sim 10 minutes

3 Systems Engineering (SYST)

3.1 Project Challenges and Constraints

There are several major challenges associated with developing a nanosatellite. Project success hinges upon understanding the complexity that comes from interfacing between subsystems. This is common to all aerospace projects. This issue is traditionally handled by a system engineering subteam. System engineers must be able to manage the project as well as fully understand the technical theory behind each subsystem. The current design team uses this approach to developing a 3U CubeSat.

Aerospace projects typically have many interrelated components and subsystems that have to be designed and assembled concurrently. Small changes in one subsystem can drastically affect the design of other components. The interdependency of subsystems is exacerbated for space projects because of mass, volume, power, and data handling constraints. Systems engineers must effectively mediate and communicate between each subsystem team in order to specify design requirements and limitations.

There are a variety of project constraints from several sources. These are general NASA requirements, RSL goals, and CubeSat Design Specifications. Meeting all of these requirements is crucial to receiving a launch opportunity. The SYST subteam has attempted to streamline the project so that future users will be able to meet these requirements relatively easily. Specific constraints that affect all subsystems are listed in Chapter 2.

3.2 Project Organization

In order to mitigate project complexity, the CubeSat was divided into seven subsystems. These are systems engineering (SYST), thermal design and analysis (THERM), structural engineering (STRU), distributed command and data handling (dCDH), communications (COMM), electronic power systems (EPS), and the active attitude control system (AACS). Each subsystem had dedicated team members. There was some personnel overlap between subteams; however, scheduling and task conflicts were avoided through use of a Gantt chart.

The design team met weekly to discuss current tasks and challenges. In addition, subteams met as needed (usually weekly) to discuss subsystem issues. Members of SYST attended other subteam meetings in addition to the larger weekly team meeting to help coordinate the project. SYST helped interface between subteams on multi-subsystem tasks. These tasks were managed using a detailed requirements flowdown and a Gantt chart. These documents can be found in Appendix D.

Table 3.1: UPAACN mass budget.

Item	Mass [kg]
STRUC Frame	0.81
Solar Panel Faces	0.24
ACR-SAT boards	0.1
BCN antenna & board	0.11
Transmitter antenna	0.031
MHX2420 boards	0.125
Sensor Board	0.013
AACS	0.12
Estimated Battery	1.0
Total	2.549

3.3 Budgeting

When applied to a space project, budgeting refers to more than just money. Due to the limitations of launch vehicles and satellite technologies, other project capacities are managed in a budget format as well. This includes mass, power, and data. The budget was broken down by subsystem in order to help control the complexity and the overall cost. The budgets for the current design team can be found in Appendix F. As an example, the project mass budget is shown in Table 3.1.

The monetary budget is dictated by the project requirements. Funding is provided directly through the RSL. The team also has access to many necessary components and hardware from previous projects. While some of these items were used in the prototyping phase, they may not all be suitable for flight as specified by the project requirements. As a result, a budget for the flight phase is described in Chapter 4. Several components, such as the space rated solar cells, are pre-existing RSL assets that do not contribute to the project budget.

To meet mission objectives, many components will be manufactured at SCU. This helps the team provide a low-cost alternative to traditional solutions for high-risk endeavors. The team purchased components through the RSL that could not be fabricated at the university level.

The SYST subteam managed all budgeting for the UPAACN. As stated above, this included the monetary budget as well as mass, volume, and power budgets. These living documents allowed the design team to keep track of project resources as well as CubeSat constraints. This documentation can be found in Appendix E.

3.4 Timeline

An important task for SYST was to manage task scheduling *via* a Gantt chart. A Gantt chart helps illustrate the time required to complete each task as well as

task interrelatedness. This allowed interdependent subsystem tasks to be completed linearly and helped prevent delays in the design process. Use of the Gantt chart allowed SYST to effectively manage the complexity of the 3U CubeSat platform. This document is found in Appendix F.

3.5 Design Process

With multiple subsystems being designed concurrently, SYST had to ensure that the designs could be assembled together and work in the way intended. Documentation was produced that helped manage interrelated subsystem tasks and interfacing.

From a top level, this process began with creating a project statement and a separate mission statement. These statements were developed into a requirements flowdown document, which can be found in Appendix D. This helped the team separate work for developing a 3U CubeSat platform and the work for prototyping and fabrication.

The Project Statement is as follows:

The goal of the project is to develop a 3U CubeSat platform capable of supporting short duration technology verification experiments while providing compelling hands-on student education opportunities.

The Mission Statement for the prototype of the 3U CubeSat, also known as the UPAACN, is as follows:

The Unspecified Payload and Active Attitude Control (UPAAC) nanosatellite will perform a 3-6 month technology verification experiment for a NASA test component and a new SCU single axis active attitude control system in Low Earth Orbit (LEO).

Some specific examples of guiding documents are the success criteria and the operating modes document. These both describe the specific functions of the spacecraft on-orbit and the means of judging whether requirements were met. Furthermore, these functions were further illustrated using a system block diagram, found in Chapter 2.

One of the main project requirements was reproducibility and manufacturability. To help with this, SYST created documents such as a Bill of Materials (BoM) and a standard formatting for all the drawings. This aided in the creation of a buildbook that can help future project teams.

3.6 Risk Mitigation

Space projects are traditionally very risky due to the impossibility of retrieval or repair of spacecraft. Mission success requires guaranteed functionality from each subsystem. Subsystem failures can often cascade and cause the entire satellite to fail. For instance, if the thermal subsystem fails, the satellite component temperatures will drift outside their operational ranges causing damage and possibly failure. The traditional approach to this problem is to design with high safety factors and introduce system redundancy. This project makes use of these ideas to a certain extent, but in order to lower the cost, some compromises were made.

An example of building to a high factor of safety is the design for the structural subsystem. It is constructed from machined aluminum and is 2 [mm] at its most thin. This dimension stems not only from design, but also from the capabilities of the SCU machine shop. Compared to other bus structures, such as a Pumpkin CubeSat bus, this is extremely thick. This means that the structural design will be very resilient during launch. The bus structure also makes use of brackets made for mounting internal components. These increase the stiffness of the structure overall, raising the natural frequency. While this design does increase the factor of safety, it was implemented primarily to facilitate machining at the university level. Therefore, any realized increase in natural frequency can be more accurately characterized as a positive externality.

System redundancy was introduced by means of using flash memory *via* an SD card. This card allows for data logging in addition to the capacity of the flight computers. This will help the satellite with anomaly management, *i.e.* dealing with disturbances on-orbit. It will also help the ground team manage the long-term health of the satellite.

4 Structural Engineering (STRUC)

4.1 Background

The structure of a satellite has several main functions. It provides the framework for the satellite as a whole and incorporates the other subsystems into its design while optimizing the use of volume and mass. The structural integrity of a satellite must be maintained throughout handling, launch, deployment, and mission life in order to provide support and protection for all subsystems. This includes the payload, the flight computers, EPS components, transmitter board, and AACs mechanism. The structure must be able to passively dissipate heat generated by internal components as well as insulate against incoming radiation.

The structural design must ensure the safety of the satellite throughout three major mechanical environments: ground, launch, and orbital. Each environment places unique stresses on the design. On the ground, the satellite must be able to survive the test, transportation, and fabrication conditions. Here, the spacecraft is exposed to thermal and atmospheric conditions that are very different from space. The second environment, the launch environment, places significant dynamic and static loads on the spacecraft. These include boundary conditions in the launch envelope, acoustic and acceleration loads, and shock from the launch vehicle/multistage rocket separation events. The satellite will spend the longest time in the space environment. It will be exposed to a vacuum, which can cause outgassing and cold welding, depending on the material composition. Radiation and ultraviolet degradation can change the material properties of the spacecraft and orbital debris could cause damage upon impact. In order to ensure a properly functioning spacecraft, the structure must be able to withstand all three of these unique environments.

Typically, the design of the structure is based on the orbit and mission type of the spacecraft. Orbits may be classified under two major categories: low-earth orbit (LEO) and geostationary orbit (GEO).

Unlike LEO satellites, GEO satellites benefit from almost never entering the Earth's shadow, but must have large communication dishes to reach Earth. They are typically larger and more massive than LEO satellites. GEO spacecraft typically have large gimballed solar panels and communication dishes. Often, GEO satellites have their own means of propulsion for precision pointing. Overall, they are far more expensive and complicated, and fulfill several missions simultaneously.

LEO satellites must be able to tolerate the temperature changes caused by the Earth's shadow, albedo (reflection of sunlight off the Earth), and Earth's own infrared radiation, but benefit from being close to the Earth. This means that satellites in LEO can be small and compact. They can have small communication dishes, small solar panels, small batteries, simple command and data handling, and small control systems.

Smaller systems have lower power requirements, so solar arrays can be body mounted, in contrast with the deployable arrays typical of GEO spacecraft. Additionally, LEO satellites can be designed to be launched to form a constellation of satellites. Smaller size lowers the cost to launch and streamlines the design process, making them a popular option.

4.2 Requirements

There are several requirements to be met in order for the satellite to be considered a structurally launch-ready 3U CubeSat. First, the natural frequency of the entire spacecraft must be kept above 100 [Hz] so that the satellite will not experience resonance during the launch. Resonance occurs when the system experiences vibration at one of its fundamental frequencies, which causes the amplitude of the oscillation to increase without bound. This could damage the satellite prior to deployment. Natural frequency, ω_n , can be loosely approximated as:

$$\omega_n = \sqrt{\frac{k}{m}} \quad (4.1)$$

where k is the stiffness of the structure and m is the mass of the overall structure. For a system as complex as the completed nanosatellite, finite element analysis and experimental verification must be used to determine the natural frequency.

Second, the 3U CubeSat has physical constraints defined by the characteristics of the P-Pod launcher. As stated in Chapter 2, the external volume of the satellite must be maintained at $100\pm0.1 \times 100\pm0.1 \times 340.5\pm0.3$ [mm]. This means the structure of the nanosatellite must be manufactured with strict tolerances. The total mass of the satellite including the payload must be kept under 4 [kg]. This will ensure that the nanosatellite will fit within the P-Pod launcher without adding significant weight to the launch. In addition to these requirements, the external structure of the satellite must include rails that will be in contact with the launcher. At least 75%, or 255.4 [mm], of the satellite rails must be in contact with the launcher rails. These rails must be made out of hard anodized aluminum to prevent damage.

A SYST level requirement for the structure of the satellite is that it must be student built. This reduces cost and turnaround time for the project because changes and problems can be managed directly by the students. However, this also meant that longer and more arduous machine processes were used due to the limited capabilities of the average university machine shop. One example of this was that the SCU machine shop lacked a metal-capable laser cutter, which could have been used to quickly fabricate the faces of the structure. Instead, these structural components had to be manufactured using a milling machine.

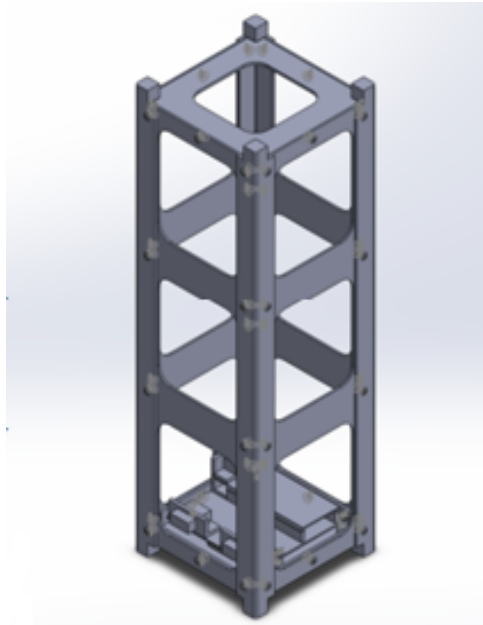


Figure 4.1: Bus structure from 2012 design team.

Finally, the arrangement of the internal components must be completed in such a way as to ensure proper mass distribution. Specifically, as per the CubeSat Design Specifications, the spacecraft center of mass must be within 2 [cm] of its geometric center.

4.3 Inherited Design

Drawing from the lessons learned from the 2011-12 nanosatellite team and the requirements for the P-Pod, a 3U structure was designed. Although the Pumpkin Inc. design only included three distinct parts, the 3U CubeSat design requires ten separate parts: four side faces, four corner brackets, one top face, and one bottom face. This design is shown in Figure 4.1. The solid side faces allow the internal components to be incorporated into the satellite. They attach to the corner brackets along the side and to the top and bottom faces. All the parts are manufactured from aluminum 6061 and the fasteners are military specification stainless steel to increase the likelihood of mission success. A detailed parts list can be found in Appendix H.

4.4 Design Updates

A thorough review of the 3U design from last year revealed that significant changes were needed to meet requirements for launch and deployment. For instance, the inherited design lacked a deactivation switch integrated with the structure and mounting and cabling were an afterthought. Considering how many subsystems and components are included in the 3U CubeSat platform, it was clear that changes were necessary.

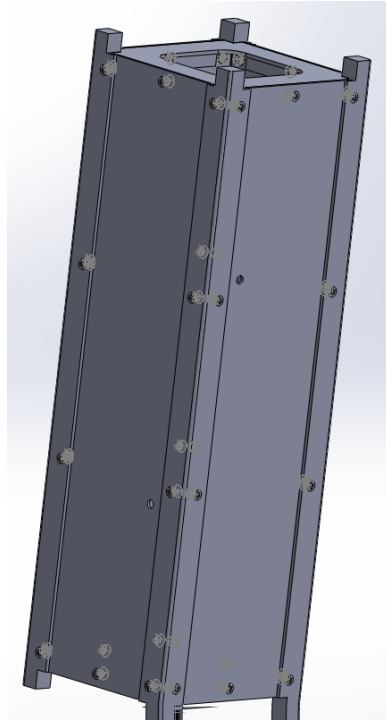


Figure 4.2: Updated bus structure design.

The structural design from last year included side faces with pockets milled out. Although this reduces the mass of the structure, it did not allow flexibility within the design. For the unspecified payload, it is crucial that the design can be modified easily to account for changes in payload and batteries. Additionally, the 2011-12 design did not consider how to incorporate the solar panels. The design was changed to have solid side faces. This allowed the design to be more flexible, and the new design includes holes for the attachment and wiring of the solar panels. The new design has also sped up and simplified the manufacturing process, because the pockets no longer needed to be milled out. This had the added bonus of increasing the natural frequency because the solid faces greatly increased the stiffness of the structure. The new assembly is shown in Figure 4.2.

In order to better incorporate the internal electronics of the nanosatellite, several hole locations were changed and added. Through-holes were added so that the AACCS payload, communication board, and solar panels could be included in the satellite. The bottom face was also redesigned so that it allows the wires to be routed along one side of the satellite and makes the wiring process much simpler.

The brackets were also redesigned. The bracket that mounts the flywheel can was designed with specifications set by the AACCS subteam. It must keep the flywheel centered within the structure to prevent anomalous system behavior. The second bracket is used to attach the payload and the communication board. It was designed

in such a way that the through-holes for the communication board lined up with the through-holes for the brackets.

4.5 Challenges

The major challenge encountered during the design and fabrication of the structure was maintaining the scale and tolerances of each component. This challenge is a result of the project requirement to manufacture and assemble the spacecraft in the university machine shop using only student labor. Machining the side faces was especially challenging; these parts were fabricated on milling machines, which is a long and arduous process compared to something more high-tech such as a metal-capable laser cutter. The top and bottom faces were milled from solid blocks of aluminum and were mounted using assembly tools. This was necessary as each part required thin flanges in order to attach to the side faces. The corner brackets had the tightest tolerances and required a special tool in order to be machined properly.

4.6 Analysis

Modal analysis was conducted using the finite element analysis (FEA) program ANSYS 14 to find the natural frequencies of the system. This analysis was completed for the assembled structure and did not include internal components. This is because it is difficult to simulate the behavior of the various electronic components, especially those that have not yet been selected, such as the battery and payload. Further FEA will be completed once the internal components are finalized. The boundary conditions of the model were chosen to simulate the constraints imposed by the P-POD. The eight corners of the nanosatellite were constrained so that they have no displacement in any direction.

The results of the finite element analysis show that the structure has a first natural frequency of 591.55 [Hz], which greatly exceeds the minimum natural frequency requirement of 100 [Hz]. The program also calculated five other modes of vibration. These natural frequency values are significantly higher than those derived from the 2012 design, as shown in Table 4.1. Despite the increased mass, the additional material increased the stiffness of the structure significantly.

Because the solid side faces are relatively thin compared to the rest of the structure, it is expected that this is where failure may occur. The mode shapes in Figure 4.3 show that the structure does vibrate as anticipated.

Table 4.1: Natural frequencies for different modes of vibration.

Mode	Updated Design [Hz]	2012 Design [Hz]
1	591.55	499.4
2	892.45	531.9
3	896.87	536.5
4	931.14	581.5
5	1151.5	717.2
6	1153.7	791.4

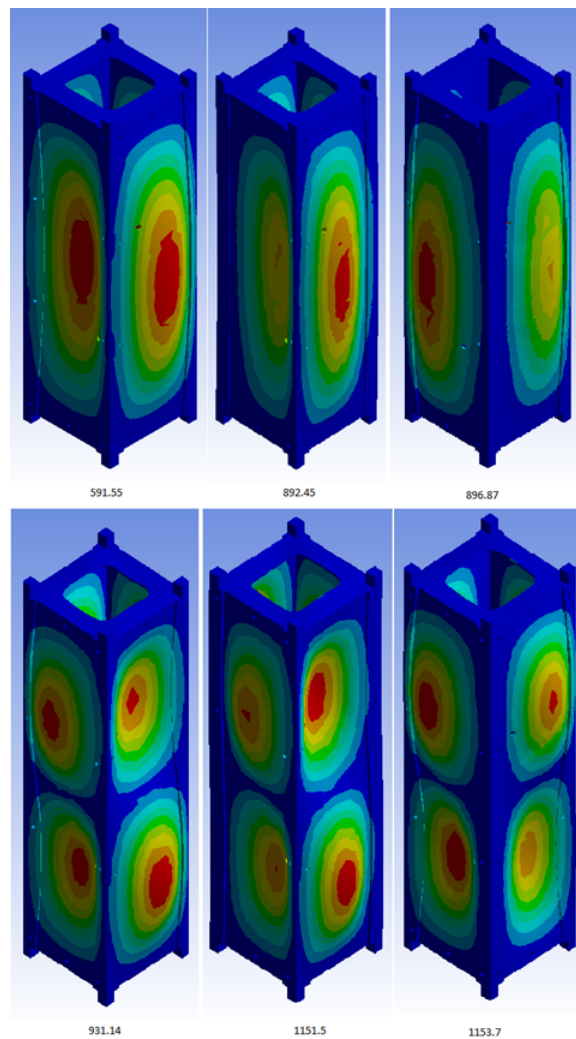


Figure 4.3: Six modes of vibration of the bus structure.

5 Thermal Design and Analysis (THERM)

5.1 Satellite Thermal Background

The thermal subsystem is vital to a satellite's functionality. It ensures other system components are not compromised in the extreme conditions of the space environment due to temperature fluctuations. Every component has an operational temperature range that must be maintained to ensure functionality. In addition to an operational temperature range, there is a survival temperature range. Generally, if the component temperatures fluctuate outside of their operational range, the systems will still function if returned to operational conditions. Unfortunately, once outside the survival temperature range, components will fail. A satellite's survival and operational temperature ranges are determined by its most sensitive components.

In LEO, the thermal inputs that affect satellites are direct internal heat generation, solar radiation from the sun, infrared radiation emitted by Earth, and albedo, which is solar radiation reflected off Earth's surface. The external thermal inputs are transferred to the orbiting spacecraft through radiation, which is illustrated in Figure 5.1. The heat flux is determined by the geometry, orientation, and material properties of the spacecraft. Internal heat generation is created by electrical components and is transferred through conduction and radiation. The only means of heat dissipation is through radiation.

Thermal analysis is necessary to simulate the behavior of the satellite while in orbit. This is typically completed using Thermal Desktop, an industry standard. Thermal Desktop is used to generate thermal models of systems that can be manipulated in a CAD environment.²⁰ Unfortunately, it has a steep learning curve, making it impractical to implement at the university level.

The current design team took a different approach to thermal analysis. This was completed using the thermal analysis tool SatTherm, which was used by the previous design team. This is described in Section 5.3.

Thermal analysis considers the worst case scenarios a satellite might sustain during its mission life. This approach determines whether a satellite will survive the most extreme environments it might encounter on orbit. It also benchmarks the temperature range the satellite will sustain. The two scenarios of interest are the “hot case,” when the satellite’s largest surface faces the sun with the inclusion of internal heat generation, and the “cold case,” when the satellite’s smallest surface faces the sun without any internal heat generation. This is typical for a satellite in LEO; alternate assumptions are made for different orbits. From this analysis, the THERM subsystem is engineered using a combination of Active Thermal Control (ATC) and Passive Thermal Control (PTC) to keep the satellite within the temperature range requirement.

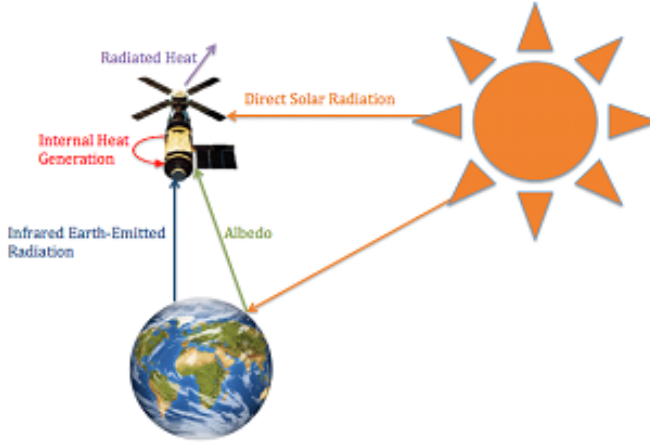


Figure 5.1: Energy balance of a satellite in LEO.

5.2 Modes of Heat Transfer

Since there is no medium in space to transport heat by convection, there are only two modes of heat transfer relevant to analysis: conduction and radiation. This analysis neglects the effects of convection in the sealed vessel for the AACs.

5.2.1 Conduction

Conduction is the transfer of energy by atomic vibrations (phonons) and electronic transitions (for metals in particular). The higher the particle energy, the higher the temperature.²¹ Heat transfer processes can be characterized by rate equations, such as Fourier's Law:

$$q'' = -k \frac{dT}{dx} \quad (5.1)$$

where q'' is the heat flux [W/m^2], k is a transport property or the thermal conductivity [$\text{W}/(\text{m}\text{K})$], and $\frac{dT}{dx}$ is the change in temperature over distance. The minus sign is used because heat is transferred in the direction of decreasing temperature.

To calculate the heat transfer rate and flux between two points i and j , Fourier's Law may be used as

$$q_{ij} = \frac{kA}{L}(T_i - T_j) \quad (5.2)$$

$$q_{ij}'' = \frac{k}{L}(T_i - T_j) \quad (5.3)$$

where q_{ij} is the heat rate in [W] between points i and j , A is the cross sectional area in [m^2] through which the heat is flowing, L is the distance in [m] between points i and j , T_i is the temperature in [K] at point i , T_j is the temperature in [K] at point j , and q_{ij}'' is the heat flux in [W/m^2] between points i and j .

5.2.2 Radiation

Thermal radiation is energy emitted at the surface of matter and is transported by electromagnetic waves. Since radiation does not require a material medium, it is most efficient in a vacuum.²² The rate at which radiation energy is emitted is contingent on the direction and wavelength of the electromagnetic waves and the surface temperature. This rate is known as the surface emissive power, E , and is measured in [W/m²].

An ideal radiator is known as a “blackbody.” A blackbody’s characteristics are that it “absorbs all incident radiation, regardless of wavelength and direction; for a prescribed temperature and wavelength, no surface can emit more energy than a blackbody; and it is a diffuse emitter.”²³ The Stefan-Boltzmann law calculates the emissive power of a blackbody as a function of surface temperature:

$$E_b = \sigma T_s^4 \quad (5.4)$$

where E_b is the emissive power of a blackbody [W/m²], σ is the Stefan-Boltzmann constant (5.67×10^{-8} [W/m²· K⁴]), and T_s is the surface temperature.

The heat flux emitted by a real surface is less than that of a blackbody because it is also dependent on the surface emissivity:

$$E = \varepsilon \sigma T_s^4 \quad (5.5)$$

where E is the emissive power and ε is the surface emissivity ($0 \leq \varepsilon \leq 1$). Furthermore, the heat flux radiated from one body to another can be calculated using:

$$q_{ij}'' = \varepsilon \sigma F_{ij} (T_i^4 - T_j^4) \quad (5.6)$$

where F_{ij} is the view factor between surface body i and surface body j .

5.3 SatTherm

SatTherm is a “thermal analysis and design tool for small spacecraft” designed by NASA Ames and San Jose State University in 2008. It is a MATLAB package that runs a nodal transient thermal analysis for small spacecraft. A benchmark comparison between SatTherm and Thermal Desktop consistently yielded temperature profiles within 4 [K] of one another.²⁴

The SatTherm package uses the finite-difference numerical method to calculate the transient temperature of each surface of a modeled satellite.

The way in which heat flux affects an object's temperature can be characterized in the transient heat flux equation of a one dimensional system:

$$k \frac{\partial^2 T}{\partial x^2} = \rho c_p \frac{\partial T}{\partial t} \quad (5.7)$$

where k is the thermal conductivity of the material in [W/mK], ρ is the material density in [kg/m³], and c_p is the material specific heat in [J/kgK]. This is a second-order partial differential equation which relates the partial derivative of temperature with respect to time to the second partial derivative of temperature with respect to position. With the use Equation 5.7 and the finite-difference method, the temperature profile as a function of time and position, $T(x, t)$, can be approximated.

The finite-difference method uses a forward difference approach to determine an object's transient temperature at each of its nodes. An approximation to the time derivative in Equation 5.7 is expressed as:

$$\frac{\partial T}{\partial t} \approx \frac{1}{\Delta t} [T(x, t + \Delta t) - T(x, t)] \quad (5.8)$$

$$\frac{\partial^2 T}{\partial x^2} \approx \frac{1}{\Delta x^2} [T(x + \Delta x, t) - 2T(x, t) + T(x - \Delta x, t)] \quad (5.9)$$

Each node n is separated by length x , making its neighboring nodes $n - 1$ and $n + 1$. This means that $T(x + \Delta x, t)$ becomes T_{n+1} , $T(x, t)$ becomes T_n , and $T(x - \Delta x, t)$ becomes T_{n-1} . Similarly, $T(x, t)$ becomes T_n and $T(x, t + \Delta t)$ becomes T'_n , which is the the temperature of node n after one time step t . Using the notation in Equations 5.8 and 5.9, Equation 5.7 simplifies into:

$$\frac{k}{(\Delta x)^2} (T_{n-1} - 2T_n + T_{n+1}) = \frac{\rho c_p}{\Delta t} (T'_n - T_n) \quad (5.10)$$

Then, both sides of Equation 5.10 are multiplied by the volume of material separating each node n , $A\Delta x$, where A is the cross-sectional area and Δx is the length. Further replacing $\frac{kA}{\Delta x}$ with the conductive resistance R , and $V\rho c_p$ with the material's thermal capacity C , one obtains:

$$\frac{T_{n-1} - T_n}{R_{n,n-1}} + \frac{T_{n+1} - T_n}{R_{n,n+1}} = \frac{C}{\Delta t} (T'_n - T_n) \quad (5.11)$$

Equation 5.11 can be generalized for a two-dimensional system as follows:

$$\sum_j \frac{T_j - T_i}{R_{ij}} = \frac{C_i}{\Delta t} (T'_i - T_i) \quad (5.12)$$

Additional consideration of radiation and internally generated heat results in the following expression for T'_i :

$$T'_i = T_i + \frac{\Delta t}{C_i} \left(\sum_j q''_{ij-cond.} + \sum_j q''_{ij-rad.} + q''_{i-int.} \right) \quad (5.13)$$

where $q''_{ij-cond.}$ is the heat flux from conduction, $q''_{ij-rad.}$ is the heat flux from radiation, and $q''_{i-int.}$ is the heat flux from internal heat generation. Equation 5.13 demonstrates that the temperature of a node can be calculated iteratively for a transient analysis, though it requires that the initial temperatures as well as the radiation and internal heat fluxes at each time step be known. The value of Δt should be bounded using an associated stability criterion to ensure that there are no numerically induced oscillations, which can cause the solution to diverge.²⁵

5.4 Active and Passive Thermal Solutions

There are several methods of thermal control to keep a satellite within its required temperature range. One popular approach taken for satellite thermal design is “cold-biasing,” meaning that the satellite is designed to operate closer to its low temperature limit than its high temperature limit. This is typically done because it is cheaper and more efficient to generate heat than it is to dissipate heat in the space environment. Another approach is to maximize PTC and minimize ATC to reduce THERM subsystem complexity and maintain minimal impact on the power budget. Since PTC will be optimized to reduce necessity of ATC, several subsystem options have been explored.

There are many traditional thermal design solutions. One example is multi-layer insulation (MLI), which minimizes heat transfer to and from the satellite, but requires space in the volume budget. A different approach is to reduce or increase the amount of thermal radiation the satellite absorbs or emits using a surface finish with appropriate thermal properties. Heat pipes are efficient devices used to dissipate heat, however they are not practical for a small satellite. A highly thermal conductive plate made out of aluminum or titanium can be used to mount the high energy producing components. This allows heat to flow from the plate to the exterior surface of the satellite and be dissipated through radiation. In some cases, satellites mount radiators to dissipate heat.

To effectively use ATC, temperature sensors are required. Some options include thermistors, resistance temperature detectors (RTD), and thermocouples. RTDs are made of conductors, such as platinum, and have a resistance that varies linearly with temperature. Thermistors are semiconductors that give a power function relationship between resistance and temperature.²⁶ In a thermocouple, a voltage is generated across the junction of two different alloys in response to temperature changes.

RTDs and thermistors are compatible with computerized systems and have an operating temperature range of 73 to 973 [K]. They generally provide temperature readings of up to two significant figures and can remain stable with little degradation. RTDs are expensive because of their material value, while both sensors are more sensitive to environmental disturbances than thermocouples. Thermocouples have a wider temperature range of 73 to 2593 [K] and do not require any power to operate. The only drawback is that thermocouples degrade more quickly than RTDs and thermistors.²⁷ Since small satellites have a relatively short mission life, thermocouples are the best option for thermal sensors.

For ATC, louvers can be used to control the thermal environment. Louvers function as shutters that open when the satellite's internal temperature is too high. A bi-metallic sensor actuates the louver blades by contracting and applying a torque as temperature increases. Using a highly reflective base-plate to reject heat, the satellite's temperature can be controlled passively.²⁸ Unfortunately, louvers are difficult to manufacture, demand too much of the mass budget, and reduce space designated for photovoltaic panels. Thermoelectric coolers can be used to dissipate excess heat, however they are not efficient in performance and are typically used for low heat flux systems.

The most practical solution to generating heat is the use of flexible electrical heaters, which exploit the heat generated from resistors. They are simple components that can be epoxied to another component and conduct heat. When the temperature measuring device indicates that the component has fallen below its operational temperature range, the heater will turn on, then turn off once the sensor indicates the component's temperature has been returned to its operational temperature range.

5.5 SatTherm Updates

Upon reviewing the SatTherm package, an error with the internal view factor function for the satellite had to be corrected. This error caused the internal view factors to not add up to 1. It was also discovered that the SatTherm package previously assumed that only the top surface of the satellite would constantly face the sun. The script was changed so that the hot and cold cases mentioned in section 5.1 could be simulated. Additionally, a hot and cold case were simulated that included Chemglaze Z306 Black paint as the surface finish for the top and bottom surfaces. The satellite's orbital parameters were changed to match the orbit of the International Space Station (ISS) as of January 21, 2013. Also, the analysis now includes different surface finishes for each surface of the satellite, including aluminum 6061, Chemglaze Z306 Black Paint, and an averaged surface finish of aluminum 6061, photovoltaic cells, and printed circuit board.

Table 5.1: Thermal properties of surface finishes.

Surface Finish	Absorptivity	Emissivity
Aluminum 6061	0.031	0.039
Averaged Composite	0.651	0.649
Chemglaze Z306 Black Paint	0.920	0.890

5.6 Work Summary

To begin, a temperature range requirement had to be defined by the UPAACN's system components temperature sensitivity, which was bounded to 242 to 358 [K]. To input the UPAACN's material properties into SatTherm, an average surface finish for the side surfaces had to be calculated to account for the composite material of aluminum 6061, photovoltaic cells, and printed circuit board. The surface thermal properties are tabulated in Table 5.1. Once the satellite's thermal properties were calculated and updated in SatTherm, the simulation was run for a period of six hours for both hot and cold cases.

Different paint surface finishes were used in the thermal analysis as part of the PTC to maintain the satellite's surfaces within the temperature range requirement. Chemglaze Z306 Black Paint was selected as the best surface finish.

5.7 Challenges

The first challenge encountered was deciphering the SatTherm package. The package had several scripts that ran different functions necessary to perform the thermal analysis, making it a tedious process. Every function was verified and modified where necessary. Another challenge stemmed from finding a surface finish with thermal properties that was ideal to maintain the satellite's surfaces within the temperature range requirement while also being cost effective.

5.8 Results

Before a surface finish was considered, a hot and cold case were simulated using aluminum 6061 material properties. These results are shown in Figures 5.2 and 5.3, respectively. The hot case results show that the UPAACN will stay within its operational temperature range. The cold case shows that the UPAACN node temperatures will drop below the lower limit of the operational temperature range. This is due to the low absorptivity of aluminum 6061. These results prompted the team to consider using a surface finish with more desirable material properties on the top and bottom faces of the UPAACN.

The hot case results with the top and bottom surface finish of Chemglaze Z306 Black Paint are shown in Figure 5.4. The cold case results with the top and bottom surface

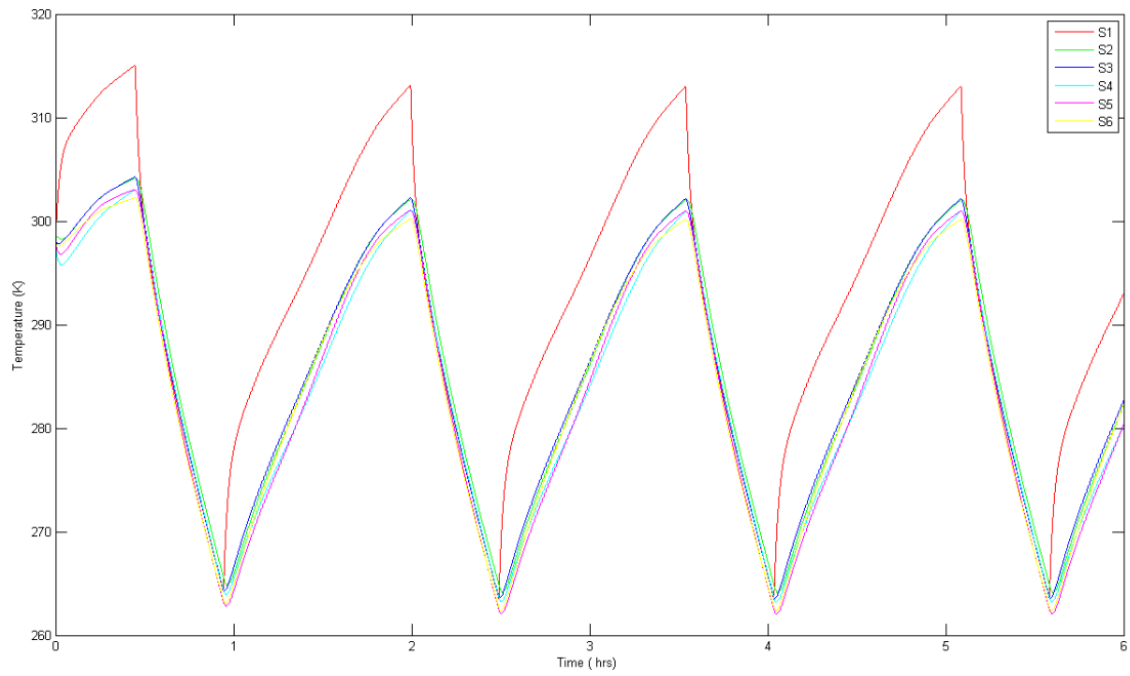


Figure 5.2: Hot case simulation over six hour period with aluminum 6061 as a surface finish on the top and bottom faces.

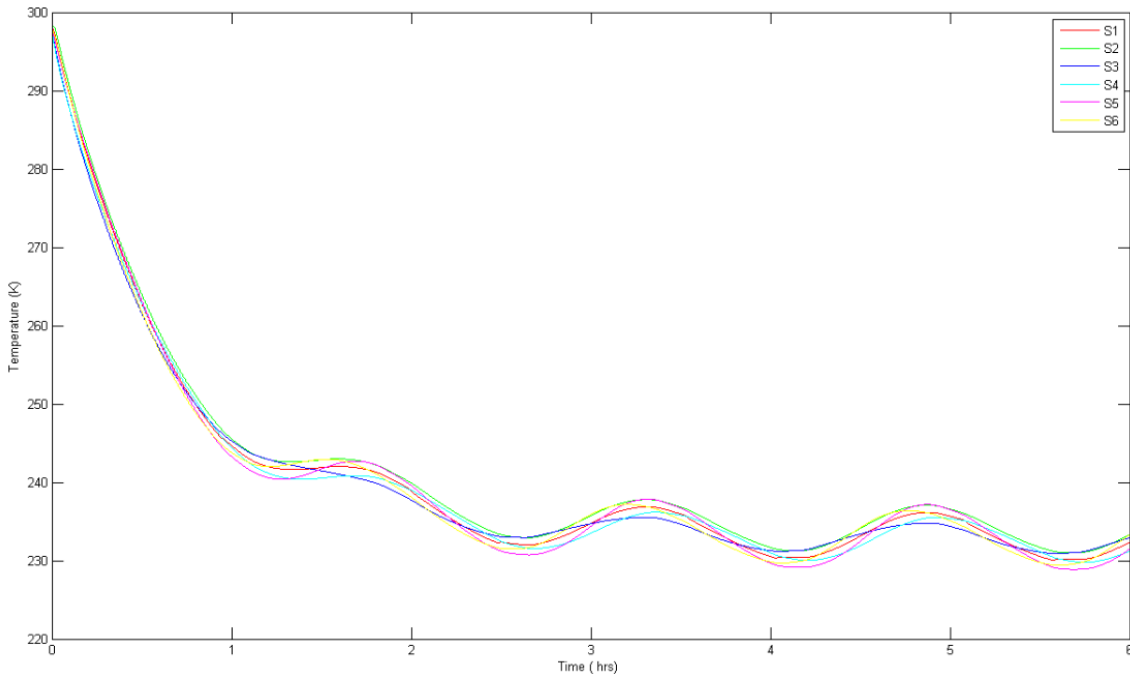


Figure 5.3: Cold case simulation over six hour period with aluminum 6061 as a surface finish on the top and bottom faces.

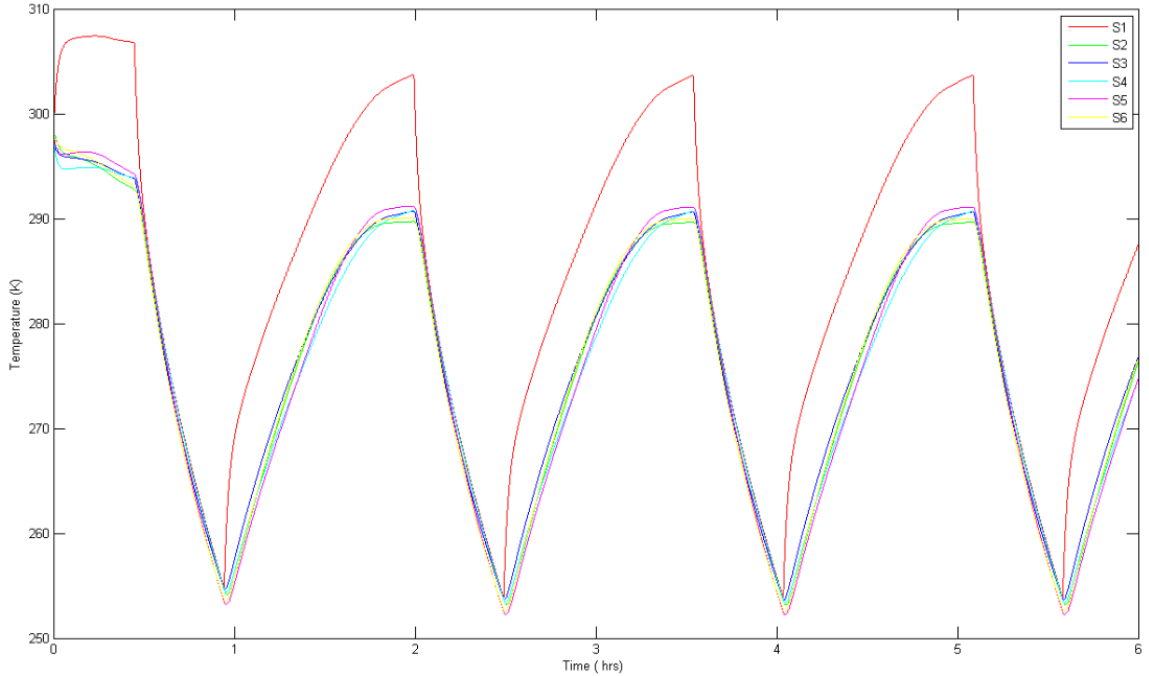


Figure 5.4: Hot case simulation over six hour period with Chemglaze Z306 Black Paint as a surface finish on the top and bottom faces.

Table 5.2: Temperature ranges for hot and cold cases with and without Chemglaze Z306 Black Paint on the top and bottom faces.

Surface Finish	Hot Case [K]	Cold Case [K]
Aluminum 6061	262-313	229-237
Chemglaze Z306 Black Paint	252-304	242-275

finish of Chemglaze Z306 Black Paint is shown in Figure 5.5. Figures 5.4 and 5.5 each contain data for the temperature of each surface of the satellite while in orbit.

The hot case shows that the UPAACN will stay within its temperature range requirement with a safety of 10 [K] above its lower limit and oscillates well below its upper limit. Similarly, the cold case stays well below its upper limit, but reaches the lower limit at 242 [K]. Since it is not expected that the UPAACN's orientation will be fixed in a cold case position for a significant amount of time, the risk of UPAACN falling out of its operating temperature range is small. These results were compared to the hot and cold cases run without the additional surface finish of Chemglaze Z306 Black Paint, which are shown in Table 5.2.

Through simulation, with the current configuration of the UPAACN and applying Chemglaze Z306 Black Paint to the top and bottom surfaces, the results show that the UPAACN should stay within its temperature range requirement.

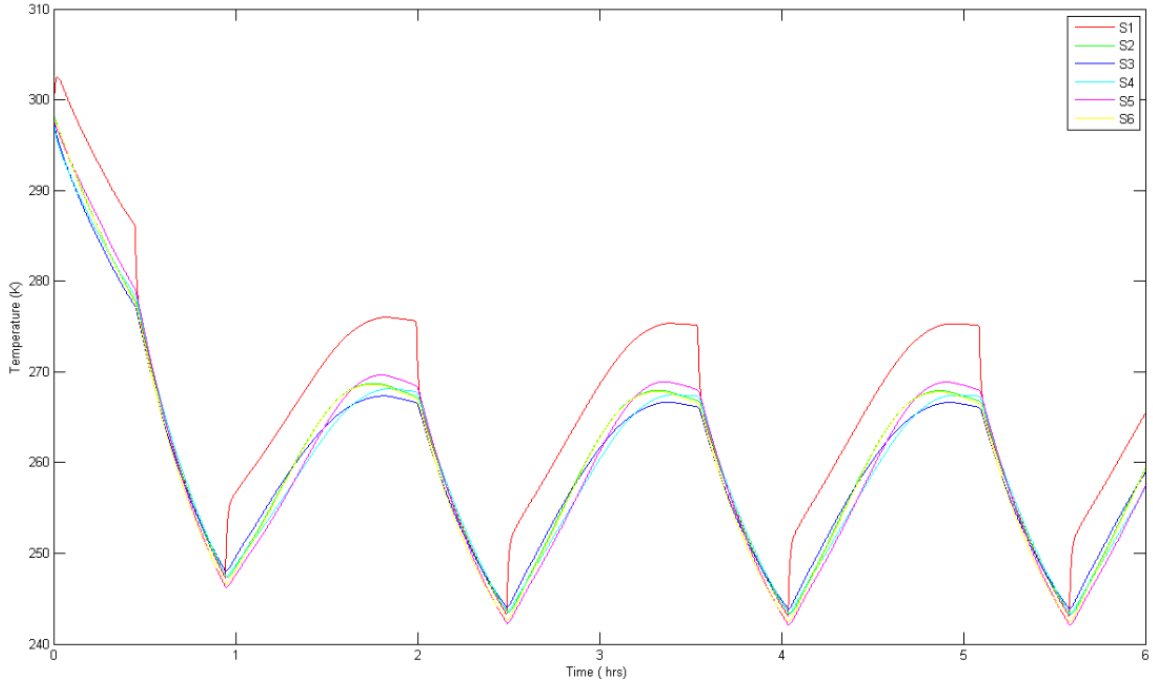


Figure 5.5: Cold case simulation over six hour period with Chemglaze Z306 Black Paint as a surface finish on the top and bottom faces.

5.9 Future Work

With the implementation of a battery and payload, the SatTherm simulation will need to be modified to adopt the new changes and be run again for new results. It is likely that new components will have more sensitive temperature ranges, which would most likely require the use of ATC in the thermal subsystem. As discussed in section 5.5, MLI can be used to minimize heat transfer while thermocouples and flexible electric heaters can be used to sense component temperatures and provide heat when necessary.

SatTherm does not have a complete graphical user interface. All variables are defined in a MATLAB script (m-file), which runs by calling the functions needed to calculate the transient temperature. Developing a graphical user interface would increase SatTherm's usability and shorten its learning curve.

6 Distributed Command and Data Handling (dCDH) and Communications (COMM)

6.1 Introduction

The Data Handling subsystem is comprised entirely of one single piece of hardware on which four main processes are installed; the Dallas-Master (DMS), the Scheduler, the Expert, and the Beacon (BCN). The main function of the dCDH subsystem is to control all the software in the satellite. It monitors the statuses of the subsystem such as current and temperature in order to make sure the system is within the operational range. The beacon continuously transmits system telemetry data packets in order to communicate the satellite operational status to the ground component. The scheduler is used to turn on the COMM subsystem after initial satellite deployment and if it has been turned off in order to save power. It will also control the frequency of the beacon packet broadcasts. The expert system will ensure the system is within the operational range.

The main functions of the COMM subsystem are to send data from the satellite to the ground station and to distribute commands from the ground station to the satellite. The COMM subsystem is necessary for dCDH as it is the only means for the ground station to communicate with and send commands to the satellite on-orbit.

6.2 Requirements

Mission success is determined by customer satisfaction. In the case of the UPAACN and its subsystems, Dr. Christopher Kitts of the RSL is the primary customer. Several RSL requirements have already been discussed in Chapters 1 and 2. For dCDH and COMM, the requirements are split into three categories: functional, non-functional, and design constraints. Functional requirements define system actions, while non-functional requirements define how these actions are completed. Design constraints restrict the means in which solutions are implemented.

There are several functional requirements. The system will send health packets and data *via* the beacon board. In addition, the flight computers will receive data and commands from the RSL ground station. The system will then execute these commands by distributing them to the various subsystems. Finally, the dCDH system will interface with the AACS mechanism.

The non-functional requirements are more general and affect the system design process. For instance, the system is designed to be as efficient and cost effective as possible while complying with all NASA and CubeSat Design Specifications. The system is also design to be expanded in future iterations so that a variety of payloads can be supported. This approach helps develop the capabilities of the 3U platform.

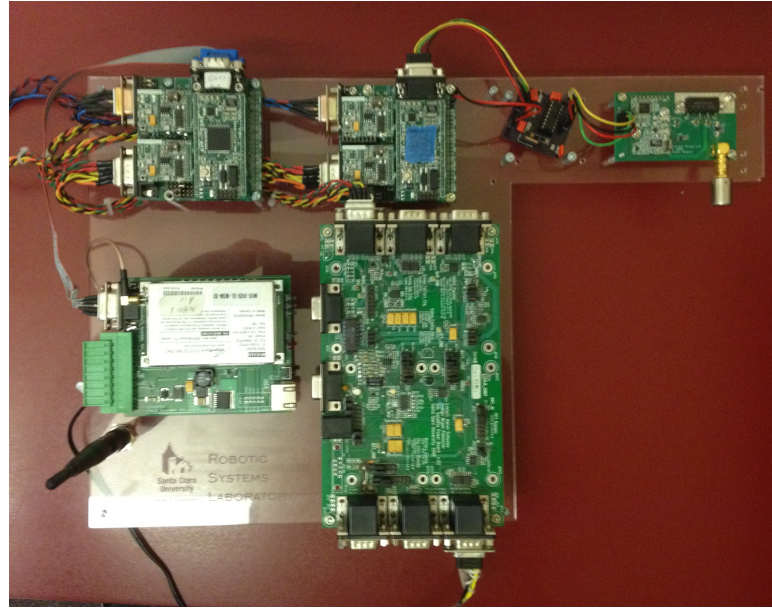


Figure 6.1: Clockwise from top left: two AVR-SAT boards, beacon board, lab power board, MHX2420 OEM Radio Transmitter board.

Finally, the dCDH and COMM systems are designed to be maintained by students in the RSL.

The dCDH/COMM subteam used AVR-SAT hardware boards in accordance with the design requirements. The system was also required to fit within the physical architecture of the 3U platform. For transmissions, a MHX2420 OEM Radio Transmitter board was used in order to maintain compatibility with existing RSL operations. This allows the RSL ground station to communicate with the UPAACN on-orbit. This hardware is shown in a lab configuration in Figure 6.1.

6.3 System Architecture

6.3.1 Conceptual Model

The first iteration of the dCDH and COMM subsystems was based on the architectural diagram shown in Figure 6.3.1. This was a client-server model adapted for the distributed flight computing approach. The diagram shows how the dCDH processes interface with the AAC mechanism.

6.3.2 Final Model

The design team eventually settled on the architectural model shown in Figure 6.3. This model was adopted after the team encountered issues with the conceptual model. This updated model more comprehensively considers the overall subsystem structure

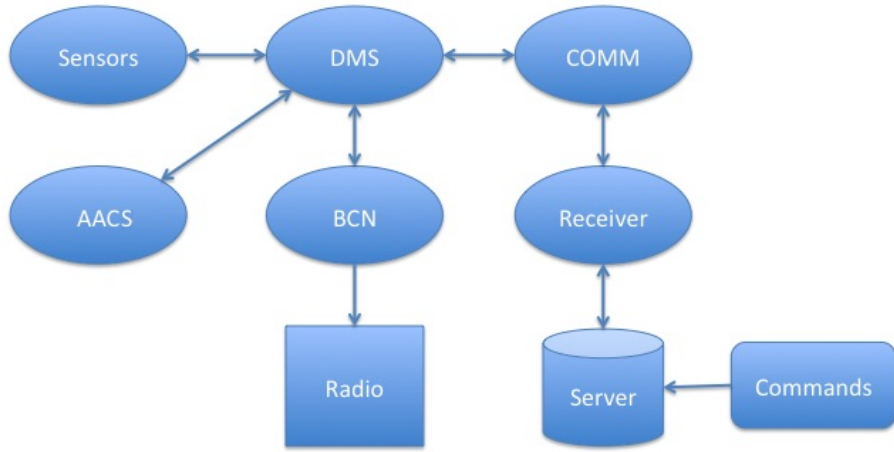


Figure 6.2: Conceptual architectural model of dCDH and COMM.

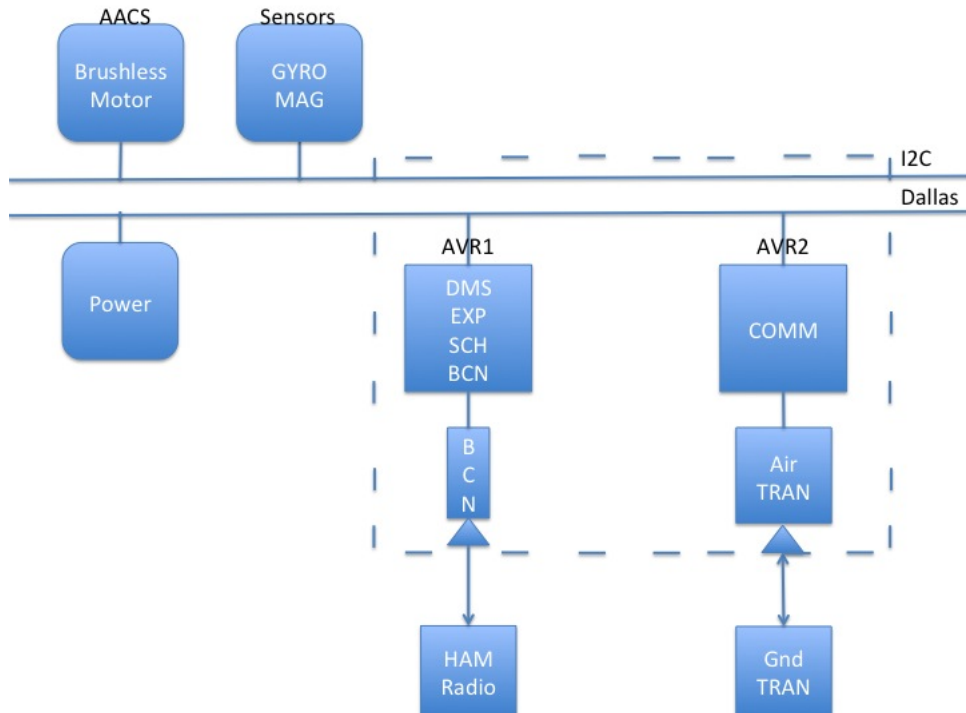


Figure 6.3: Final architectural model for dCDH and COMM.

of the 3U platform. The main update is that Beacon is now included in the dCDH hardware instead of COMM due to memory overlap issues.

6.4 Use Cases

The following use cases explain the main functions of the dCDH and COMM subsystems. They include the components that perform a function, or the actors, the goal of the function, the conditions that must be satisfied before and after the function is performed, and the step-by-step process of completing the function.

6.4.1 Sending Commands *via* the Transmitter

- Actors - RSL Ground Station.
- Goal - Send commands to the UPAACN from the RSL Ground Station.
- Pre-Condition - Satellite is powered, ground antenna is able to broadcast.
- Post-Condition - Commands were sent and received.
- Exceptions - Transmitter is non-functional.
 1. Seek out UPAACN.
 2. Establish link between ground station and UPAACN.
 3. Broadcast command to UPAACN.
 4. End broadcast.

6.4.2 Sending Beacon Packets

- Actors - RSL Ground Station.
- Goal - Initialize beacon in order to send packets.
- Pre-Condition - Satellite is powered, ground antenna is able to broadcast, HAM radio is on.
- Post-Condition - Commands were sent and received, beacon is transmitting packets.
- Exceptions - Transmitter is non-functional, satellite is out of HAM radio range.
 1. Seek out UPAACN.
 2. Establish link between ground station and UPAACN.
 3. Broadcast to UPAACN.
 4. Initialize beacon command for set time interval.
 5. End broadcast.

6.4.3 System Power On

- Actors - UPAACN.
- Goal - Turn on all subsystems individually.
- Pre-Condition - UPAACN has gone through reboot or has powered off individual subsystems.
- Post-Condition - All UPAACN subsystems are powered on.
- Exceptions - N/A.
 1. Dallas-Master detects subsystems that are powered off.
 2. Dallas-Master executes commands that redirect power to subsystems in question.

6.4.4 System Power Off

- Actors - UPAACN.
- Goal - Turn off all subsystems individually.
- Pre-Condition - UPAACN has power and is receiving commands, hardware sensors are functioning.
- Post-Condition - UPAACN subsystems are powered off.
- Exceptions - N/A.
 1. UPAACN sensors detect that criteria is met for full system reboot or for individual subsystems to be powered off.
 2. Dallas-Master sends commands to power off to subsystems in question.

6.4.5 AACS Motor Control

- Actors - UPAACN.
- Goal - Receive data from and send control commands to AACS motor.
- Pre-Condition - UPAACN has power, RSL ground station is able to broadcast.
- Post-Condition - Motor response is controlled.
- Exceptions - Sensors are non-functional.
 1. Dallas-Master reads information from sensors.
 2. Dallas-Master will send control command to motor depending on telemetry data/system functional criteria.

3. Telemetry/AACS data is relayed to RSL ground station.
4. End broadcast.

6.5 Activity Diagrams

The activity diagrams show the flow of the dCDH and COMM processes. They separates each into logical and graphical components while describing the flow of each process. Each diagram shows how processes interact with and lead into other processes. These diagrams were taken from previous RSL projects that used the same boards and processes. They can be found in Appendix F.

6.6 Technologies Implemented

6.6.1 Software

The code used for the 3U CubeSat platform flight computing subsystems is written in C. Programmer's notepad was used to compile the code. It was then flashed onto the hardware boards using AVR Studio 4. When running the code on the hardware, the commands and data can be monitored and sent *via* the Terminal program or any serial compatible program.

6.6.2 Hardware

In keeping with project requirements, the hardware used was provided by the RSL. This includes:

- 2 AVR-SAT Microcontroller Boards (based on ATMega128)
- 2 MHX2420 Transmitter Boards
- 1 Beacon board with antenna
- 1 Faulhaber 1202 Brushless DC Penny-Motor with speed controller
- Various sensors:
 - Gyroscope
 - Magnetometer

6.7 Design Rationale

The purpose of the dCDH subsystem is to process the commands and telemetry data and relay it to the RSL ground station. It was important to ensure that the hardware used was reliable and compatible with all subsystems. The AVR-SAT boards used are outdated, but they have a flight heritage, which is highly desirable in the space industry. In other words, these boards have been proven on-orbit, so they can be implemented in the 3U CubeSat platform with confidence. These boards communicated

Table 6.1: Risk analysis chart for dCDH and COMM subsystems.

Risks	Consequences	Probability	Severity	Impact	Mitigation Strategy
Dynamic requirements	Requirements not met	0.9	8.5	7.65	Frequent communication with adviser, make system adaptable
Difficult board integration	UPAACN will not function	0.9	8.0	7.20	Become familiar with documentation and AVR libraries
Unfamiliarity with hardware	Requirements not met	1.0	7.0	7.00	Become familiar with documentation, read previous thesis
Bugs in existing code	Spend time fixing bugs	0.8	8.0	6.40	Compile and check code after every change, read comments left by previous authors
Time	Miss project deadline	0.6	7.0	4.20	Have weekly group meetings, communicate with SYST

through I²C protocol, which allows for easy integration with compatible payloads. While it would be possible to design and implement more capable boards, it would be too time consuming and the value offered by the flight heritage would be lost. Finally, the beacon has been chosen to broadcast over HAM radio protocols as this has been proven on-orbit as an effective approach for LEO spacecraft.

The COMM subsystem is used by the dCDH subsystem on-orbit to send and receive commands from the RSL ground station. This function is handled by the MHX2420 transmitter board. Like the AVR-SAT boards, the MHX2420 has flight heritage and helpful documentation from previous satellite missions, making it easy to implement in the 3U CubeSat platform. The antenna used by the COMM subsystem is flat and flexible, allowing it to fit within the bus structure without interfering with other hardware. This helps optimize volume and functionality.

6.8 Project Risks

The risk analysis chart, found in Table 6.1, helped the team better understand potential design obstacles. The chart is organized by decreasing impact on the group, measured on a scale from zero to ten, ten being project failure.

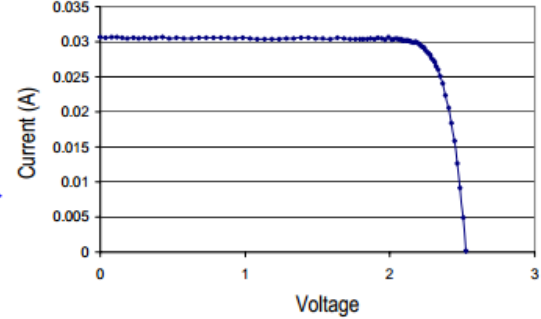


Figure 7.1: IV curve for Triangular Advanced Solar Cell.

7 Electronic Power System (EPS)

7.1 Background

The EPS is responsible for providing power all electrical components on a satellite. In general, it has several major functions. This includes generating power; storing power in batteries for use during eclipse/peak power draw periods; conditioning, regulating, converting, and distributing power; and protecting against power failures.²⁹ In addition to functional requirements, satellite power systems must also consider system degradation, orbital parameters, and spacecraft configuration. The power system in a satellite is also used to handle mission specific applications.

7.2 System Architecture

All satellite power systems have the same basic components. This includes a means of power generation, a regulating system, a means of storage, and the satellite loads.

For a CubeSat, power generation is typically handled through photovoltaics assembled into body mounted panels. These are designed in order to produce desired current and voltages. When a photovoltaic cell is exposed to electromagnetic radiation, it generates a voltage and causes current to flow. The voltage across the cell is dependent on the current through the cell. This relationship is expressed through the use of a Current vs. Voltage graph, also known as an IV curve. The IV curve for the triangular advanced solar cells (TASC) used in the solar panel design for the UPAACN is shown in Figure 7.1.³⁰

The regulating functions of the EPS are handled by a power board. The main functions of this board are to control the power generated by the solar array, to regulate the voltage of the satellite, and to charge the battery. Different satellites use different levels of power regulation.

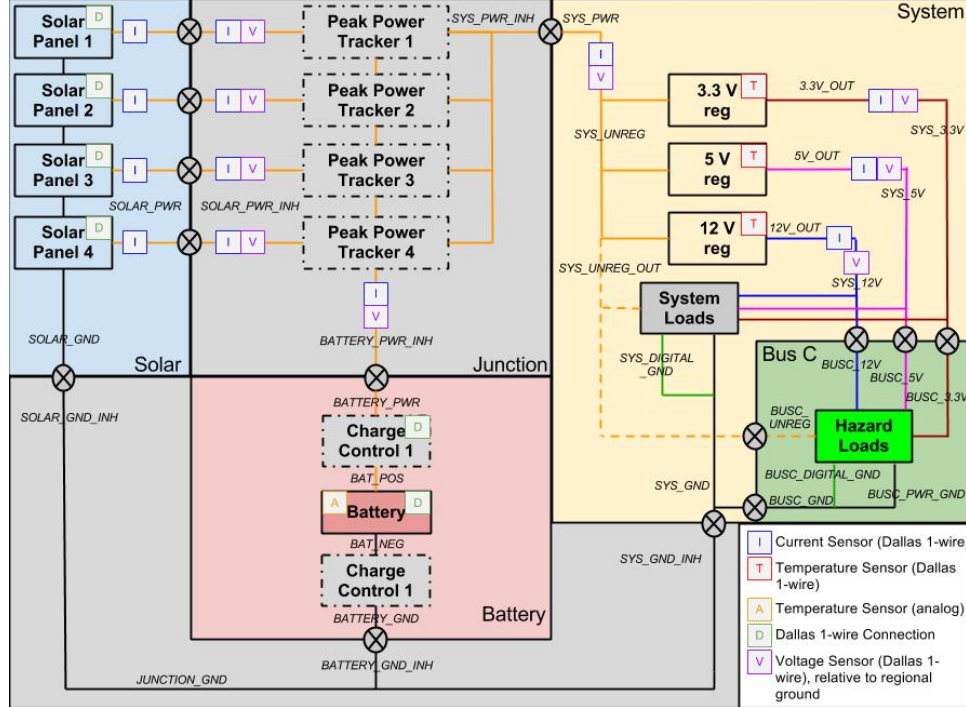


Figure 7.2: EPS block diagram.

Power storage in a satellite is typically handled by rechargeable batteries. For a satellite in LEO, the battery is charged by the solar array when exposed to solar radiation. The battery provides power to the satellite when it is in eclipse. It is also used to supplement the solar array during times of peak power draw. These batteries are typically Nickel-Cadmium or Lithium Ion.

The 3U CubeSat platform will use a power system that includes four body mounted solar panels that each feed into individual peak power trackers (PPT). The PPTs are used to dynamically optimize the power output of the solar arrays. This then feeds into a power board which regulates the bus voltage and current. The power board also controls the charging and discharging of a Lithium Ion battery. The 3U CubeSat platform also includes a kill switch that ensures no systems start up before 30 minutes after deployment. A system block diagram can be found in Figure 7.2.

The power from each panel on the UPAACN is fed into a peak power tracker. The peak power tracker regulates the input current from the cells in order to keep the input power and voltage at a predetermined level based on the power curve of the cells. The output voltage is then bucked to a level suitable to charge the battery. The output of the battery feeds into the startup comparator. The startup comparator is responsible for the 30 minute delay between launch from the pod and systems turn on. The output of the comparator is fed to both boosting and bucking converters. The output of these converters are fed to the various other boards as voltage supply rails.

7.3 Solar Array Design and Assembly

Solar panel arrays are created by placing multiple cells in series to create strings, and then these strings are placed in parallel to form an array. Cells are combined in series in order to produce a desired voltage. These strings are placed in parallel in order to produce a desired current output. Diodes are often included at the end of each string in order to protect the solar cells from reverse charging. For CubeSats, these arrays are typically mounted to the satellite body.

The solar panel design for the UPAACN is similar to that of the Brown Cube Satellite. Each panel utilizes a two layer PCB. This PCB is the body of the panel, it is where each of the cells associated with the panel will be mounted. The PCB also holds the traces that form the electrical connections between cells. Each panel will span the length of the CubeSat, and the width between rails along the long edges of the satellite. Four of these panels will be used to cover the rectangular surfaces of the satellite. The top and bottom, square surfaces of the satellite, will not contain solar panels.

The panel dimensions are 321 x 68.58 [mm]. Each panel will contain fifty Triangular Advanced Solar Cells or TASCs. These cells will be connected in strings of five cells. These strings will be connected in parallel to form ten strings per panel. The trace width used for the series connections was determined based on the current expected to flow through each one of these traces. It was made wider than necessary to avoid resistive losses, and to better dissipate heat. These traces were selected to be 0.76 [mm] in width. At the cathode of each string a vishay B120 schottky diode was placed, with the anode of the diode placed at the anode of the string. These diodes serve the purpose of blocking current from flowing through a string from anode to cathode in the presence of a string at a higher potential. These strings were then connected in parallel via 2.54 [mm] traces. These traces were again larger than necessary for the amount of current traveling through them, however, the increased width meant better thermal conduction and less resistivity. Two vias were provided at the back of each panel to provide a soldering point for the anode and the cathode of the panel.

The electrical characteristics of each panel are as follows under peak power conditions. Peak power conditions include exposure to 1 Sun or 136 [mW/cm²], and max power point operation. The max power point for each cell was determined using the TASC data sheet. It can be found by taking the product of current and voltage for a solar cell's IV curve as shown in Figure 7.3. Note that this curve is not derived from a TASC.

Operating at the maximum power point (MPP) of 28 [mA] and 2.19 [V], each string produces 10.95 [V] and 28 [mA] of current for a total of 306 [mW]. The maximum power output of each panel is therefore ten times this number or 3.067 [W].

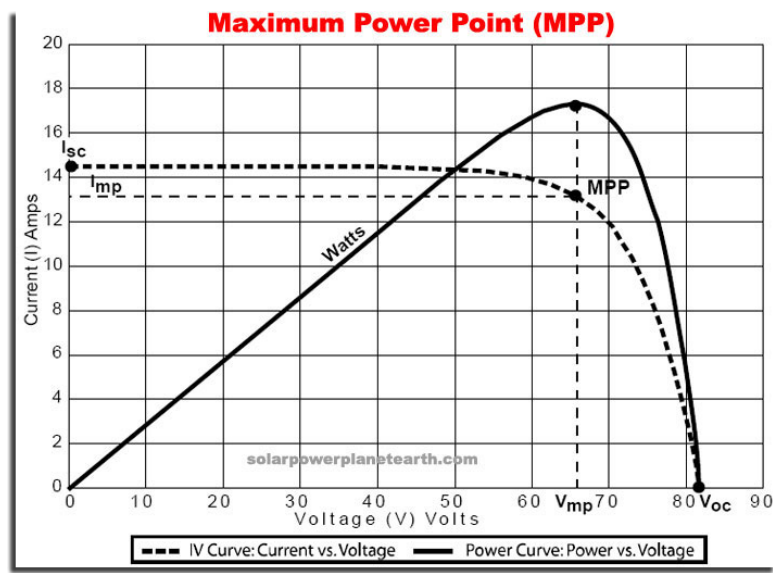


Figure 7.3: IV curve for a solar cell and maximum power point (MPP).

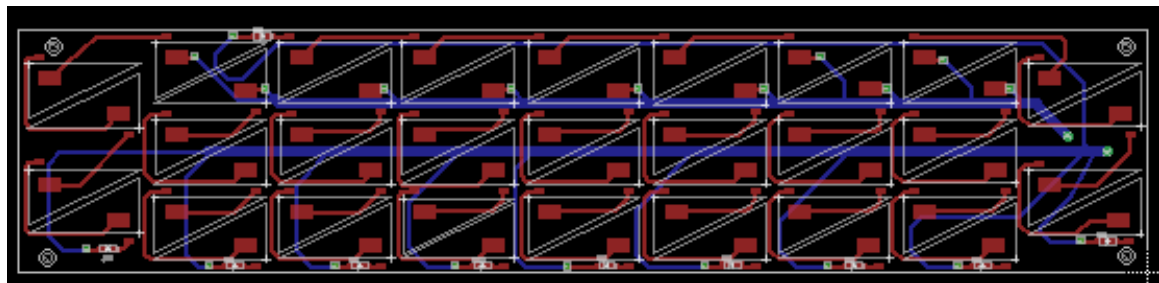


Figure 7.4: Solar panel PCB layout showing top traces in red and bottom traces in blue.

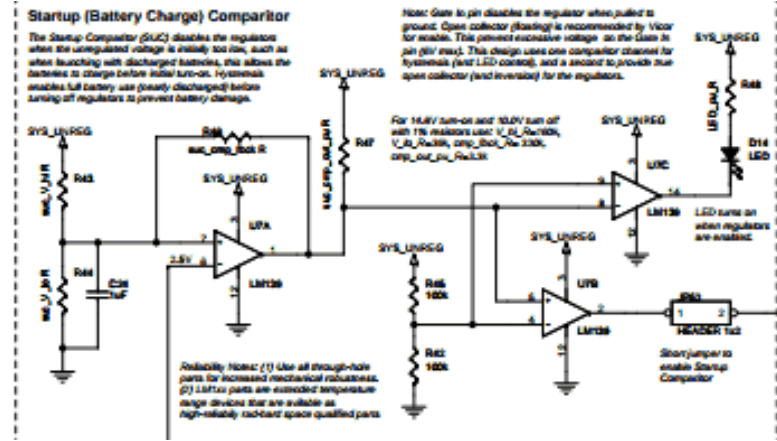


Figure 7.5: Start-up comparator circuit design.

The following assembly procedure was found in the 2012 Brown CubeSat design.³¹ First a solder mask must be created. We created our mask out of a laser cut plastic polymer. The purpose of the mask is to assist in the placement of each cell on the panel. The mask itself is the same size as the panel and contains cutouts in the shape of each cell to be placed. By placing the mask over the PCB it would be possible to place each cell in precisely the right place without having to worry about accidentally shorting two cells. EPO-TEK H20E Electrically Conductive Silver Epoxy can be used to form both the electrical and physical connection between the back end of each solar cell or the anode of the cell, and the appropriate solder pad for the cell. To place each cell a handivac should be used to prevent damage to the cells. Once the cells have been placed the anode of each cell can be soldered to the appropriate solder pad *via* 30 AWG Wires. The layout of the solar panels is shown in Figure 7.4.

7.4 Battery and Support Circuitry

The output of the battery in the UPAACN goes to the start-up comparator circuit. The purpose of the start-up comparator is to determine whether or not power should be delivered from the battery to the load. If the battery is charging for the first time, it is important that it does not deliver power to the load until it has been adequately charged. In order to accomplish this a circuit was constructed based on the 2009 designs. This design is shown in Figure 7.5.

7.5 Peak Power Tracker

In photovoltaic systems, solar panels are usually connected directly to a battery. While this configuration is simple and requires no support circuitry, it is not efficient. In order to extract the maximum available power from a solar panel, it must be operated at the maximum power point (MPP). The MPP is located at the knee of an IV curve. Unfortunately, the voltage of the battery, which is often lower than the MPP, limits the solar panel output voltage. In order to prevent power losses, a

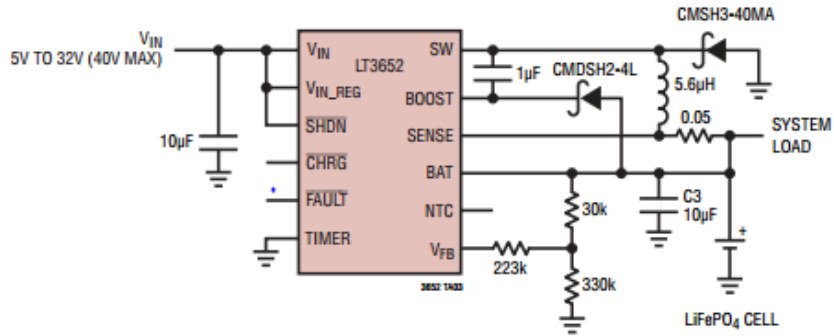


Figure 7.6: LT3652 PPT circuit design.

step-down converter is implemented between the solar array and the battery. This circuitry, known as a peak power tracker (PPT), increases system complexity, but can extract up to 20% more power from the array by operating it at the MPP.³² In a small satellite application, it is extremely important to maximize the power output of the body mounted solar array as its area is limited by the surface area of the spacecraft.

The PPT regulates the input voltage in order to get the most power out of each panel. The MPP voltage and current for the UPAACN solar array are listed in Section 7.3. The PPT also bucks this voltage to provide a regulated voltage to the battery. If the PPT was to regulate the input to that of the voltage needed by the battery, efficiency would be lost due to the power curve of the solar panels. A buck converter is used to provide maximum efficiency between the input from the panels and the input of the battery. The UPAACN EPS will use the LT3652 PPT in order to charge a 7.4 [V] battery. Unfortunately, because a battery has not been selected, the PPT designs are not definite as they depend on the battery voltage. However, we have a basic configuration as shown in Figure 7.6. Charging time and current will be adjusted based on battery input voltage specifications.

7.6 Power Board Design Updates

The power board consists of two buck converters and one boost converter in addition to the PPT and charging circuitry. The buck converters take an approximate battery input voltage of 7.4 [V] and buck to 5 and 3.3 [V]. Two non-synchronous switching converters are used to accomplish this. Both converters are exactly the same except for their inputs to the voltage sensor, which is the input to the control loop that determines the duty cycle. As $D = V_o/V_{in}$, the duty cycle for the respective buck converters is expected to vary with the input to the converter. Each buck converter uses a TPS 5450 switching chip. The circuitry for the buck converters can be seen in Figure 7.7. The boost converter uses a TPS55340 chip. The schematic for this chip is shown in Figure 7.8. Like the buck converters, the TPS55340 uses feedback to

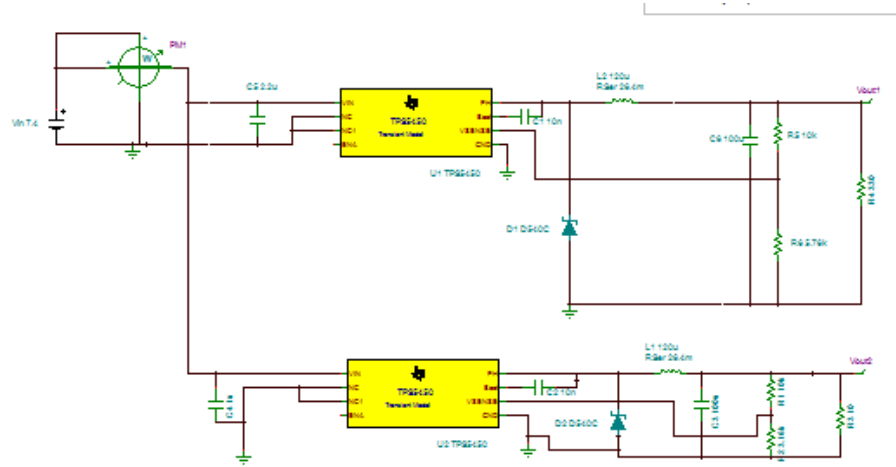


Figure 7.7: Buck converter circuitry schematic.

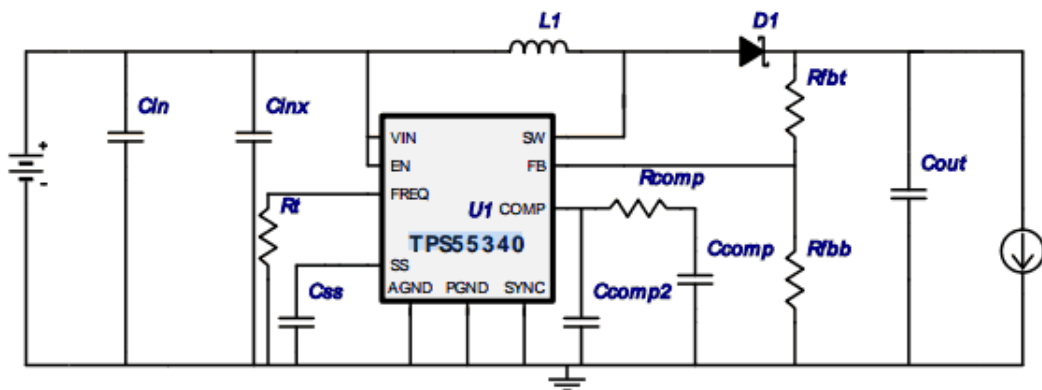


Figure 7.8: Boost converter circuitry schematic.

determine the switching duty cycle. This feature could be very important depending on battery performance.

8 Active Attitude Control System (AACS)

8.1 Purpose

The purpose of the AACS is to determine and control the orientation of the spacecraft as it orbits Earth. The AACS uses a reaction flywheel to control rotation of the spacecraft about one axis. Using the law of conservation of momentum, the AACS uses rotation of a reaction flywheel to cause rotation of the spacecraft. A nested closed loop control approach is used to achieve the desired performance of the subsystem. The inner control loop is comprised of the actuator, a brushless DC motor, and its own controller, a motor controller developed by the motor manufacturer. This control system is directly attached to the reaction flywheel. Feedback is provided by Hall effect sensors built into the motor, closing the inner control loop. The outer loop is comprised of the spacecraft, the inner control loop, and the controller implemented on the flight computers. The outer loop is closed by using a rate gyro to provide feedback. The rate gyro used on this spacecraft measures angular speed about three axes, though only one axis is used by the AACS. The AACS is able to control angular speed about one axis using this approach. This is necessary to de-spin the spacecraft, a process which counteracts the unknown angular speed of the spacecraft when it is deployed. This process is expected to take up to ten minutes.

8.2 Requirements

The AACS is an experimental proof of concept and the success of the sub-system will be defined as such. Experiments will be performed on the ground pre-launch and repeated on orbit. Performance in space will be quantified and recorded. Discrepancies that are thought to be results of the space environment will be of particular interest. Specific subsystem requirements are defined by other subsystems, RSL, and Cal Poly CubeSat requirements. The total subsystem mass is to be less than 0.5 [kg]. Total power consumption is required to be less than 5 [Whr] every fifteen minutes.

Table 8.1: Summary of AACS requirements.

Specification	Requirement	Achieved
Mass	< 0.5 [kg]	0.12 [kg]
Power	< 20 [W]	0.975 [W]
Performance	2 [RPM] de-spin	2 [RPM] de-spin within 3 minutes
Cost	< \$500	\$402.82

For performance requirements, the AACS needs to be capable of de-spinning a 3U CubeSat from 2 [RPM] on orbit in under ten minutes. Finally, the total subsystem cost needs to be under \$500. See Table 8.2 for a summary of these requirements. All physical and monetary requirements were met. The performance requirement was achieved using combinations of proportional, derivative, and integral (PID) control.

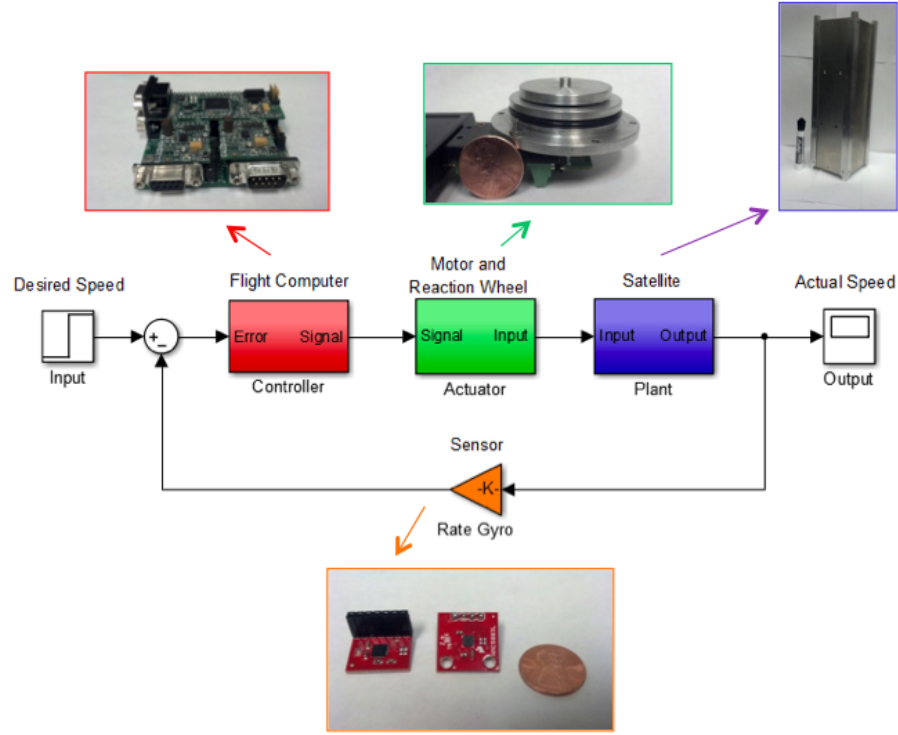


Figure 8.1: AACS architectural diagram.

8.3 System Architecture

The AACS is composed of four primary parts, just like any closed loop control system. The plant, or what is to be controlled, is the spacecraft in this case. The rate gyro sensor provides feedback to the controller about the motion of the plant. The controller, which is control code implemented on the dCDH flight computers, sends the input signal to the actuator. The actuator is composed of a brushless DC motor with an attached flywheel. The AACS architecture is shown in Figure 8.1.

The AACS is limited by the internal volume of the spacecraft and the need for a sealed container. The size of the flywheel is determined by the mass of the spacecraft. The flywheel must have enough mass so it can sufficiently affect the spacecraft's rotation, but must also be small enough to fit within the spacecraft. The flywheel mechanism is vulnerable to the space environment, so it must be encased in a sealed container. The sealed container further limits the size of the flywheel, but will ensure that the flywheel can run properly for the mission life.

8.4 Control System Design

The mechanics of rotational control using a flywheel rely upon the mass moment of inertias of the flywheel and spacecraft and the torque output of the motor. The equations of motion that govern rotational speed and position are derived from Newton's

Second Law. The equations of motion were derived in this fashion for the spacecraft and reaction wheel. These are found in Equations 8.1 and 8.2, respectively. The mass moment of inertias are denoted by I , and the angular speeds are denoted by ω . The subscripts refer to the spacecraft, s , and the reaction flywheel, f . The input torque from the motor is τ . Note that τ is negative in Equation 8.2 due to Newton's Third Law. These two equations are cross-coupled by the friction, b , that exists between the flywheel and spacecraft. These friction values are from the friction in the motor, and the friction in the bearing that pins the end of the flywheel.

$$I_s \omega_s = \tau - b(\omega_s - \omega_f) \quad (8.1)$$

$$I_f \omega_f = -\tau - b(\omega_f - \omega_s) \quad (8.2)$$

This simulation was completed using Simulink, as shown in Appendix C. The first model is for the open loop analysis of the spacecraft. The equations of motion were put in a state-space realization. A ramp input was used to simulate the torque from the motor. Realistically, the torque supplied by the motor is not constant; it will decrease as the motor speed increases. The ramp input is of a negative slope to simulate spinning the motor from standstill to full speed in ten seconds. This has inaccuracies as the motor does not gain speed linearly and was found to be a second order system. The motor dynamics will be explained later. Also, this analysis only examines one axis. The other two axes of rotation are cross-coupled, relating rotation about one axis to rotation about three axes. However, it is assumed that the forces resulting from this cross-coupling are negligible. These cross-coupled forces are too weak compared to other forces that can influence the rotation of the spacecraft.

The second Simulink model is for the closed-loop analysis of the spacecraft. In this model, the actuator, controller, and sensor are also modeled. The actuator is a second-order transfer function derived from experimental data collected from the motor and motor controller. Again, the motor dynamics will be explained later. The controller uses PID control, which will also be justified later. The sensor used here has a unity gain as its signal, which is not amplified in any way. The saturation block in this model is to simulate the loss in available torque as the motor gains speed. The speed of the flywheel used to determine the torque limits is taken from the law of conservation of momentum. This is inaccurate because friction between the flywheel and spacecraft would decrease rotational speeds over time. By adjusting the physical sizes of the simulated flywheel, the model was used to help determine what size of flywheel would fit within operating and budget constraints. By adjusting the control gains of the model, safe gain values could be found for use in an actual test of the AACCS. This allows tests to be run without damaging the motor or motor controller.

By examining these equations of motion in Simulink, it was found that a larger flywheel is capable of controlling a larger spacecraft. However, using a larger flywheel consumes more power and takes up more of the mass and volume budget. Also, a large

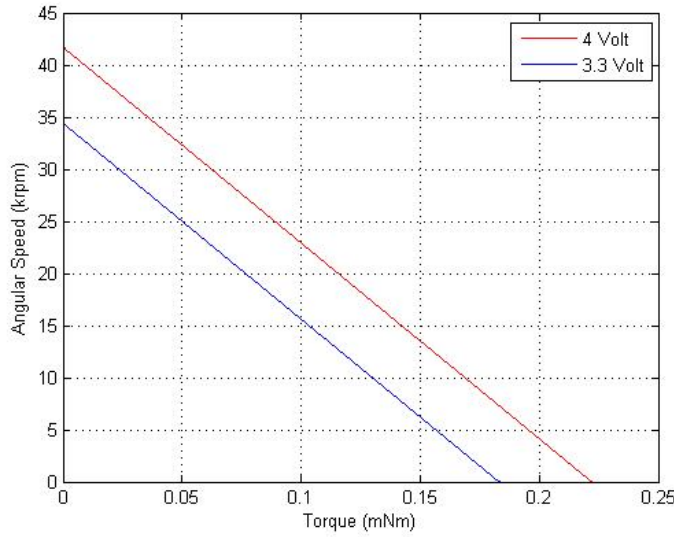


Figure 8.2: Torque and angular speed relationship for Faulhaber DC motor.

flywheel requires more torque to overcome its static friction. A small flywheel cannot affect the spacecraft quickly, but consumes little power and mass. For this subsystem, a small flywheel with a diameter of 31 [mm] and height of 3 [mm] was chosen to be well under budget and allow more mass to be used for the sealed container. A small flywheel also requires little power to spin, further keeping the subsystem below budget. However, the flywheel must be able to produce a desired angular position or rotation within a designated amount of time. The longer the AACCS takes to produce a desired output, the more power is used. Fortunately, issues regarding power can be approached with motor selection.

Several factors were considered when selecting a motor. It was first decided to use a brushless DC motor. This decision was largely based on research done in the 2010 “Nanosatellite Attitude Determination and Control” senior design project.³³ Other factors considered were power consumption, torque and the angular speed it was capable of providing. The motor’s physical configuration was also a major influence in the selection process. The 1202H004BH Brushless Flat DC Penny Motor produced by Faulhaber, seen in Appendix F, was chosen. The factors that were highly weighted in this decision were low power consumption, ability to attain high speeds, and the flat physical configuration. The model chosen also incorporated Hall effect sensors which made the motor easily controlled using a closed-loop strategy that incorporated a speed controller.

Once the motor was selected, an iterative process was used to size the flywheel. First, a steady state analysis was used to quantify the motor’s performance. Speed was related to torque, as seen in Figure 8.2, so that a target optimum operating region was defined. DC motors run more efficiently at high speeds and low torque, so a

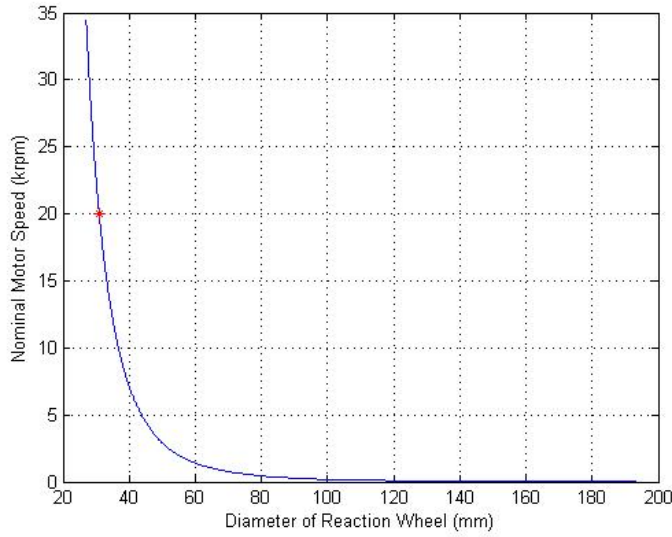


Figure 8.3: Flywheel diameter plotted against operating speeds for Faulhaber DC motor.

nominal operating speed of 20,000 [RPM] was selected. It should be noted that while the motor can operate at 4 [V], it is implemented in the AACCS at 3.3 [V].

After the desired nominal operating speed of the motor was determined, the flywheel was sized. Based upon the principle of the conservation of angular momentum, a MATLAB script, found in Appendix C, was used to calculate the diameter of the flywheel based on system properties. These parameters included angular speed of the spacecraft, mass of the spacecraft, and height of the flywheel. A flywheel diameter of 31 [mm] was chosen. As seen in Figure 8.3, a small change in flywheel diameter greatly affects the nominal operating speed of the motor. Needless to say, the system will still function while the motor is operating at different speeds, but the system should perform best at the nominal speed.

The flywheel is controlled using PID control. This form of control relates a desired output with the current output and conditions the input based on the output values. The difference between desired output and current output is referred to as the error value. PID control uses three individual terms to generate the input. The first term, proportional, is simply the error multiplied by a proportional gain, K_p . The second term, integral, is the sum of all errors multiplied by a different gain, K_i . The final term, differential, is the difference in error values multiplied by another gain, K_d . These three terms added together form the input into the actuator. This is shown in Equations 8.3 and 8.4 below. The discrete version of this is used for actual implementation in the control code, found in Appendix C.

$$u(t) = K_p e(t) + K_i \int_0^{\infty} e(t) dt + K_d \frac{de(t)}{dt} \quad (8.3)$$

$$u(t) = K_p e(t) + K_i \sum_{i=1}^n e_i(t) \Delta t + K_d \frac{e(t) - e(t - \Delta t)}{\Delta t} \quad (8.4)$$

PID control is effective at setting desired response mechanics, such as settling time and overshoot. This control is also easy to implement, and allows easier integration and coordination with the dCDH system. PID control can also be modular to accommodate different payloads. Using programs to control the gains of PID control will allow the AACCS to properly function with virtually any practical payload. These gains can also be set to change the response mechanics depending on the payload. Some applications may require little to no overshoot, while other cases will desire a short rise time at the expense of overshoot or settling time.

Optimal control is another viable option that could perform better than PID control. This kind of control attempts to minimize the energy spent achieving a good response. However, it is very difficult to implement and requires knowledge outside of the undergraduate curriculum. Other forms of control, such as lag-lead compensation or basic observer-state feedback, are also capable of functioning for the AACCS. Currently, PID control is the preferred method, as it is easily accessible and versatile enough to function for this project.

8.5 Flywheel Mechanism Design

Due to the nature of the mission, a number of considerations had to be taken into account for the physical mechanism design, and the machine design process. When making the initial decisions about design and materials at the beginning of the 2012-2013 academic year, it was decided that the AACCS would be made entirely from aluminum. The system had to be made of metal because of the outgassing constraints specified in Chapter 2. Aluminum was chosen as the best choice for this application based on a number of factors. First, compared to other materials such as steel, aluminum is somewhat cheaper and easier to machine. It is light metal, which made it a logical choice in trying to budget weight to the different subsystems. Second, in looking at many of the other projects in the RSL, aluminum is a widely used material that has proven its success in space applications.

With this decided, other design decisions had to be made. The motor selected by the AACCS subteam has lube in the motor bearings that has a TML above 1%. In other words, it will not satisfy the CubeSat Design Specifications stating that every material exposed to the space environment must have a TML of less than 1%. While there was discussion about switching to a space rated motor, because of the abilities of the motor and the volume saving form factor, it was decided to create a sealed can held at 1 [atm] to protect the motor from the space environment. To do this, a flanged cylindrical tube was designed, as seen in Appendix B, with two different lids that would be screwed down with an o-ring inside to complete the air seal. The

o-ring chosen is 3/16 [in] thick and sits in a groove in the can lids. The material is Viton Fluoroelastomer which has a TML of 0.4%.³⁴

The AACCS subteam chose to use o-rings as opposed to other sealing options for a number of reasons. One option brought up was to try to machine incredibly close tolerances and then used a press fit to seal the can. This would be difficult to repeat multiple times if the can had to be opened and closed. Additionally, aluminum, because it is a softer material, would not be able to hold the tight tolerances necessary with machining processes used. Another option explored was to use a gasket. This was abandoned in favor of the o-ring option, mostly because for a gasket, a flat surface is needed to insure a seal. Due to the machining process and the tolerances held in aluminum, the AACCS subteam was unsure if the flanged can body and the lids could be machined to meet requirements. Additionally, the o-ring option would be cheaper and easier to implement.

From the beginning of the 2012-2013 academic year, the design for the AACCS mechanism has changed in a number of different ways. From sizing changes to the sealing of the system, each decision has offered new design challenges. As stated before, the flywheel was resized based on the dynamics of the smaller spacecraft. With the smaller flywheel, the system could be reduced in size, which as a whole benefited the mission-specific portion of the project. For instance, characteristics such as power requirements, mass, and volume were all decreased. While the original mission power and mass budget had allowed for 20 [W] and 0.5 [kg] respectively, the smaller attitude control system only used 0.975 [W] and 0.12 [kg]. Unfortunately, from a machine design standpoint, because the system reduced in size, it meant that there were new design and fabrication challenges that had to be addressed.

The first assembly decision that had to be made was how to attach the flywheel to the motor. As can be seen in the specification sheet in Appendix D, the size of the motor shaft is small compared to other more robust control system mechanisms. To mount their flywheel, the 2010 “Nanosatellite Attitude Determination and Control” team used a compression technique with set screws to create a collar around the motor shaft.³⁵ Unfortunately, this method could not be reproduced by the UPAACN system. Because the motor shaft of the chosen motor is only 3 [mm] tall, it would be difficult to make a flywheel thick enough to actuate the system as well as withstand deformation forces in everyday handling and launch, while still being able to create a usable collar on the shorter shaft.

To solve this problem, a number of design alternatives were considered. The first was to use a shrink fit in which the hole in the flywheel could be expanded using heat and then fit over the esteel shaft. In practice, the hole in the flywheel would expand to a larger diameter than the shaft, and then shrink back down to size, thus attaching itself to the shaft with a snug fit. Unfortunately, this method proved not to be viable due

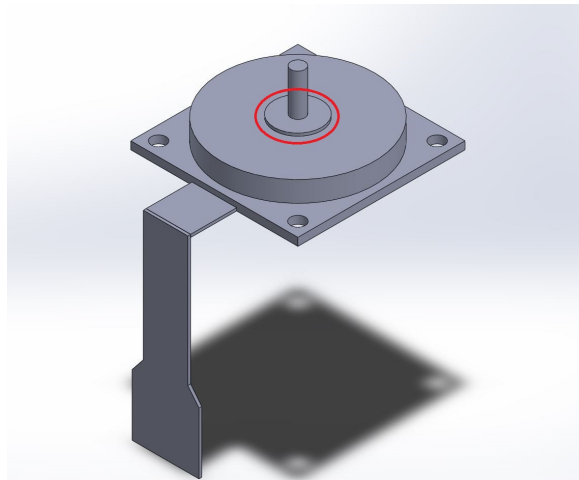


Figure 8.4: SolidWorks model of Faulhaber DC motor showing boss in red.

to the fact that the required temperature would be higher than the melting point of the aluminum.

The next option for attaching the flywheel to the motor shaft was to use a press fit in which the hole on the flywheel is the same as the shaft diameter, and the wheel is pushed onto the motor, again with a secure and snug fitting end product. The problem with this method, however, is that there would be no way to insure that the flywheel would be mounted parallel to the motor. Additionally, the force required to push the aluminum onto the steel shaft could damage the motor. The motor chosen is a flat motor that has all of its circuitry in the base. Because of this, any normal force applied to the motor risks damaging the electronics.

With these options ruled out, the last option was to use glue on the flywheel and motor shaft. To do this, a hole was drilled and reamed to be slightly larger than the diameter of the motor shaft. The flywheel then slipped easily over the motor shaft and rested parallel on a small boss protruding from the the spinning disk. This boss is shown in Figure 8.4.

Another design challenge encountered was trying to mount the motor onto the aluminum lid. The flat motor form factor meant that the motor could be mounted flat on the aluminum lid by using holes on the PCB board. One of the advantages to this is that a clamp system did not have to be implemented to hold in a cylindrical motor, as is often done. The problem that was encountered, however, again had to do with the scale of the system. Because the motor is so small relative to other motors, the mounting holes were clearance holes for an M1 screw. The issue arose as drilling and tapping M1 screw holes into aluminum on the SCU Machine Shop machines would be incredibly difficult. In the interest of staying true to the project requirement to fabricate all hardware in house, a mounting bracket was utilized, as can be seen in Figure 8.5.

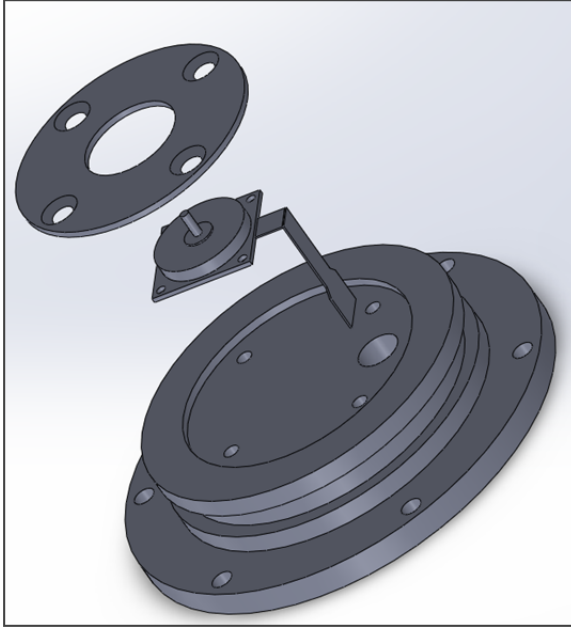


Figure 8.5: SolidWorks model of AACS bracket, DC motor, and can lid.

This bracket utilized 3/16 [in] screw holes in the lid that were more manageable to drill and tap. This configuration of mounting the motor lead to a very interesting observation. Once all the parts were machined and the motor mounted, testing began. While it was expected for the motor with no load from the flywheel on it to output about 30,000 [RPM] and draw 30 [mA] of current, this was not the case. Instead of what was expected, the motor was drawing about 120 [mA] of current, but only outputting 12,000 [RPM]. After some research it was concluded that the magnets in the motor were producing eddy currents in the conductive aluminum can lid. An eddy current is current induced by changing magnetic fields in conductors. The theory behind this concept comes from Lenz's Law, shown in Equation 8.5.

$$\varepsilon = -\frac{\delta \Phi_B}{\delta t} \quad (8.5)$$

In this equation, ε stands for the induced electromotive force which is proportional and opposite to the magnetic flux $\delta \Phi_B$. In other words, as the magnets in the motor spin, they create a magnetic field perpendicular to the spin, and so into the aluminum lid. This changing magnetic field then induces currents in the lid that opposes the direction of the magnetic field.³⁶ This opposing magnetic field then induces a sort of drag, and quickly dissipates power. In this case, because power is a function of current, the observed increase in current draw for a slower rotation speed led to the confirmation of the hypothesis that eddy currents were the problem.

To solve this problem, two different solutions were explored. The first was to eliminate the metal lid altogether. By using a low outgassing plastic as the lid material, it was issue could be solved. Due to the price of plastics like Techtron and Vespel Polyimide,

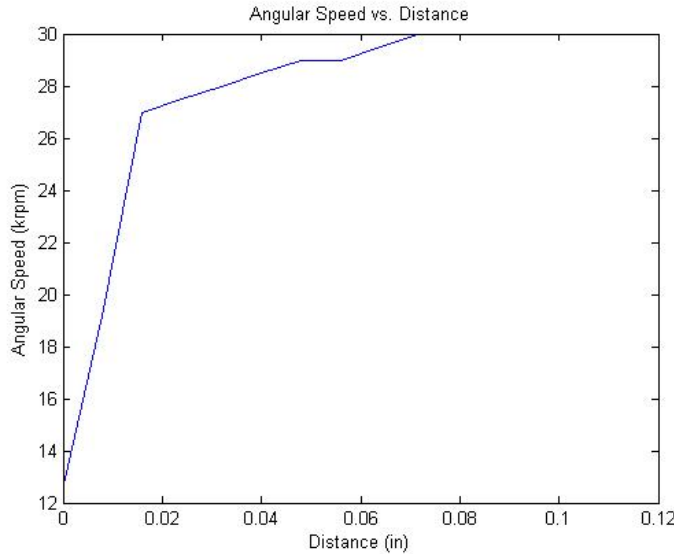


Figure 8.6: Effects of distance between motor and lid on system performance.

as well as the time left in the year, it was impractical to fabricate a new lid from these materials.³⁷

The distance between the conductor and the magnetic field greatly impacts the drag effects of eddy currents.³⁸ With this in mind, iterative tests were performed to determine the amount of spacing actually needed to dissipate the effects. Using 0.008 [in] increments, and measuring the current draw and output speed, it was found that the effects on the speed of the motor dissipated at about 0.070 [in] from the lid, but the current draw did not reach the desired 30 [mA] until about 0.120 [in] distance was reached. This behavior can be seen in Figures 8.6 and 8.7.

The AAC team decided that a plastic spacer, made of Delrin, could be a viable option. This spacer was machined and recessed into the lid. The final height was chosen to be 0.130 [in] in order to ensure that the effects from eddy currents dissipated completely.

8.6 Passive Control

While the AAC controls the spin of the spacecraft about one axis, other control strategies are used to control the other axes. Passive control using bar magnets will be employed to stabilize the spacecraft on-orbit by using the Earth's magnetic field. Passive control techniques exploit features of the space environment without drawing energy from the EPS.

Examples of other passive control strategies include mass bias, which takes advantage of gravity gradients, or use of solar pressure, which is caused by photons from the sun

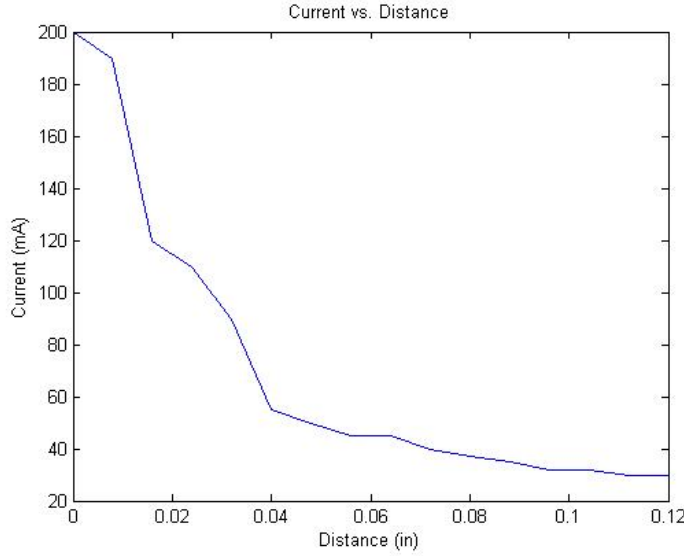


Figure 8.7: Effects of distance between motor and lid on system current draw.

hitting light and dark surfaces. For this spacecraft, bar magnets were oriented along the long axis. For this discussion, yaw is defined as the rotation about the long axis while roll and pitch are defined about the other two axes. In orbit, the bar magnets will align with the field lines of the Earth’s magnetic field, which minimize the roll and pitch of the spacecraft. Consequently, the spacecraft is free to yaw, which is the motivation for the design and development of the AACCS. As the passive control components were not the focus of this project, they are not discussed in any further detail.

8.7 Future Work

The AACCS meets requirements. In practice, it could be implemented in a more massive spacecraft as is, or could be reduced in size for the UPAACN. Should the size be reduced, it could be possible to include three of these systems to control all three axes of rotation. However, this would require further simulation to determine what sizes of flywheels would be effective for this task. As such, the model used to determine the size of the flywheel for one axis would need to be updated to accommodate three axes of control.

Another improvement would be to use a different motor that has a built-in encoder for speed control. The current motor uses digital Hall effect sensors which can only provide an estimation of rotational speed. An encoder is more accurate, so the motor speed would be smoother and provide a less noisy response. When the motor is set to operate at a fixed speed, the Hall effect sensors show that the speed fluctuates several thousand [rpm]. While the motor speed is probably fluctuating to a certain extent under steady state conditions, it is most likely not changing by a few thousand rpm

as the signal sometimes indicates.

Since the feedback from the Hall effect sensors is used to close the speed control loop, noise in the sensory signal could negatively affect performance. The noise issue, resulting in steady state error, must be addressed if the AACCS is to achieve a higher level of functionality such as angular position control. The AACCS could be used to control angular position. Orienting the spacecraft at specific angle can have uses for the unspecified payload. Any device or experiment that requires a specific level of light or the view of another object such as the sun or Earth would benefit from controlling angular position.

In terms of hardware improvements, there are a number of different areas of design reworked. The first being the wiring from the motor. The current design leaves a small hole through which the leads can leave the can to connect to the speed controller. Obviously, this defeats the purpose of a sealed can, and so the current configuration calls for a space rated epoxy to be used to seal the hole around the motor leads. While there are certain plugs that could accomplish a true seal, they were more expensive than what the team could spend. While it is not the most elegant of designs, it is effective. Space-rated epoxy is also expensive and there is a risk of ruining the subsystem during assembly. It is possible to get epoxy on the motor or reaction wheel while filling the hole. Consequently, it is justifiable to design a sealed plug in future iterations.

The second design that could be improved upon is the way that the motor and flywheel are pinned on the opposite can lid. The concern is that because the motor shaft is so small in comparison to the flywheel, the weight on the end of the shaft will act as a lever arm and could shear the motor shaft off. One design solution explored was to put a small boss on the top of the flywheel that could sit within a bearing seated in the opposite can lid. This would assume a pinned-pinned configuration without any moments being enacted on the shaft. While the AACCS team has done considerable research into suitable bearings, because of the size and performance necessary, they would be expensive and rather rare.

Another possible design improvement would be the inclusion of a pressure sensor inside the can. It would be of interest to log the pressure inside the can throughout the duration of the mission. As small pressure transducers are readily available on the market, it could be possible to incorporate one into the design. The leads could exit through the same hole as the motor leads. Regardless, the internal layout of the subsystem components would have to be reconfigured to include the sensor. Quantification of the leak rate would aid in future design. Also, it would be of interest to see if there is improved system performance if the reaction wheel was operated in a reduced air environment. In a reduced air environment, there would be less aerodynamic drag on the reaction wheel, potentially increasing motor efficiency. Nonetheless, efficiency would only be increased to a certain point. Once the can is sufficiently depressurized,

the lubrication in the subsystem's bearings would evaporate and the motor would seize. Optimizing the pressure inside the can might be a cheap and effective way to increase the performance of the subsystem.

9 Subsystem Functionality Verification and Testing (TEST)

9.1 Introduction

Satellites must undergo thorough testing before launch and deployment. As it is extremely difficult to service satellites on-orbit, these testing procedures must ensure that failure does not occur. In general, environmental testing of a new product involves examining modes of failure. This gives engineers valuable information about the behavior and shortcomings of a design. Unfortunately, satellites cannot be taken to failure during testing; the high cost of the spacecraft means that all testing is performed on the flight unit.

Strict testing requirements have been developed by NASA to ensure that satellites do not fail on-orbit. These are extremely important during the development process as failure on-orbit could damage more than just the satellite; collateral damage could include other payloads in the launch vehicle and contribute to the already dangerous amount of space debris. The testing requirements are documented in the NASA document GSFC-STD-7000.³⁹

9.2 Requirements

In addition to the GSFC-STD-7000 document, the design team must meet requirements from the CalPoly CubeSat Design Specification and from the RSL. During development, the team compiled these documents into the requirements flowdown. From here, the requirements were split into project requirements and mission requirements. These can be found in Appendix D.

9.3 Methodology

The purpose of testing the 3U CubeSat is to verify that the design has met all requirements. In the industry, special environmental chambers are constructed to simulate the launch environment. Access to these chambers is generally only given to projects with launch dates. To help increase the likelihood of using these chambers, the design team developed basic environmental testing procedures to be completed at SCU. This simultaneously allowed the team to test the platform as well as develop the testing capabilities of the RSL.

In the industry, there are several types of testing. These include vacuum testing, thermal testing, vibration testing, and acoustic testing. Functionality verification testing is also performed on the satellite components, but this varies between projects. Here at SCU, the design team performed basic thermal testing, vibration testing, and vacuum testing.

9.4 Shock and Vibration Testing

Finite element analysis is a powerful tool and offers a reliable approximation of the natural frequency for a perfect system. However, experimental verification is necessary to account for the real world launch stresses the satellite will encounter. The UPAACN was tested using two methods: impact testing and vibration table testing.

Impact testing is used to determine the natural frequency of the system by striking the satellite with a special hammer, which causes the system to vibrate at its fundamental frequency. The response of the system was measured using accelerometers. The acceleration of the system was first plotted against time, an example of one of the plots can be seen in Figure 9.1. Logarithmic decay was then used to find the natural frequency of the system. The accelerometers were placed in several different locations including the top, bottom, and center of gravity of the nanosatellite. From the plot of the acceleration versus time, the logarithmic decrement, δ , is defined as

$$\delta = \frac{1}{n} \ln \left(\frac{x_1}{x_{n-1}} \right) \quad (9.1)$$

Where n refers to the peaks of the second order response shown in Figure 9.1, x_1 is the amplitude of the first peak, and x_{n-1} is the amplitude of the peak prior to the last peak. After the logarithmic decrement was found, the damping ratio, ζ , was calculated to be:

$$\zeta = \left[1 + \frac{2\pi^2}{\delta} \right]^{-\frac{1}{2}} \quad (9.2)$$

The damping frequency, w_d , was found by taking the inverse of the period, T , of the satellite's response. From the damping frequency and damping ratio, the natural frequency was found with Equation 9.3:

$$w_n = w_d [1 - \zeta^2]^{-\frac{1}{2}} \quad (9.3)$$

The average natural frequency from the impact tests was determined to be 116.78 [Hz] with a standard deviation of 1.16 [Hz]. This result shows that the natural frequency of the satellite was above the 100 [Hz] requirement. Obviously, this data is much lower than the natural frequencies calculated *via* FEA, the lowest value being 591.55 [Hz]. This error is likely due to the experimental set-up. This test was completed using the best equipment available at SCU, which is at best an improvised version of what is completed in the industry. The experimental set-up is shown in Figure 9.2. Professional impact testing uses a special hammer that can account for its own frequency response while also measuring the natural frequency of the test components. The design team is satisfied with these results as they do meet the design requirements, but additional testing is required to further verify the natural frequency.

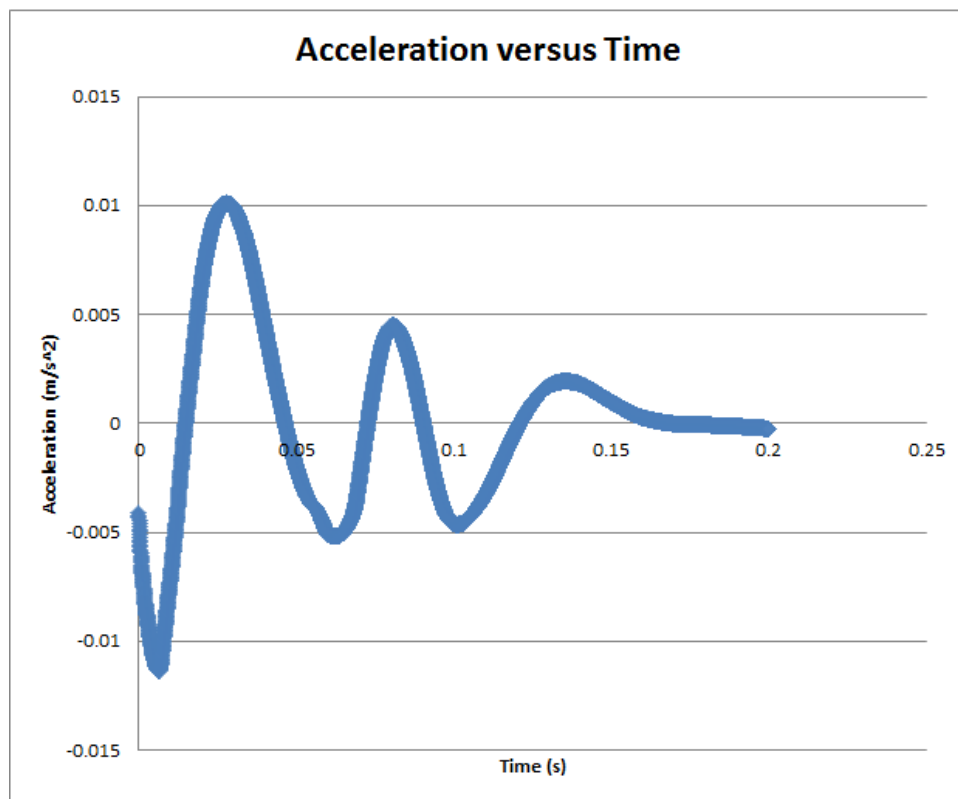


Figure 9.1: Accelerometer response to impact testing.

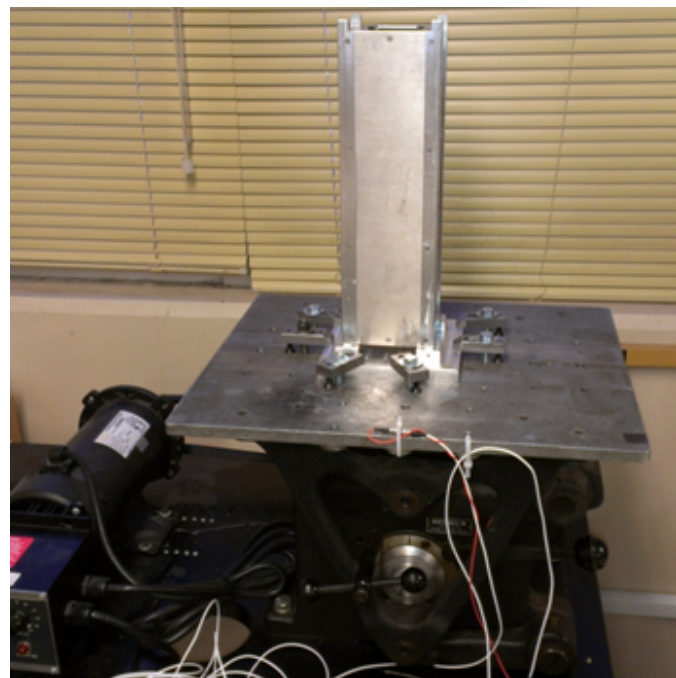


Figure 9.2: Set-up for baseline vibration table testing.

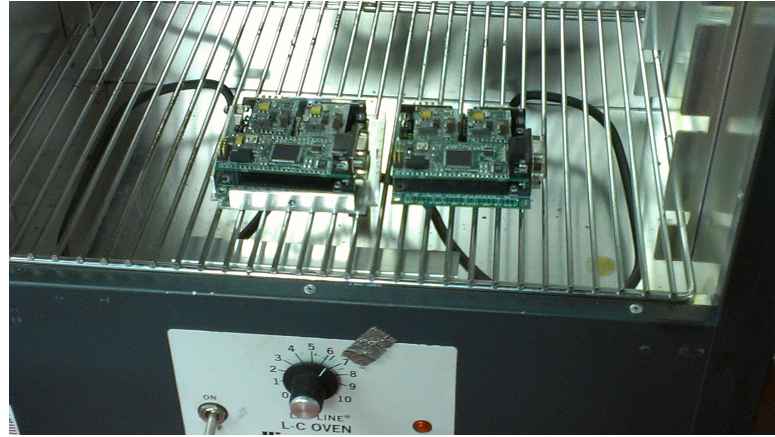


Figure 9.3: Thermal cycling experimental setup.

The second step is to complete vibration testing on a table capable of reaching 100 [Hz] or above. This still only simulates base excitation, which is simpler than what the system will experience during launch. To simulate the launch properly, the satellite will be placed within the P-Pod launcher and then placed on the vibration table. Accelerometers will be used to measure the response of the system to ensure that the amplitude does not increase significantly during any of the tested frequencies.

9.5 Thermal Cycling

Theoretical calculations and transient thermal analysis offer a reliable projection of how a system will behave on-orbit. However, there are far too many variables in real world applications that are not accounted for in calculations and computer analyses. Thermal cycling testing was completed on UPAACN components as well as on the assembled spacecraft. This simulated the on-orbit thermal environment. The only problem with this method is the mode of heat transfer; on-orbit heat will be transferred via radiation where the test uses conduction and convection. This is an acceptable trade-off for preliminary testing. The satellite health was monitored throughout the test via the beacon signal from the dCDH subsystem.

Preliminary testing was performed on the AACS mechanism in order to characterize behavior resulting from thermal cycling. Before thermal cycling tests were run, a control bump test was necessary to benchmark the system's performance. See section 9.8.1 for more details about the bump test. The preliminary tests were completed using an oven and freezer in the SCU materials lab. This setup is shown in Figures 9.3 and 9.4. These were used to simulate a 90 minute LEO orbit, where components were moved between the oven and freezer every 45 minutes. The temperatures of the oven and freezer were about 320 [K] and 250 [K], respectively.

The thermal cycle was run three times to simulate three complete orbits. The ambient temperature as well as flywheel motor temperature were measured before and after



Figure 9.4: Oven used for thermal cycling.

each cycle, as seen in Table 9.1. Because the oven and freezer used were not in a vacuum environment, condensation was observed on the test components after each cold cycle, increasing the convective coefficient. The satellite health was monitored between test cycles using a bump test to observe the control system's behavior. These tests were plotted against the control test as seen in Figure 9.5.

The results in Figure 9.5 show no significant difference between the control test and those tests run between cycles. The temperatures that UPAACN will endure on-orbit should have minimal effect on the control system's health and functionality.

9.6 Acoustic Testing

In the industry, thorough vibration testing is performed in an acoustic chamber. This chamber simulates the high intensity acoustic noise experienced by a satellite during launch.⁴⁰ Vibroacoustic testing is extremely valuable during the testing process. Unfortunately, it is not practical to reproduce this test at the university level. Therefore, the design team has forgone acoustic testing and focused on basic vibration testing.

9.7 Vacuum Testing

Aerospace companies perform thermal-vacuum tests to demonstrate a spacecraft's ability to operate in a vacuum at on-orbit temperatures. This test is extremely useful in uncovering defects and design faults. It can help the engineers observe the effects of outgassing on various spacecraft components. Outgassing occurs when volatile

Table 9.1: Thermal cycling temperature results on AACS mechanism.

Cycle	Start/End	Environment	Time [min]	Ambient Temperature [K]	Component Temperature [K]	Comments
1	Start	Hot	0	318.2	307.8	
	End		45	318.0	318.0	
	Start	Cold	45	258.0	315.0	
	End		90	258.1	261.1	Visible Condensation
2	Start	Hot	90	317.0	289.2	
	End		135	311.5	313.6	Dry
	Start	Cold	135	257.0	309.5	
	End		225	256.4	283.6	Visible Condensation
3	Start	Hot	225	305.0	287.2	
	End		315	312.0	316.3	
	Start	Cold	315	256.9	310.0	
	End		405	258.8	261.5	Visible Condensation

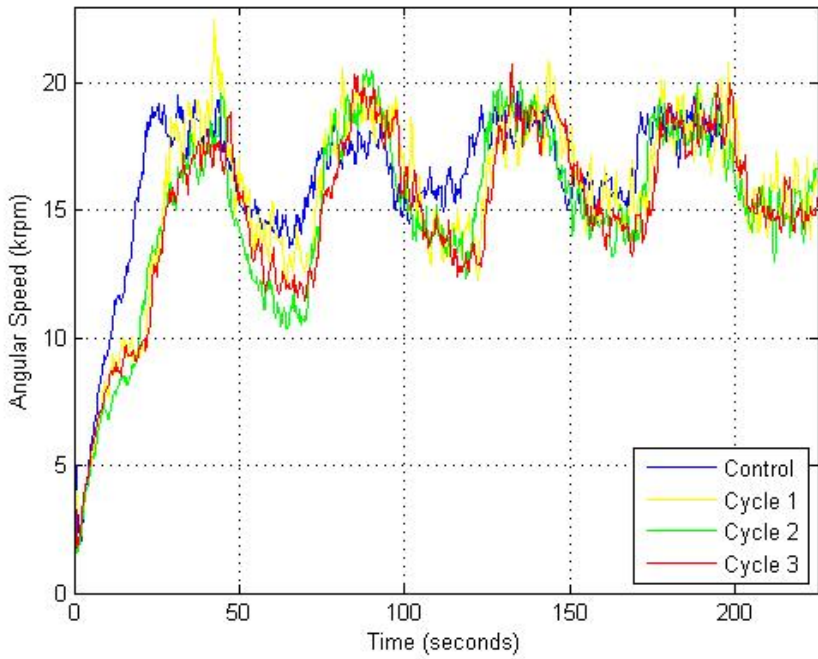


Figure 9.5: Bump test results of AACCS mechanism in between thermal cycles.

materials emanate from surfaces under vacuum conditions. This results in mass loss and material condensation on other surfaces.⁴¹ CalPoly CubeSat Design Specifications state that the total mass loss (TML) of the spacecraft must be less than 1% and the collected volatile condensable material must be less than 0.1%.⁴²

At SCU, it is not possible to complete thorough thermal-vacuum testing. However, as the AACCS mechanism is located in a sealed container, it is important that it be tested with a pressure gauge to quantify the rate at which leakage occurs. As stated in Chapter 8, the bearing lube used in the AACCS motor was a high outgassing material, requiring the use of a sealed vessel. Though a functional vacuum chamber was not available to the design team, the AACCS mechanism was subjected to a water leak test.

After sealing the system, the vessel was submerged to a depth of fifteen feet and allowed to sit for ten minutes. The system was then brought to the surface and allowed to dry before being opened. Once opened, there was no measurable evidence of leakage. The future plan for testing is to subject the system to a more robust depth test. This will be performed in the ocean at a depth of 10 [m] which will create a pressure differential of 1 [atm], which is what the system will experience on-orbit.

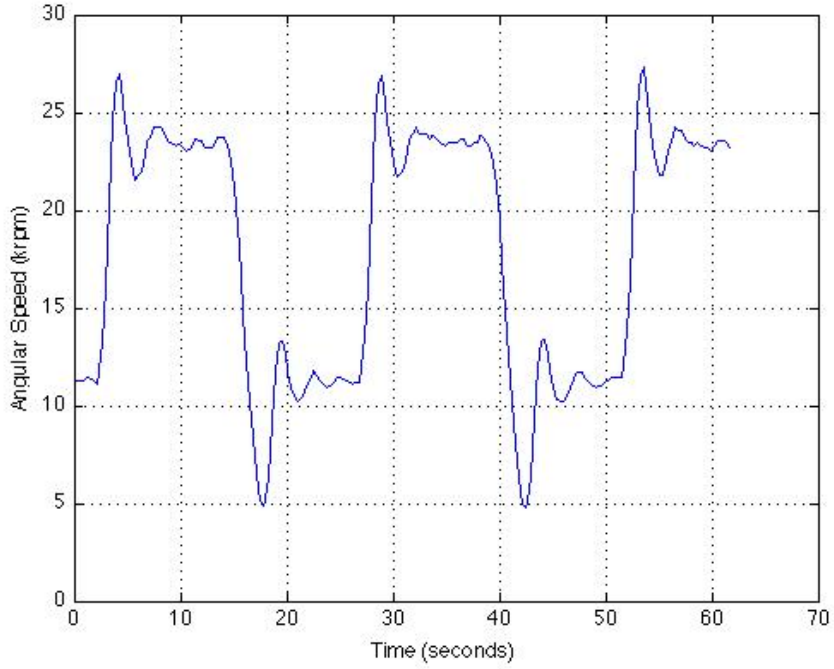


Figure 9.6: Bump test of AACS motor.

9.8 Subsystem Verification of Functionality

Before launch, it is extremely important to test all subsystems to verify functionality. This testing is completed for each separate subsystem as well as for the assembled 3U CubeSat. The goal of this testing is to prove that all systems will behave as expected on-orbit as well as to characterize any anomalous behavior. Explicit functionality verification requirements are outlined in section 2.1 of the GSFC-STD-7000 document.⁴³

The primary functionality verification tests were performed on the AACS, dCDH, COMM, and EPS subsystems. Functionality verification tests differ between subsystems; however, success criteria for these tests is given by the requirements flowdown found in Appendix D.

9.8.1 Active Attitude Control System

Testing of the AACS was conducted in two phases. First, the functionality of the actuator was tested and quantified. That information was used to make a more robust model of the entire control system. The functionality for the control system as a whole was then tested and that performance was quantified.

In order to model the dynamic response of the actuator accurately, a bump test was performed on the motor. The motor was set to run at a fixed speed and then was

provided with a step input to raise the speed. In the test, the motor started at 12,000 [rpm] and was bumped to 23,000 [rpm]. The actuator response to the step input was recorded and plotted. This response resembles a second order system, as shown in Figure 9.6.

Based on this data, response characteristics were determined. An overshoot of 15.2% and peak time of 0.168 [s] were calculated. The damping ratio, ζ , was found to be 0.514 using Equation 9.4, where % is the percent overshoot. Using the damping ratio and the peak time, T_p , the natural frequency was determined using Equation 9.5. These values were incorporated into the Simulink models to improve accuracy. The transfer function for this model is shown in Equation 9.6.

$$\zeta = \frac{-\ln (\%OS/100)}{\sqrt{\pi^2 + \ln^2 (\%OS/100)}} \quad (9.4)$$

$$\omega_n = \frac{\pi}{T_p \sqrt{1 - \zeta^2}} \quad (9.5)$$

$$G(s) = \frac{\omega_n^2}{s^2 + 2\zeta\omega_n s + \omega_n^2} \quad (9.6)$$

Luckily, comprehensive AACS testing can take place before launch. The ideal testing environment would be to suspend the UPAACN using a low-friction swivel in a vacuum. This can simulate the space environment and allows for rotation about one axis. However, this testing apparatus goes beyond the resources available at SCU, so the system was tested at ambient atmospheric pressure while hanging from a string. The testing apparatus consisted of a wooden frame with a hook used to suspend the UPAACN with fishing line. While the bus structure is suspended, the AACS is run using an Arduino microcontroller. This helped eliminate extra programming work. Ideally, the COMM infrastructure would be used to relay the angular speed from the rate gyro to a computer.

These tests were performed without a functional power system, so on-board communication could not be used. A full circle protractor was positioned beneath the satellite in order to measure angular speed. A reference point was marked on the satellite in order to prevent error from estimation. Each test used a desired angular speed of 2 [rpm]. The PID control gains were adjusted between tests in order to determine the capabilities of the system. At an interval of 5 [s], the angular position of the satellite was recorded and used to generate a table of angular speeds. These tables were used to generate graphs to determine the response characteristics for each set of gains.

Ground testing is useful when verifying functionality, but it can provide results very different than what is expected on-orbit. For instance, drag forces from the atmosphere on Earth can affect the rotation of the UPAACN during testing. These limit

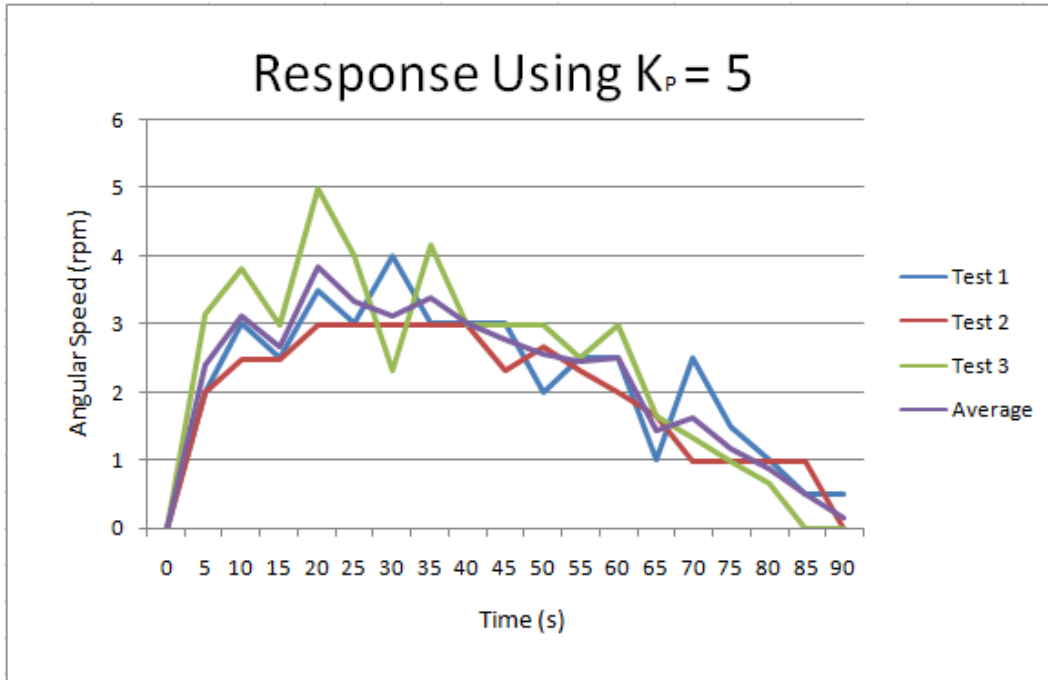


Figure 9.7: Angular speed response of UPAACN for three tests.

the total available motor torque and the damping of the response. In addition, torsion in the fishing line applies a spring force that counteracts the torque of the motor. This is avoided by suspending the satellite with a longer string.

Another shortcoming of this setup is that fishing line cannot fix the UPAACN to one axis of rotation. Environmental disturbances can cause it to swing. This was especially prevalent whenever the system was powered up for a test run. The forces from the ground environment are not insignificant, but luckily they are not strong enough to prevent testing altogether.

The first tests used only proportional control. The gains were set by the Simulink model. Beginning with a gain of 5, three tests were run to check the error associated with the testing method as well as to determine if the length of fishing line was sufficient for a two minute test. The results of these three tests, including an average of the runs, are compiled in Figure 9.7.

The results from these tests are noisy due to the poor resolution. The angular speed of the UPAACN began to diminish after 40 [s] of each test run. This is due to the torque of the fishing line. The testing apparatus could not support a string long enough to prevent this from occurring.

Similar testing was performed with the UPAACN suspended from a spiral staircase spanning 3 floors. This prevented the fishing line from tangling. Note that the average

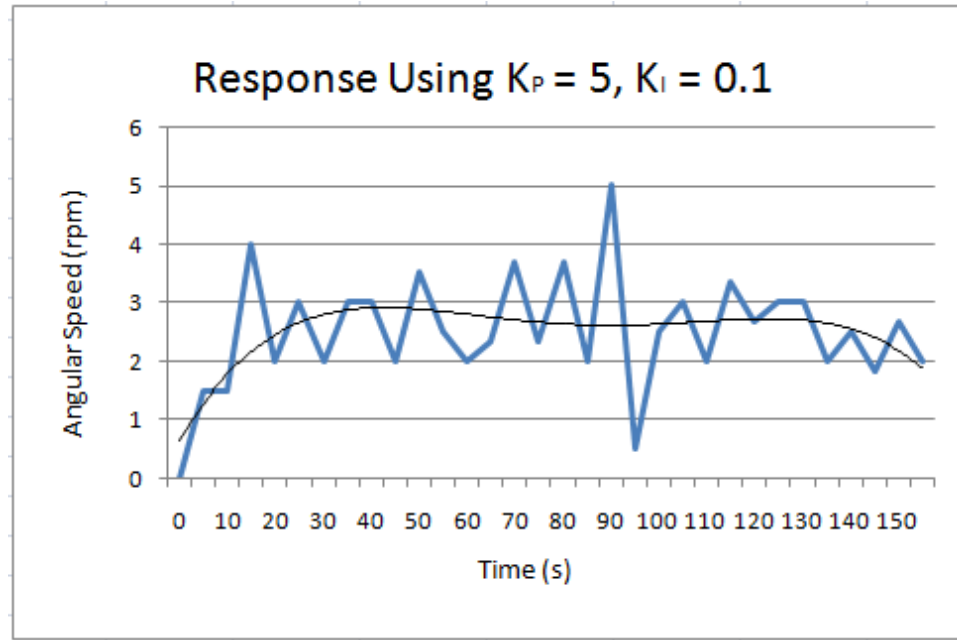


Figure 9.8: Response of AACCS from PI control.

response has a settling time between 25 and 35 [s]. This suggests that proportional control is capable of achieving steady state before the spring forces overcame the system response. The results also suggest that using only proportional control will have a steady state error. This is consistent with the theory that pure proportional control on second order closed-loop systems will involve steady state error. For practical uses, proportional control can be tuned to minimize this error at the expense of other response characteristics.

Adding integral control to proportional control can help eliminate steady state error. This is important when a tuned proportional controller may saturate its actuator in order to achieve a small steady state error. In this system, saturating the motor is detrimental as it quickly uses the available torque to control satellite spin. Integral control can overcome the steady state error while also reducing saturation time. However, using integral control will increase overshoot and settling time. These characteristics are demonstrated in Figure 9.8 which shows the response from PI control generated by the AACCS. Note the perceived steady state error and gradual decline towards the desired angular speed of 2 [rpm].

In this response curve, the overshoot is approximately 50% and the settling time is much longer than the total test time. By decreasing either the proportional or integral gains, the overshoot and settling time can be reduced. This will allow the response to be within the desired response characteristics defined in Chapter 8. Figure 9.9 shows the response curve when the proportional gain is lowered from 5 to 1.

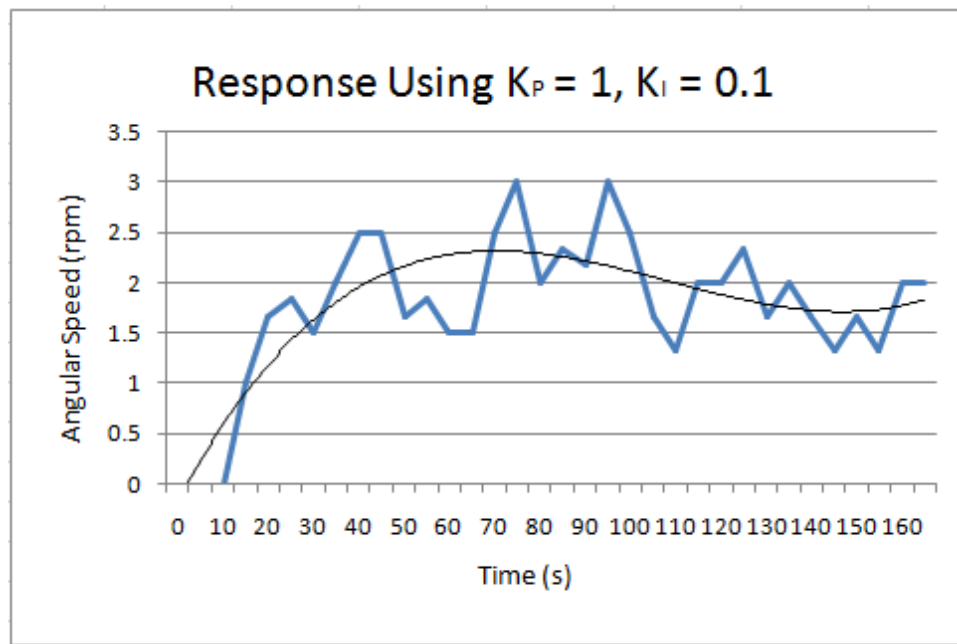


Figure 9.9: Response of AACS from PI control with lowered proportional gain.

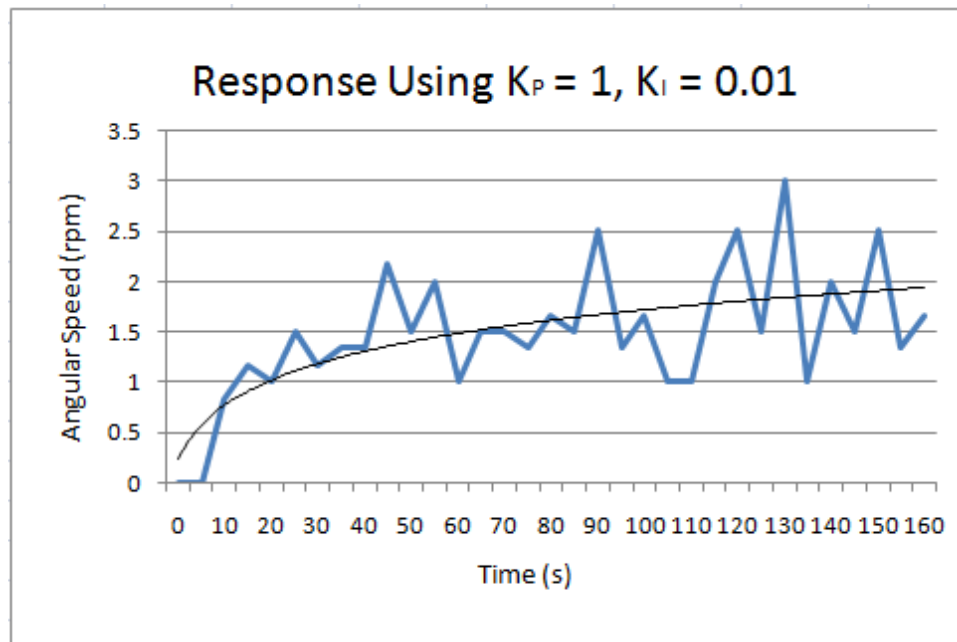


Figure 9.10: Response of AACS from PI control with lowered integral gain.

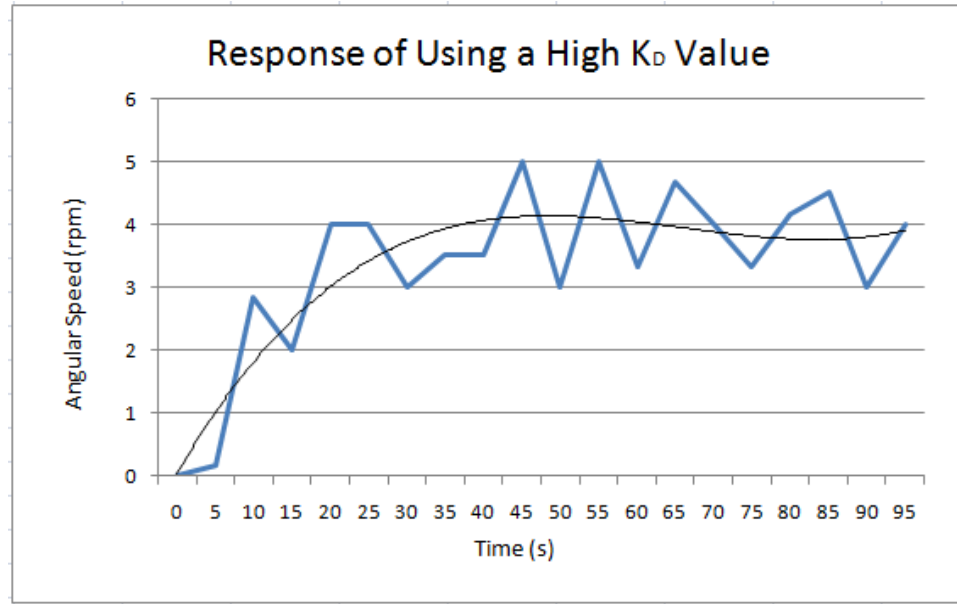


Figure 9.11: Response of AACCS with PID control.

In this response, the overshoot is now approximately 15%. However, the settling time appears to still be larger than the test time. By further tuning gains, a favorable response can be determined. Figure 9.10 is the response curve where the integral gain has been lowered from 0.1 to 0.01. In this graph, there is no overshoot or visible settling time. The best fit line for the response, however, was generated with a logarithmic function. The responses shown in Figures 9.8 and 9.9 use third order polynomials to generate best fit lines. This approach produced an unstable response when applied to the data in Figure 9.10. Third order polynomials work well for characterizing the data of short underdamped second order responses, but tend to fail for critically or overdamped second order responses. A logarithmic best fit line is more appropriate for a response in which there is no significant overshoot or settling time. This response is ideal for this application because overshoot and steady state error are undesirable. This suggests that a proportional gain of 1 and an integral gain of 0.01 generate a response that meets design requirements. One shortcoming of this is that the response has a high rise time. Although it still meets the design requirements, it could be further improved by introducing derivative control.

Derivative control is capable of reducing overshoot and settling time. Proportional and integral control can reduce rise time at the expense of increasing overshoot and settling time. While derivative control cannot technically reduce rise time, it can reduce the overshoot and settling time incurred by increasing proportional and integral control. In this way, derivative control mitigates the weaknesses of proportional and integral control. However, too much derivative control can cause a response to be overdamped with an apparent steady-state error. This is shown in Figure 9.11.

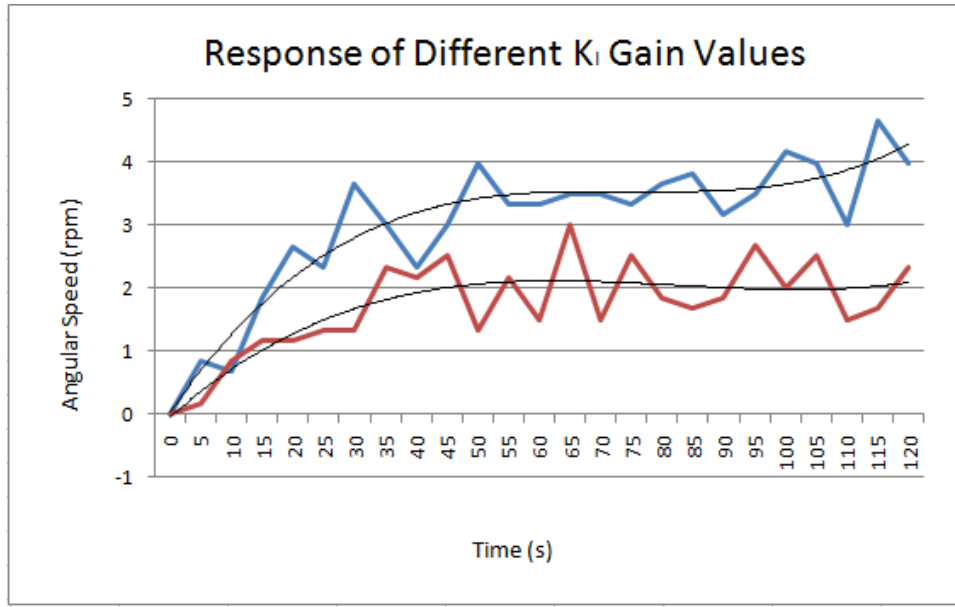


Figure 9.12: Response of AACCS from different integral gains; 0.1 is in blue and 0.001 is in red.

The response shown used a proportional gain of 1, a derivative gain of 0.5, and an integral gain of 0.1. The derivative gain is too high at half the proportional gain value. While it may appear that there is a steady-state error, the integral gain will eventually cause the response to match the desired value. These gains were still successful in reducing the rise time, as it has been reduced from over 2 minutes to approximately 10 seconds. However, this is a case in which the gains are producing a response well outside the design requirements. By reducing the derivative gain, a better response may be produced. Figure 9.12 shows this response as the blue line.

While the blue response uses a much smaller derivative gain than in Figure 9.11, the responsive still has an excessive overshoot and settling time. The red response uses a significantly smaller integral gain of 0.001. This response has a desirable short rise time, though it has some unwanted overshoot. With further tuning, a response with a similar rise time and favorable overshoot could be generated. This red response successfully shows that Proportional-Integral-Derivative control is effective for the satellite. However, there are multiple sets of gains that can generate a desired response. Changing the proportional gain instead of the integral gain could also work. In Figure 9.13, two sets of gains using different proportional values are compared. For both responses, the differential gain value is 0.1 and the integral gain value is 0.01.

These responses use an integral gain higher than in Figure 9.12. Note that the blue response in this graph is a less excessive version of the blue response in Figure 9.12. By changing the proportional gain to only 0.8, a 20% decrease, the response changes dramatically. The response no longer reaches the desired value before it peaks, meaning it has an undesirable rise time. While a proportional gain of 0.8 does

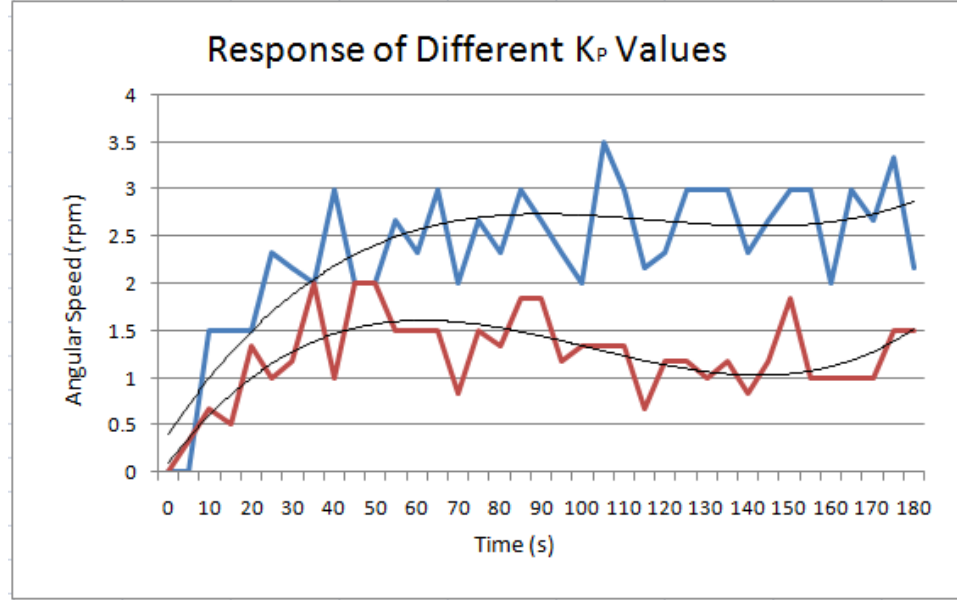


Figure 9.13: Response for proportional gains of 1 in blue and 0.8 in red.

not meet the design requirements, it shows that a properly tuned proportional gain can also generate a favorable response. Should the response peak near the desired value, it is expected that the response will be within or near the design requirements like the red response in Figure 9.12. With additional tuning, more sets of gains could be found to fit within the specified design requirements. These tests have shown that the AACCS is an effective controller that can meet the design requirements set for the satellite.

9.8.2 Distributed Command and Data Handling (dCDH) and Communications (COMM)

To verify dCDH and COMM functionality, each component was tested individually. For these subsystems, there are five main processes: COMM, beacon (BCN), Dallas-Master (DMS), scheduler (SCH), and expert (EXP). Unit testing was needed in order to verify each process separately. The test cases for each of these processes are shown below.

1. COMM

- (a) Verify communication *via* computer over serial port.
- (b) Verify communication from COMM to other boards.
- (c) Verify communication from COMM to computer wirelessly.

2. BCN

- (a) Verify that BCN is sending packets over the correct frequency.

- (b) Verify that packets are received over the HAM radio.
- (c) Verify that packets can be constructed from data given by other units (for example, temperature and current from DMS and EXP).

3. DMS

- (a) Test operating conditions of over- and under-current
- (b) Test operational temperature range.
- (c) Verify that DMS will automatically turn on if there is power.

4. SCH

- (a) Verify that schedules are ran at the proper time.

5. EXP

- (a) Verify that a rule can be created.
- (b) Verify that a variable can be added.
- (c) Verify that a variable can be changed.
- (d) Verify that the EXP rules can be turned on and off.
- (e) Test what happens when the board loses power.

Once unit testing was complete, components were tested together. This helped the team verify that the processes were functioning over the hardware interfaces. This phase required the most in-depth testing as it had to cover all use cases while ensuring that the system is error-free.

First, DMS and BCN were tested together to verify that they could communicate directly through serial. SCH and EXP were then similarly tested. Once full dCDH functionality was verified, COMM was tested by directly connecting to the COMM AVR-SAT board and verifying that commands were received and executed. Finally, wireless testing of the MHX2420 transmitter board was completed. This was carried out by verifying the board could send and receive commands wirelessly and execute commands correctly.

Previously, the system architecture had BCN and COMM on the same AVR-SAT board. During testing, this created a memory overlap. This occurred when the BCN was collecting and broadcasting data while COMM was sending or receiving data/commands. There were two solutions to this problem: add external memory or change the system architecture. As adding external memory would increase system complexity, the design was changed so that COMM ran on its own board while BCN was integrated with DMS, SCH, and EXP.

9.8.3 Electronic Power System (EPS)

The primary source of power generation for the 3U CubeSat platform comes from Triangular Advanced Solar Cells (TASC) which are made from gallium-arsenide on a germanium substrate. These cells are designed for high power aerospace applications. The manufacturer recommends that two solar cells can be arranged within an approximate rectangular area of 1.55 x 3.18 [cm] with a cell of gap of 0.046 [cm]. These solar cells were chosen over more conventional silicon cells due to their voltage output, efficiency, and antireflective coating. The TASC cells deliver four times greater voltage than silicon cells; i.e., one TASC cell can generate the same voltage as four silicon cells in series. Additionally, the TASC cells are twice as efficient as the silicon, therefore they deliver more than twice the power from the same area. Lastly, these cells have a built in multi-layer which provides low reflectance over the wavelength range of 0.3 to 1.8 [μm].

Mechanically, the power team decided to attach the solar cells on a printed circuit board (PCB) as shown in Figure 7.4. This approach helps maintain the electronic circuit characteristics without introducing parasite capacitance. With proper circuit board design, component wiring and assembly can be manufactured by a PCB printing company. These PCBs offer uniformity of electrical characteristics, simplified component identification and equipment maintenance, and reduced inspection time. The printing process eliminates the possibility of error during assembly and therefore prevents miswiring and shorts.

The board design placed the triangular cells in rectangular pairs in order to maximize space, as shown in Figure 7.4. Each rectangular area was 17.4 x 31.8 [mm], which complies with the manufacturer's recommendations. This orientation is oversized in the x-axis by 12.25% in order to compensate for possible errors during fabrication and assembly. The design accommodates 25 pairs of solar cells (50 total) per panel, which could ideally provide an output of 10.95 [V] at 280 [mA] with an estimate of 3.07 [W]. The top layer routes are 0.76 [mm] and the bottom are 2.54 [mm], which gives enough physical space for electrons to move through the board without causing it to overheat or damage the routes. The board also includes four drill holes (4.49 [mm] diameter) to attach the panels to the bus structure structure.

The board layout includes Schottky diodes, which have a small voltage drop between 0.15 to 0.45 [V]. This provides the circuit with a higher switching speed and minimizes unused voltage. The diodes are capable of blocking up to 30 [V]. This prevents one string of solar cells at a higher voltage from forcing the current to flow towards a lower potential string.

The power board holds the regulators and voltage converters. It receives input from the solar array and is capable of outputting three different bus voltages: 3.3, 5, and 12 [V]. The power board is also responsible for charging the battery, as detailed in Figure 7.5.

The startup comparator schematic used to charge up the battery was tested using comparators (LM139), two DC power sources, and an oscilloscope. After tests, the circuit had to be modified as each comparator has an open voltage collector. This means a pull-up resistor is needed in the output of node 2. After adding a 10 [$k\Omega$] resistor connected to the unregulated bus in parallel with the JP52 Header 1x2, the results on node 2 showed that the circuit has a turn on voltage of 8.85 [V] and a 5.9 [V] turn off point with a reference voltage of 2.5 [V].

Both the 3.3 and 5 [V] regulators feed into a package with a PowerPad at the bottom of the case. This PowerPad would have to be grounded in order to turn on the IC. This means customized PCBs would be required or special tools (not available at SCU) would have to be used. In order to save resources, the EPS team decided to perform SPICE simulations.

Simulations were run for the comparators and buck converters. For the buck simulations, TINA spice was used on a TPS5450 chip from a 7.4 [V] input. In the setup, two buck converters were created and a voltage analysis was taken at the output of each. For the first buck, an output voltage of 3.3 [V] was created. The settling time was 8.1 [ms], and had a peak overshoot of 80 [mV]. The transient analysis showed that during the first 0.53 [ms], there was little activity at the output, which was a steady 1.05 [mV]. The Vout quickly began to ramp up before it settled to a constant rate of increase, finally settling at its 3.3 [V] output. For the second buck converter, an output of 5 [V] was achieved. The settling time was also 8.1 [ms], however, there was a peak overshoot of 150 [mV]. This was expected as $\frac{dV}{dt}$ was higher for this converter as it climbed to a higher voltage in the same time period as the 3.3 [V] converter. The initial rise in voltage also occurred at 0.53 [ms].

For the the startup comparator, all simulations were run on LT SPICE. The comparator circuit as seen above was simulated using an LM139 chip. From this simulation, it was determined that there was a turn on voltage of 15 [V] and a turn off voltage of 9.75 [V]. However, this was not compatible with system requirements. Therefore, the values were adjusted in the input voltage divider so that a turn on voltage of 7 [V] and a turn off voltage of 5 [V] was achieved.

10 Business Plan and Cost Analysis

10.1 Introduction

Traditionally, the nanosatellite industry has revolved around NASA and its subsidiaries. Launch opportunities are highly regulated, and as stated in previous chapters, difficult to obtain without the proper connections. Luckily, the success of aerospace start-ups such as Space-X is changing the industry for the better. Investors are increasingly interested in similar ventures, and NASA is attempting to facilitate the process.

There are several successful nanosatellite companies, such as Pumpkin Inc. As stated in Chapter 1, Pumpkin has developed a platform similar to the design team's CubeSat, but at a much higher cost. Several other start-ups are attempting to meet the pre-fabricated CubeSat demand, so it is obvious that this is a growing industry.

10.2 Goals and Objectives

The goal of the team is to use the 3U CubeSat platform as an educational tool for universities and as a low-cost alternative for start-ups. The 3U CubeSat platform will be marketed as accessible and easy to customize rather than compete directly with Pumpkin Inc. As a comparison, the difference between each product is similar to that of the Basic Stamp and an Arduino board.

The previous design team did not believe that their CubeSat was commercially viable because the nanosatellite market was too small at the time. Just a year later, the team now believes that there is significant demand for an accessible 3U CubeSat platform. Regardless, the purpose of the platform is primarily educational. Business plans would start at the university level, and if there is significant interest from the industry, then expansion would be considered.

10.3 Product Description

The 3U CubeSat platform is a viable option for university space programs interested in producing a functioning nanosatellite. While the previous design team produced several iterations of their designs, the current team has focused on the 3U form factor.

The structural design is comprised of four major components: corner brackets, side faces, and a top face, and a bottom face. These parts are attached using undercut screws and locknuts. In addition to the bus structure, there are cross brackets for mounting internal components. This design meets all CubeSat Design Specifications. All parts are fabricated on a standard milling machine, making it easy to customize each part. The assembled bus is shown in Figure 10.1.

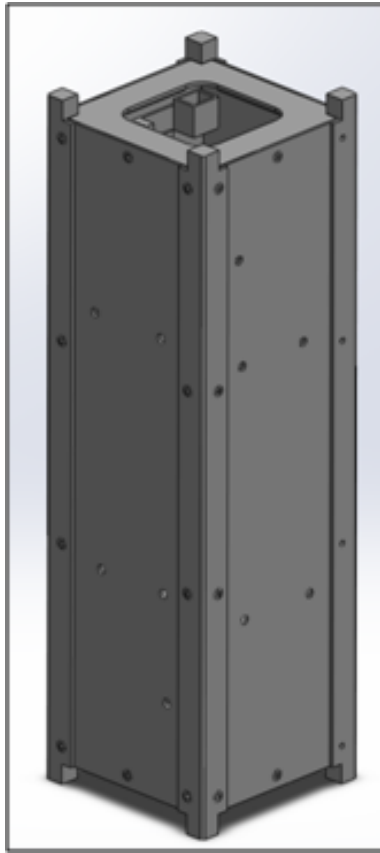


Figure 10.1: Assembled bus structure for 3U CubeSat platform.

In addition to the structure, the 3U platform will offer a distributed command and data handling flight computing system and a power regulator board. These are designed to fit inside of the bus structure and can be stacked vertically, therefore saving space. The flight computing system also handles communications through a HAM radio beacon and an S-Band transmitter.

Optionally, the 3U CubeSat platform can include the active attitude control system mechanism in order to offer basic pointing capabilities. This system can control the position and rotation of the spacecraft about its long axis. It will be stabilized through the use of passive magnets that work with the Earth's magnetic field.

10.4 Potential Market

As previously mentioned, the primary market is educational institutions wishing to develop their nanosatellite programs. This will potentially allow these institutions to complete experiments and research on-orbit while minimizing the design cycle and cost. The 3U CubeSat platform will also be marketed to start-ups for similar applications.

Pumpkin Inc., via CubeSat Kit, markets its products to start-ups as well, but its use of complex manufacturing processes increases the overall cost. For Pumpkin, this will only payoff once sales surpass the initial investment. While previously this was seen as a risky venture, this has been offset by increased demand. This is a good time to attempt to break into the prefabricated nanosatellite market.

It should be noted that the low cost of the 3U CubeSat platform is partially due to student labor, which for the purpose of the project is free. The team has assumed that potential customers will have basic machining capabilities. Industry labor will obviously increase the overall cost of the platform, however the value offered via its ease of customization should offset this.

10.5 Manufacturing

The 3U CubeSat platform can be manufactured on a standard milling machine. Reusable fixtures are used to manufacture the bus structure. Aluminum 6061 is used for all bus structure components. The manufacturing process is simple enough such that university students trained to work in a machine shop can complete it. Realistically, this process fits best at the university level, hence why the primary market is educational institutions. The same process can be used in the industry, however, trained machinists will decrease manufacturing time and increase cost.

10.6 Cost Analysis

The total cost of the 3U CubeSat platform bus structure is about \$500. This includes the cost of tooling, raw materials, and fixtures. However, once fixtures and tooling are procured, the cost of machining multiple bus structures is about \$100 a piece. As a comparison, the Pumpkin 3U structure is about \$10,000. It should be noted that the other subsystems offered with the platform will increase the overall cost. Reusing the manufacturing fixtures designed by 2011-2012 nanosatellite also helped reduce cost. The nanosatellite must still undergo rigorous testing and meet certain standards for handling before it can be considered flight ready. Both of these will add significant costs. The specific costs are further detailed in Appendix F.

10.7 Financial Outlook

The primary market for the 3U CubeSat platform is educational institutions. Success of the project hinges upon accessibility, therefore, future financials depend on outside donations and grants. Luckily, this money can be applied in other areas as the cost of machining the platform at a university is low. Future funding depends on adapting the platform to developing needs.

11 Engineering Standards and Constraints

11.1 Sustainability

It is well known that the proliferation of satellite technology has led to a high level of debris orbiting Earth. Similar to air pollution, this is an issue that will lead to dire consequences if action is not taken. Fundamentally, this is a sustainability issue. If space debris is not curbed, it will become impossible to launch and operate spacecraft. This is known as Kessler Syndrome. It refers to the exponential increase in space debris due to collisions and erosion of existing spacecraft to the point at which it becomes impossible to safely operate new satellites.⁴⁴

There are several ways to avoid Kessler Syndrome. The easiest means of prevention is to follow all design specifications given by NASA and other space agencies as they are designed to limit on-orbit decay of spacecraft. These requirements also specify that rigorous testing must occur to verify that the spacecraft will survive the launch environment.⁴⁵ In addition to following correct procedure during the design cycle, there are several solutions actively being pursued by NASA as means to limit space debris. Typically this involves re-entry of old spacecraft from orbital decay or boosting these satellites into a graveyard orbit. In addition, there are some satellite based methods of debris retrieval in development.

About 19,000 pieces of debris larger than 5 [cm] are currently being tracked by NASA. It is estimated that another 300,000 pieces smaller than 1 [cm] are currently orbiting below 2000 [km] altitude.⁴⁶ This debris is most highly concentrated at about 800 [km] altitude, or near geosynchronous orbit (GEO).⁴⁷ This is likely because GEO orbits are popular for large communication satellites, but these orbits take extremely long to decay. There is still significant debris in LEO, and even though it decays relatively quickly compared to GEO, it is a threat to many spacecraft, including the ISS. In fact, just recently a piece of debris penetrated one of the solar arrays of the ISS. We hope to avoid contributing to this problem by properly following all CubeSat Design Specifications as well as any other requirements given by NASA. This will help ensure that UPAACN will survive the launch environment and will not decay on-orbit.

11.2 Economics

The project has a success criteria in reducing the cost to manufacture the satellite. Machining the components in the Santa Clara University's machine shop and creating in-house testbeds will significantly reduce the satellite's total cost. All the labor will be completed by students so that this cost will be minimized. While utilizing these resources will reduce the cost, some components will need to be purchased because they can not be manufactured at the university level.

Our team successfully lowered the total cost of producing a satellite. The UPAACN nanosatellite can be produced at approximate \$2,000 whereas most satellites of a

similar size will cost approximately \$10,000 or more to produce. We hope that this will make the technology more accessible to newcomers to the space industry, including universities and start-ups. Since the cost is significantly lowered, hopefully more people will be exposed to the technology, hopefully making a beneficial impact on the space industry.

11.3 Manufacturability

The manufacturability of the UPAACN nanosatellite project was designed to improve both the social and environmental impacts. The project was designed to make the nanosatellite able to be built cheaper, rapidly, and at an university level. This aspect of the design creates a huge social impact. It allows college students to get hands-on experience with building a satellite, and allows them to create or expand their very own projects. This gives rise to more research to be done at a university level, which, in turn, can lead to more students becoming interested in the aerospace field and ultimately more research to be done in and about the space environment. This research could create more improvements for technology which will impact society as a whole.

The manufacturability of the UPAACN nanosatellite project was also designed to have solid side faces. These solid side faces, which are used for more mounting capabilities, allow about 20% more material in the exterior frame to be in use where in most nanosatellites the sides would be cut-out. This value was determined by an exterior frame mass of 0.4 [kg], which is the mass of the 2012 3U CubeSat exteriors with cut-out sides, compared to the UPAACN design which has an exterior mass of 0.5 [kg]. Of the 20% of the material (aluminum) that is cut out, even if it is used to be recycle not all of the aluminum scraps can be recycled for it is often mixed in scraps of other metals and plastic from the machine shops. This will have an environmental impact because it will prevent less aluminum waste to go into the environment.

11.4 Ethics

The UPAACN is a project that may use private information from NASA. This private information includes intellectual property and other sensitive details. It is unethical to share this information with any person or organization outside of this project. This information could cause damage to NASA or become a threat to national security, and as such, must be protected. To do so, all private information is kept within the RSL. This lab is only open to members of this project. There is also an off campus location where a cleanroom is maintained to store and test components of the spacecraft. This cleanroom is also only accessible to members of the project. By keeping all information and work on this project contained in private locations, the information from NASA can be kept safe.

11.5 Political

While one might not think of politics when discussing a satellite, in recent years politics has found its way into aerospace discussions. In the last year alone, President Obama and the U.S. government have cut NASA's budget by over 20%. This is due to several reasons, including the sequester, the national debt, but most notable the fact that the government and the general public do not place enough importance in space research and education. In the past there has been much excitement in terms of learning about and sending missions to space. In recent years, however, people have begun to view this kind of work as superfluous and unnecessary when there are other more pressing issues.

Among the hardest hit departments in NASA are the Mars exploration as well as the educational departments. The first mentioned has the potential to make history, and yet a large amount of funding has been taken away from it and allocated elsewhere. Space industry has always been at the forefront of innovation, and by cutting funding, the risk is that some of these inventions will never see the public light. Inventions like water filters, Velcro, and infrared thermometers all began at NASA. Cutting funding to the sciences like the space industry will only inhibit innovation.

In terms of education, NASA has always worked to educate employees as students, and chosen to instill an excitement for aerospace in them. Without the proper funding, however, it becomes difficult to impart the same enthusiasm. This is where nanosatellites are useful. This project allows for a general payload system that is easy and cheap to manufacture and assemble ($\sim \$5,000$ vs $\sim \$50,000$). It can be used by future students as a platform for experimentation or as a starting point for future innovation. While NASA will continue to be the leader in space research and applications in the U.S., with the government cutting spending, it is only natural that other projects will arise to help bridge the gap left by the lack of funds.

12 Conclusion

12.1 Summary

The objective of this project was to develop a 3U CubeSat platform capable of supporting short duration technology verification experiments in LEO while providing valuable experience to university students. The project made use of existing technologies within the RSL. This design methodology allows for easy customization, minimizes cost, and shortens the design cycle for future CubeSat projects. This platform can be manufactured at the university level and is capable of supporting student projects. Along with the platform, the satellite development capabilities of the RSL have been improved through the use of various testbeds and methods of analysis.

The 3U CubeSat platform has several major subsystems. The bus structure is an updated design based on the work completed by the 2011-12 design team. The flight computing is handled by the dCDH and COMM subsystems, which make use of RSL flight computers. The EPS was updated based on a previous RSL power board and solar panel design which now includes a PPT system. Basic attitude control capabilities are provided by the AACS mechanism, another RSL project. This platform was prototyped; the resulting CubeSat is called the UPAACN. It was assembled in the RSL cleanroom at NASA Ames.

To ensure that all requirements were met, especially the CubeSat Design Specifications, the SYST subteam provided necessary documentation and completed management tasks. Thermal analysis was completed using the SatTherm MATLAB package. This tool is also available to future CubeSat design teams at SCU. Finite element analysis was completed on the updated bus structure to ensure that the natural frequency was above 100 [Hz].

Several baseline tests were completed on the UPAACN and its subsystems. Vibration testing was completed on the SCU vibe table to ensure resonance did not occur. Impact testing was also performed on the empty structure as well as on the assembled CubeSat. Thermal cycling was performed on the electronic components. This was done by moving the components between an oven and a freezer in the SCU materials lab. This process simulated the thermal environment experience by satellites in LEO. Vacuum testing was completed on the AACS mechanism to ensure that air did not leak from the sealed vessel. Once integrated into the UPAACN, the AACS mechanism functionality was tested via a spin test. These procedures and their results are compiled here for use by future design teams.

12.2 Lessons Learned

During the project, the design team learned many valuable lessons about the design process, project management, and working in the aerospace industry. This began with becoming familiar with the CubeSat Design Specifications as well as all general

requirements for satellites. These constraints helped the team formulate and understand the engineering problems present when designing and fabricating a satellite.

The most valuable lessons came from learning the processes commonly used in the industry. It was fascinating to discover the issues that arise on-orbit due to the extreme environment of space. From a management perspective, it was interesting to learn how systems engineers manage a design team while maintaining a thorough understanding of the technical underpinnings, which is something not found outside the aerospace industry. The approach to analysis and testing is also very unique. The team enjoyed balancing redundancy with design and fabrication constraints. During the machining process, the mechanical engineering team members developed their knowledge of design for manufacturability.

Overall, the team believes that this project has helped its members prepare for careers in the aerospace industry. It has provided the team with valuable hands-on experience that can be applied in the field. As the project relied heavily on the design process, this experience would be extremely valuable in other design focused capacities.

12.3 Future Work

The scope of the project was limited due to the lack of a launch date. While this may change in the future, this limited the work of the team. Before the 3U CubeSat platform can be made flight-ready, several important components must be integrated and thorough environmental testing must be completed.

The EPS requires assembled solar panels, a power board, and a space-rated battery. Designs and prototypes exist for the solar array and power board, but these have not yet been purchased. Passive magnets must be integrated into the bus so that the satellite's orientation will be fixed on-orbit.

While the team has completed baseline testing here at SCU that has yielded promising results, the platform must be tested to industry standards. This includes vibro-acoustic and thermal-vacuum testing. More in depth FEA should be completed that includes all bus components and better simulates the launch environment.

Most importantly, the 3U platform needs a payload. The UPAACN prototype is valuable as a demonstration of the technology, but it lacks a mission payload. It is difficult to call a satellite complete that lacks a payload, as there is a not insignificant amount of customization required to support one. Once the design team presents the project to engineers at NASA, it is possible that a payload and a launch opportunity will be granted. The responsibility of updating the platform in this case would be left to a future design team. Hopefully, the documentation left by the current design team will help the future team achieve success.

Bibliography

1. "CubeSat." About Us. California Polytechnic State University, n.d. Web. 17 May 2013.
2. "Robotic Systems Laboratory - Expeditions & Operations." Index. Santa Clara University, n.d. Web. 17 May 2013.
3. Boyle, Rebecca. "DARPA Wants Swarms of Cheap, Disposable Satellites That Take Pictures on Demand." Popular Science. Popular Science, 13 Mar. 2012. Web. 17 May 2013.
4. Tsitas, Stephen. "6U CubeSat Commercial Applications." 6U CubeSat Low Cost Space Missions Workshop. The University of New South Wales, Canberra. 18 July 2012. Lecture.
5. "CubeSat Kit." Home. N.p., n.d. Web. 17 May 2013.
6. Galysh, I., K. Doherty, J. McGuire, H. Heidt, D. Niemi, and D. Dutchover. CubeSat: Developing a Standard Bus for Picosatellites. The StenSat Group. CubeSat, n.d. Web. 17 May 2013.
7. Toorian, Armen, Emily Blundell, Jordi Puig Suari, and Robert Twiggs. CubeSats as Responsive Satellites. CubeSat. 3rd Responsive Space Conference 2005, n.d. Web. 17 May 2013.
8. Harrison, Sam, Patrick Scott, and Victor Zapien. Nanosatellite Fabrication and Analysis. Thesis. Santa Clara University, 2012. Santa Clara: Santa Clara University, Department of Mechanical Engineering, 2012. Print.
9. VanOutryve, Cassandra Belle. A Thermal Analysis and Design Tool for Small Spacecraft.Thesis. San Jose State University, 2008. San Jose: San Jose State University, 2008. Print.
10. "Thermal Modeling Software Using FEM, FD and FNM Methods, Thermal Desktop." C&R Technologies, n.d. Web. 17 May 2013.
11. Munakata, Riki, Wenschel Lan, Armen Toorian, Amy Hupputanasin, and Simon Lee. CubeSat Design Specification. CubeSat. The CubeSat Program, Cal Poly SLO, n.d. Web. 17 May 2013.
12. Op. cit., "Robotic Systems Laboratory - Expeditions & Operations."
13. "Artemis." Artemis. N.p., n.d. Web. 06 June 2013. <<http://screem.engr.scu.edu/artemis/>>.
14. Op. cit., "Robotic Systems Laboratory - Expeditions & Operations."
15. "NASA - National Aeronautics and Space Administration." NASA. N.p., n.d. Web. 27 May 2013.

16. Op. cit., "Robotic Systems Laboratory - Expeditions & Operations."
17. Op. cit., CubeSat Design Specification.
18. United States. NASA. Goddard Space Flight Center. General Environmental Verification Standard. By Abigail Harper, Michael Ryschkewitsch, Arthur Obenschain, and Richard Day. NASA, n.d. Web. 17 May 2013.
19. Op. cit., CubeSat Design Specification.
20. Op. cit., C&R Technologies.
21. Incropera, Frank P., David P. DeWitt, Theodore L. Bergman, and Adrienne S. Lavine. Fundamentals of Heat and Mass Transfer. 7th ed. John Wiley & Sons, 2011. Print.
22. Strong, John, and Henry Victor Neher. Procedures in Experimental Physics. New York: Prentice-Hall, 1938. Print.
23. Op. cit., VanOutryve.
24. Op. cit., Harrison, Sam, et. al.
25. Ibid.
26. Boghossian, A., Brown, A., & Zak, S. (2006). Temperature Sensors. <<https://controls.engin.u>>. 12 November 2012.
27. Ibid.
28. Orbital Sciences Corporation. Thermal Control Louvers. Beltsville, MD: Orbital Sciences Corporation, 2013. Thermal Louvers Brochure. Orbital Sciences Corporation. Web. 8 June 2013.
29. Kitts, Christopher. "Power Systems." Santa Clara University, Santa Clara. Lecture.
30. Spectrolab Inc. Triangular Advanced Solar Cells (TASC). Sylmar, CA: Spectrolab, 2002. Web. 8 June 2013. <http://www.spectrolab.com/DataSheets/PV/PV_NM_TASC>.
31. Carrere, Alexander L. Solar Panel Design Decision and General Information Sheet. N.p.: ISAT Group, 1 Jan. 2012. PDF.
32. "Solar Peak Power Trackers." Solar Peak Power Trackers. N.p., n.d. Web. 09 June 2013.
33. Backus, Andrew, Honeyman, Parker, Nahlik, Matthew. "Nanosatellite Attitude Determination and Control." Thesis. Santa Clara University, 2010. Santa Clara: Santa Clara University, Department of Mechanical Engineering, 2010. Print.

34. "Outgassing Data for Selecting Spacecraft Materials System." Outgassing Data for Selecting Spacecraft Materials System. NASA, n.d. Web. 20 May 2013.
35. Op. cit., "Nanosatellite Attitude Determination and Control"
36. Giancoli, Douglas C. Physics for Scientists & Engineers. Upper Saddle River, NJ: Pearson Prentice Hall, 2008. Print.
37. "Outgassing of Engineering Plastics In High-Vacuum Applications." Boedeker Plastics : Outgassing of Engineering Plastics. Boedeker Plastics, Inc., 2013. Web. 20 May 2013.
38. Op. cit., Giancoli
39. Op. cit., General Environmental Verification Standard
40. Ibid.
41. Ibid.
42. Op. cit., CubeSat Design Specification
43. Op. cit., General Environmental Verification Standard
44. Kessler, Donald J., "Derivation of the collision probability between orbiting objects: the lifetimes of jupiter's outer moons." Icarus, Volume 48, Issue 1, October 1981, Pages 39-48, ISSN 0019-1035, 10.1016/0019-1035(81)90151-2.
45. Op. cit., CubeSat Design Specification
46. NASA. The Threat of Orbital Debris and Protecting NASA Space Assets from Satellite Collisions. OD Media Briefing. NASA, 28 Apr. 2009. Web.
47. NASA. USA Space Debris Environment, Operations, and Policy Updates. US OD Presentation to 2008 STSC. United Nations Office for Outer Space Affairs, 11 Feb. 2008. Web. 8 June 2013.

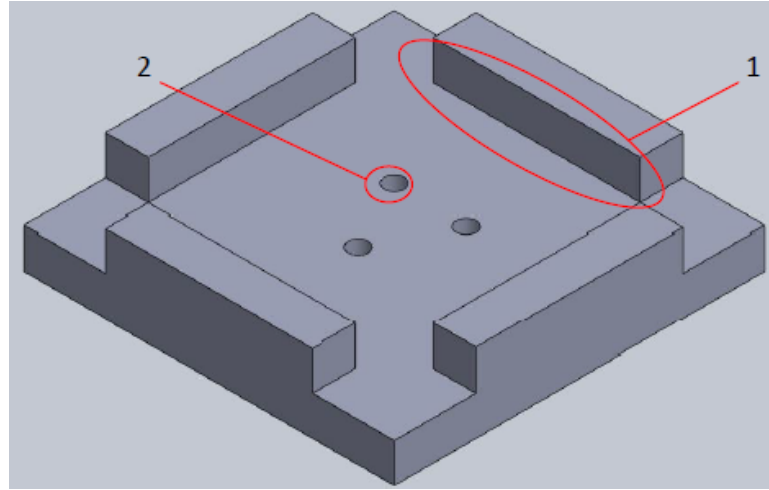


Figure A.1: Bottom fixture for top and bottom faces.

A Build Book

The following describes the machining and assembly process used to prototype the 3U CubeSat platform. These procedures rely heavily upon the work of the 2012 design team; their procedures are included in part along with pertinent updates in the following sections.

A.1 Top and Bottom Faces and Fixtures

In order to construct the top and bottom faces, two fixtures were machined. They were constructed out of solid blocks of aluminum 6061 on a milling machine. The procedure for these fixtures are as follows. These instructions rely upon the drawings included in Appendix B.

A.1.1 Bottom Fixture

1. Bring the block of aluminum down to size on the milling machine.
2. Machine out the central pocket to the appropriate depth. This is done so that the flanges (1) seen in Figure A.1 actually connect all the way around the perimeter of the piece.
3. Machine out the corner materials to the appropriate depth. This leaves four flanges that are the exact height and length required.
4. Drill and tap the three holes (2).

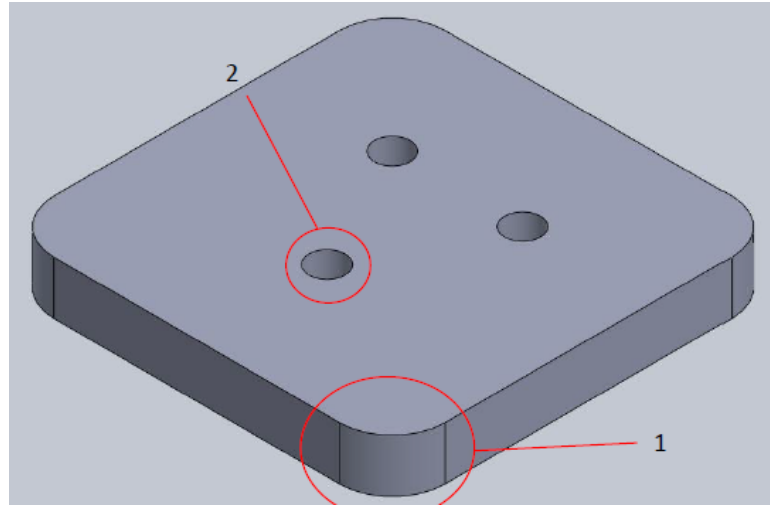


Figure A.2: Top fixture for top and bottom faces.

A.1.2 Top Fixture

1. Machine the aluminum block down to the appropriate size.
2. Machine the radii on the corners (1) one at a time.
3. Drill the three holes (2) in the middle of the fixture. These are through holes. See Figure A.2 for detail.

A.1.3 Top and Bottom Faces

The procedure for machining these faces is mostly the same, however, mounting requirements will affect the locations of through holes.

1. Bring the aluminum block down to size.
2. Machine out the four corner notches (1) shown in Figure A.3.
3. Drill the four mounting holes (2) for the captive nuts.
4. Drill and countersink the mounting holes (3) on the bottom of the face. These locations will vary based on mounting requirements.
5. Machine out the pocket (4).
 - (a) Machine out a pocket large enough to fit the top fixture down to the final thickness of the face. Be sure to make the pocket larger than the fixture.
 - (b) If not machining a pocket all the way through the part, then three holes will need to be drilled to accommodate the fixtures.
 - (c) Attach the part to both fixtures, using properly sized bolts to hold the parts together. This assembly is shown in Figure A.4.

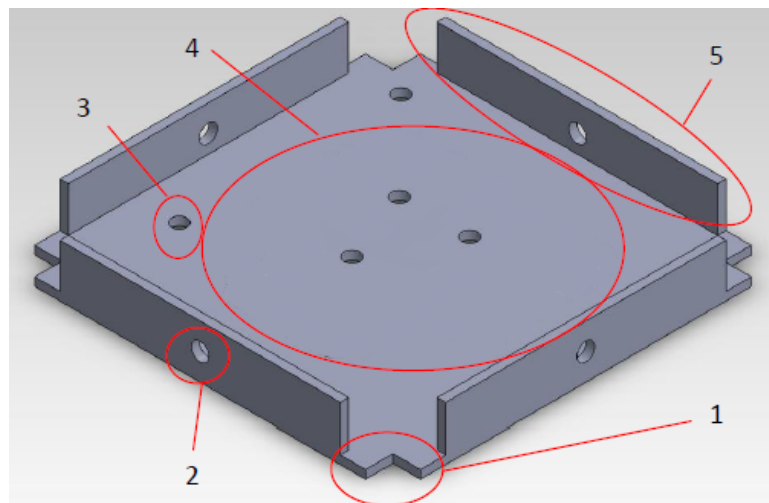


Figure A.3: Top/bottom face.

- (d) Without taking material off the top fixture, continue to machine out the pocket until the flanges are the proper thickness.

A.2 Side Faces and Fixtures

In order to construct the four side faces, two fixtures were machined. They were constructed out of solid blocks of aluminum 6061 on a milling machine. The procedure for these fixtures are as follows. These instructions rely upon the drawings included in Appendix B.

A.2.1 Bottom Fixture

1. Bring the aluminum block down to size.
2. Machine out the pocket (1) leaving three walls as shown in Figure A.5.
3. Drill and tap the twelve holes (2).

A.2.2 Top Fixture

1. Bring the aluminum block down to size.
2. Drill the twelve through holes (2) as shown in Figure A.2.2.

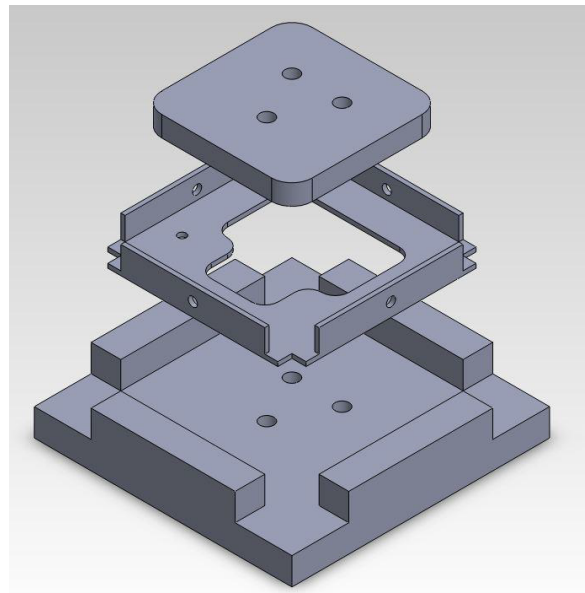


Figure A.4: Top/bottom face fixture assembly.

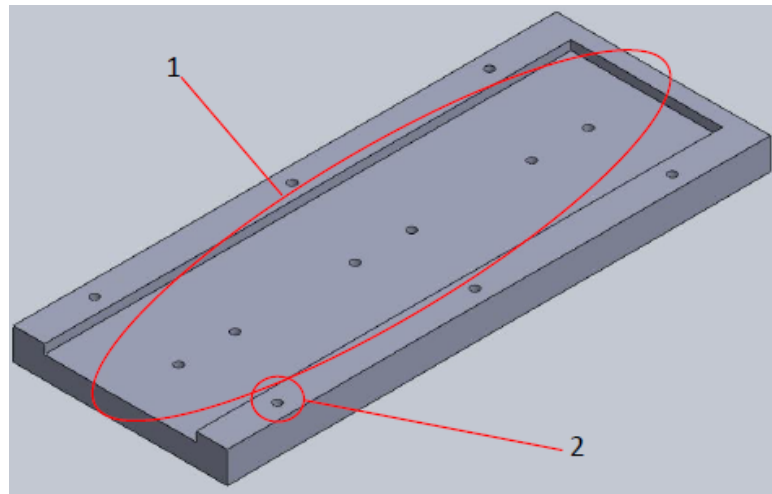


Figure A.5: Bottom fixture for side faces.

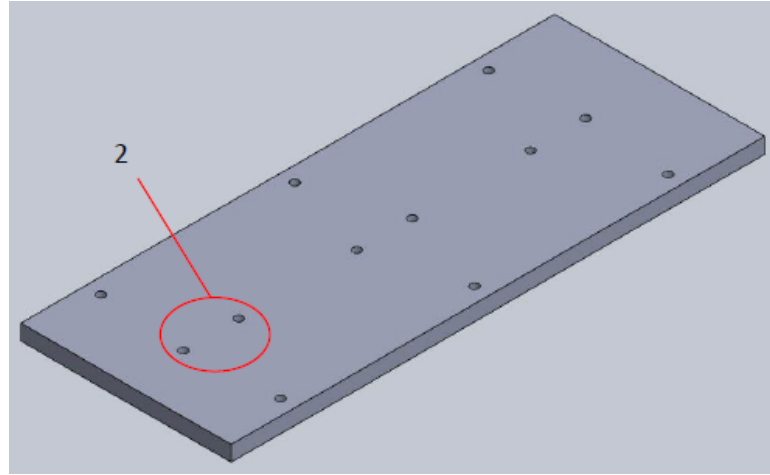


Figure A.6: Top fixture for side faces.

A.2.3 Side Faces

1. As the side faces are very thin, all four are clamped together and machined concurrently.
2. Bring down the clamped faces to the correct size.
3. With the faces clamped onto the bottom fixture, drill the eight through holes for the captive nuts (1).
4. If pockets are desired in the side faces, drill the six through holes (2) so that the top fixture can be attached.
5. Drill and countersink the two holes on the top and bottom (3) as shown in Figure A.7.
 - (a) To countersink with the faces clamped together, start with the top face.
 - (b) Carefully remove the top face, leaving the other faces in the fixture to maintain dimensions.
 - (c) Countersink the next face.
 - (d) Repeat steps (b) and (c) until all faces are complete.
6. If pockets are desired, put all faces into the fixtures and bolt down using the six through holes (2) as seen in Figure A.8.
7. Machine out pockets.

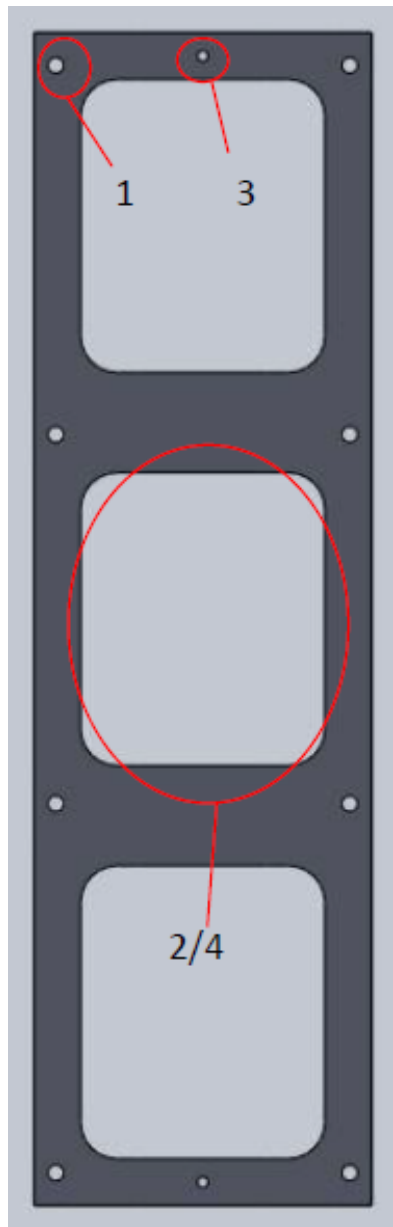


Figure A.7: Side faces.

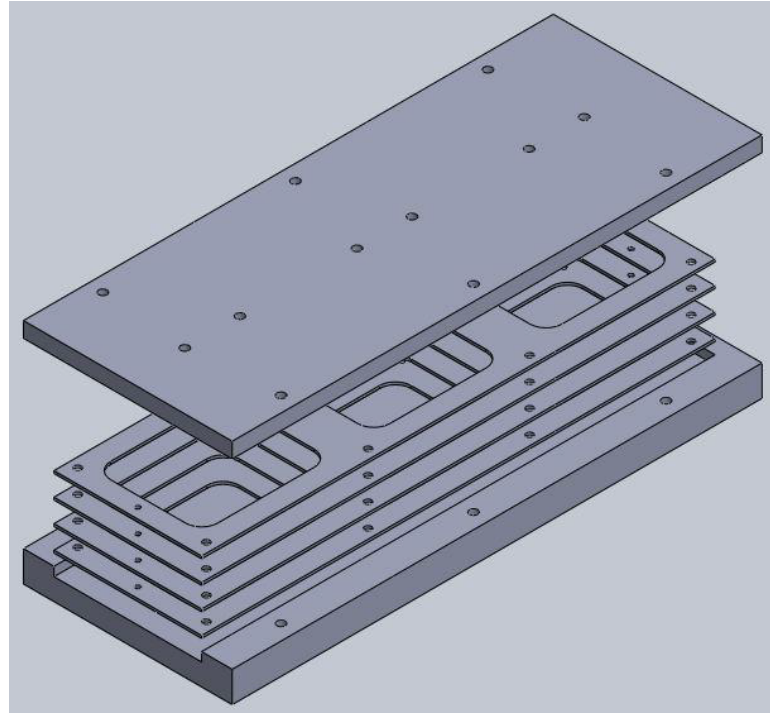


Figure A.8: Side faces fixture assembly.

A.3 Corner Brackets and Fixture

A.3.1 Fixture

1. Bring the aluminum block down to size.
2. Machine out the material on both sides of the fixture (1) as shown in Figure A.9.
3. Machine down the platforms that will have two holes to the proper height (2).
4. Just inside of the platforms (2), there is a small pocket. Machine this down to the proper height on both sides.
5. Machine the center pocket (3) down to the correct size.
6. Drill and tap the four holes (4).
7. Drill and tap the eight holes in the floor of the center pocket (3).

A.3.2 Corner Brackets

Two brackets are machined at once and come from the same block of aluminum. These are attached along the long side and split into two pieces once attached to the fixture.

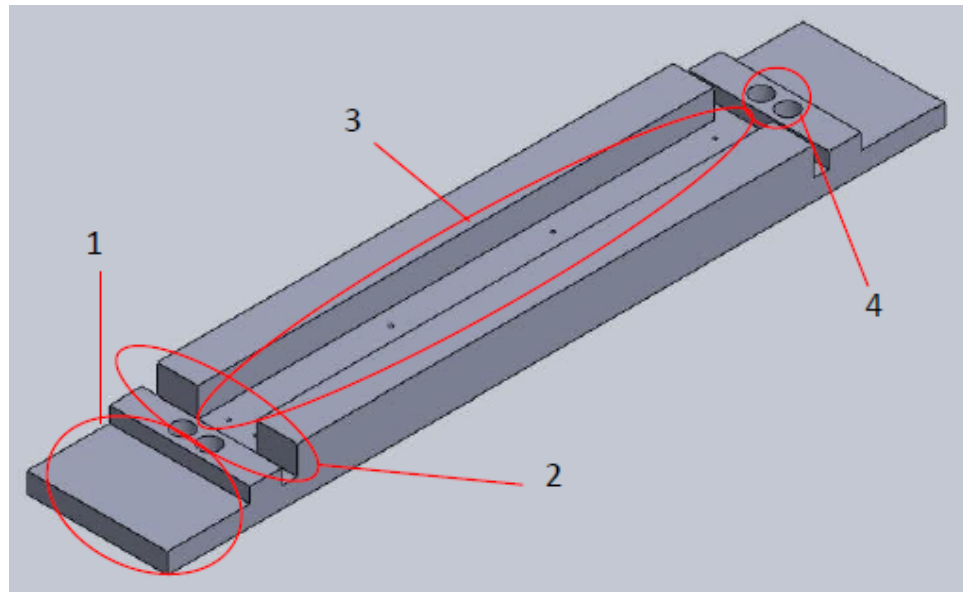


Figure A.9: Fixture for corner brackets.

1. Bring the aluminum down to size.
2. Machine out the radii that run the length of the part.
3. Machine out one side of the cubes (1) as shown in Figure A.3.2.
4. Holes are then drilled and countersunk in the appropriate locations (2).
5. Place the part into the fixture with the radii facing down, clamping the cubes (1) to the fixture as shown in Figure A.11.
6. Machine out the pocket in the middle (3).
 - (a) Use a large cutting tool to bring the pocket to the appropriate depth.
 - (b) Use a small cutting tool to clean up the corners of the pocket.
7. Remove the clamps and fasten the brackets to the fixture using the eight holes that were drilled and tapped (2).
8. Finish the cubes (4).
9. Split the piece down the middle using the same small cutting tool.
10. Switch the brackets in the fixture so that the sides of the brackets facing down are now on the sides of the fixture.
11. Machine out the leftover material.

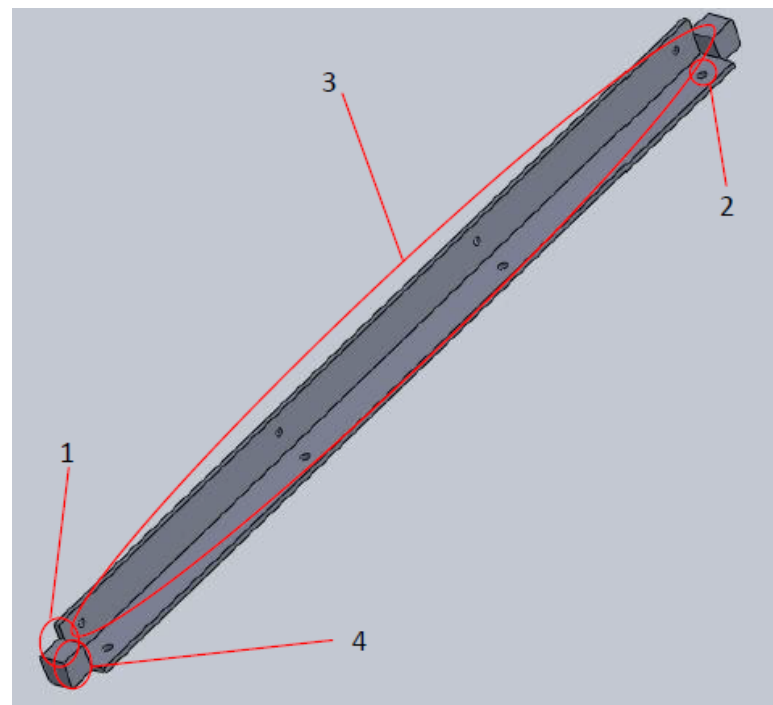


Figure A.10: Corner bracket.

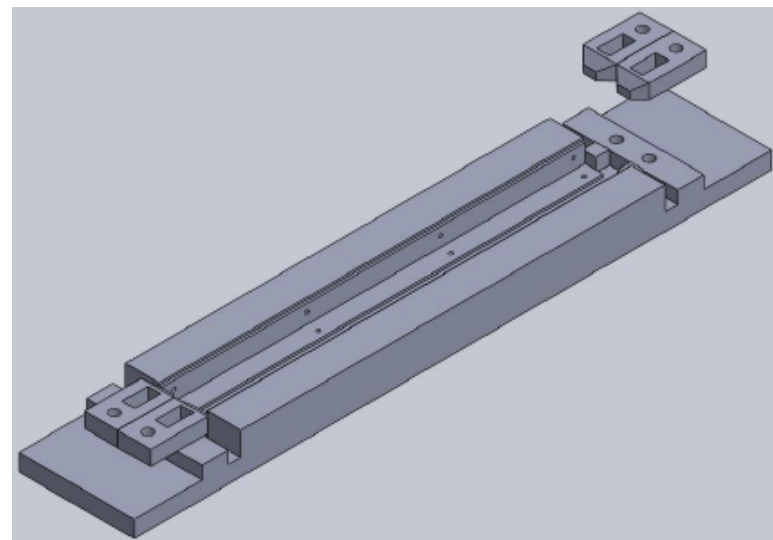


Figure A.11: Corner bracket fixture assembly.

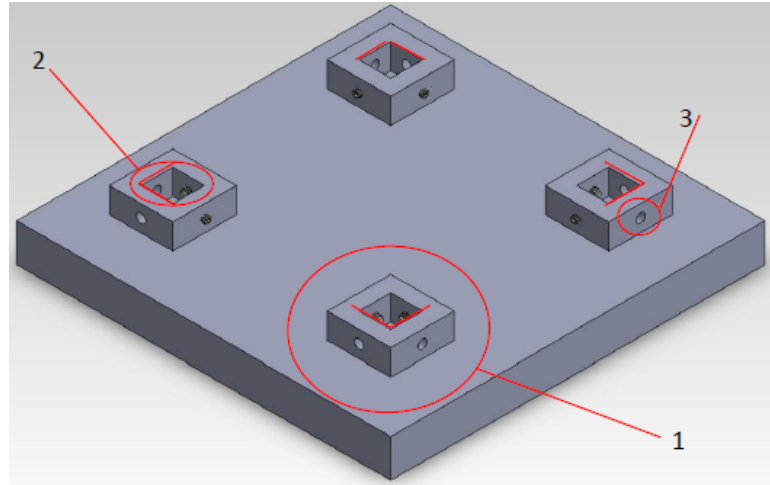


Figure A.12: Assembly tool.

A.4 Assembly Tools

1. Bring the aluminum block down to size.
2. Remove all material except for the base and the four protruding cubes (1) as shown in Figure A.12.
3. The cubes are then machined one at a time.
 - (a) Drill out the corners of the inside pocket that will be made.
 - (b) Pocket each cube down to the appropriate depth (2).
 - (c) Drill and tap the holes (3).

A.5 AACs Fixtures

In order to machine the small scaled AACs two pieces of fixturing were needed. The first was a set of aluminum soft jaws which allowed the circular pieces of the system to be held in the mill during machining. The second was a soft collet used to hold the flywheel in place on the lathe. The procedure for the machining of these fixtures is described below.

A.5.1 Soft Jaws

1. Mount the soft jaws in the mill vice and find the center point using an indicator.
2. Mill the largest diameter and take steps down for the smaller diameters, as shown in Figure A.13.

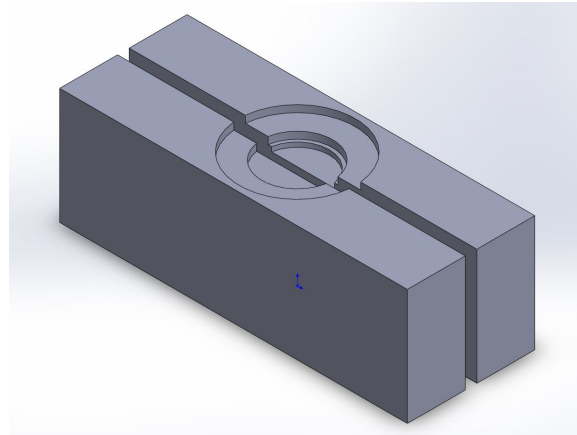


Figure A.13: Soft jaws.



Figure A.14: Soft collet.

A.5.2 Soft Collet

1. Mount soft collet in lathe.
2. Machine pocket in collet 0.100 [in] deep, as shown in Figure A.14.

A.6 AACs Parts

Due to the nature of the tolerances, make sure to test fit all components while machining.

A.6.1 Can Body

1. Use the lathe cutting tool to set outer diameter of can body flanges.
2. Use boring bar to machine inner diameter.

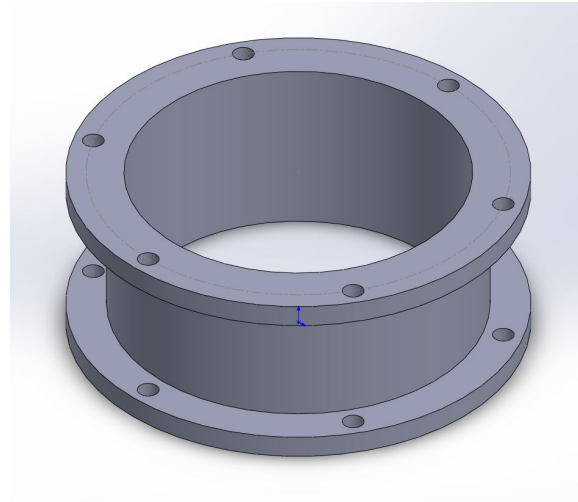


Figure A.15: Can body.

- (a) Must be done at high speeds to insure that the finish will be smooth.
- (b) Finish must be smooth to create best seal with the O-rings.
3. Use parting tool to create the groove between the two flanges.
4. Use parting tool to part off the part from the original stock.
5. Place part in soft jaws on the mill.
6. Drill holes on one flange (6).
7. Remove part and flip over.
8. Drill holes on second flange (6). Part is shown in Figure A.6.1.

A.6.2 Top Can Lid

1. Machine aluminum rod stock to final outer diameter on lathe.
2. Use lathe to machine the boss.
3. Use parting tool on lathe to create groove for the O-ring.
4. Use parting tool to separate part from stock.
5. Place part in soft jaws on mill.
6. Machine circular pocket to depth.
7. Drill and tap 2-56 holes to depth.
8. Drill #11 through hole.
9. Drill flange clearance holes (6). Final part is shown in Figure A.16.

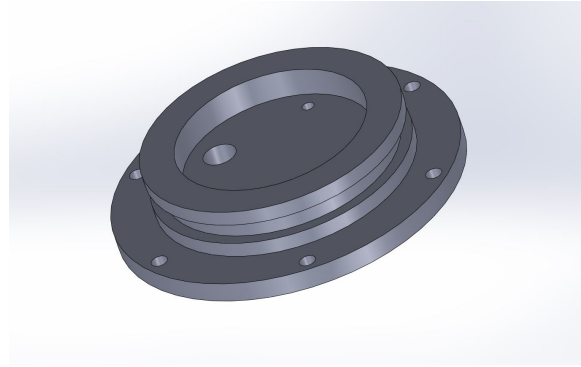


Figure A.16: Top can lid.

A.6.3 Bottom Can Lid

1. Machine aluminum rod stock to final outer diameter on lathe.
2. Use lathe to machine boss.
3. Use parting tool on lathe to create groove for the O-ring.
4. Use parting tool to separate part from stock.
5. Place part in soft jaws on mill.
6. Machine circular pocket for the bearing.
 - (a) Test with bearing so that the fit is snug on the bearing but it can still slip in and out of the pocket.
7. Drill #10 hole on the surface of the pocket.
8. Drill flange clearance holes (6). Final part is shown in Figure A.17.

A.6.4 Flywheel

1. Machine aluminum rod stock to final diameter on lathe.
2. Use bandsaw to cut a piece larger than the final height of the flywheel.
3. Clamp part in soft jaws.
4. Drill #61 through hole.
5. Ream hole with 1 [mm] reamer.
6. Mount part in soft collet.
7. Face part to size and create boss on top. Final part is shown in Figure A.18.



Figure A.17: Bottom can lid.

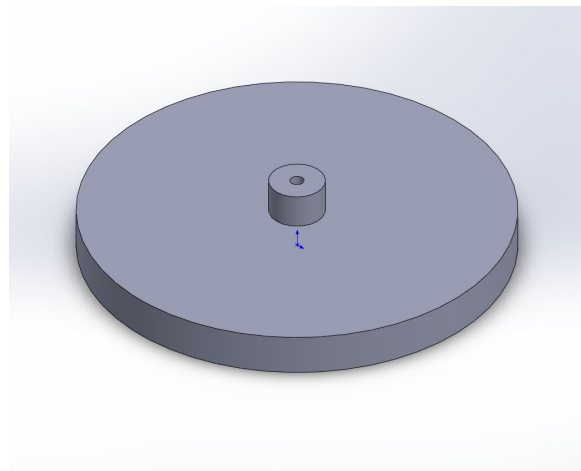


Figure A.18: Flywheel.

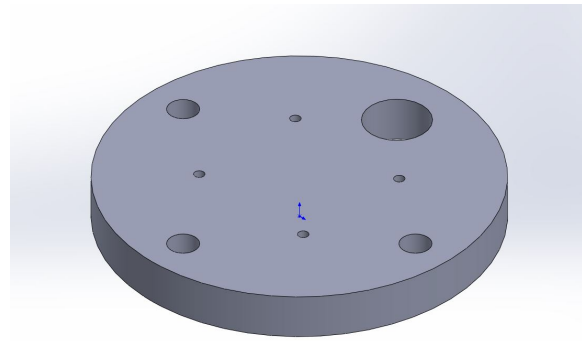


Figure A.19: Motor spacer.

A.6.5 Motor Spacer

1. Use lathe to bring Delrin to size.
2. Use parting tool to part off to height.
3. Use laser cutter to cut appropriate holes. Final part is shown in Figure A.19.

A.6.6 Motor Mounting Bracket

1. Machine stock to size.
2. Use bandsaw to cut off part of the sized stock.
3. Place part into soft collet and face it to size.
4. Clamp part (softly) in soft jaws.
5. Machine circular pocket through all.
6. Drill #43 through holes.
7. Use 82 degree countersink to create chamfer for flat head screws. Final part is shown in Figure .

A.6.7 Assembly

1. Use M1 screws to attach motor to motor spacer.
2. Use 2-56 screws to attach motor mounting bracket over the brushless DC motor, through the motor spacer, and finally to the top can lid.
 - (a) Make sure the motor lead wires fit through the clearance hole.

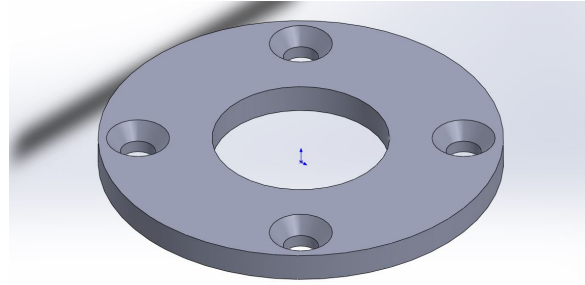


Figure A.20: Motor bracket.

- (b) Make sure bracket is snug on top of the motor but not so tight as to crush the PCB on the motor.
3. Slip o-rings over both can lids into the machined grooves.
4. Use (6) M2 screws and nuts to attach the top can lid to the can body.
5. Use general quick set epoxy to attach flywheel to the motor shaft.
 - (a) Use the small boss to ensure a parallel seating of the reaction wheel on the motor.
6. Slip the bearing over the reaction wheel boss.
7. Slip the lower part of the assembly into the bottom can lid.
8. Secure the bottom can lid to the rest of the can body with the remaining (6) M2 screws. Assembly is shown in Figure A.21.

A.7 System Integration

System integration of the UPAACN occurred at the RSL building at NASA Ames. A low grade cleanroom was built using RSL supplies. This cleanroom had a HEPA filter mounted on the roof of the cleanroom and was lined with plastic. Smocks, masks, gloves, and foot-covers were used by team members. All furniture and tools used in the cleanroom were cleaned before being brought in.

All satellite components were cleaned using a combination of rubbing alcohol and acetone. This helps to minimize the potential of outgassing.

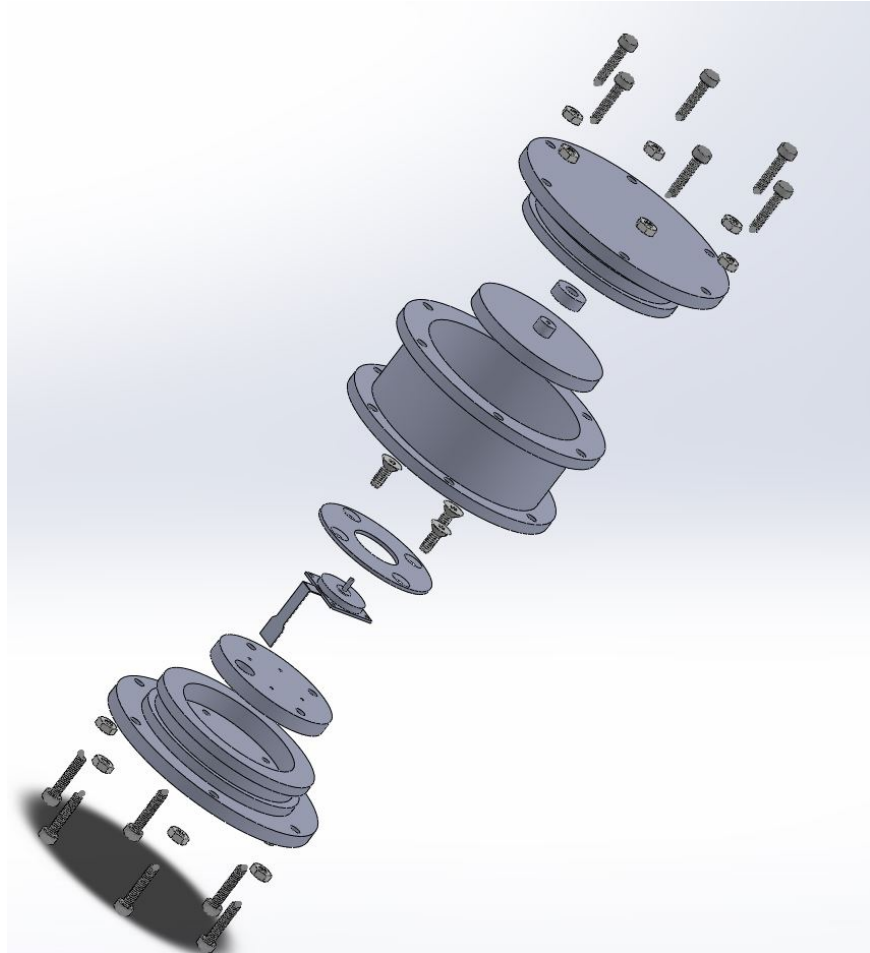


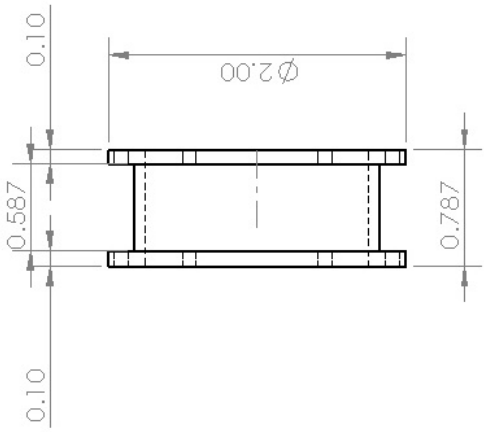
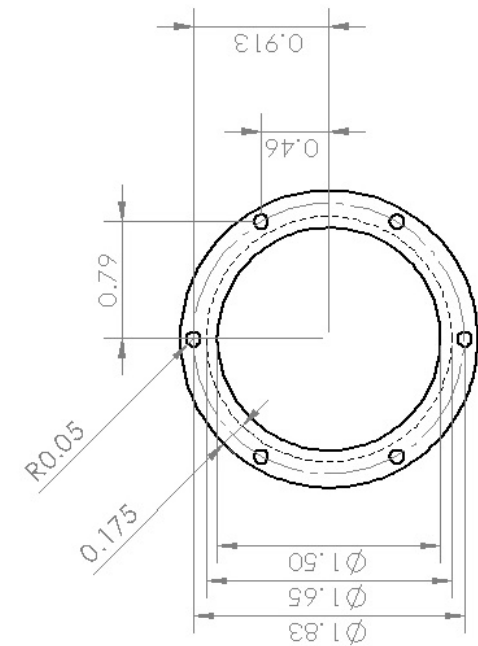
Figure A.21: AACS assembly.

B Drawings

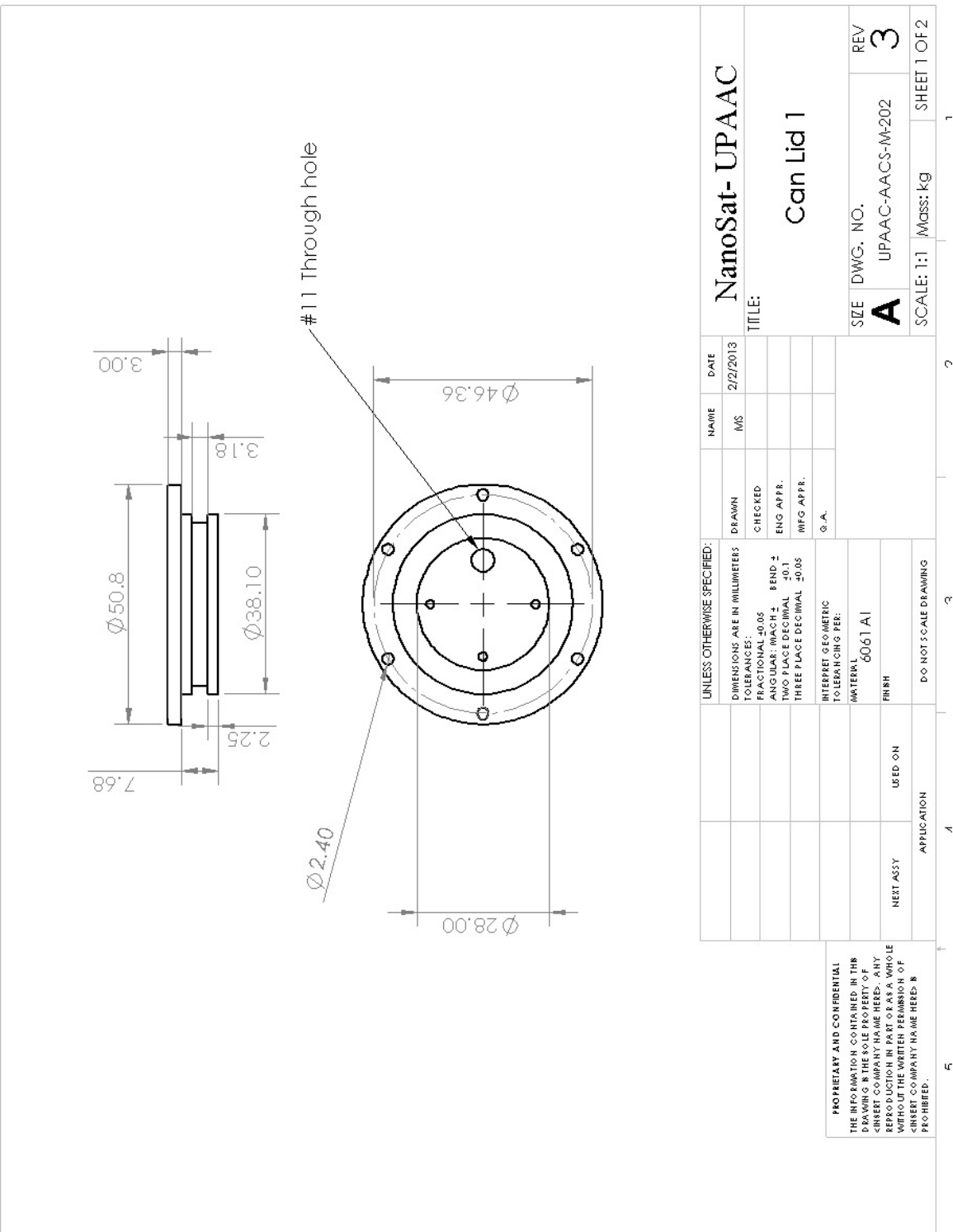
1. AACS-101 - Reaction Wheel
2. AACS-201 - Can Body
3. AACS-202 - Can Lid 1 - Sheet 1
4. AACS-202 - Can Lid 1 - Sheet 2
5. AACS-203 - Can Lid 2
6. AACS-204 - Motor Spacer
7. AACS-205 - Motor Mounting Bracket
8. AACS-2A - Flywheel Assembly
9. AACS-301 - Soft Jaws
10. STRUC-101 - Side Faces
11. STRUC-102 - Corner Brackets Overview
12. STRUC-102 - Corner Brackets Dimensioned
13. STRUC-102 - Corner Brackets End Detail
14. STRUC-103 - Top Face Overview
15. STRUC-103 - Top Face Dimensioned
16. STRUC-104 - Bottom Face Overview
17. STRUC-104 - Bottom Face Dimensioned
18. STRUC-105 - Payload/Transmitter Board Bracket
19. STRUC-106 - Flywheel Can Bracket
20. STRUC-201 - Side Face Bottom Fixture
21. STRUC-202 - Side Face Top Fixture
22. STRUC-203 - Top/Bottom Face Bottom Fixture
23. STRUC-204 - Top/Bottom Face Top Fixture
24. STRUC-205 - Corner Bracket Fixture
25. STRUC-206 - Assembly Tool
26. STRUC - Assembly

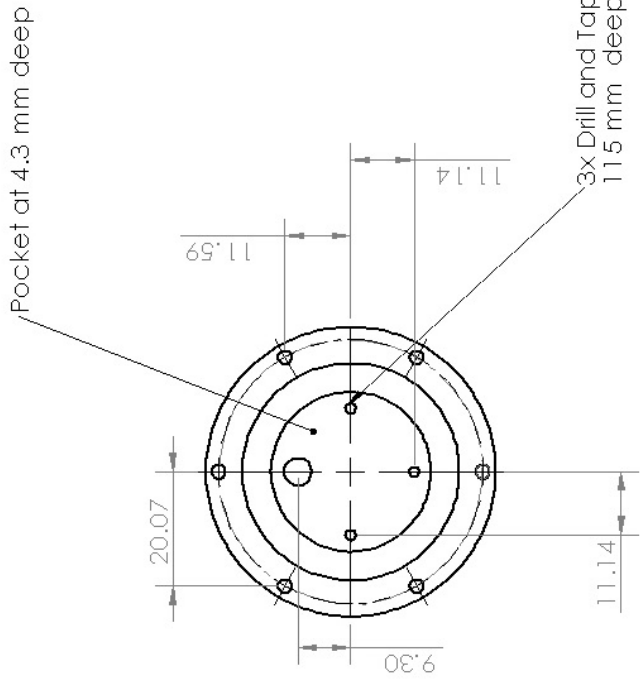
27. STRUC-401 - Payload Can
28. STRUC-402 - Payload Can Lid Overview
29. STRUC-402 - Payload Can Lid Groove Detail
30. STRUC-402 - Payload Can Lid Back Detail

		<p>NanoSat- UPaac</p> <p>Reaction Wheel</p>	
UNLESS OTHERWISE SPECIFIED:	DRAWN BY:	NAME:	DATE:
DIMENSIONS ARE IN MILLIMETERS	M.S.	M.S.	3/15/2013
TOLERANCES:	CHECKED		
FRACTIONAL: +0.05	ENG APP.		
ANGULAR: MACH \pm	MFG APP.		
ONE PLACE DECIMAL	Q.A.		
TWO PLACE DECIMAL			
INTERPRET GEOMETRIC			
TO TOLERANCING PER:			
MATERIAL:			
6061 Aluminum			
FINISH:	None		
USED ON:			
NEXT AS STY:			
APPLICATION:	DO NOT SCALE DRAWING		
5	4	3	2
			1
			SHEET 1 OF 1
			REV 1
		A	UPAAC-AAC5-M-101
		SCALE: 2:1	Mass: kg

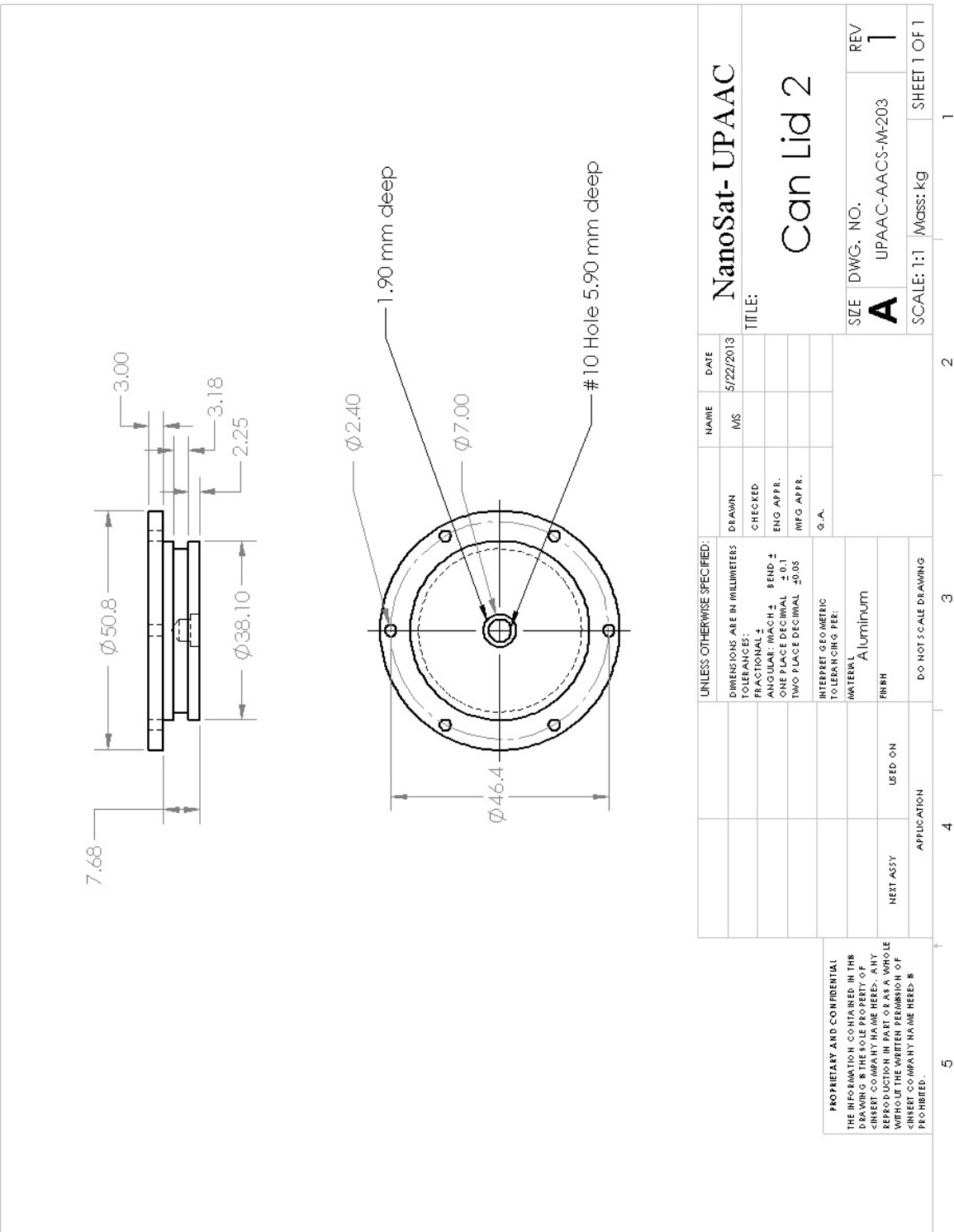


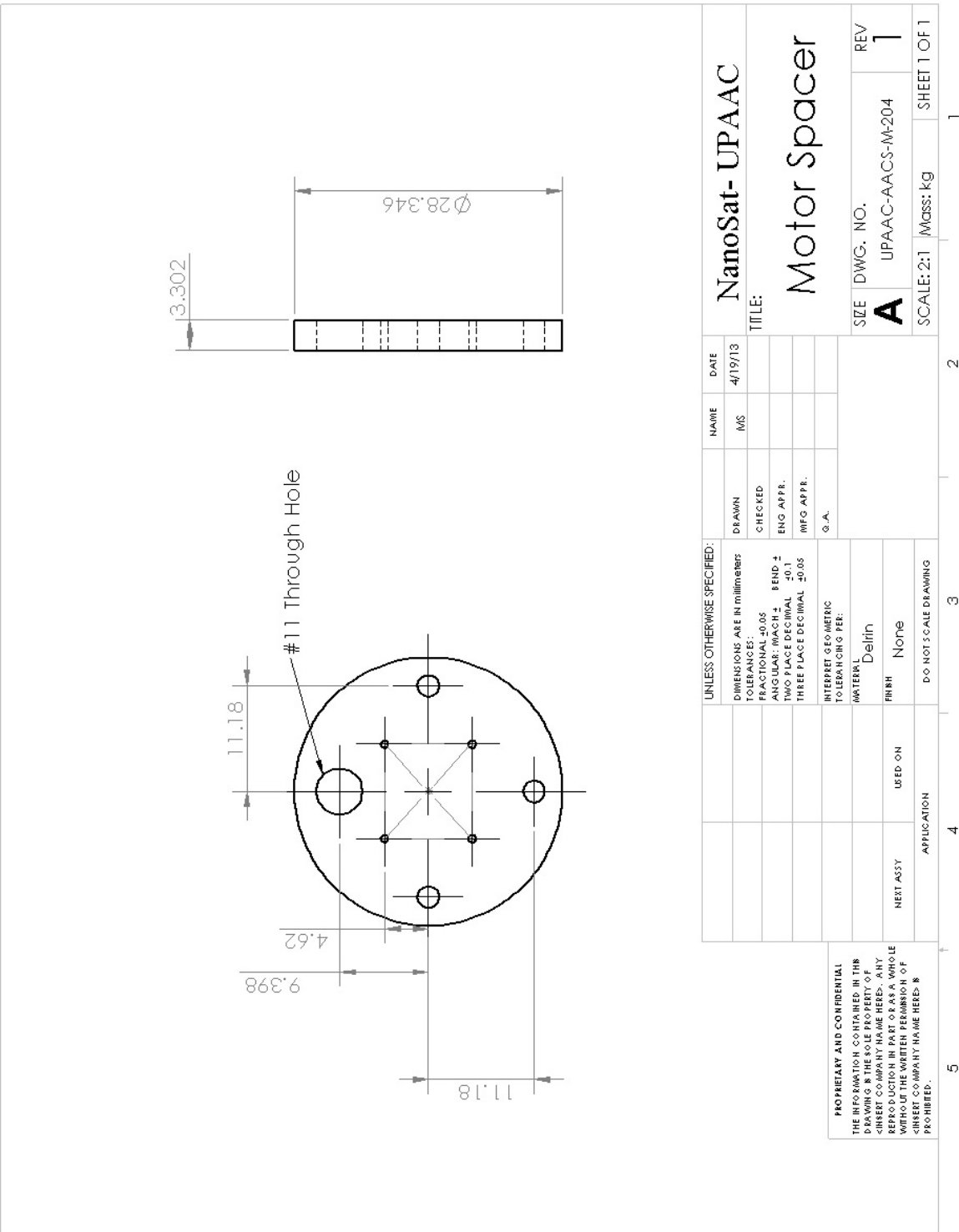
UNLESS OTHERWISE SPECIFIED:		NAME M.S.	DATE 2/3/2013	TITLE: NanoSat- UPaac Reaction Wheel Can Body
SIZE	DWG. NO.			
A	UPAAC-AACS-M201			REV 1
SCALE: 1:1	Mass: kg			SHEET 1 OF 1
Material	Ø0.61 Aluminum			
Finish	USED ON			
Interpret Geometric Tolerancing per:	DO NOT SCALE DRAWING			
Proprietary and Confidential	The information contained in this drawing is the sole property of <insert company name here>. Any reproduction in part or as a whole without the written permission of <insert company name here> is prohibited.			

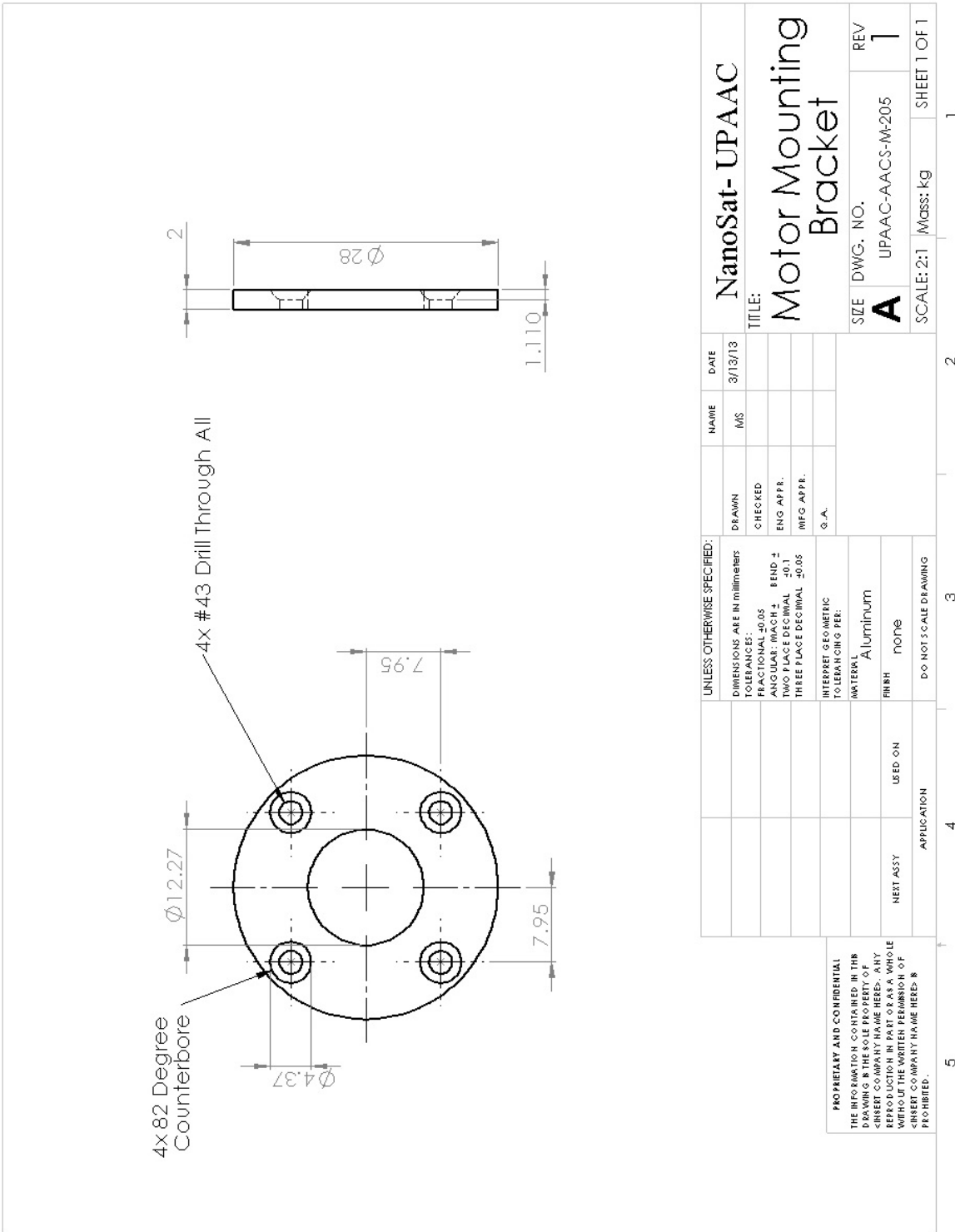




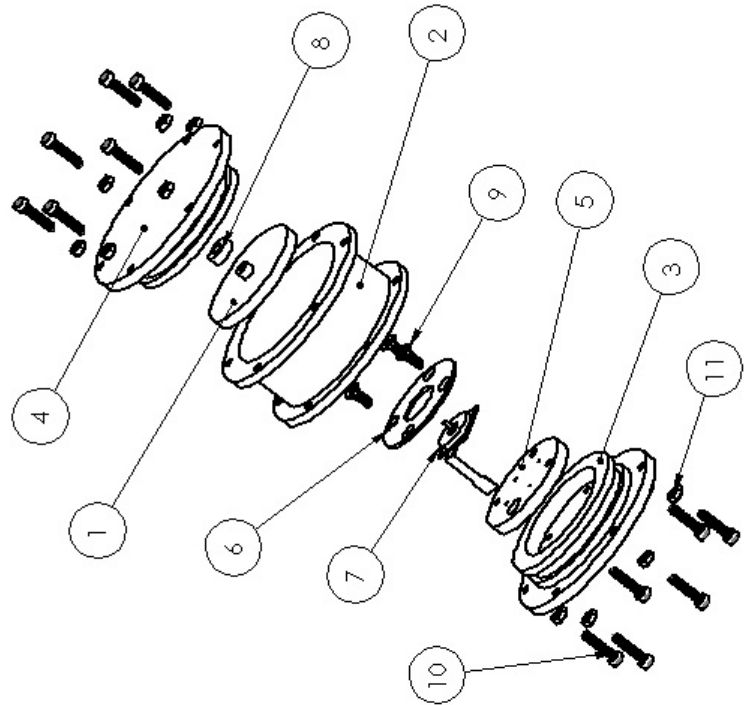
UNLESS OTHERWISE SPECIFIED:	
DIMENSIONS ARE IN millimeters	
TOLERANCES:	
FRACTIONAL: ± 0.05	DRAWN
ANGULAR: MACH + B END \pm	CHECKED
TWO PLACE DECIMAL: ± 0.1	ENG APPR.
THREE PLACE DECIMAL: ± 0.05	INFO APPR.
INTERPRET GEOMETRIC TO EXACTNESS PER:	Q.A.
MATERIAL	Aluminum
FINISH	None
Do NOT SCALE DRAWING	
NEXT ASSY	USED ON
APPLICATION	
PROPRIETARY AND CONFIDENTIAL THE INFORMATION CONTAINED IN THIS DRAWING IS THE SOLE PROPERTY OF CIBERTEK COMPANY NAME HERE. ANY REPRODUCTION IN PART OR AS A WHOLE WITHOUT THE WRITTEN PERMISSION OF CIBERTEK COMPANY NAME HERE, IS PROHIBITED.	
TITLE: Can Lid 1	
NAME: MS DATE: 2/21/13	
SIZE: DWG. NO. A UPAAAC-AACS-M-202	
SCALE: 1:1 MASS: kg REV 1	
SHEET 2 OF 2	



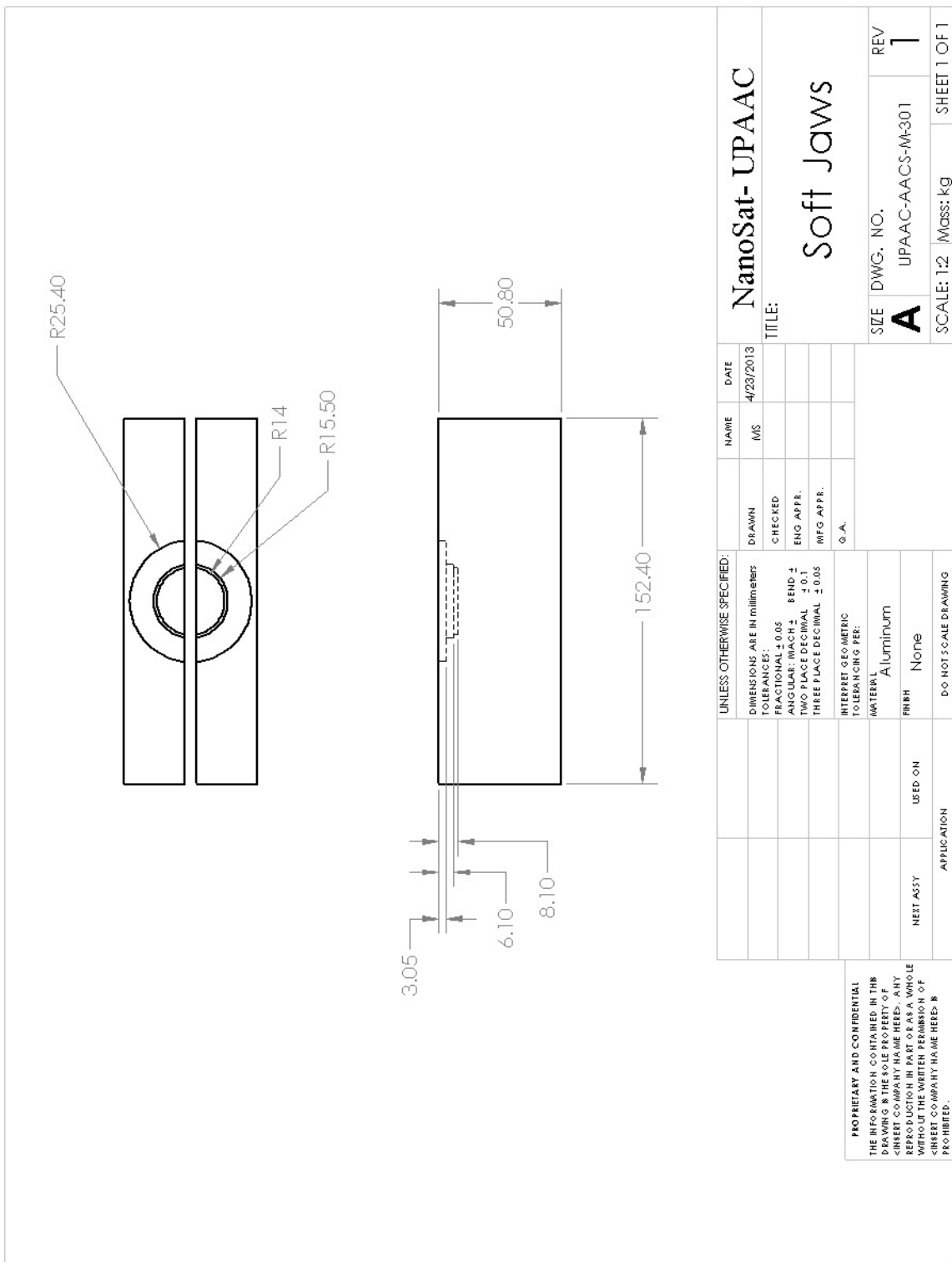


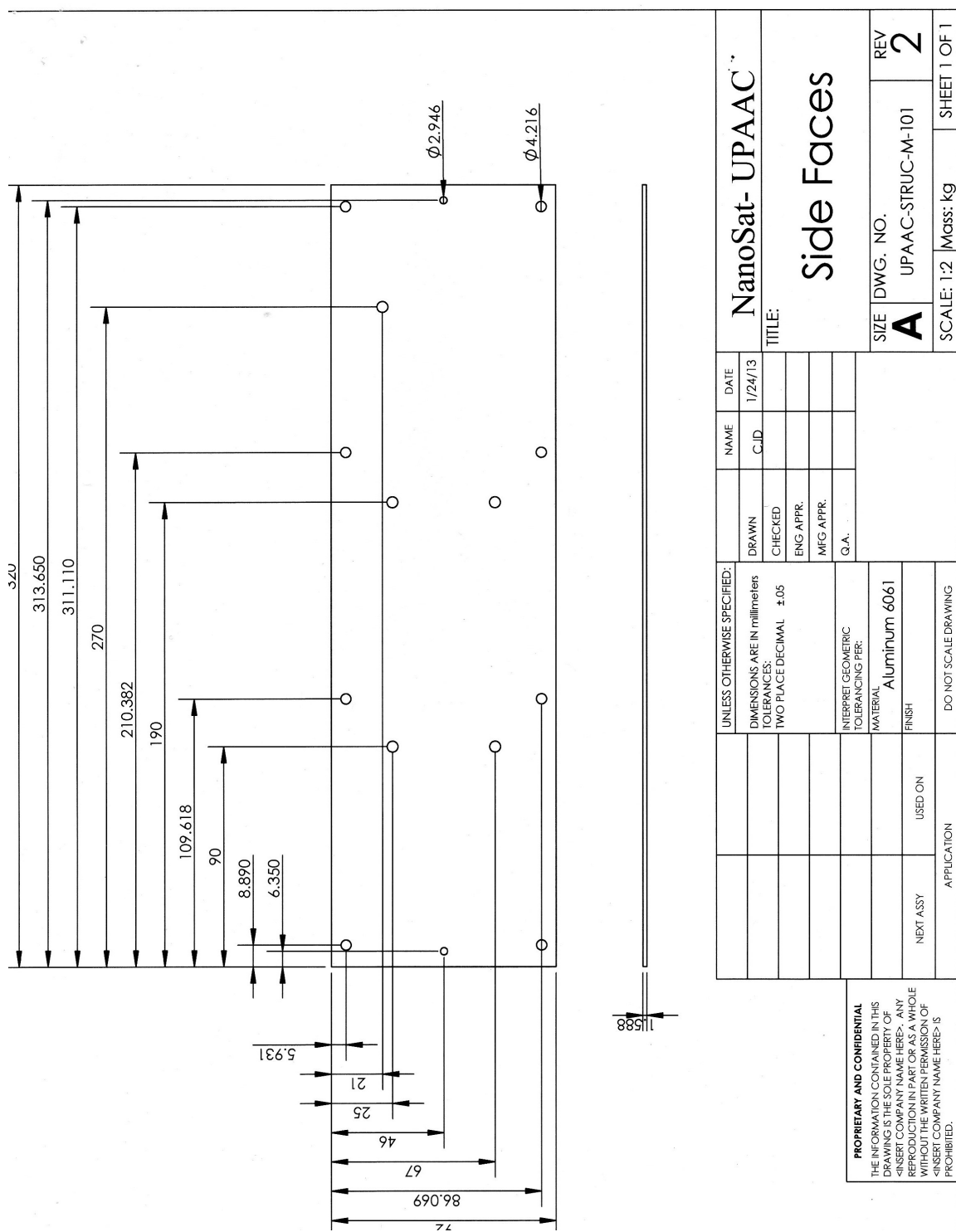


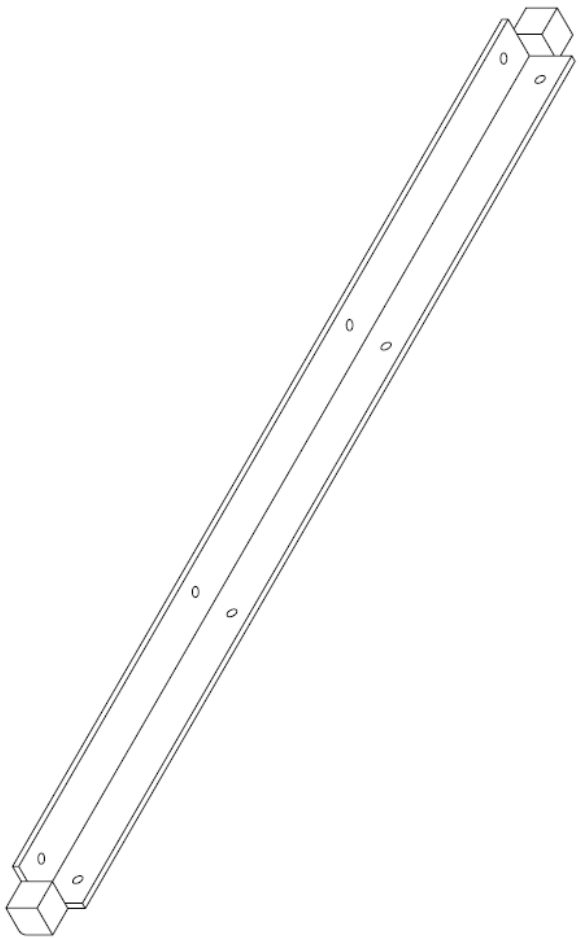
ITEM NO.	PART NUMBER	DESCRIPTION	QTY.
1	AACS-101	Reaction Wheel	1
2	AACS-201	Can Body	1
3	AACS-202	Can Lid 1	1
4	AACS-203	Can Lid 2	1
5	AACS-204	Motor Spacer	1
6	AACS-205	Motor Mounting Bracket	1
7	1202H004BH	Brushless DC Motor	1
8	DDL-740ZZ.HA3P25L01	Bearing Placeholder	1
9	91253A077	FH 2-56x0.25" Screws	3
10	91290A017	M2x10mm Screws	12
11	91828A111	M2 Nut	12



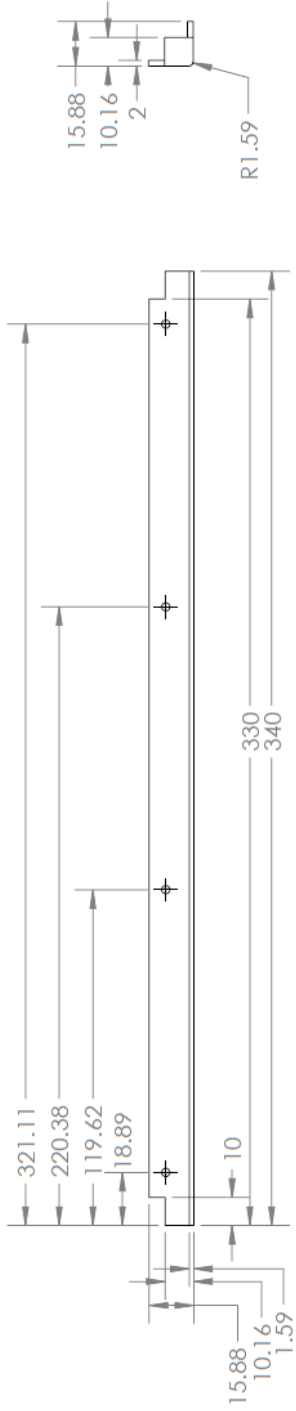
UNLESS OTHERWISE SPECIFIED:			
DIMENSIONS ARE IN millimeters	DRAWN BY:	NAME:	DATE:
TOLERANCES: FRACTIONAL 0.5 DECIMAL: .005 ANGLE: .005° LEADS PLACED DECIMAL .001 THREE PLACED DECIMAL .0001	CHECKED:	M/S	4/16/13
TITLE: NanoSat- UPAAC			
Exploded Assembly			
PROPRIETARY AND CONFIDENTIAL			
INFORMATION CONTAINED IN THIS DRAWING IS UNCLASSIFIED AND IS NOT SUBJECT TO THE COMPANY'S SECURITY POLICY. INFORMATION CONTAINED HEREIN, ANY PART THEREOF, AND THE METHODS, ANY EDITIONS, REPRODUCTIONS, OR DERIVATIVES THEREOF, WHICH ARE MADE, USED, OR DISCLOSED IN PART OR AS A WHOLE, WILL NOT BE DIVULGED OUTSIDE THE COMPANY OR ITS CONTRACTORS OR SUBCONTRACTORS. < INSERT COMPANY NAME HERE > © PROHIBITED.			
SIZE	DWG. NO.	REV	
A	UPAAC-AACS-A-401	1	
SCALE: 2:3		Mass: kg	SHEET 1 OF 1
APPLIED		DO NOT SCALE DRAWING	
NEXT ASSY		LED ON	LINES
		None	None







Title:			
Corner Brackets Overview			
Size	Dwg. No.	Rev	
A	UPAAC-STRU-C-M-102	1	SHEET 1 OF 1
Unless otherwise specified: Dimensions are in millimeters Tolerances: Two place decimal ±0.05			
DRAWN	NAME QJ	DATE 2/3/13	
CHECKED			
ENG APPR.			
MFG APPR.			
G.A.			
Interpret Geometric Tolerancing per: Material			
6061 Aluminum			
FINISH	None		
NEXT ASSY	USED ON		
APPLICATION	Do Not Scale Drawing		
Proprietary and Confidential The information contained in this drawing is the sole property of Insert Company Name Here. Any reproduction in part or as a whole without the written permission of Insert Company Name Here is prohibited.			



NanoSat- UPAAC

TITLE:

Corner Brackets

UNLESS OTHERWISE SPECIFIED:
DIMENSIONS ARE IN millimeters
TOLERANCES:
TWO PLACE DECIMAL 4.05

DRAWN
CHECKED
ENG APPR.
MFG APPR.
Q.A.

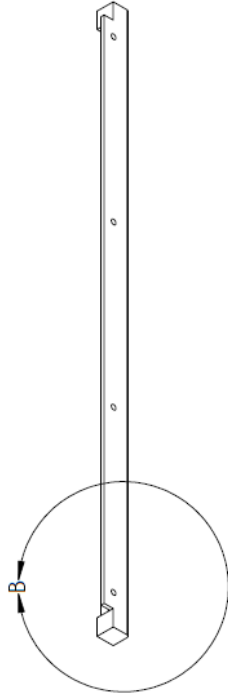
SIZE	DWG. NO.	REV
A	UPAAC-STRUC-M-102	2
SCALE: 1:2	Mass: kg	SHEET 1 OF 1
2	3	1
4		
5		

PROPRIETARY AND CONFIDENTIAL

THE INFORMATION CONTAINED IN THIS DRAWING IS THE SOLE PROPERTY OF [REDACTED COMPANY NAME HERE]. ANY REPRODUCTION IN PART OR AS A WHOLE WITHOUT THE WRITTEN PERMISSION OF [REDACTED COMPANY NAME HERE] IS PROHIBITED.



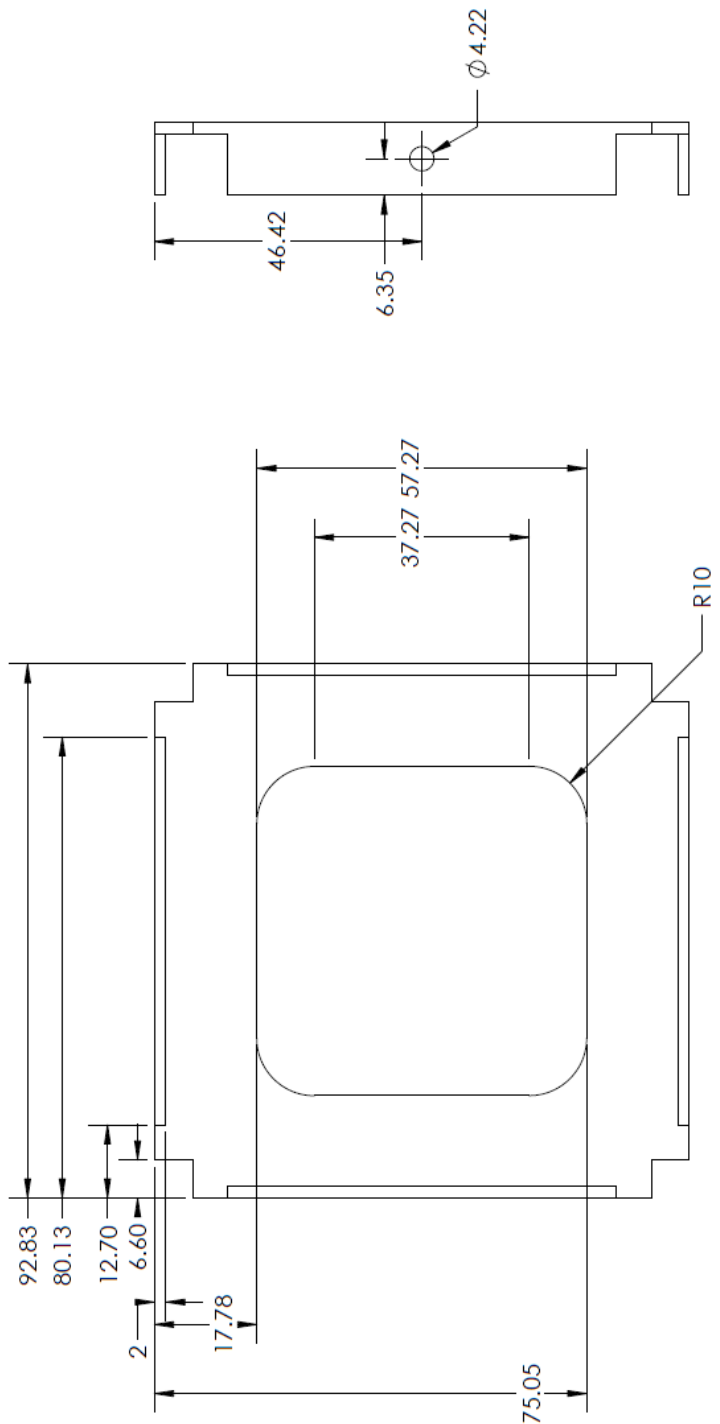
DETAIL B
SCALE 1 : 1



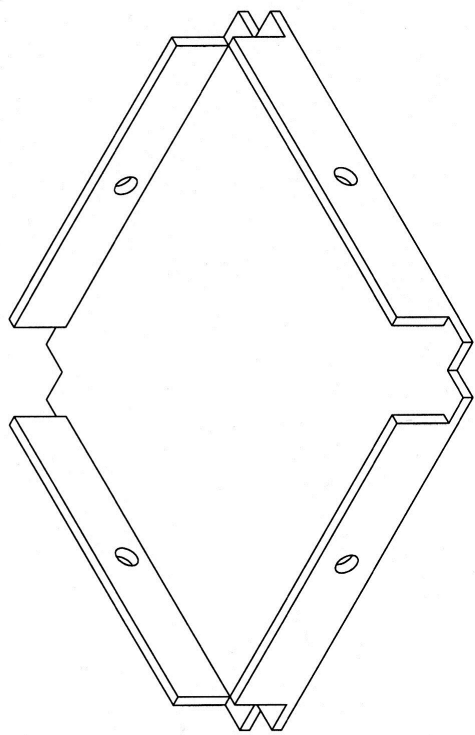
UNLESS OTHERWISE SPECIFIED:		NAME	DATE	NanoSat- UPAAC	
DIMENSIONS ARE IN millimeters		OJ	2/3/13	TITLE:	
TOLERANCES:		DRAWN	CHECKED		
FRACTIONAL: ± 0.05		BEND	+	Corner Brackets	
ANGULAR: MACH ²	ONE PLACE DECIMAL	MACH ²	± 0.1	End Detail	
TWO PLACE DECIMAL: ± 0.05		ENG APPR.			
INTERPRET GEOMETRIC		MFG APPR.			
TOLENCING PER:		Q.A.			
MATERIAL	6061 Aluminum				
FINISH	None				
NEXT ASSY	USED ON				
APPLICATION	DO NOT SCALE DRAWING				
4	3				
5	2				
	1				

PROPRIETARY AND CONFIDENTIAL
THE INFORMATION CONTAINED IN THIS
DRAWING IS THE SOLE PROPERTY OF
<INSERT COMPANY NAME HERE>. ANY
REPRODUCTION IN PART OR AS A WHOLE
WITHOUT THE WRITTEN PERMISSION OF
<INSERT COMPANY NAME HERE> IS
PROHIBITED.

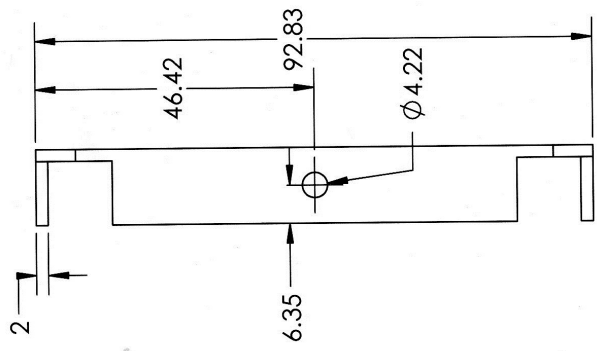
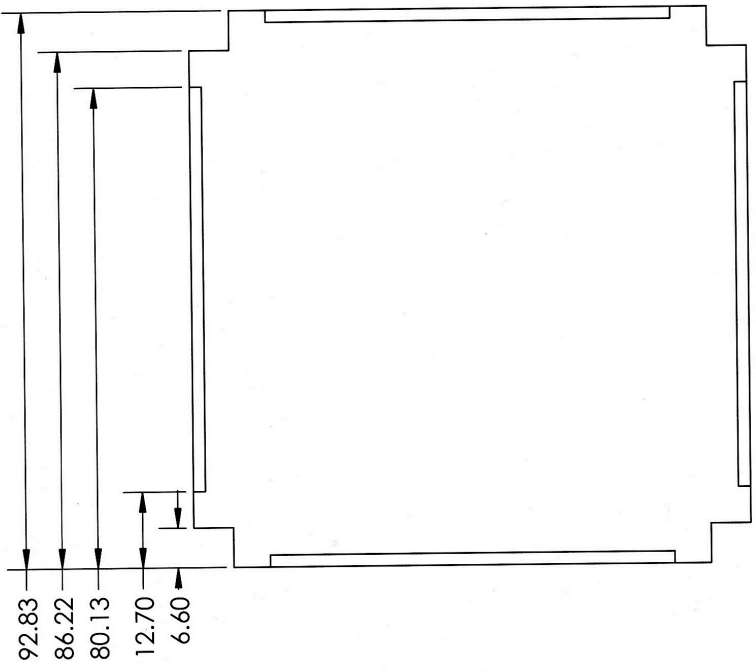
		<p>UNLESS OTHERWISE SPECIFIED: DIMENSIONS ARE IN millimeters TOLERANCES: TWO PLACE DECIMAL ±0.05</p> <table border="1"> <tr><td>DRAWN</td><td>NAME OJ</td><td>DATE 2/3/13</td></tr> <tr><td>CHECKED</td><td></td><td></td></tr> <tr><td>ENG APPR.</td><td></td><td></td></tr> <tr><td>MFG APPR.</td><td></td><td></td></tr> <tr><td>Q.A.</td><td></td><td></td></tr> </table> <p>INTERPRET GEOMETRIC TOLENCING PER: MATERIAL: 6061 Aluminum</p> <table border="1"> <tr><td>NEXT ASSY</td><td>USED ON</td><td>FINISH None</td></tr> <tr><td>APPLICATION</td><td colspan="2">DO NOT SCALE DRAWING</td></tr> </table>		DRAWN	NAME OJ	DATE 2/3/13	CHECKED			ENG APPR.			MFG APPR.			Q.A.			NEXT ASSY	USED ON	FINISH None	APPLICATION	DO NOT SCALE DRAWING	
DRAWN	NAME OJ	DATE 2/3/13																						
CHECKED																								
ENG APPR.																								
MFG APPR.																								
Q.A.																								
NEXT ASSY	USED ON	FINISH None																						
APPLICATION	DO NOT SCALE DRAWING																							
<p>NanoSat- UP AAC Title: Top Face Overview</p>		<p>SIZE DWG. NO. A UP AAC-STRUC-M-103 REV 1</p>																						
<p>PROPRIETARY AND CONFIDENTIAL THE INFORMATION CONTAINED IN THIS DRAWING IS THE SOLE PROPERTY OF [REDACTED] COMPANY. NAME HERE; ANY REPRODUCTION IN PART OR AS A WHOLE WITHOUT THE WRITTEN PERMISSION OF [REDACTED] COMPANY. NAME HERE, IS PROHIBITED.</p>		<p>SCALE: 1:1 SHEET 1 OF 1</p>																						



UNLESS OTHERWISE SPECIFIED:		DRAWN	NAME	DATE
DIMENSIONS ARE IN millimetres		O.J.		2/3/13
TOLERANCES:		CHECKED		
TWO PLACE DECIMAL ±0.05		ENG APPR.		
		MFG APPR.		
		O.A.		
INTERPRET GEOMETRIC TOLERANCING PER:				
MATERIAL		6061 Aluminum		
FINISH		None		
NEXT ASSY		USED ON		
APPLICATION			DO NOT SCALE DRAWING	
NanoSat- UPAAC Top Face TITLE: SHEET 1 OF 1				
PROPRIETARY AND CONFIDENTIAL		THE INFORMATION CONTAINED IN THIS DRAWING IS THE SOLE PROPERTY OF <INSERT COMPANY NAME HERE>. ANY REPRODUCTION IN PART OR AS A WHOLE WITHOUT THE WRITTEN PERMISSION OF <INSERT COMPANY NAME HERE> IS PROHIBITED.		



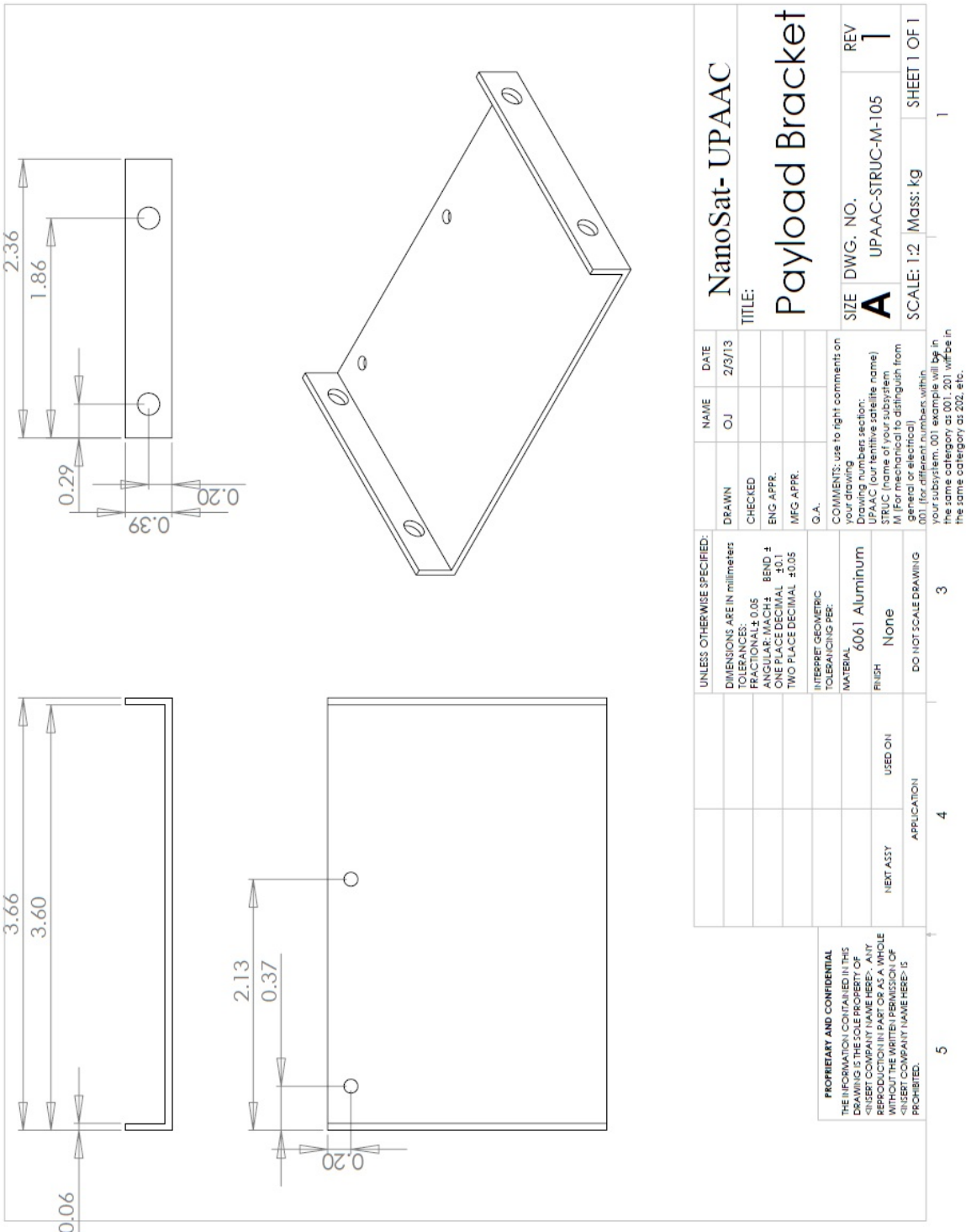
UNLESS OTHERWISE SPECIFIED:		NAME	DATE
DIMENSIONS ARE IN millimeters		OJ	2/3/13
TOLERANCES: TWO PLACE DECIMAL. ±0.05		CHECKED	
		ENG APPR.	
		MFG APPR.	
		Q.A.	
INTERPRET GEOMETRIC TOLERANCING PER:			
MATERIAL:		6061 Aluminum	
FINISH:		None	
USED ON:		DO NOT SCALE DRAWING	
APPLICATION			
PROPRIETARY AND CONFIDENTIAL THE INFORMATION CONTAINED IN THIS DRAWING IS THE SOLE PROPERTY OF <INSERT COMPANY NAME HERE>. ANY REPRODUCTION IN PART OR AS A WHOLE WITHOUT THE WRITTEN PERMISSION OF <INSERT COMPANY NAME HERE> IS PROHIBITED.		SIZE	DWG. NO.
		A	UPAAC-STRUC-M-104
		REV	1
TITLE:		Bottom Face Overview	
SCALE: 1:1		SHEET 1	

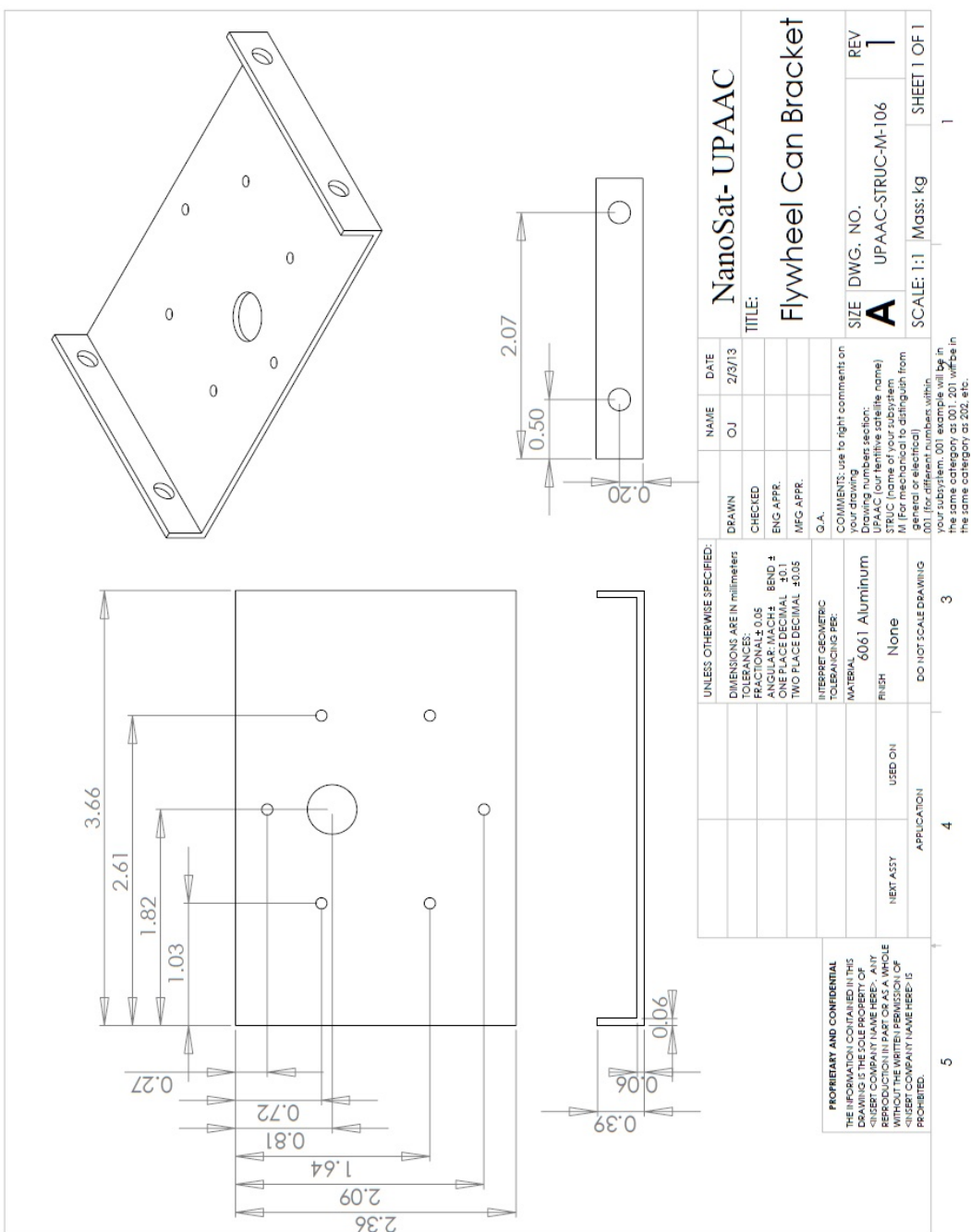


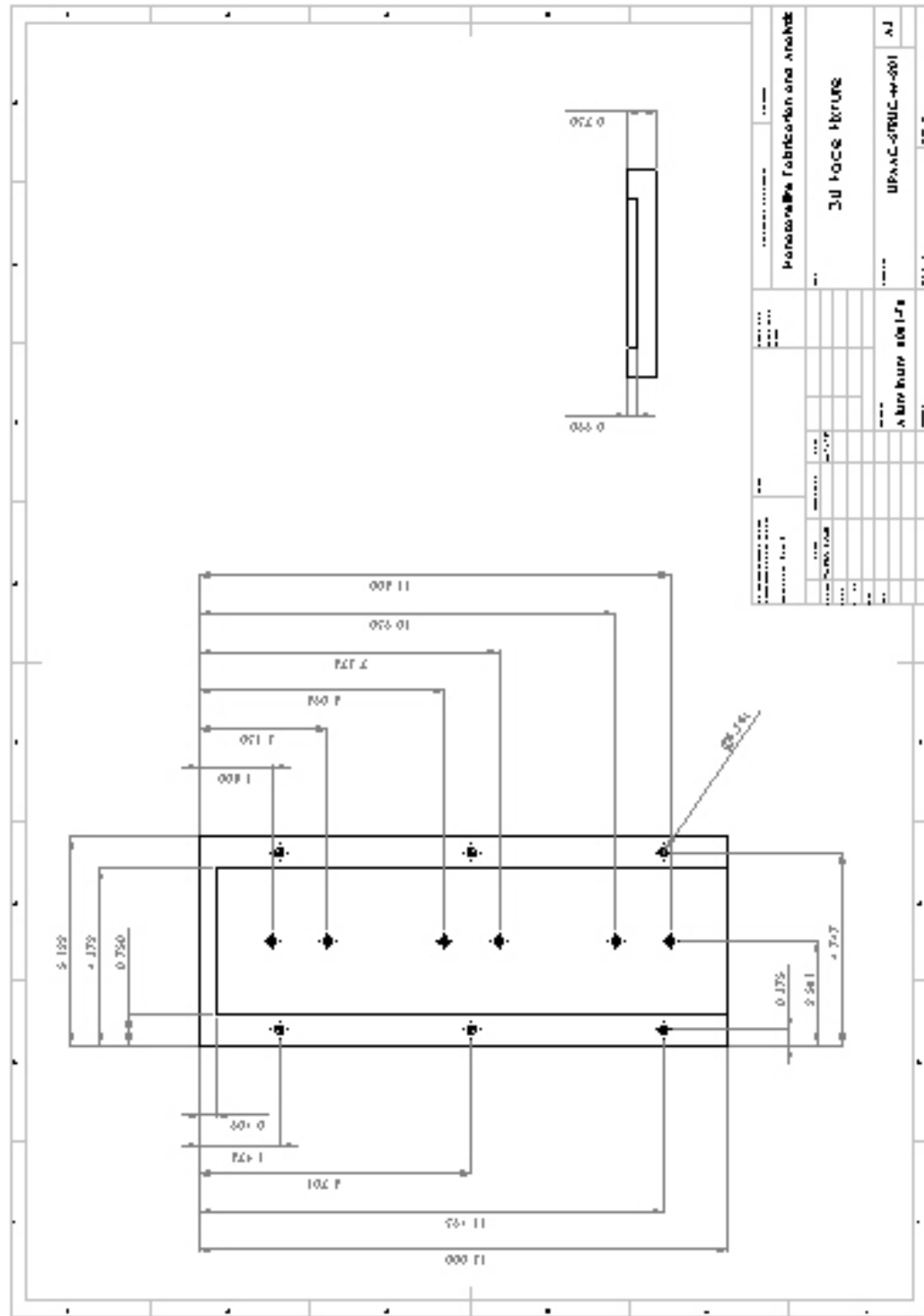
UNLESS OTHERWISE SPECIFIED: DIMENSIONS ARE IN millimeters TOLERANCES: TWO PLACE DECIMAL ±0.05		NAME O.J.	DATE 2/3/13
DRAWN	CHECKED	ENG APPR.	MFG APPR.
INTERPRET GEOMETRIC TOLERANCING PER:	Q.A.		
MATERIAL	6061 Aluminum	FINISH	None
NEXT ASSY	USED ON	APPLICATION	DO NOT SCALE DRAWING

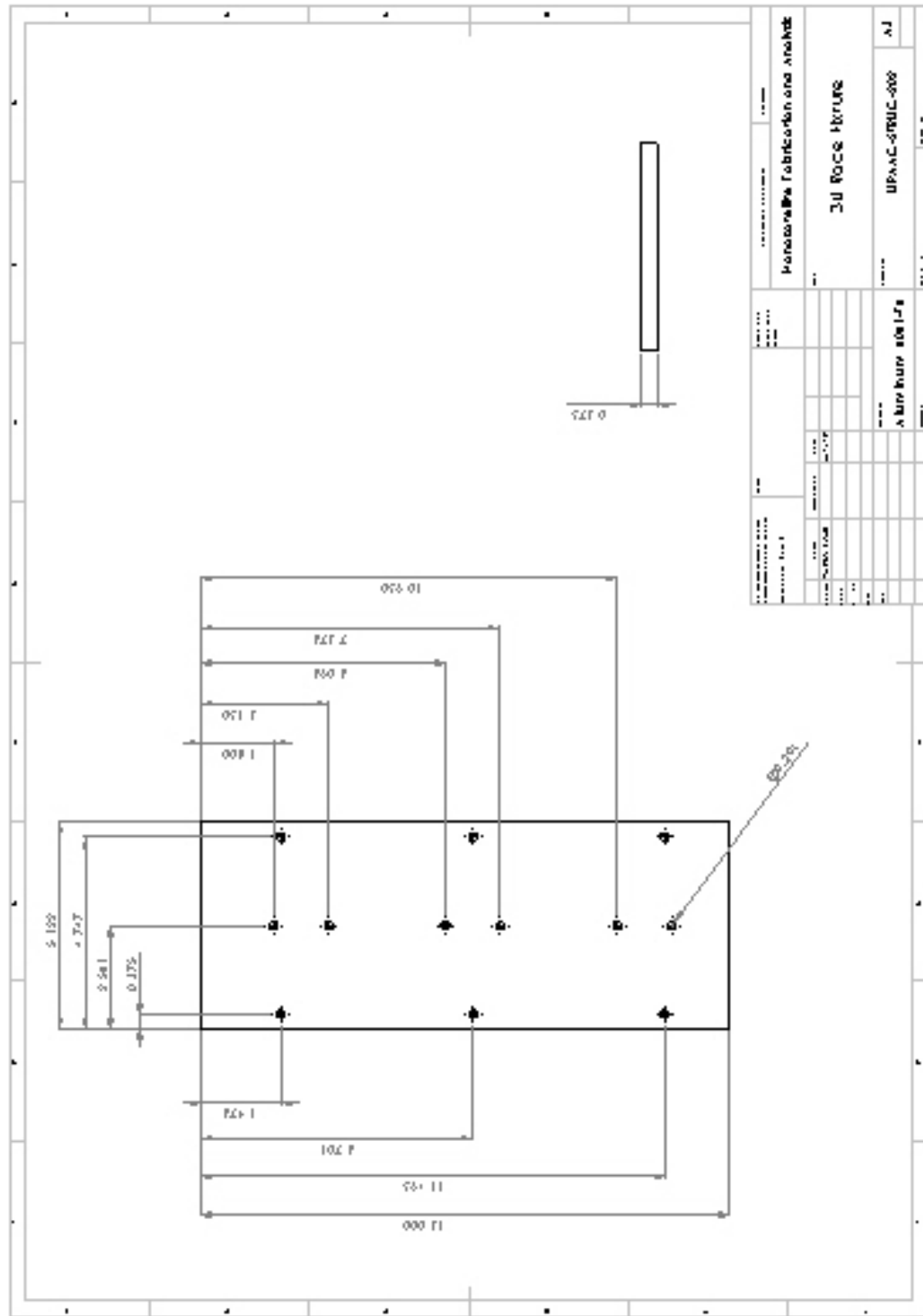
PROPRIETARY AND CONFIDENTIAL
THE INFORMATION CONTAINED IN THIS
<INSERT COMPANY NAME HERE>, ANY
REPRODUCTION IN PART OR AS A WHOLE
WITHOUT THE WRITTEN PERMISSION OF
<INSERT COMPANY NAME HERE> IS
PROHIBITED.

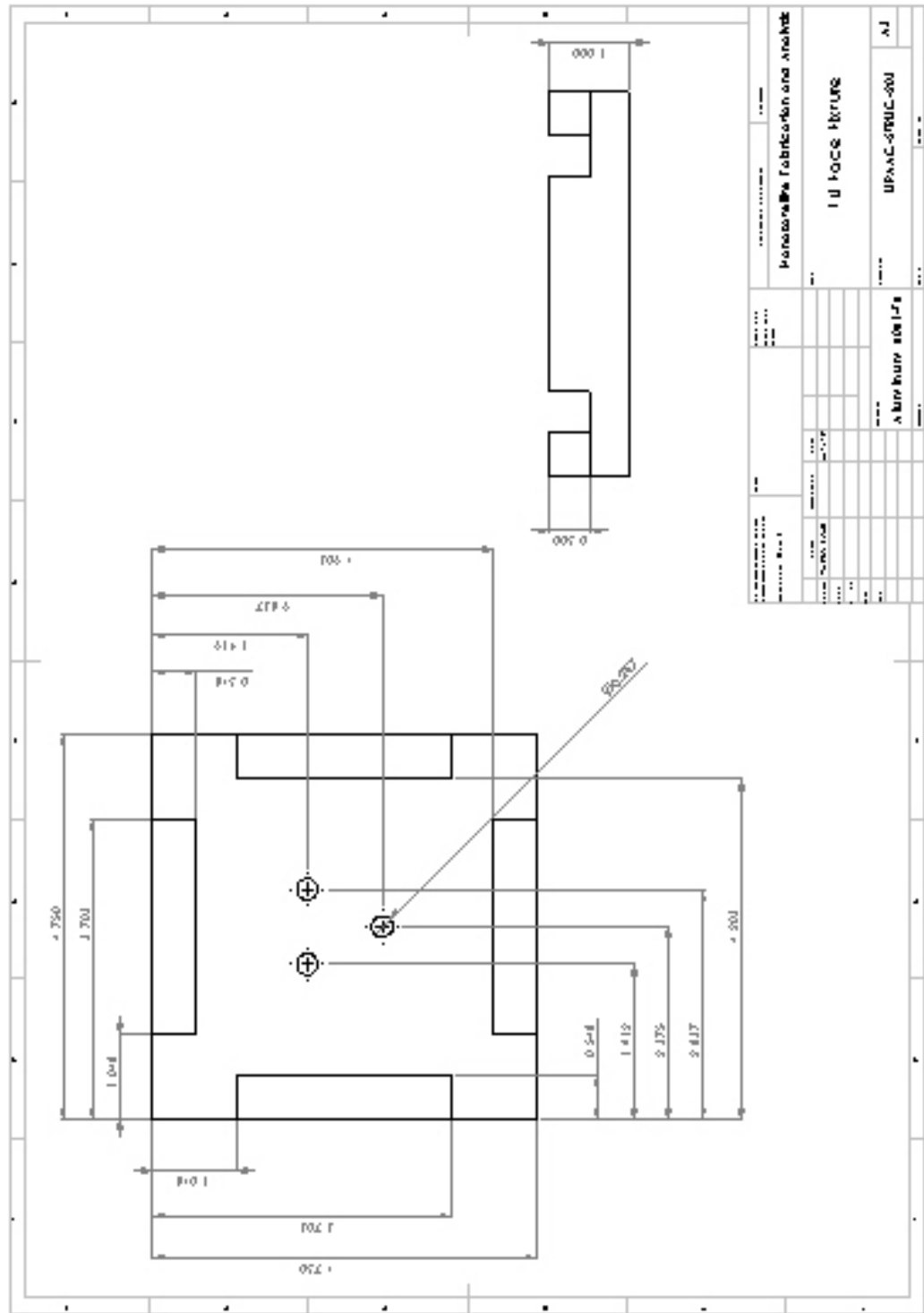
SIZE	DWG. NO.	REV
A	UPAAC-STRUC-M-104	1
SCALE: 1:1		SHEET

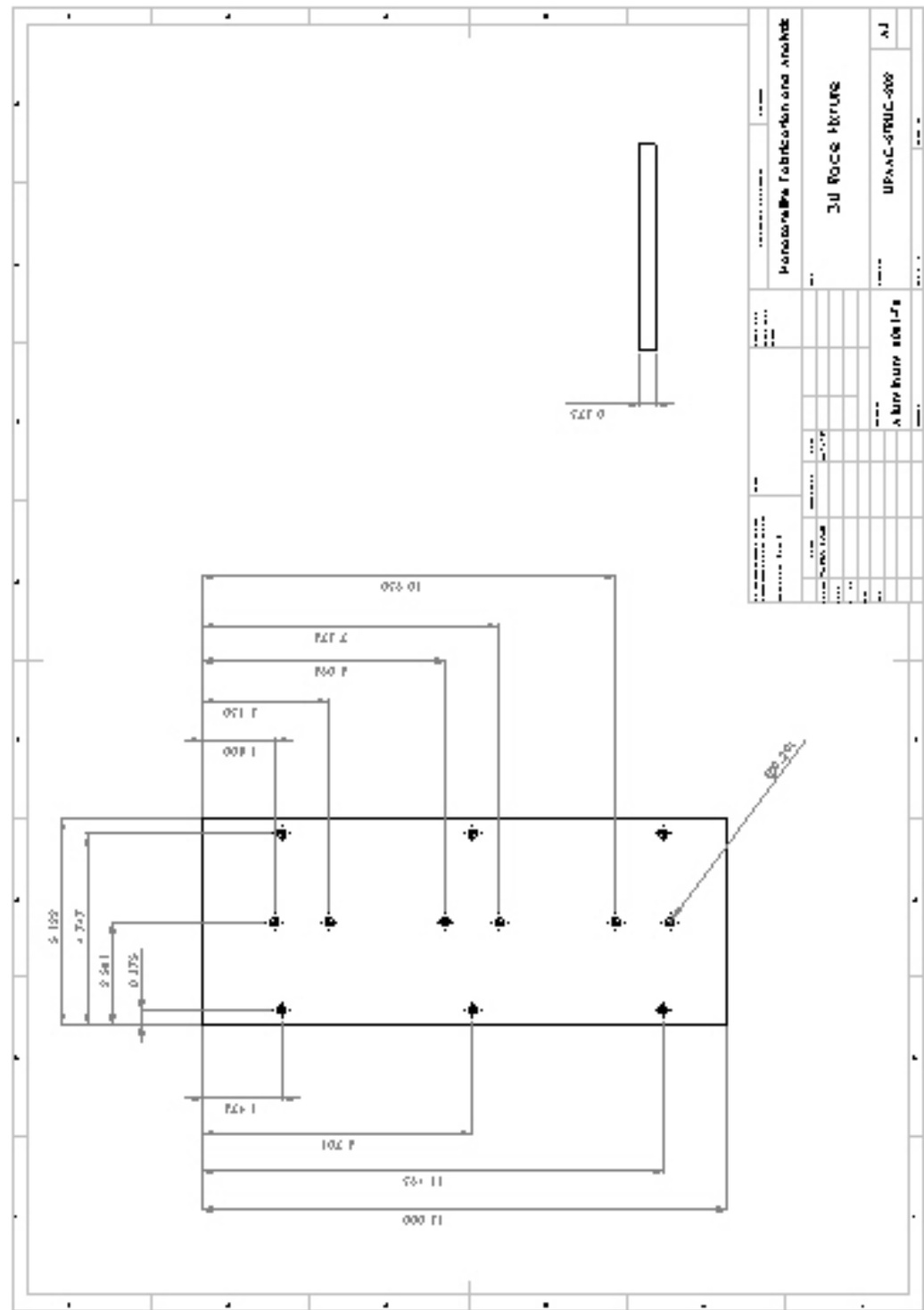


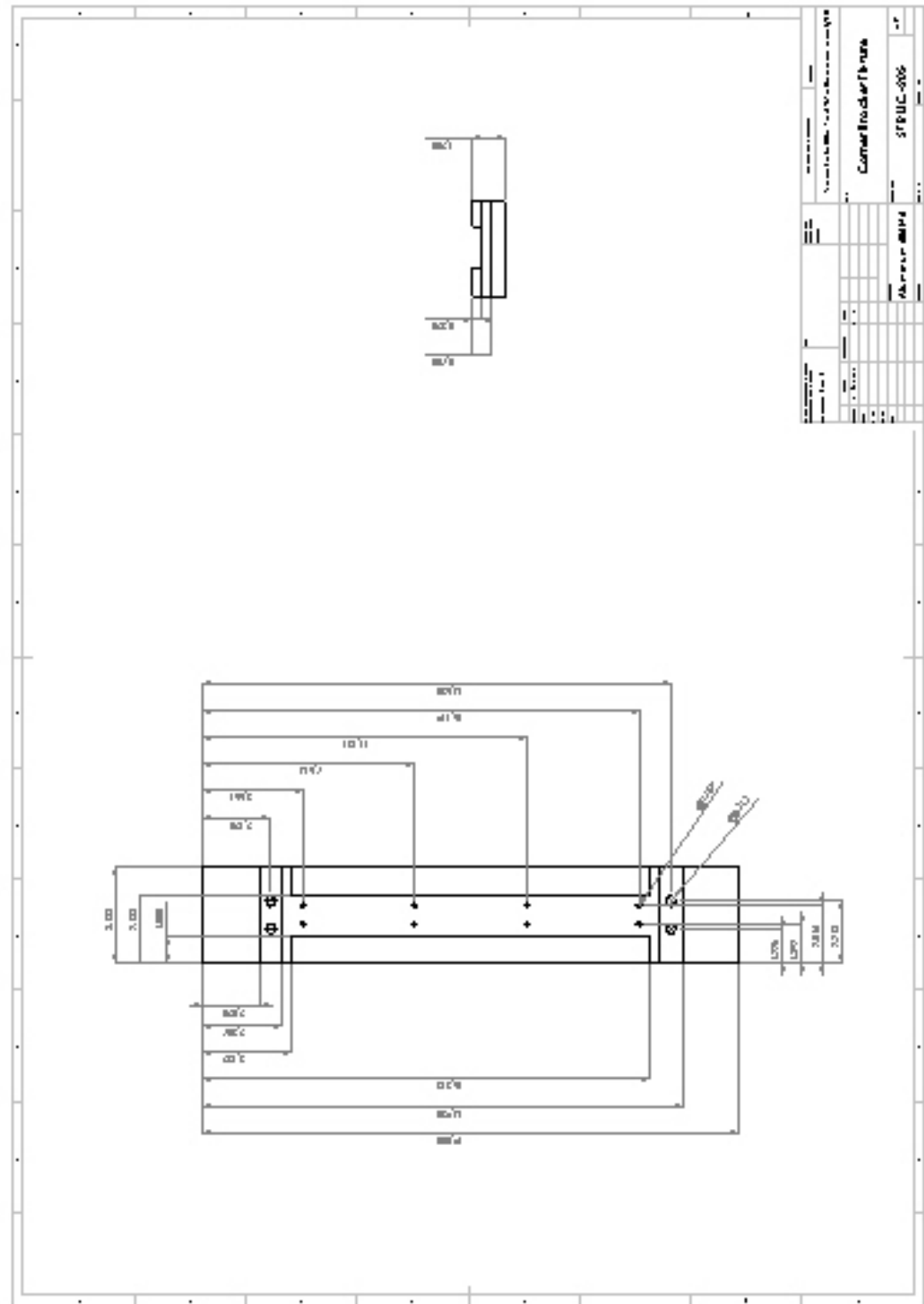


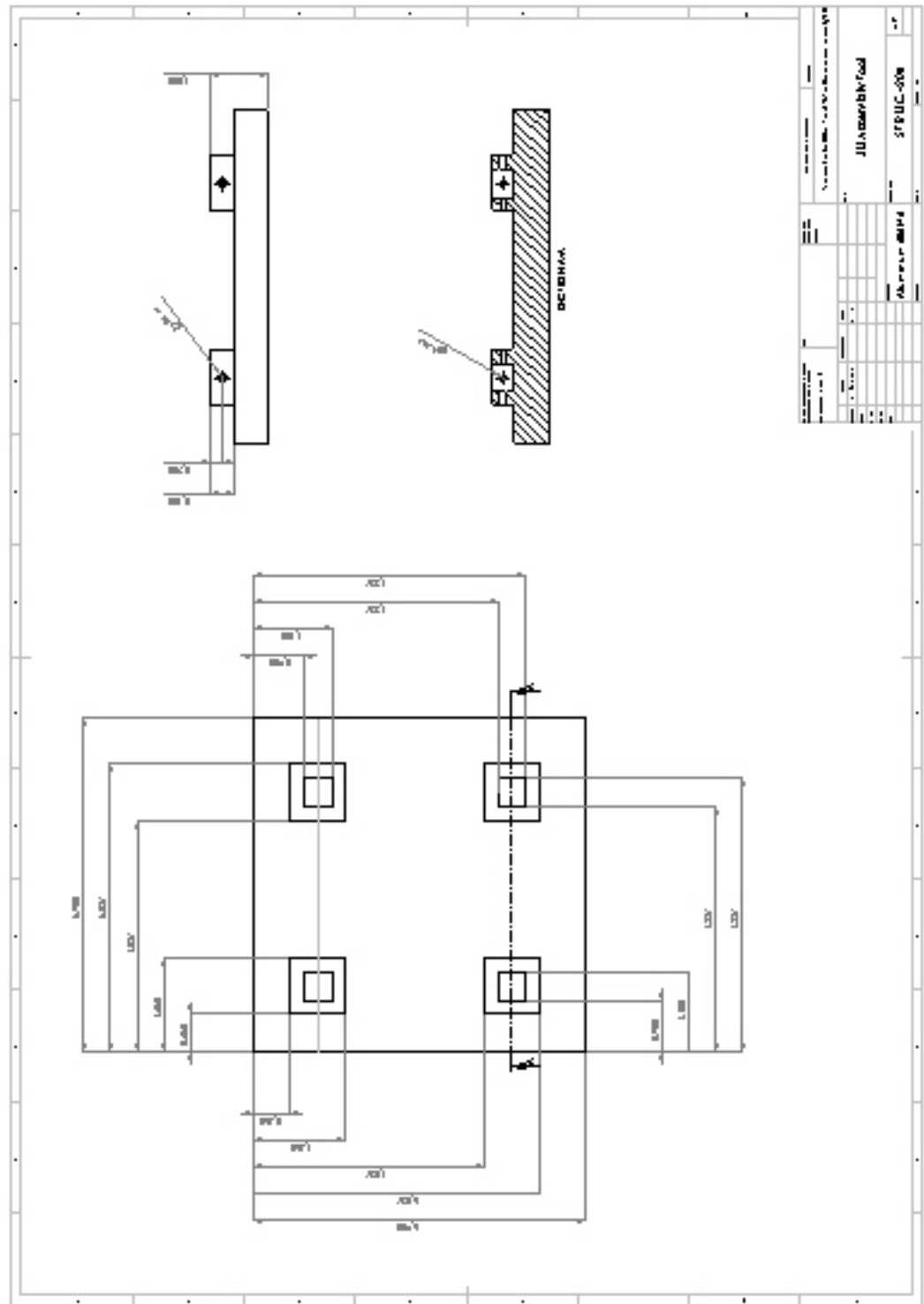


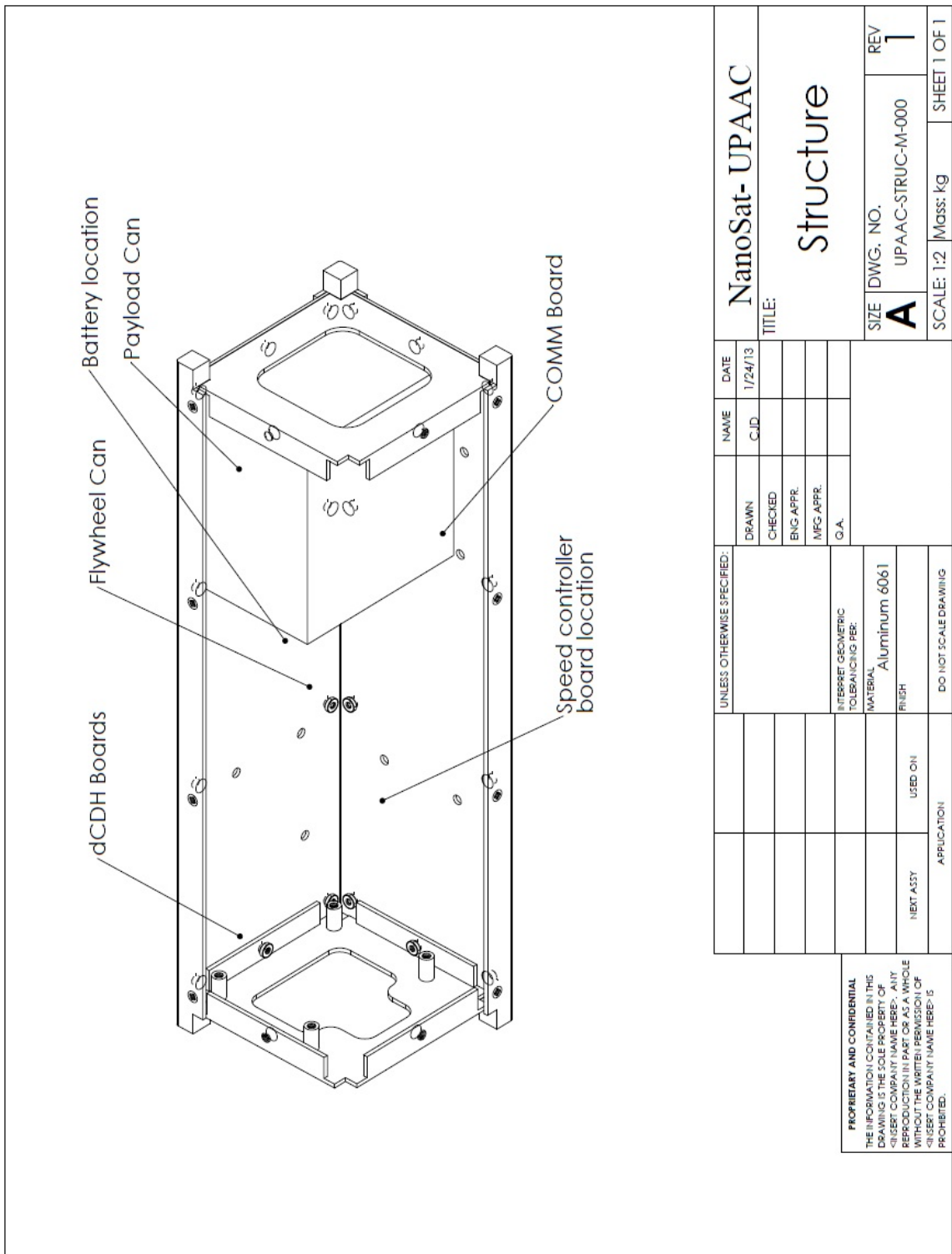


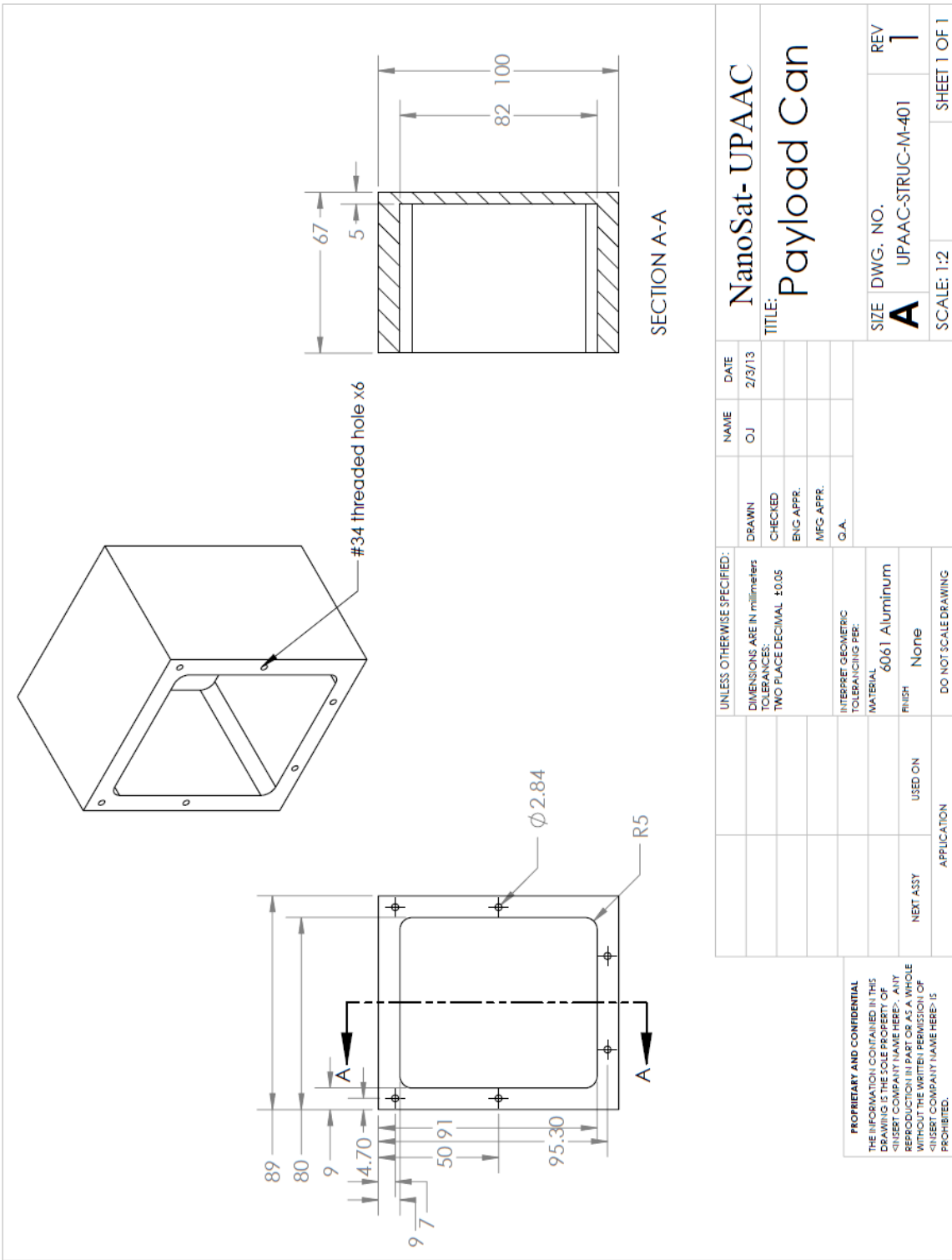


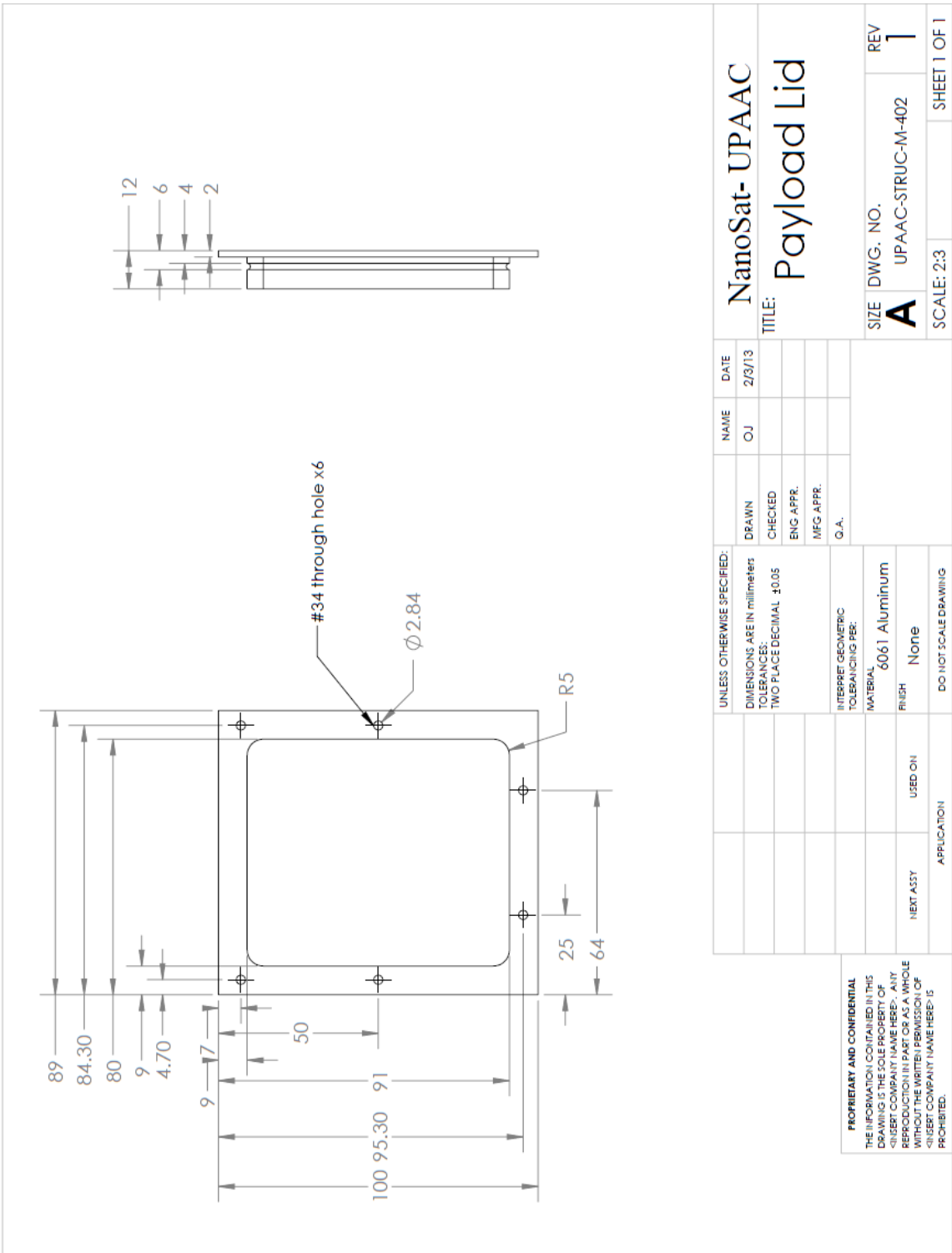




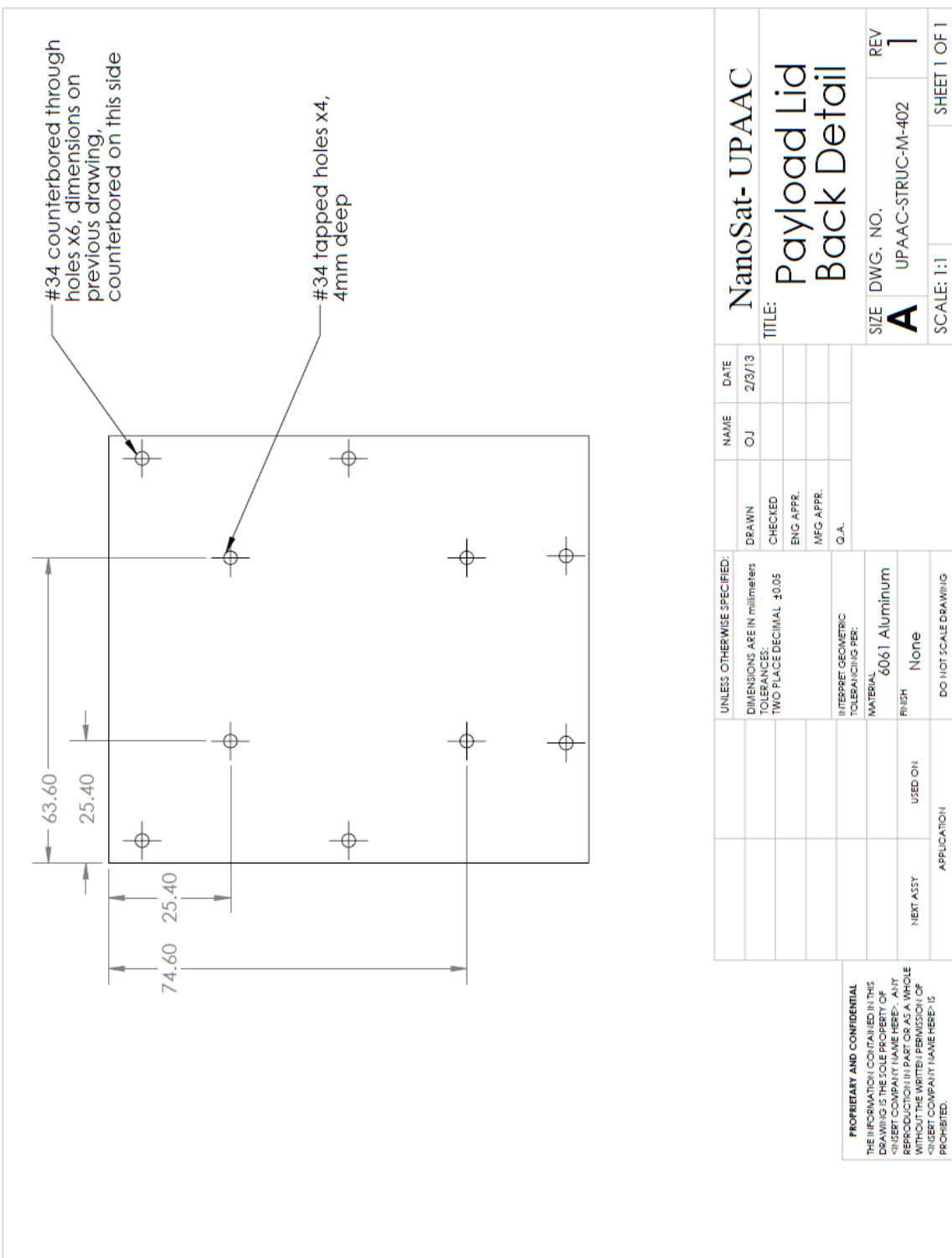








		<p>DETAIL B SCALE 2 : 1</p>		<table border="1"> <tr> <td colspan="2">UNLESS OTHERWISE SPECIFIED:</td></tr> <tr> <td>DIMENSIONS ARE IN millimeters</td><td>DRAWN</td></tr> <tr> <td>TOLERANCES: TWO PLACE DECIMAL .005</td><td>CHECKED</td></tr> <tr> <td></td><td>ENG APPR.</td></tr> <tr> <td></td><td>MFG APPR.</td></tr> <tr> <td></td><td>Q.A.</td></tr> <tr> <td colspan="2">INTERPRET GEOMETRIC TOLERANCING PER:</td></tr> <tr> <td colspan="2">MATERIAL: 6061 Aluminum</td></tr> <tr> <td>FINISH: None</td><td>USED ON</td></tr> <tr> <td>NEXT ASSY</td><td>APPLICATION</td></tr> <tr> <td colspan="2">DO NOT SCALE DRAWING</td></tr> </table>		UNLESS OTHERWISE SPECIFIED:		DIMENSIONS ARE IN millimeters	DRAWN	TOLERANCES: TWO PLACE DECIMAL .005	CHECKED		ENG APPR.		MFG APPR.		Q.A.	INTERPRET GEOMETRIC TOLERANCING PER:		MATERIAL: 6061 Aluminum		FINISH: None	USED ON	NEXT ASSY	APPLICATION	DO NOT SCALE DRAWING	
UNLESS OTHERWISE SPECIFIED:																											
DIMENSIONS ARE IN millimeters	DRAWN																										
TOLERANCES: TWO PLACE DECIMAL .005	CHECKED																										
	ENG APPR.																										
	MFG APPR.																										
	Q.A.																										
INTERPRET GEOMETRIC TOLERANCING PER:																											
MATERIAL: 6061 Aluminum																											
FINISH: None	USED ON																										
NEXT ASSY	APPLICATION																										
DO NOT SCALE DRAWING																											
				<p>PROPRIETARY AND CONFIDENTIAL THE INFORMATION CONTAINED IN THIS DRAWING IS THE SOLE PROPERTY OF <INSERT COMPANY NAME HERE>. ANY REPRODUCTION IN PART OR AS A WHOLE WITHOUT THE WRITTEN PERMISSION OF <INSERT COMPANY NAME HERE> IS PROHIBITED.</p>																							
				<p>NAME: O.J. DATE: 2/3/13 TITLE: NanoSat- UPAAAC Payload Lid Groove Detail REV: 1 SIZE DWG. NO. A UPAAAC-STRUC-M-402 SCALE: 1:1 SHEET 1 OF 1</p>																							



C Detailed Calculations

C.1 SatTherm Code

The SatTherm code package that was used by the 2013 design team is included on a USB stick submitted with this thesis.

C.2 AACS Code and Calculations

C.2.1 Control Code

AACS Control Code for Arduino Platform:

```
//The Wire library is used for I2C communication
//Note: Mega 2560 uses pins 20 and 21 instead of A4 and A5
#include <Wire.h>

//This is a list of registers in the ITG-3200. Registers are parameters that determine how the sensor will behave, or they can hold data that represent the sensors current status.
//To learn more about the registers on the ITG-3200, download and read the datasheet.
char WHO_AM_I = 0x00;
char SMPLRT_DIV= 0x15;
char DLPF_FS = 0x16;
char GYRO_XOUT_H = 0x1D;
char GYRO_XOUT_L = 0x1E;
char GYRO_YOUT_H = 0x1F;
char GYRO_YOUT_L = 0x20;
char GYRO_ZOUT_H = 0x21;
char GYRO_ZOUT_L = 0x22;

//This is a list of settings that can be loaded into the registers.
//DLPF, Full Scale Register Bits
//FS_SEL must be set to 3 for proper operation
//Set DLPF_CFG to 3 for 1kHz Fint and 42 Hz Low Pass Filter
char DLPF_CFG_0 = 1<<0;
char DLPF_CFG_1 = 1<<1;
char DLPF_CFG_2 = 1<<2;
char DLPF_FS_SEL_0 = 1<<3;
char DLPF_FS_SEL_1 = 1<<4;

//I2C devices each have an address. The address is defined in the datasheet for the device. The ITG-3200 breakout board can have different address depending on how
//the jumper on top of the board is configured. By default, the jumper is connected to the VDD pin. When the jumper is connected to the VDD pin the I2C address
```

```

//is 0x69.
char itgAddress = 0x69;

//Calibration for offsets
int xbias=-10;
int ybias=42;
int zbias=-12;
double rawtorpm=0.0128; //value to convert raw data to rpm
double rpmtorads; //value to convert rpm to rad/sec

int motorpin=6;
int direcpin=5;

//In the setup section of the sketch the serial port will be configured, the i2c
communication will be initialized, and the itg-3200 will be configured.

//Controller variables
double wsdes=0.0; //Reference r(t), aka desired speed in rpm

double Kp=2.0; //Controller gains
double Kv=1.0;
double Ki=0.1;

double actuator=250.0; //This is the value that relates input u (rad/sec) to tau
(Nm).

//Note that u is actually converted into a PWM which the motor controller un-
derstands as our desired tau.

//Also, this value might be dynamic, as in it changes with time.

double x0=0; //Or use another known initial value.
double error=wsdes-x0; //Error value e(t) that becomes u(t) through PID control.
double ws; //Output y(t), aka the actual speed in rad/sec.
double lasterror,interror=0; //Variables for I control
double differror; //Variable for D control
double P,I,D,u; //Variables for input
int direc=LOW; //CW (LOW) and CCW (HIGH)
//Check if directions are correct

//Timer variables
double previousMillis=0;
double interval=100.0; //Control loop runs each 50 ms.
double delta_t=interval/1000.0; //Time step for differential input

void setup(){
//Create a serial connection using a 9600bps baud rate.
Serial.begin(9600);

//Initialize the I2C communication. This will set the Arduino up as the 'Master'
device.

Wire.begin();

```

```

//Read the WHO_AM_I register and print the result
char id=0;
id = itgRead(itgAddress, 0x00);
Serial.print("ID: ");
Serial.println(id, HEX);

//Configure the gyroscope
//Set the gyroscope scale for the outputs to +/-2000 degrees per second
itgWrite(itgAddress, DLPF_FS, (DLPF_FS_SEL_0|DLPF_FS_SEL_1|DLPF_CFG_0));
//Set the sample rate to 100 hz
itgWrite(itgAddress, SMPLRT_DIV, 9);

rpmtorads=2.0*PI/60.0;
wsdes=wsdes*rpmtorads; //Convert rpm to rad/sec

pinMode(motorpin,OUTPUT);
pinMode(direcpin,OUTPUT);
}

void loop(){
//Create variables to hold the output rates.
int xRate, yRate, zRate;
double xrpm, yrpm, zrpm;
double xrads, yrads, zrads;
unsigned long currentMillis = millis();

//Each interval is 50ms. Consider using nested loop to separate sensor readings
and motor output.
if(currentMillis - previousMillis > interval) {
    previousMillis = currentMillis;

//Sensors: Read the x,y and z output rates from the gyroscope.
xRate = readX(); //Figure out which one to use for ws.
yRate = readY();
zRate = readZ(); //It's this one, right?
xrpm=(xRate+xbias)*rawtorpm; //Convert to rpm
yrpm=(yRate+ybias)*rawtorpm;
zrpm=(zRate+zbias)*rawtorpm;
xrads=xrpm*rpmtorads;
yrads=yrpm*rpmtorads; //Convert to rad/sec
zrads=zrpm*rpmtorads;
/*Serial.print(xrpm); //Biases included
Serial.print('\t'); //This will output the data used to generate graphs.
Serial.print(yrpm);
Serial.print('\t');
Serial.print(zrpm);
Serial.print('\t');
Serial.println(currentMillis);*/
}

```

```

//Wait 10ms before reading the values again. (Remember, the output rate was
set to 100hz and 1reading per 10ms = 100hz.)

//Control code:
ws=yrads; //Feedback, y(t)
lasterror=error;
error=wsdes-ws; //r(t)-y(t)=e(t)
P=Kp*error; //Proportional control term
interror=interror+error*delta_t;//int(error*dt) 0 to inf
I=Ki*interror; //Integral control term
differror=error-lasterror; //e(t)-e(t-deltat)
D=Kv*differror/delta_t; //Differential control term
u=P+I+D;
u=u*actuator; //Convert input, u (rad/sec) to PWM which generates the input
on the plant, tau (Nm).

if(error<0)
direc=LOW;
else
direc=HIGH;
if(u<0)
u=-u;
if(u>255.0)
u=255.0;
analogWrite(motorpin,u);
digitalWrite(direcpin,direc);
/*Serial.print(error);
Serial.print('\t');
Serial.print(direc);
Serial.print('\t');
Serial.println(u);*/
}

void itgWrite(char address, char registerAddress, char data)
{
//Initiate a communication sequence with the desired i2c device
Wire.beginTransmission(address);
//Tell the I2C address which register we are writing to
Wire.write(registerAddress);
//Send the value to write to the specified register
Wire.write(data);
//End the communication sequence
Wire.endTransmission();
}

```

```

//This function will read the data from a specified register on the ITG-3200 and
return the value.
//Parameters:
// char address: The I2C address of the sensor. For the ITG-3200 breakout the
address is 0x69.
// char registerAddress: The address of the register on the sensor that should be
read
//Return:
// unsigned char: The value currently residing in the specified register
unsigned char itgRead(char address, char registerAddress)
{
//This variable will hold the contents read from the i2c device.
unsigned char data=0;

//Send the register address to be read.
Wire.beginTransmission(address);
//Send the Register Address
Wire.write(registerAddress);
//End the communication sequence.
Wire.endTransmission();

//Ask the I2C device for data
Wire.beginTransmission(address);
Wire.requestFrom(address, 1);

//Wait for a response from the I2C device
if(Wire.available()){
//Save the data sent from the I2C device
data = Wire.read();
}

//End the communication sequence.
Wire.endTransmission();

//Return the data read during the operation
return data;
}

//This function is used to read the X-Axis rate of the gyroscope. The function
returns the ADC value from the Gyroscope
//NOTE: This value is NOT in degrees per second.
//Usage: int xRate = readX();
int readX(void)
{
int data=0;
data = itgRead(itgAddress, GYRO_XOUT_H)<<8;
data |= itgRead(itgAddress, GYRO_XOUT_L);

return data;
}

```

```

}

//This function is used to read the Y-Axis rate of the gyroscope. The function
returns the ADC value from the Gyroscope
//NOTE: This value is NOT in degrees per second.
//Usage: int yRate = readY();
int readY(void)
{
    int data=0;
    data = itgRead(itgAddress, GYRO_YOUT_H)<<8;
    data |= itgRead(itgAddress, GYRO_YOUT_L);

    return data;
}

//This function is used to read the Z-Axis rate of the gyroscope. The function
returns the ADC value from the Gyroscope
//NOTE: This value is NOT in degrees per second.
//Usage: int zRate = readZ();
int readZ(void)
{
    int data=0;
    data = itgRead(itgAddress, GYRO_ZOUT_H)<<8;
    data |= itgRead(itgAddress, GYRO_ZOUT_L);

    return data;
}

```

C.2.2 Controller

Equations C.1 and C.2 show the state-space realization of the equations of motion for the spacecraft and reaction wheel rotation. Note that these are cross-coupled first order equations. The open loop Simulink model used is shown in Figure . The motor block is explained in depth in Chapter 8.

$$\begin{bmatrix} \dot{\omega}_s \\ \dot{\omega}_f \end{bmatrix} = \begin{bmatrix} -b/I_s & b/I_s \\ b/I_f & -b/I_f \end{bmatrix} \begin{bmatrix} \omega_s \\ \omega_f \end{bmatrix} + \begin{bmatrix} 1/I_s \\ 1/I_f \end{bmatrix} \tau(t) \quad (\text{C.1})$$

$$y(t) = [1 \ 0] \begin{bmatrix} \omega_s \\ \omega_f \end{bmatrix} + [0] \tau(t) \quad (\text{C.2})$$

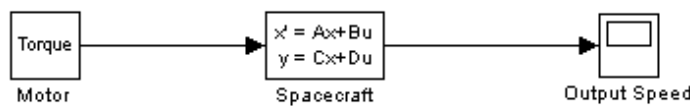


Figure C.1: Open loop Simulink model.

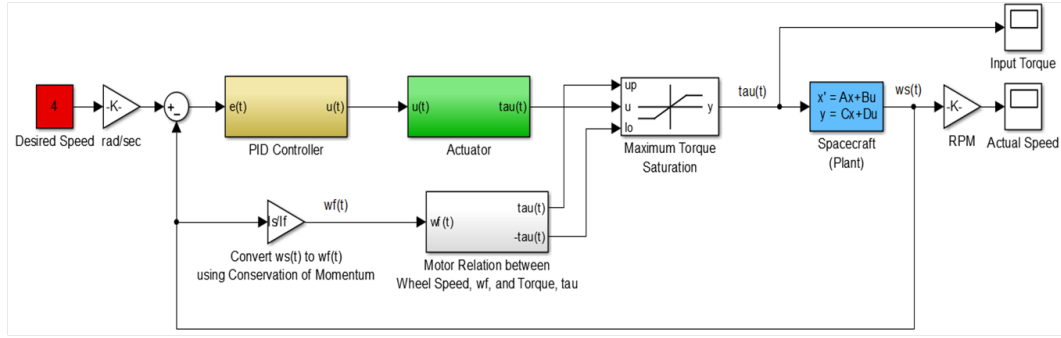


Figure C.2: Closed loop Simulink model.

The open loop Simulink model used is shown in Figure C.1. The motor block is explained in depth in Chapter 8. The closed loop Simulink model used is shown in Figure C.2. Components to this system are also explained in Chapter 8.

C.2.3 Steady State Motor Analysis MATLAB Script

```

clear; close all
% AAC
%
% Steady State Motor Analysis
%
% Elliott Martin
% 4/30/13
% w = v/kt - R/(ktke)*Tm
% 4 Volt Supply
V4 = 4; % V
w_nl = 41740; % rpm
Tstall4 = 0.222; % mNm
kt = V4/w_nl; % mNm/A
slope = 187793; % rpm/mNm
Tm4 = [0:.0001:Tstall4]; % mNm
w4 = -slope.*Tm4 + V4/kt; % rpm
w4 = w4/1000; % krpm
% 3.3 Volt Supply
V3 = 3.3; % V
Tstall3 = V3/(slope*kt);
Tm3 = [0:.0001:Tstall3];
w3 = -slope*Tm3 + V3/kt; % rpm
w3 = w3/1000; % krpm
plot(Tm4,w4,'r');
hold on;
plot(Tm3,w3,'b');
grid on

```

```

xlabel('Torque (mNm)');
ylabel('Angular Speed (krpm)');
%title('Angular Speed vs. Torque of Brushless DC Motor');
legend('4 Volt', '3.3 Volt')
% Current Draw vs. Torque
% v = 4V
I4 = Tm4/kt + Tstall4/kt; % A
figure;
plot(Tm4, I4);

```

C.2.4 Reaction Wheel Sizing MATLAB Script

```

clear; close all
% AAC
% Momentum Exchange Analysis and Reaction Wheel Sizing
% Using Faulhaber Brushless Flat Penny Motor:
% Series 1202H004BH
% Elliott Martin
% May 3, 2013
% Rev 2.0
% Note: Steady State Motor Analysis completed in Matlab file "
%% Motor Characteristics
% Target Motor Speed and Output Torque
% Corresponding Motor output Torque
% 3.3 Volt Supply to Motor
V3 = 3.3; % V
kt = 9.5831e-05; % mNm/A
slope = 187793;
Tstall3 = V3/(slope*kt);
Tm3 = [0:.0001:Tstall3];
w3 = -slope*Tm3 + V3/kt; % rpm
w3 = w3/1000; % krpm
% Corresponding Disk Speed
spin_disk = w3*1000; % rpm
w_disk = spin_disk*2*pi/60; % rad/s
plot(Tm3,w3,'b');
xlabel('Torque (mNm)');
ylabel('Speed (krpm)');
title('Speed vs. Torque of Brushless DC Motor');
legend('3.3 Volt')
%% Properties of Spacecraft
% Note: subscript sc refers to Spacecraft
% Note: z-axis is defined to run along longest dimension (h) of Spacecraft
% Mass
m_sc = 4.0; % kg

```

```

% Dimensions
h_sc = 0.34; % m
a = 0.1; % m
b = 0.1; % m
% Mass Moment of Inertia
Izz = m_sc*(a^2+b^2)/12; % kgm^2
I_sc = Izz; % kgm^2
%% Spin of Spacecraft
% Note: Typical Spin of Spacecraft about z-axis after histerisis
% stabelisation is 1-2 rpm.
spin_sc = 2; % rpm
w_sc = spin_sc*2*pi/60; % rad/s
%% Momentum Transfer
% Momentum is conserved: H(sc) + H(disk) = 0
% where H = I*w
% The target speed of the motor and acutal speed of the spacecraft are used
% to determine the required moment of inertia of the flywheel
I_disk = I_sc*w_sc./w_disk; % kgm^2
figure;
plot(I_disk, w3);
grid on
xlabel('Moment of Inertia (kg*m^2)');
ylabel('Nominal Operating Speed of Flywheel(krpm)');
title('Moment of Inertia vs. Speed of Flywheel');
%% Determined Dimentions of the Flywheel
% Chosen Material: 6061 Al Alloy
% Density
rho = 2700; % kg/m^3
% Given Flywheel hight
% Note: m = rho*V, where V is volume
% V = pi*r^2*h
% I_disk = 0.5*m*r^2
r = (2*I_disk./(rho*pi*h)).^0.25; % m
d = 2*r; % m
d_mm = 1000*d; % mm
V = pi*r.^2*h; % m^3
m = rho.*V; % kg
w_target = 20; % krpms d_20 = 30.95; % mm
figure;
plot(d_mm,w3 );
hold on
plot( d_20,w_target,'*r')
xlabel('Diameter of Reaction Wheel (mm)');
ylabel('Nominal Motor Speed (krpm)');
%title('Diameter of Reaction Wheel vs. Nominal Motor Speed');

```

```

grid on
figure; d_mm_2 = d_mm(200:900);
w3_2 = w3(200:900);
plot(d_mm_2,w3_2);
hold on
plot( d_20,w_target,'*r')
xlabel('Diameter of Reaction Wheel (mm)');
ylabel('Nominal Operating Speed of Motor(krpm)');
title('Zoomed: Diameter of Reaction Wheel vs. Nominal Motor Speed');
grid on
% figure;
% plot3(Tm3,w3,d_mm)
% zlabel('Diameter of Flywheel (mm)');
% xlabel('Torque (mNm)');
% ylabel('Nominal Operating Speed of Flywheel(krpm)');
%
% grid on

```

C.2.5 Bump Test Arduino Sketch

```

#define AVGL 4 //rolling average length
volatile unsigned long ticks = 0;
unsigned long prevMillis = 0;
unsigned long interval = 100000<<1;
int state = false;
unsigned int avgArray[AVGL];
unsigned int avgCounter = 0;
volatile long lastTick = 0;
volatile long period = 0;
void setup()
{
pinMode(6, OUTPUT);
Serial.begin(9600);
// Use Pin 2 (interrupt # 0) for input to Arduino
attachInterrupt(0, isr_ticks, RISING);
TCCR0B = TCCR0B & 0b11111000 | 0x02;
Serial.println("Press any key to start the test...");
while(!Serial.available());
analogWrite(6, 100); }
void loop()
{
int b = 100;
int c = 200;
int i; // for(i = 0; i < 500; i++)
unsigned long currentMillis = millis();
```

```

if( currentMillis - prevMillis > interval )
{
//Serial.print("\tinterval: ");
//Serial.println(currentMillis - prevMillis); prevMillis = currentMillis;
if( state )
analogWrite(6, b);
else
analogWrite(6, c);
state = !state;
} if( avgCounter == AVGL )
{
avgCounter = 0;
//avgSum = 0;
}
avgArray[avgCounter] = period;
//avgSum += period;
avgCounter++;
// analogWrite(6, 100);
Serial.print(currentMillis);
//Serial.print(":");
//Serial.print(avgCounter);
//Serial.print("-");
Serial.print("\t");
Serial.print(period >> 3);
Serial.print("\t");
Serial.println((average(avgArray))>>3);
delay(300 << 3); //delay(10000<<3);
}
void isr_ticks()
{
//unsigned long m = micros();
//unsigned int p = m - lastTick; //new period
ticks++;
period = micros() - lastTick;
lastTick = micros();
//the new period shouldn't be much smaller than the old one.
/* if( period > (p >> 2) )
{
period = p;
lastTick = m;
} */
/*
unsigned int getPeriod()
{

```

```

int t = micros();
ticks = 0;
int p = 0;
interrupts();
delay(4<<3); //delay for 4 milliseconds
p = (micros() - t) / ticks ;
noInterrupts();
return p;
}
*/
unsigned int average(unsigned int * a)
{
int i = 0;
unsigned long s = 0; //sum
for( i = 0; i < AVGL; i++)
s += a[i];
/* Serial.print("\ts: ");
Serial.print(s);
Serial.print("\t");*/
return (s / AVGL);
}

```

C.3 dCDH and COMM Code

The code for the dCDH and COMM subsystems is included on a USB stick submitted with the physical copy of this thesis.

D Requirements Flowdown

Appendix A - Project/Mission Objectives		Requirement Color Codes		
	Rev Date: 1/31/13	Project Statement/Objectives	Requirement Met and Verified	Status Color Codes
	Project Requirement	Requirement Met via Design but not Verified	Requirement Not yet Adequately met via design	
Project Statement Develop a 3U NanoSatellite bus capable of short duration technology verification experiments while providing compelling hands-on student education opportunities.				
Project Objectives				
1	Develop baseline 3U bus that exploits existing subsystem designs when possible and develop new subsystem design as necessary.			
2	Demonstrate 3U bus is easily manufacturable and tested at a university facility on a university level			
3	Use operations that exploit existing mission control systems			
4	Provide educational opportunity for university students			
5	Meet the Santa Clara University's Robotic System Laboratory (RSL) Criteria			
Req.	Project Requirements	Priority	Status	Status Comments
P01	Develop baseline 3U bus that exploits existing subsystems designs when possible and develop a new subsystem design as necessary.	High	Green	
P01-1	Existing subsystem(s) shall be used when appropriate	High	Green	
P01-2	Revisions shall be made on one existing subsystem(s) being used when necessary	High	Green	
P01-3	New subsystem(s) shall be designed and implemented	High	Yellow	Some designs have been implemented, others have not; ex: EPS
P01-4	An interface with existing ground segment shall be used	High	Yellow	Can connect with ground station, but not prepared to handle
P01-5	A sealed box for an unspecified payload shall exist	Low	Yellow	incomming data, more programming necessary Box exists but is not top priority
P02	Demonstrate 3U bus is easily manufacturable and tested at a university facility on an university's level	High	Green	
P02-1	The 3U bus shall be able to be reproduced at an university level funding	High	Green	
P02-2	The 3U bus shall be able to be developed with standard university facility	High	Green	
P02-3	The integration and testing (I&T) process shall be student centric	High	Green	
P02-4	The I&T process shall use in-house testing equipment for testing	High	Green	
P03	Use operations that exploit existing mission control systems	High	Green	
P03-1	The 3U bus shall be able to communicate with existing ground segment	High	Green	Can connect with ground station, but not prepared to handle
P03-2	The 3U bus shall be able to use digital command and data handling (dCDH) to send data to and from ground segment	High	Green	incomming data, more programming necessary
P03-3	The satellite shall be able to communicate data from the unspecified payload box	High	Yellow	Design is in place, but need a payload to verify
P04	Provide educational opportunity for university students	High	Green	
P04-1	Project shall provide hands-on involvement by university students	High	Green	
P04-2	Project shall provide better understanding of development of space products	Medium	Green	
P04-3	The design and development of the project and components shall be done mainly by university students	High	Green	
P05	Meet appropriate criteria	High	Green	
P05-1	The system shall meet all CubeSat constraints	High	Green	
P05-2	The system shall meet all RSL constraints	High	Green	

UPAACN Requirements Spreadsheet											
	Rev Date: 1/31/31										
Requirement Color Codes <table border="1"> <tr> <td>Mission Statement/Objectives</td><td>Requirement Met and Verified</td></tr> <tr> <td>Mission Requirement</td><td>Requirement Met via Design but not Verified</td></tr> <tr> <td>System Requirement</td><td>Requirement not yet adequately met via design</td></tr> <tr> <td>Subsystem Requirement</td><td></td></tr> </table>				Mission Statement/Objectives	Requirement Met and Verified	Mission Requirement	Requirement Met via Design but not Verified	System Requirement	Requirement not yet adequately met via design	Subsystem Requirement	
Mission Statement/Objectives	Requirement Met and Verified										
Mission Requirement	Requirement Met via Design but not Verified										
System Requirement	Requirement not yet adequately met via design										
Subsystem Requirement											
Mission Statement	The Unspecified Payload and Active Attitude Control (UPAAC) nanosatellite will perform a 3-6 month technology verification experiment for a NASA test										
Mission Objectives											
1	Prove and characterize new bus subsystems for this class of mission										
2	Demonstrate it meets all of the University Nanosatellite Program constraint for a 3U system										
3	Demonstrate and characterize parts for active attitude control system (ACCS)										
4	Demonstrate and characterize new capabilities for satellite command and control										
Req.	Mission Requirements	Priority	Status								
MO1	Prove and characterize new bus subsystems for this class of mission An analysis shall be used to show that each existing subsystem being used is appropriate for the mission The revisions made on existing subsystem(s) being used shall be provided Data and analysis of new subsystems shall be provided	High Medium Low	Designs are in place, full verification requires more thorough testing and flight-ready assembly								
MO1-1		High									
MO1-2		High									
MO1-3		High									
MO2	Demonstrate it meets all of the CubeSat Design Specifications for a 3U system The satellite's volume shall not exceed 10 cm x 10 cm x 30 cm The satellite shall power up in a safe mode for 30 min after being deployed from peek-pod The satellite's mass shall exceed 4kg The satellite shall remain in a range of temperature from 253 to 358 degrees Kelvin	High									
MO2-1		High	Designs are in place, need to be prototyped and integrated								
MO2-2		High	Can only be met with inclusion of a payload								
MO2-3		High	Proven via SatTherm MATLAB code								
MO2-4		High	Physical components in place, but need to test on power board								
MO2-5	The satellite shall have a kill switch on rail prior to launch	High	Can only be met with inclusion of flight components which are still unknown								
MO2-6	The satellite center of gravity shall be located within 2 cm from the geometric center	High	Verified via FEA and basic impact testing, but more thorough testing is needed								
MO2-7	The satellite shall have a fundamental frequency above 100 Hz given a fixed base condition	High	Current configuration meets this requirement, but unknown flight components may change this								
MO2-8	The satellite shall not produce more than 15W-hr in a 15 min period	High									
MO3	Demonstrate and characterize parts for active attitude control system (ACCS)	High									

MO3-1	The satellite shall power the active attitude control flywheel mechanism during specified times.	High					
MO3-2	The satellite shall control the flywheel mechanism based on input from the mission operations center.	High					
MO3-3	The satellite shall be able to verify the functionality of the flywheel system through sensing	High					
MO3-4	The satellite shall be able to send and receive data to and from the flywheel system based on data handling capabilities	High					
MO4	Demonstrate and characterize new capabilities for satellite command and control	High	Yellow	Yellow	Green		
MO4-1	The satellite shall be able to communicate necessary data to the mission operations center	High					
MO4-2	The mission operations center shall be able to send controls to the satellite	High		Yellow	Green	Ground station database capabilities must be developed	
MO4-3	The satellite shall be able to interpret commands from the mission operations center and relay them to the corresponding subsystems	High					
	S1: UPAAC Satellite Requirements						
	Req	Status					
S1-1	The UPAAC satellite shall meet all CubeSat Design Specifications.	High				Based on current configuration, all specifications are met	
S1-2	The UPAAC satellite shall meet all RSL Program constraints.	High					
S1-3	The UPAAC satellite shall be designed for a 3-6 month nominal mission life in space.	Medium					
S1-4	The UPAAC satellite shall include a testbed for an unspecified payload that could include a sealed container or mounting brackets to ensure stability and survival.	High					
S1-5	The UPAAC satellite shall support the payload testbed with appropriate data handling, power, mechanical, attitude, fixturing, and thermal services.	High	Yellow	Yellow	Green	This requires a payload to be fully verified, basic support is offered currently	
S1-6	The UPAAC satellite shall support the Active Attitude Control System (AACS) flywheel mechanism and sealed container equipment.	High					
S1-7	The UPAAC satellite shall use a software suite for dCDH services.	High					
S1-8	The UPAAC satellite shall use the AACS subsystem with appropriate data handling, power, mechanical, fixturing, and thermal services.	High					
S1-9	The UPAAC satellite shall support the dCDH subsystem with appropriate power, mechanical, fixturing, and thermal services.	High					
S1-10	The UPAAC satellite shall support radio communications with RSL's ground operations center for command and telemetry operations.	High					
	Req	UPAAC Satellite Sub-System Requirements					
		Payloads					
S1.1	Active Attitude Control System (AACS)						
S1.1-1	AACS shall meet all CubeSat Requirements					High	

S1.1-2	AACS shall meet all RSL Program constraints	High	High	
S1.1-3	AACS shall be meet success criteria defined in documentation	High	High	Can only be verified on-orbit
S1.1-4	AACS shall be able to collect sensor data in order to verify satellite orientation	High	High	
S1.1-5	AACS shall conform to AACS-EPS interface requirements regarding signal compatibility	High	High	
S1.1-6	AACS shall conform to AACS-STRUC interface requirements regarding mechanical configuration, volume, and fixturing	High	High	
S1.1-7	AACS shall conform to the power/data interface standard	High	High	
Bus Subsystems				
S1.2	Structure (STRUC)			
S1.2-1	STRUC shall meet all CubeSat Mechanical requirements for a 3U CubeSat	High	High	
S1.2-2	STRUC must survive launch, have a natural frequency higher than 100Hz	High	High	Requires thorough FEA and environment testing
S1.2-4	STRUC must ensure survival of all subsystems on-orbit	High	High	Can only be verified on-orbit
S1.2-5	STRUC shall meet all subsystem and payload fixturing requirements	High	High	
S1.2-6	STRUC shall meet all RSL Program constraints	High	High	
S1.2-7	STRUC shall be designed for a 3-6 months of operation in space	Medium	High	
S1.2-8	STRUC shall be designed to incorporate the existing structural design of the 2011-2012 senior design team team with updates when applicable	High	High	
S1.2-9	STRUC shall be designed to be manufactured and assembled in the SCU machine shop and integrated at the RSL cleanroom space at NASA Ames	High	High	
S1.3	Electrical Power System (EPS)			
S1.3-2	EPS shall meet all RSL Program constraints.	High	High	
S1.3-3	EPS shall meet all CubeSat Electrical Requirement for a 3U CubeSat	High	High	Requires more prototyping/testing of flight components
S1.3-4	EPS shall provide power services to satellite components; this includes ground, regulated 3.3V, 5V, and 12V buses and 50mA and 150mA outputs	High	High	
S1.3-5	EPS shall generate and store power sufficient to support the execution of all minimal success criteria operations over a 3-6 month period assuming nominal operations	High	High	Designs are in place, but flight components are required to verify
S1.3-6	EPS shall enforce all subsystems are powered off for the first 30 minutes after deployment	High	High	Designs are in place, but flight components are required to verify
S1.3-7	EPS shall conform to EPS-STRUC interface requirements regarding mechanical configuration, volume, and fixturing	High	High	
S1.3-8	EPS shall conform to EPS-AACS interface requirements regarding signal type	High	High	
S1.4	Communication System (COMM)			
S1.4-1	COMM shall meet all RSL Program constraints	High	High	
S1.4-3	COMM shall receive radio commands from the ground with radio frequency and data parameters that are compatible with the RSL Ground Operations Center	High	High	
S1.4-5	COMM shall demodulate and decode radio commands and forward them to the dCDH subsystem in a compatible command packet structure and data rate	High	High	

S1.4-1	COMM shall encode and modulate dCDH packets and transmit them to the ground with radio frequency and data parameters compatible with the RSL Ground Operations Center	High							
S1.4-2	COMM shall conform to COMM-STRUC interface requirements regarding mechanical configuration, volume, and fixturing	High							
S1.4-3	COMM shall conform to the power interface standard	High							
S1.4-5	COMM shall meet all payload subsystem requirements	High			Payload is required to verify				
S1.5	Distributed Command and Data Handling (dCDH)								
S1.5-2	dCDH shall meet all RSL Program constraints.	High							
S1.5-3	dCDH shall be designed using the Dallas-master suite and standards	High							
S1.5-4	dCDH shall relay commands from the COMM subsystem to the appropriate target subsystems	High							
S1.5-5	dCDH shall relay status and experimental data from subsystems to the COMM subsystem	High							
S1.5-6	dCDH shall provide/schedule command execution in support of mission objectives with a command queue capacity	High							
S1.5-7	dCDH shall store aggregated mission data as documented in data budget	High							
S1.5-8	dCDH shall conform to dCDH-STRUC interface requirements regarding mechanical configuration, volume, and fixturing	High							
S1.5-9	dCDH shall conform to dCDH-COMM interface requirements regarding signal compatibility and software interface	High							
S1.5-10	dCDH shall meet all payload subsystem requirements	High			Payload is required to verify				
S1.6	Thermal System (THERM)								
S1.6-1	THERM shall be meet success criteria defined in documentation	High							
S1.6-3	THERM shall meet all CuObsSat Requirements	High							
S1.6-4	THERM shall meet all RSL Program constraints	High							
S1.6-5	THERM shall be designed to maintain component temperatures within their thermal limits consistent with nominal operating modes during the mission lifetime (253 to 358 degrees Kelvin)	Requirement is met based on current components, may change depending on flight							
S1.6-6	THERM shall provide additional support to the payload if necessary	High							
S2	Ground Segment								
S2.1	Mission Operations Center (MOC)	High							
S2.1-2	The MOC shall meet all RSL Program constraints.	High							
S2.1-3	The MOC shall monitor the state of the system	High							
S2.1-4	The MOC shall display raw mission data products to the operators	High							
S2.2	Ground Communications Station (GCS)								

S.2.2-2	The GCS shall meet all RSL Program constraints, to specifically include:	High	Green								
S.2.2-3	The GCS shall receive satellite data via radio communications with radio frequency and data parameters (e.g., frequencies, modes, rates, encoding formats, etc.) that are compatible with the satellite COMM subsystem.	High	Green								
S.2.2-4	The GCS shall relay satellite data to the MOC	High	Green								
S.2.2-5	The GCS shall receive satellite commands from the MOS	High	Green								
S.2.2-6	The GCS shall relay satellite commands to the satellite via radio communications with radio frequency and data parameters (e.g., frequencies, modes, rates, encoding formats, etc.) that are comparable with the satellite COMM subsystem.	High	Green								
S.2.2-7	The GCS shall accept configuration commands from the MOC	High	Green								
S.2.2-8	The GCS shall provide status data to the MOS	High	Green								
<hr/>											
S.3	Ground Support Equipment	Yellow	Yellow								
S.3.1	Mechanical Ground Support Equipment (MGSE)	Yellow	Yellow								
S.3.1-2	The MGSE shall meet all RSL Program constraints.	High	Green								
S.3.2	Electrical Ground Support Equipment (EGSE)	Yellow	Yellow								
S.3.2-2	The EGSE shall meet all RSL Program constraints.	High	Green								
S.3.3	Testing (TEST)	Yellow	Yellow								
S.3.3-2	TEST shall meet all RSL Program constraints	High	Green								
S.3.3-3	Test shall meet all CubeSat Testing Requirements	High	Green								
S.3.3-4	Test shall use an analysis on the satellite using computer program to determine if satellite meets the temperature constraints	High	Yellow								
S.3.3-5	TEST shall use an analysis to verify its natural frequency falls within acceptable boundaries	High	Yellow								
S.3.3-6	TEST shall determine if satellite meets P-POD requirements	High	Green								
S.3.3-7	TEST shall verify pre-flight subsystem functionality	High	Green								
S.3.3-8	TEST shall demonstrate a connection between the assembled spacecraft and the RSL Ground Operations Center before launch	Medium	Yellow								
S.3.3-9	TEST shall verify proper payload integration	High	Red								
S.3.3-10	TEST shall verify AACS can provide single-axis control to the satellite	High	Green								

E Timeline

Main Deadlines	
1. Parts list, detailed schedule, and hardware goals for Winter Quarter	1/14/2013
2. Ethics/Professionalism, Budget Update	1/28/2013
3. Presentation/Design Review goals due	1/30/2013
4. Detail drawings, informal oral presentation, lifelong learning	2/4/2013
5. Analysis report/Oral presentations	2/25/2013
6. Formal written and oral progress report	3/11/2013
7. Assembly drawings and hardware completion	3/20/2013
8. Thesis TOC and introduction due	4/8/2013
9. Senior Design conference	5/9/2013
10. Societal/environmental impact report	5/15/2013
11. Thesis draft due	5/20/2013
12. Patent search or business plan due	5/29/2013
13. Experimental results due	6/3/2013
14. Open house (hardware due)	6/5/2013
15. Final thesis due	6/12/2013
Systems (SYST)	
1. Complete detailed timeline for Winter and Spring Quarters.	1/14/2013
2. Set hardware goals for Winter Quarter.	1/14/2013
3. Set manufacturing schedule for Winter Quarter.	1/21/2013
4. Order parts.	1/30/2013
5. Machining	5/30/2013
6. Assembly	5/20/2013
7. Controls Programming	4/15/2013
8. Hanging Test	5/9/2013
9. Pool Seal Test	5/9/2013
10. Vibration Test	6/1/2013
11. Tuning of Gains	5/9/2013
12. Develop Gantt chart as project progresses.	5/10/2013
13. Develop separate mission objectives and project objectives.	1/30/2013
14. Update budget.	1/28/2013
15. Prepare for NASA Ames presentation/design review.	1/30/2013
16. Prepare analysis report.	2/25/2013
17. Complete operating modes document	3/13/2013
18. Update power budget	3/18/2013
19. Update mass budget	3/20/2013
20. Coordinate drawings and assembly drawings	3/20/2013
21. Update internal layout	3/20/2013
22. Update budget	3/20/2013
23. Prepare testing schedule for Winter and Spring Quarters.	4/15/2013
24. Design AACs Test Bed	2/11/2013
19. Research Alternative Design	2/11/2013
Structures (STRUC)	
A. Learn how to operate the tools/machine in the Santa Clara machine shop	11/30/2012
B. Research cheap materials that can be used while remaining effective	10/30/2012
C. Communicate with dCDH, AACs, dCDH, THERM, EPS and COMM for lay-out	11/30/2012
D. Create initial sketch/lay-out	10/31/2012
E. Determine what frequency structure needs to be tested at	10/31/2012
F. Determine fasteners to be used in final assembly	10/31/2012
G. Design initial payload bay	10/31/2012
H. Integrate payload bay design and lay-out design	10/31/2012
I. Update lay-out design	1/31/2013

1. Complete parts list.	1/14/2013
2. Complete part drawings.	1/30/2013
3. Set manufacturing schedule for Winter Quarter.	1/21/2013
4. Order parts.	1/30/2013
5. Manufacture parts.	3/20/2013
6. Complete assemblies.	4/10/2013
7. Test assembled structure (vibration, heat, cold, fit test).	5/6/2013
Active Attitude Control System (AACS)	
A. Arduino Tutorials (LED and DC motor)	11/2/2012
B. Momentum Calculations	11/2/2012
1. Develop equations of motion	11/16/2012
2. Conservation of Momentum	11/16/2012
3. Optimize iteratively	11/22/2012
C. Initial Flywheel Designs	12/2/2012
D. Research integration of sensors	11/5/2012
E. Research of Senior Thesis	11/9/2012
F. Create Initial Control System Block Diagram	12/12/2012
G. Incorporate hardware and software	3/16/2012
J. Attend Mech 371 AACS Lecture	10/30/2012
1. Set goals for Winter Quarter.	1/14/2013
2. Complete parts list.	1/14/2013
3. Work with STRUC to complete drawings/designs.	1/30/2013
4. Prepare demo showing input/output mechanism functionality.	4/5/2013
5. Manufacture/assemble final iteration of flywheel design.	4/5/2013
6. Complete AACS subsystem.	3/20/2013
7. Test AACS subsystem.	5/6/2013
Thermal Systems (THERM)	
1. Set goals for Winter Quarter.	1/14/2013
2. Learn and understand the thermal code for the exterior of the spacecraft based on the orbit	10/31/2012
3. Research best materials to use on a Low Earth Orbit (LEO)	10/31/2012
4. Analyze the results of the analysis program	11/30/2012
5. Communicate with EPS team to see the internal produce heat	11/30/2012
6. Analyze the predicted heat flux in the interior of the spacecraft	12/31/2012
7. Research ways to dissipate heat from a satellite	12/31/2012
8. Develop initial design to dissipate heat	1/31/2012
9. Design thermal test bed (hot and cold test beds, low pressure test bed)	12/31/2012
10. Compile initial thermal analysis into document for presentation.	1/30/2013
11. Compile operating temperature information.	1/30/2013
12. Define operating and survival temperature ranges.	1/30/2013
13. Set thermal constraints on payload.	1/30/2013
14. Make predictions of thermal effects on electronics based on operating temperatures.	1/30/2013
15. Work to develop thermal testing chamber and testing plan.	4/5/2013
16. Complete final thermal analysis of finished spacecraft.	4/5/2013
17. Test assembled satellite for functionality in thermally controlled environments.	5/6/2013
18. Improve SatTherm code package.	6/2/2013
Electronic Power Systems (EPS)	
A. Research solar cells and how to implement solar panels	11/7/2012

B. Communicate with Systems team to determine how much power is needed for each subsystem	11/21/2012
C. Communicate with THERM team to determine the internal heat generated	11/28/2012
D. Develop initial design of the EPS	1/2/2013
E. Develop design to test the EPS	1/16/2013
6. Distributed Command and Data Handling (dCDH)	
3. Prepare plan for power board.	3/11/2013
4. Order parts.	4/5/2013
5. Update power board layout and components	4/20/2013
6. Build solar panels.	4/20/2013
7. Assemble power system.	5/20/2013
8. Test for functionality.	6/2/2013
Distributed Command and Data Handling (dCDH) and Communications (COMM)	
1. Work on beacon code	11/28/2012
2. Work on COMM code integration	12/12/2012
3. Integrate beacon and Dallas Master code	1/14/2012
4. Set goals for Winter Quarter.	12/5/2012
5. Began testing scheduling of beacon broadcasts	2/25/2013
6. Began working with Sensors (Gyroscope & Magnetometer)	3/25/2012
7. Prepare beacon demo	3/2/2013
8. Integrate AACSB functionality onto same boards as dCDH and main CPU.	3/20/2013
9. Work with AACSB on flywheel functionality/data interface	4/18/2013
10. Complete programming for COMM and dCDH systems.	5/10/2013
11. Test for functionality in assembled spacecraft.	6/2/2013

F Budgets and Spreadsheets

F.1 Operating Modes

F.1.1 Purpose

The goal of this document is to define the different operating modes of the UPAACN (Unspecified Payload Active Attitude Control Nanosatellite) system. Specifically, this includes the power requirements and operating times of each subsystem used for each mode. Note: this document does not speculate as to what the power requirements of a payload would be, rather it assumes that future revisions would take this additional power draw into account. These power requirements would have to stay within the constraints of UPAACN.

F.1.2 Relevant Subsystems

The power drawing components from each subsystem mentioned in this document are as follows:

- Beacon - A component of Communications (COMM), located on the Dallas Master board. It also includes the BCN antenna.
- COMM Board - A component of COMM. This board is separate from the Dallas Master board, but cannot function independently.
- Transmitter Antenna/Board - Components of COMM. They are used to transmit and receive commands, which are then relayed through the COMM board.
- Dallas Master Board - A component of the distributed command and data handling subsystem (dCDH). Must be running for all other power drawing components to function, excluding beacon and the power board.
- Scheduler/Expert - Components running off of the same board as Dallas Master. Work as parts of dCDH.
- Power Board - Component of the electronic power system (EPS). This will include the peak power tracker circuit.
- Arduino - Controller of the active attitude control system (AACS). Used to send commands to and receive data from the flywheel mechanism and its feedback loops. This may be replaced by a motor driving board.
- DC Micromotor - Actuator of the AACS.

F.1.3 Operating Modes

The following are the expected operating modes for UPAACN. They are essentially combinations of the powered components listed above.

1. Idle - both dCDH boards, Beacon, COMM Board, EPS Power Board
 - (a) Voltage Range - 5 to 12 [V]
 - (b) Power Draw - 5 [W]
2. AACS Experiment - both dCDH boards, Beacon, COMM Board, EPS Power Board, AACS motor and driver board
 - (a) Voltage Range - 4 [V] for motor, 5 to 12 [V] for other components
 - (b) Power Draw - 12 W
3. Transmitting - both dCDH boards, Beacon, COMM Board, EPS Power Board, Transmitter antenna/board
 - (a) Voltage Range - 5 to 12 V
 - (b) Power Draw - 20 W

F.1.4 Operating Schedule

Below is the expected schedule for each of the three modes to be operated. UPAACN will likely remain in Idle mode most frequently. For power budgeting reasons, the AACS system will not be run at the same time that data is being transmitted to and from the ground station. It is expected there will be more time transmitting during the initial weeks after launch in order to establish normalized telemetry. The AACS system will not be operated until the orbit has settled and the payload functionality has been established.

- Phase 1:
 - Idle: 97% or 163 hours per week
 - Transmitting: 3% or 5 hours per week
- Phase 2:
 - Idle: 91% or 153 hours
 - Transmitting: 3% or 5 hours per week
 - AACS Experiment: 6% or 10 hours per week
- Phase 3:
 - Idle: 95% or 159 hours per week
 - Transmitting: 2% or 4 hours per week
 - AACS Experiment: 3% or 5 hours per week

- Phase 4:
 - Idle: 97% or 163 hours per week
 - Transmitting: 2% or 4 hours per week
 - AACSB Experiment: 1% or 1 hour per week

In Phase 1, UPAACN will be checked by the ground team during every available pass to verify system functionality and troubleshoot any system errors. Once telemetry data is collected and the spacecraft has settled into a normalized orbit, the AACSB experiment will be operated as part of Phase 2. The ground team will continue to communicate with the system during every available pass to collect telemetry and results data from the satellite and from the AACSB. During Phase 3, use of the AACSB will diminish, as will transmitting time. Phase 4 will take the mission to its end of life. The UPAACN system will mainly transmit to verify survival. AACSB usage will be minimal.

F.2 Activity Diagrams

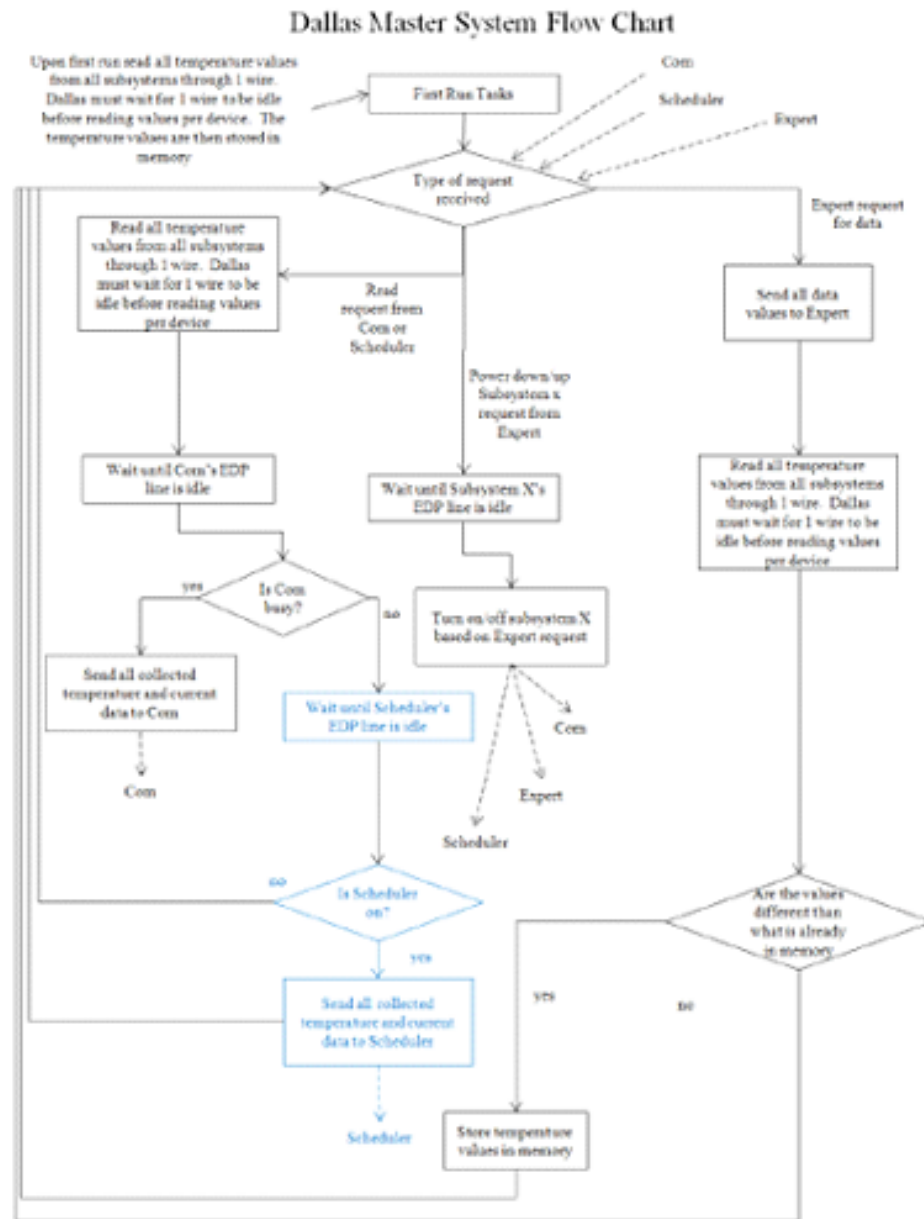


Figure F.1: Activity diagram for Dallas-Master.

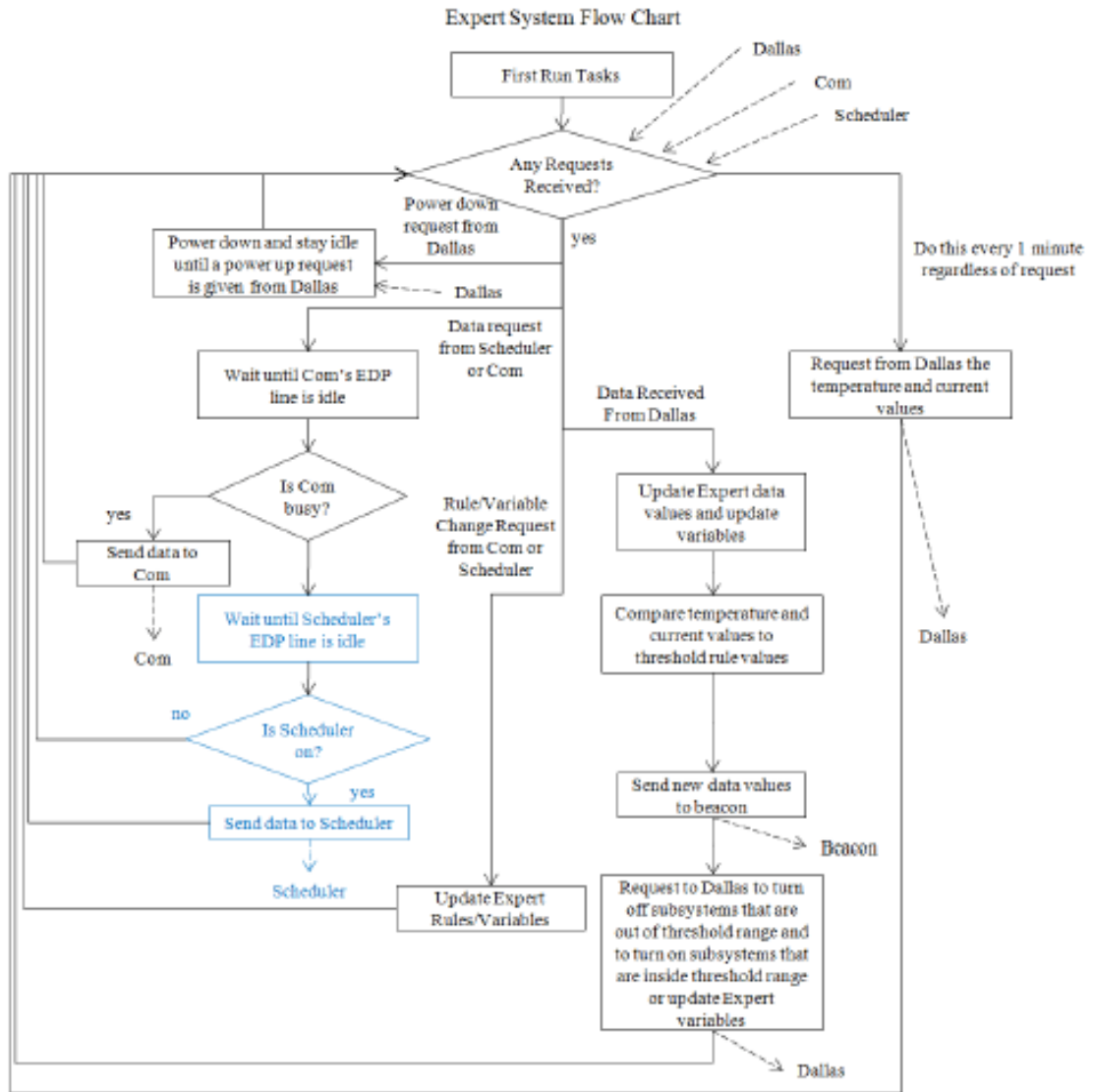


Figure F.2: Activity diagram for Expert.

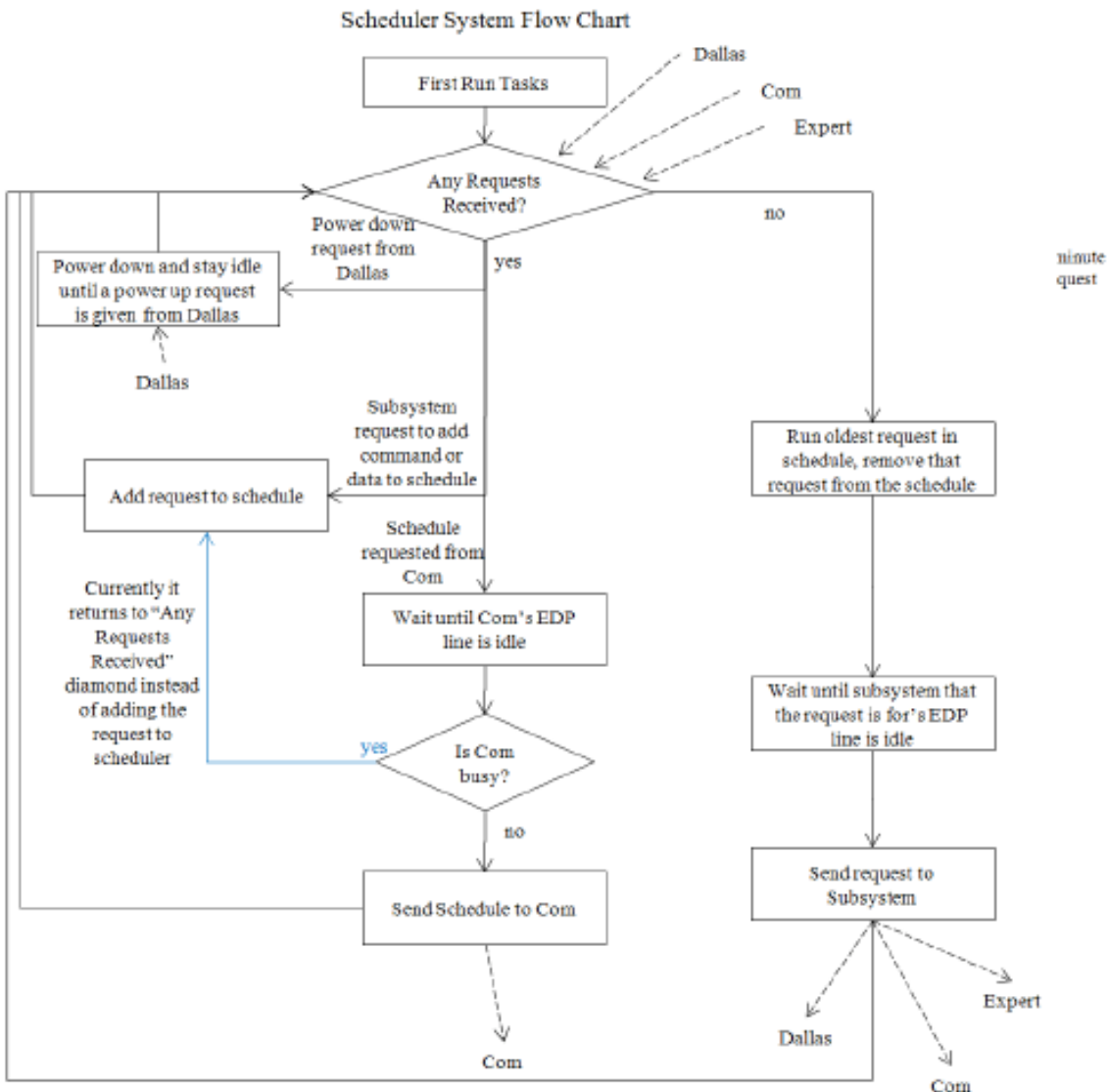


Figure F.3: Activity diagram for Scheduler.

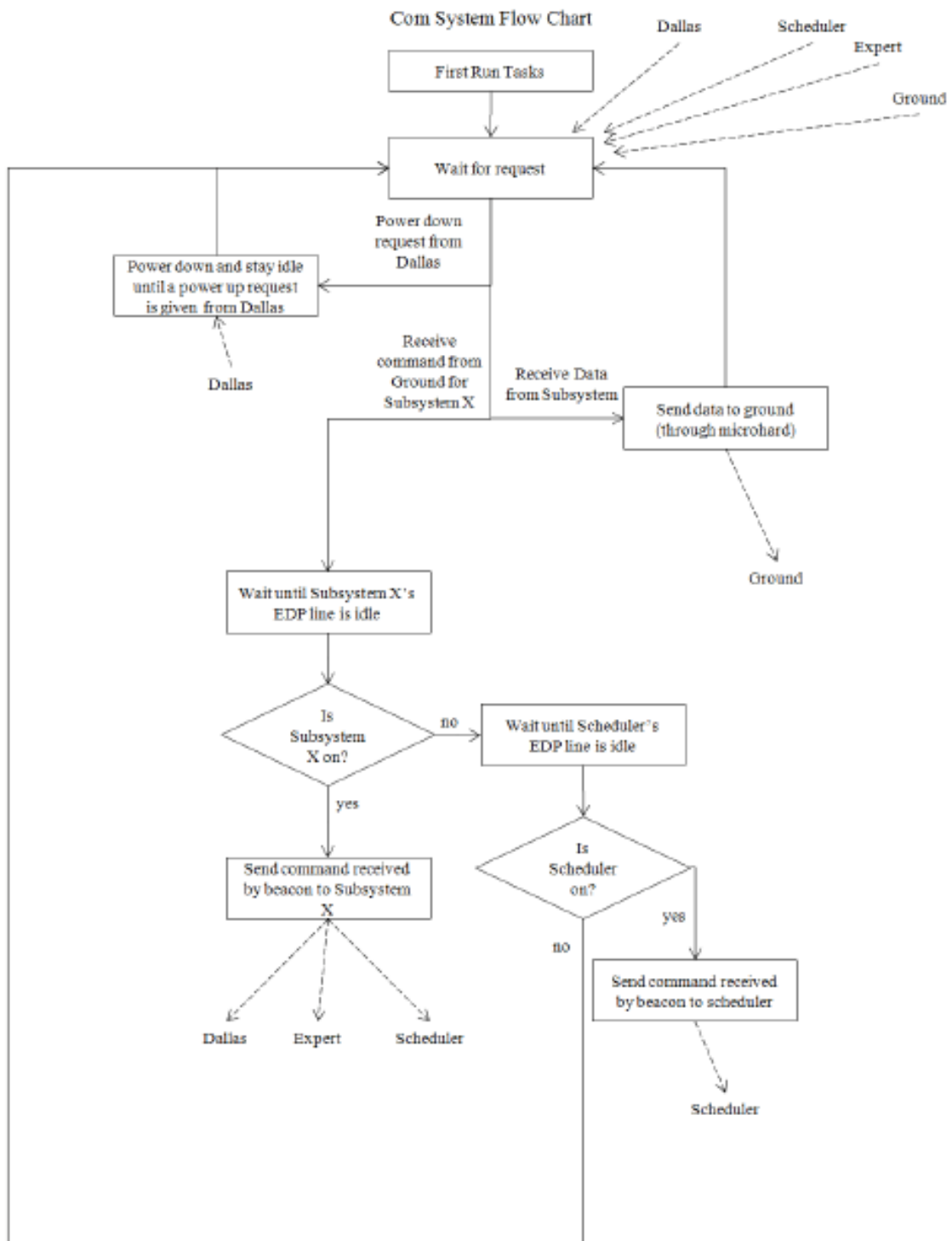


Figure F.4: Activity diagram for COMM.

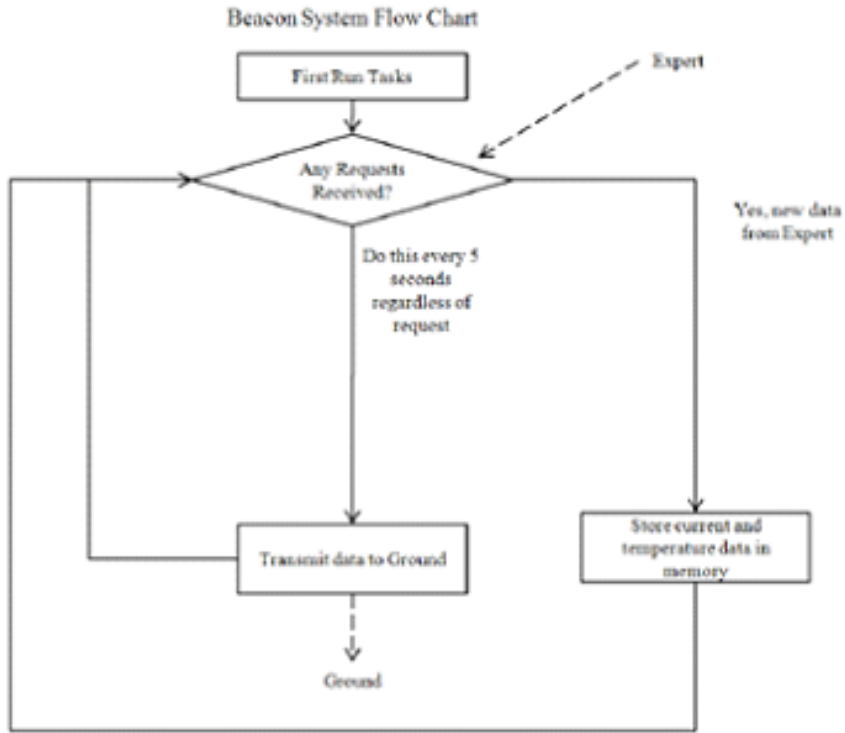


Figure F.5: Activity diagram for Beacon.

F.3 Success Criteria

F.3.1 Mission Statement

During a short term low Earth orbit mission, the spacecraft will operationally validate NASA components while testing an active single axis attitude control system and providing hands-on experience for university students.

F.3.2 Primary Mission Success Criteria

1. Complete a fully functional launch-ready spacecraft capable of supporting an unspecified payload.
 - (a) Payload possibilities will be restricted based on power, mass, and volume capabilities of the spacecraft.
 - (b) First iteration of the spacecraft will include the Active Attitude Control System (ACAS) flywheel mechanism.
 - (c) Functional criteria will be defined by Requirements Flowdown.

F.4 Mass Budget

Table F.1: Mass budget for UPAACN.

Item	Mass [kg]
STRUC Frame	0.81
Solar Panel Faces	0.24
ACR-SAT boards	0.1
BCN antenna & board	0.11
Transmitter antenna	0.031
MHX2420 boards	0.125
Sensor Board	0.013
AACS	0.12
Estimated Battery	1.0
Total	2.549

F.5 Monetary Budget

Budget Category	Subsystem	Component	Part Number	Qty	Cost/Part	Total Cost
Income	SYS					
	THERM					
	EPS					
	AACS					
	dCDH					
	COMM					
	STRUC					
	TEST					
	Total					
Expenses	SYS					
	Subsystem Total:					
	THERM	Circuit Heater		\$15-\$20	\$20.00	
		Thermocouple			\$50.00	\$50.00
		Z 306	1 gal.		\$150.00	\$150.00
	Subsystem Total:					\$70.00
	EPS	Solar Cells				
		Panels			\$200.00	\$50.00
		Battery	1	-\$200	\$200.00	
		Power Board		-\$100	\$100.00	
		Supplies			\$58.48	\$50.00
		Protoboard			\$60.83	\$82.38
	Subsystem Total:					\$482.38
	AACS	Speed Controller	1		\$86.80	\$86.80
		Programming Board	1		\$116.70	\$116.70
		A/D Converter	1		\$21.40	\$21.40
		Brushless DC Motor	1		\$60.00	\$60.00
		Magnetometer	1		\$67.60	\$67.60
		Rate Gyro			\$20.00	\$20.00
		Mounting Hardware	1		\$25.00	\$25.00
		Aluminum Stock			\$70.00	\$70.00
	Subsystem Total:					\$395.00
	dCDH	AVR Boards	2		\$30.00	\$60.00
		Cables	5		\$5.00	\$25.00
	Subsystem Total:					\$85.00
	COMM	Antennas & MicroHard boards	3		\$30.00	\$120.00
		Cables	4		\$5.00	\$20.00

	Subsystem Total:				
STRUC	Fasteners	1	\$85.00	\$85.00	\$140.00
	Tool for Fabrication	1	\$195.00	\$195.00	
	Materials	1	\$550.00	\$550.00	
	Subsystem Total:				
TEST	Singe Axis Testbed (AACS)	1	\$35.00	\$35.00	
	Subsystem Total:				
	Grand Total:				\$1,872.38

G Senior Design Conference Presentations

G.1 Nanosatellite - Design, Fabrication, and Systems

The presentation entitled “Nanosatellite - Design, Fabrication, and Systems” was given by Charles Dorsey, Thomas Hoye, Owen Jacobs, and Kadja Klarreich-Giglio at the 2013 Senior Design Conference. This presentation gives the overview of the 3U CubeSat platform as well as its major mechanical subsystems. These include SYST, STRUC, THERM, and TEST.

G.2 Active Attitude Determination and Control Subsystem

The presentation entitled “Active Attitude Determination and Control Subsystem” was given by Todd Chun-Van Osdol, Elliott Martin, and Michael Schlesselmann at the 2013 Senior Design Conference. This presentation focuses on the AACCS mechanism. This includes the control strategy, actuator design, as well as system testing and characterization.

G.3 Nanosatellite - Communications and Data Handling

This presentation entitled “Nanosatellite - Communications and Data Handling” was given by Jake Hedlund, Michael Ruiz, and Zachary Singh at the 2013 Senior Design Conference. This presentation focuses on the dCDH and COMM subsystems. This includes an overview of technologies implemented, the processes of each subsystem, and a functional demonstration.

SANTA CLARA UNIVERSITY



Nanosatellite – Design, Fabrication, and Systems

**Charles Dorsey, Thomas Hoye, Owen Jacobs,
Kadja Klarreich-Giglio**

Robotic Systems Laboratory
Department of Mechanical Engineering
Advisors: Dr. Christopher Kits, Dr. Robert Marks

www.scsu.edu SCHOOL OF ENGINEERING 

Topics to Cover

- History of Nanosatellites
- Project Overview
 - SCU Right Heritage
 - Value Proposition
- Subsystem Breakdown
 - Systems Engineering (SYST)
 - Structural Engineering (STRU)
 - Thermal Design and Analysis (THERM)

www.scsu.edu SCHOOL OF ENGINEERING 

SANTA CLARA UNIVERSITY



Satellite Services

- Communications
 - Media – TV, radio, broadband
- Remote Sensing
 - Weather
 - Military
- Science and Exploration
 - Hubble, James Webb Space Telescope
 - Cassini



Saylor FASTSAT navigator

www.scsu.edu SCHOOL OF ENGINEERING 

Small Satellites

- Cheaper, more focused missions
 - Smaller in scale
 - Less risk because of lower cost and complexity
- Variety of potential uses
 - On-orbit technology demonstration
 - Science payloads
- Accessible to smaller organizations



Saylor Phasmat, nasa.gov

www.scsu.edu SCHOOL OF ENGINEERING 

SANTA CLARA UNIVERSITY



SCU Flight Heritage

- RSL has worked with NASA to build and operate nanosatellites
 - Pharsat
 - QIOREOS
 - FASTRAC
 - Genesat-1
 - Sapphire



www.scsu.edu SCHOOL OF ENGINEERING 

Value Proposition

- Develop a competitive small satellite platform
 - Can support any payload that meets basic constraints
- Design, manufacture, and assemble at the university
 - Faster design cycle
 - Cheaper and less risky to build
 - Opportunity for students to gain hands-on experience
 - Can potentially send university payloads into orbit
 - Develop university space program
 - Attracts support from NASA and other aerospace companies

www.scsu.edu SCHOOL OF ENGINEERING 

SANTA CLARA UNIVERSITY



Platform Capabilities

- Power:**
 - 3.3, 5, and 12 [V] support, 650 [mA] current budget
 - 10 [Watt] energy capacity
- Structural:**
 - $10 \times 10 \times 30$ [cm] volume
 - < 4 [kg] mass
- Attitude Control:**
 - Position and rotation control about Z-axis
 - Total de-spin in ~10 minutes
 - Passive stabilization via magnets and hysteresis rods

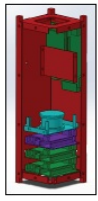
[www.santacruz.edu](#) SCHOOL OF ENGINEERING 

SANTA CLARA UNIVERSITY



System Architecture

- **(STRUC)** Structural Engineering
- **(EPS)** Electronic Power System
- **(DCDH)** Distributed Command and Data Handling/Communications
- **(AACS)** Active Attitude Control System – RSL payload

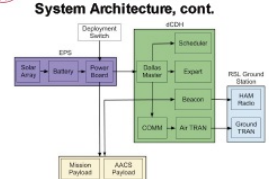


[www.santacruz.edu](#) SCHOOL OF ENGINEERING 

SANTA CLARA UNIVERSITY



System Architecture, cont.



[www.santacruz.edu](#) SCHOOL OF ENGINEERING 

SANTA CLARA UNIVERSITY



(SYST) Systems Engineering

- Requirements and constraints
- Trade-off analysis
- Subsystem integration
- Planning and scheduling



[www.santacruz.edu](#) SCHOOL OF ENGINEERING 

SANTA CLARA UNIVERSITY



(SYST) Mission Requirements

- Volume shall not exceed $10 \times 10 \times 30$ [cm]
- Satellite shall power up in safe mode for 30 min after deployment
- Mass shall not exceed 4 [kg]
- Satellite shall be maintained at 242 to 358 [kg]
- Center of gravity shall be within 2 [cm] of geometric center
- Must have a natural frequency > 100 [Hz]
- Satellite shall not consume more than 15 [Whr] in 15 minutes

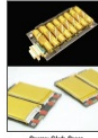
[www.santacruz.edu](#) SCHOOL OF ENGINEERING 

SANTA CLARA UNIVERSITY



(SYST) Trade-Off Analysis

- Example: Battery Selection
 - Ni-cad batteries
 - Lithium ion
- Example: Structure Design
 - Faces with pockets
 - Solid faces



Source: CiteSpace
[www.santacruz.edu](#) SCHOOL OF ENGINEERING 

SANTA CLARA UNIVERSITY



(STRUC) Structural Engineering

- Framework for components
- Protection during launch and on-orbit
 - Natural frequency $\omega > 100$ Hz
 - Desirable thermal environment
 - Meets deployment constraints
- Easy to alter for different missions
 - Semi-modular
 - Manufactured at university machine shop



Source: CubeSat3D.com

source: srujan arora **SCHOOL OF ENGINEERING** Part of Santa Clara University

SANTA CLARA UNIVERSITY



(STRUC) Inherited Design

- 2011-2012 senior design team
 - Build book and parts list
 - Fixtures for machining
- Baseline analysis
 - FEA via ANSYS
 - SetTherm
- Significant changes were necessary to meet requirements



source: srujan arora **SCHOOL OF ENGINEERING** Part of Santa Clara University

SANTA CLARA UNIVERSITY



(STRUC) Design Updates

- Solid side faces
- Flight computer location
- Mounting holes for electronics
- Cross brackets
- Deployment switch



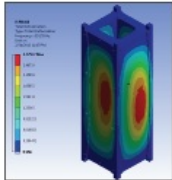
source: srujan arora **SCHOOL OF ENGINEERING** Part of Santa Clara University

SANTA CLARA UNIVERSITY



(STRUC) FEA Results

- Determine natural frequency
- Pinned corners as boundary condition
- Results:
 - Empty structure: 591.55 – 1153.7 Hz
 - Must be > 100 Hz



source: srujan arora **SCHOOL OF ENGINEERING** Part of Santa Clara University

SANTA CLARA UNIVERSITY



Vibration & Impact Testing

- SCU vibe table
 - Capable of < 15 Hz
 - Accelerometers and LabView
- Empty structure & integrated satellite
 - Verify resonance does not occur
 - Impact testing



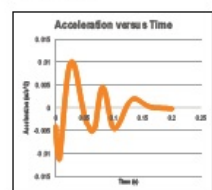
source: srujan arora **SCHOOL OF ENGINEERING** Part of Santa Clara University

SANTA CLARA UNIVERSITY



Vibration & Impact Results

- No resonance < 15 Hz
- Natural Frequency:
 - Frame: 117Hz
 - Integrated: 156Hz
- Future testing



source: srujan arora **SCHOOL OF ENGINEERING** Part of Santa Clara University

SANTA CLARA UNIVERSITY

(THERM) Thermal Design and Analysis

- Function
 - Control thermal environment
- Requirements
 - Maintain operational temperature range: 242 to 368 [K]
- Approach
 - Design for cold biasing
 - Low Earth Orbit (LEO)
 - Maximize passive thermal control
 - Minimize active thermal control

SCHOOL OF ENGINEERING

SANTA CLARA UNIVERSITY

(THERM) SatTherm MATLAB Package

- Nodal thermal transient analysis tool
 - Developed by SJSU grad student with NASA Ames
- Updates
- Assumptions:
 - Internal heat flux will stay within range set by hottest and coldest nodes
 - Hot case: largest node always normal to sun, 10 [W/hr] heat gen
 - Cold case: smallest node always normal to sun, no heat gen
 - Averaged side surface emissivity and absorptivity

SCHOOL OF ENGINEERING

SANTA CLARA UNIVERSITY

(THERM) SatTherm Output

Cold Case Hot Case

SCHOOL OF ENGINEERING

SANTA CLARA UNIVERSITY

(THERM) Results

	Cold Case Temperature Range [K]	Hot Case Temperature Range [K]
Aluminum Top and Bottom Node Surface Finish	224 to 230	268 to 314
Z305 Black Paint Top and Bottom Node Surface Finish	242 to 273	256 to 303

SCHOOL OF ENGINEERING

SANTA CLARA UNIVERSITY

(THERM) Design

- Surface finish
- No active thermal control
- Active control for future components
 - Batteries
 - Resistance heater with a temperature sensor

SCHOOL OF ENGINEERING

SANTA CLARA UNIVERSITY

Thermal Cycling/Vacuum Test

- Thermal Cycling Goals:
 - Oven/Freezer
 - Simulate LEO orbit
 - Monitor system health
- Vacuum Test Goals:
 - Test assembled satellite
 - Verify functionality

SCHOOL OF ENGINEERING

SANTA CLARA UNIVERSITY



Future Work

- Acquire high-tech components
 - Space rated battery
 - Order solar panel PCBs and power boards
 - Hysteresis rods
 - NASA payload
- Test to industry standards
 - Up to 100 Hz vibe testing
 - High-tech thermal chamber
 - Potential acoustic testing
- Present at NASA Ames

www.scu.edu SCHOOL OF ENGINEERING 

SANTA CLARA UNIVERSITY



Conclusion

- Developed a mature small satellite platform
- Designed, manufactured, and assembled at the university
- Improved satellite capabilities of the RSL
- Provide opportunities to SCU students for hands-on experience

www.scu.edu SCHOOL OF ENGINEERING 

SANTA CLARA UNIVERSITY



Questions?






www.scu.edu SCHOOL OF ENGINEERING 

SANTA CLARA UNIVERSITY



Active Attitude Determination and Control Subsystem

Todd Chun-Van Osdol
Elliott Martin
Michael Schleselmann

service project website SCHOOL OF ENGINEERING Todd Chun-Van Osdol

SANTA CLARA UNIVERSITY



Introduction

service project website SCHOOL OF ENGINEERING Todd Chun-Van Osdol

SANTA CLARA UNIVERSITY



Overview

- Robotic Systems Laboratory
- Mission Statement and Requirements
- Subsystem Breakdown
- Testing and Analysis
- Machine Design Process
- Future Improvements
- Conclusion

service project website SCHOOL OF ENGINEERING Todd Chun-Van Osdol

SANTA CLARA UNIVERSITY



The Robotic Systems Laboratory

Nanosatellite Program

- Multidisciplinary team of 10 Seniors and 4 Juniors
 - Computer Engineering
 - Electrical Engineering
 - Mechanical Engineering
- Seven subsystems

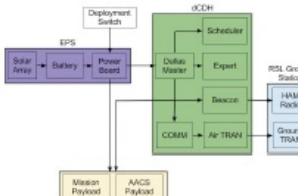


service project website SCHOOL OF ENGINEERING Todd Chun-Van Osdol

SANTA CLARA UNIVERSITY



System Block Diagram



service project website SCHOOL OF ENGINEERING Todd Chun-Van Osdol

SANTA CLARA UNIVERSITY



Mission Statement

“During a short term low Earth orbit mission, the spacecraft will operationally validate NASA components and test an active single axis attitude control system while providing hands-on experience for university students.”

service project website SCHOOL OF ENGINEERING Todd Chun-Van Osdol

SANTA CLARA UNIVERSITY



Attitude Control

- Passive, active and hybrid solutions
- Space Environment
 - Small torques dominate
 - Magnetic field
 - Gravity gradients



www.scmnews.com

SCHOOL OF ENGINEERING Santa Clara University

SANTA CLARA UNIVERSITY



Requirements

Subsystem Specific

- Experimentally validate (proof of concept) subsystem's ability to de-spin Nanosatellite from 2 rpm in under 10 minutes
- Meet system requirements
 - Mass < 0.5 kg
 - Power Consumption < 5 Wh per 15 minutes
 - Total Cost < \$500

SCHOOL OF ENGINEERING Santa Clara University

SANTA CLARA UNIVERSITY



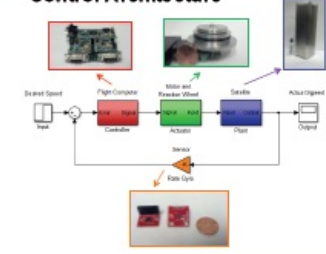
Subsystem Breakdown

SCHOOL OF ENGINEERING Santa Clara University

SANTA CLARA UNIVERSITY



Control Architecture



Block diagram illustrating the control architecture:

```

graph LR
    Input[Input] --> DesiredSpeed[Desired Speed]
    DesiredSpeed --> FlightComputer[Flight Computer]
    FlightComputer --> AttitudeSensor[Attitude Sensor]
    AttitudeSensor --> MotorAndReactionWheel[Motor and Reaction Wheel]
    MotorAndReactionWheel --> Satellite[Satellite]
    Satellite --> ActualOutput[Actual Output]
    MotorAndReactionWheel -- Rate Gyro --> RateGyro[Rate Gyro]
  
```

SCHOOL OF ENGINEERING Santa Clara University

SANTA CLARA UNIVERSITY



Control Strategy

Satellite Dynamics

- Satellite technically has 3 axes of rotation
- Passive control from magnets and hysteresis rods are assumed to fix 2 axes of rotation
- Equations of Motion:

$$T_x = I \omega_z^2 + b_z(\omega_x - \omega_i)$$

$$T_y = I \omega_i^2 + b_z(\omega_y - \omega_i)$$

$$T_z = -T_x$$

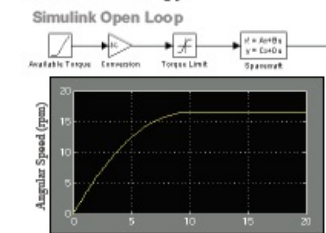
SCHOOL OF ENGINEERING Santa Clara University

SANTA CLARA UNIVERSITY



Control Strategy

Simulink Open Loop



Block diagram of the Simulink Open Loop:

```

graph LR
    AvailableTorque[Available Torque] --> Expression[Expression]
    Expression --> TorsionLimit[Torsion Limit]
    TorsionLimit --> Controller["I = 0.0018, C = 0.0001"]
    Controller --> Spanner[Spanner]
    Spanner --> OutputSpeed[Output Speed]
  
```

Graph showing Angular Speed (rad/s) vs Time (seconds):

Time (seconds)	Angular Speed (rad/s)
0	0
2	5
4	10
6	12
8	14
10	16
12	17
14	18
16	19
18	20
20	20

SCHOOL OF ENGINEERING Santa Clara University

SANTA CLARA UNIVERSITY



Control Strategy

Implementation

- Initially planned to use an Arduino Microcontroller
- Using satellite computers to run control code
- Motor inputs handled by a separate motor controller
- Motor controller values and gains are fixed once implemented in the satellite
- Ability to change satellite controller gains from ground station



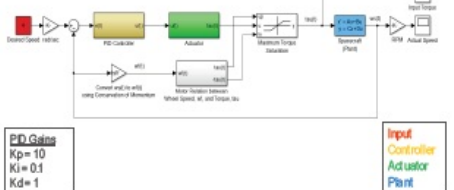
SCHOOL OF ENGINEERING 

SANTA CLARA UNIVERSITY



Control Strategy

Simulink Closed Loop



PID Gains
 $K_p = 10$
 $K_i = 0.1$
 $K_d = 1$

Input Controller Adulator Plant

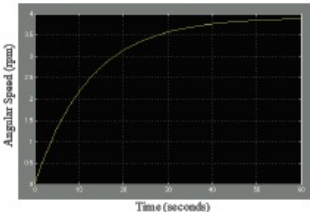
SCHOOL OF ENGINEERING 

SANTA CLARA UNIVERSITY



Control Strategy

Simulink Closed Loop Response



Angular Speed (rad/s)

Time (seconds)

SCHOOL OF ENGINEERING 

SANTA CLARA UNIVERSITY



Sensors

- Rate Gyro provides feedback for control code
- Magnetometer may be used in satellite for experimental purposes
- Motor has built Hall effect sensors to determine the pole position of the motor
- Hall effect sensor data is handled by the motor controller to determine motor speed



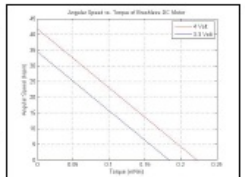
SCHOOL OF ENGINEERING 

SANTA CLARA UNIVERSITY



Actuator Design

- Motor selection**
 - Brushless flat DC Motor from Faulhaber
 - Physical configuration
 - 4 volt nominal voltage
 - Low power consumption
 - High speed
 - no load speed: 40,000 rpm
- Steady State Analysis**



Angular Speed vs. Torque of Faulhaber 30 Motor

Angular Speed (rad/s)

Torque (N-m)

4 VDC
2.5 VDC

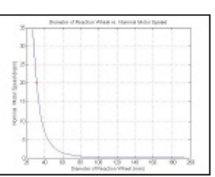
SCHOOL OF ENGINEERING 

SANTA CLARA UNIVERSITY



Actuator Design (cont.)

- Iterative reaction wheel sizing**
 - Conservation of angular momentum
- Advantages**
 - Minimal power draw
 - Flat physical configuration
 - Smaller reaction wheel
- Limitations**
 - Small amount of available torque



Reaction Wheel Mass vs. Reaction Wheel Power Draw

Reaction Wheel Mass (kg)

Power Draw (W)

SCHOOL OF ENGINEERING 

SANTA CLARA UNIVERSITY



Testing and Analysis

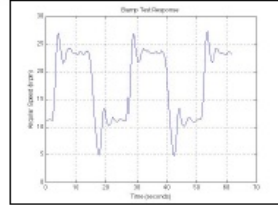
- Testing methods
- School of Engineering
- Santa Clara University

SANTA CLARA UNIVERSITY



Motor Bump Test

- Actuator's transient response to step input
- Resembled 2nd order system response
 - Rise Time: 0.96 sec
 - Setting Time: 4.5 sec
 - 15% Overshoot



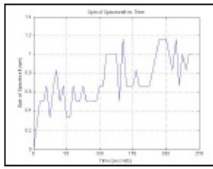
- Testing methods
- School of Engineering
- Santa Clara University

SANTA CLARA UNIVERSITY



Spin Test

- Ground vs. Space
- Steady State Error
- Difficult to Quantify



- Testing methods
- School of Engineering
- Santa Clara University

SANTA CLARA UNIVERSITY



Machine Design Process

- Testing methods
- School of Engineering
- Santa Clara University

SANTA CLARA UNIVERSITY



Components



- Testing methods
- School of Engineering
- Santa Clara University

SANTA CLARA UNIVERSITY



Subsystem Sizing

- Weight
 - 0.12 kg vs. 0.5 kg
- Volume
 - Payload Volume vs. Subsystem Volume
- Industry benchmarking
 - www.cubesatkit.com



- Testing methods
- School of Engineering
- Santa Clara University

SANTA CLARA UNIVERSITY



Pressurized Environment

- Outgassing
- O-Ring Seal
 - Alternatives
 - Sizing
 - Viton® Fluoroelastomer
 - 0.4 TML %
 - Motor Leads



[View more details](#) [SCHOOL OF ENGINEERING](#) [Santa Clara Engineering](#)

SANTA CLARA UNIVERSITY



Assembly Challenges

- Flywheel to Motor Attachment
 - Press Fit, Shrink Fit, Glue
- Motor Mounting
 - Size problems
 - Eddy Current Redesign
- Precision and Tolerance



[View more details](#) [SCHOOL OF ENGINEERING](#) [Santa Clara Engineering](#)

SANTA CLARA UNIVERSITY



Eddy Currents

- Drag Induced
 - Opposing Magnetic field
- Alternatives
 - DuPont Vespel Polyimide
 - Techtron
 - Too Expensive/Time
- Machine Response
 - Delrin Buffer (0.130")
 - Motor Mounting



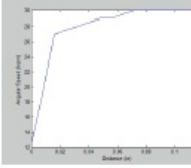
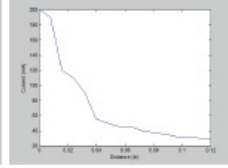
[View more details](#) [SCHOOL OF ENGINEERING](#) [Santa Clara Engineering](#)

SANTA CLARA UNIVERSITY



Eddy Currents

Angular Speed vs. Distance Current Draw. Distance

[View more details](#) [SCHOOL OF ENGINEERING](#) [Santa Clara Engineering](#)

SANTA CLARA UNIVERSITY



Future Improvements

[View more details](#) [SCHOOL OF ENGINEERING](#) [Santa Clara Engineering](#)

SANTA CLARA UNIVERSITY



Hardware Improvements

- Bearing Configuration
- Motor Lead Sealing
- Mounting of Flywheel
- Alternate Materials



[View more details](#) [SCHOOL OF ENGINEERING](#) [Santa Clara Engineering](#)

SANTA CLARA UNIVERSITY



Control Improvements

- 3-Axis Analysis
- Scale of System
- Running Motor at Low Speeds
- Encoder vs. Hall Effect Sensors



SCHOOL OF ENGINEERING 

SANTA CLARA UNIVERSITY



Conclusion

SCHOOL OF ENGINEERING 

SANTA CLARA UNIVERSITY



System Requirement

	Requirement	Actual
Mass	< 0.5 kg	0.12 kg
Power Consumption	< 20 W	0.975 W
Total Cost	< \$500	\$402.82
Performance	2 rpm	1.17 rpm

SCHOOL OF ENGINEERING 

SANTA CLARA UNIVERSITY



Summary

- Successfully met subsystem requirements
- Designed, fabricated and tested subsystem functionality
- Future improvements



SCHOOL OF ENGINEERING 

SANTA CLARA UNIVERSITY



Sources

- "CubeSat Design Specification," CubeSat, California Polytechnic State University, n.d. Web. 24 Feb. 2013.
- Harrison, Sam, Patrick Scott, and Victor Zaplen. Nanosatellite Fabrication and Analysis. Thesis. Santa Clara University, 2012. Santa Clara: Santa Clara University, 2012. Print.
- (2012). Goliat Nanosatellite [Photograph]. <http://www.cubesatkit.com/content/specs.html>
- (2010). Satnews Daily [Photograph]. <http://www.satnews.com/story.php?number=2092558544>

SCHOOL OF ENGINEERING 

SANTA CLARA UNIVERSITY



Acknowledgements

- Entire UPACCN student team
- Dr. Chris Kitts and Dr. Robert Marks
- Don MacCubbin and Calvin Sellers
- Jeff Fisher from Lockheed Martin
- Patrick Dell from Micromo
- Mechanical Engineering Department TA's
- RSL and School of Engineering

SCHOOL OF ENGINEERING 

SANTA CLARA UNIVERSITY



Nanosatellite – Communications and Data Handling

Jake Hedlund, Michael Ruiz, Zachary Singh
Advisor: Dr. Christopher Kitts

[View Project](#) [SCHOOL OF ENGINEERING](#) [TUTORING SERVICES](#)

SANTA CLARA UNIVERSITY

Background

- The Santa Clara University Robotics System Laboratory (RSL) has a decade's worth of history sending satellites into orbit
 - OOREOS
 - GeneSat-1
 - Artemis
 - PharmaSat
 - MAST
- SCU also does mission control for several NASA satellites

[View Project](#) [SCHOOL OF ENGINEERING](#) [TUTORING SERVICES](#)

SANTA CLARA UNIVERSITY



Current Project Objective

- Develop a new Nanosatellite framework to support future missions
- It will be designed for use with arbitrary payloads, using a low-cost and low-risk spacecraft
- This spacecraft will also facilitate the development of design capabilities at space system programs at the university level
- It will utilize an active attitude control system developed by other members of our team

[View Project](#) [SCHOOL OF ENGINEERING](#) [TUTORING SERVICES](#)

SANTA CLARA UNIVERSITY

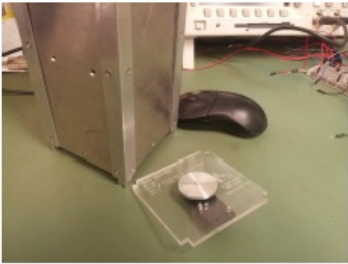
Nanosatellite Specifications

- 10 x 10 x 30 cm
- Less than 4 kg
- S-Band and UHF Communications
- Single-axis active attitude control
- Passive thermal control



[View Project](#) [SCHOOL OF ENGINEERING](#) [TUTORING SERVICES](#)

SANTA CLARA UNIVERSITY

[View Project](#) [SCHOOL OF ENGINEERING](#) [TUTORING SERVICES](#)

SANTA CLARA UNIVERSITY

Communications and Data Handling Subsystems

[View Project](#) [SCHOOL OF ENGINEERING](#) [TUTORING SERVICES](#)

SANTA CLARA UNIVERSITY



Functional Requirements

- System will send health packets and data via the beacon board
- System will receive information and data from the ground station
- System will execute commands received from the ground station
- System must communicate amongst itself to execute subsystem commands
- System will interface with the Active Attitude Control mechanism

Nonfunctional Requirements

- The system will be efficient
- The system will be compliant to the NASA and Cal Poly CubeSat standards
- The system will be extensible
- The system will be maintainable by future students
- The system will be cost effective

SCHOOL OF ENGINEERING

SANTA CLARA UNIVERSITY



Design Constraints

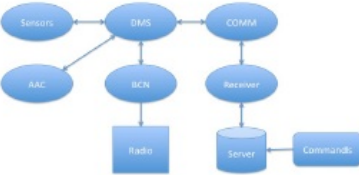
- The system will use existing AVR-SAT boards
- The system must fit within the architecture of the 3-U Nano satellite
- The system must use the MicroHard MHX2420 Radio Transmitter board to maintain compatibility with existing operations
- The system must be able to communicate to the SCU ground station

SCHOOL OF ENGINEERING

SANTA CLARA UNIVERSITY



Conceptual Model



```

graph LR
    Sensors((Sensors)) --> DMS((DMS))
    DMS --> COMMA((COMMA))
    AAC((AAC)) --> DMS
    BCN((BCN)) --> DMS
    DMS --> Receiver((Receiver))
    Receiver --> Server((Server))
    Server --> Commands[Commands]
    Radio((Radio)) --- Server
  
```

SCHOOL OF ENGINEERING



SANTA CLARA UNIVERSITY



Uses Cases

- Sending via Microhard transmitter
- Sending beacon packet
- Power on COM
- Power off COM
- Control motor

SCHOOL OF ENGINEERING

SANTA CLARA UNIVERSITY



Technologies Used

SCHOOL OF ENGINEERING

SANTA CLARA UNIVERSITY



Hardware

- 2 AVR-SAT microcontroller boards (based on ATmega128)
- 2 Microhard Transmitter boards
- 1 Beacon board with antenna
- 1 Faulhaber 1202 Brushless DC Penny-Motor and speed controller
- Various sensors
 - Gyroscope
 - Magnetometer

Software

- AVR Studio 4
- C programming language with RSL-developed AVR libraries
- Serial Terminal Program

ECHO OF ENGINEERING  

SANTA CLARA UNIVERSITY



Design Rationale

ECHO OF ENGINEERING  

SANTA CLARA UNIVERSITY



AVR-SAT boards

- have been used by previous satellite projects (flight heritage)
- space-hardened
- inexpensive

Beacon board

- Broadcasts on HAM radio frequencies

Microhard transmitter board

- Easy integration with AVR-SAT boards' data protocol

Brushless low-profile motor

- Compact
- Low current draw
- Easy integration

C language

- Consistency

AVR Studio 4

- Necessary to flash program on boards

Terminal

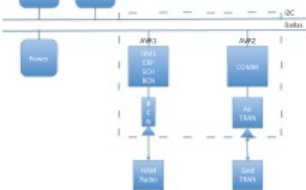
- Convenient way of interfacing with RS-232 serial port

ECHO OF ENGINEERING  

SANTA CLARA UNIVERSITY



Architectural Diagram



ECHO OF ENGINEERING  

SANTA CLARA UNIVERSITY



Project Risks

ECHO OF ENGINEERING  

SANTA CLARA UNIVERSITY



Risk	Consequences	Probability	Severity	Impact	Mitigation Strategy
Dynamic Requirements	Requirements not met	0.9	8.5	7.85	Constant updates from advisor Make systems adaptable
Difficulty integrating boards	Hardware will not work properly	0.9	8.0	7.20	Become familiar with board documentation Learn how AVR Libraries work at a low level
Unfamiliarity with hardware	Unable to complete project	1.0	7.0	7.00	Read board documentation Get information from previous thesis
Bugs within given code	Spends too much time fixing bugs	0.8	8.0	6.40	Compile and check code after every change Read comments and changes from previous authors
Time	Miss project deadline	0.6	7.0	4.20	Have weekly group meetings Create a timetable

ECHO OF ENGINEERING  

SANTA CLARA UNIVERSITY



Testing

- **Test Plan**
 - Use cases
 - Wind testing
 - Wireless testing
 - Integration testing
 - Acceptance testing
- **Test Results**
 - Initial design had to be redone
 - With current antennas, wireless works
 - Able to respond with and get information from sensors

source: clarkson.edu SCHOOL OF ENGINEERING Project Name Page 185

SANTA CLARA UNIVERSITY



Future Plans

- **Data Logging**
 - Integration of an SD card to store information of the satellite's current state
 - Downlink logs to ground station
- **More testing**
 - Ensure that the system is robust and as bug-free as possible
 - Regression testing with the completed subsystem

source: clarkson.edu SCHOOL OF ENGINEERING Project Name Page 185

SANTA CLARA UNIVERSITY



Demo

source: clarkson.edu SCHOOL OF ENGINEERING Project Name Page 185

H Parts List

Subsystem	Component Description	Part #	# of Item	BIN	Vendor	Cost per part (\$)	Responsible Person	Man-hours	Design	Procurement	Build time (each part)	Assembly	Order or start date	Received Date
Structures (STRU)	Nylon Tip 18-8 SS Socket Set Screw 4-40 Thread, 3/8" Length	STRU-C-001	20	B	McMaster-Carr	7.37 per	Owen, Elliott, Todd, Tom, Michael, Kadja	0.2	0	0.2	0	0	1/16/2013	3/15/2013
	Type 316 SS Fully Threaded Hex Head Cap Screw 1/4"-20 Thread, 1" Length	STRU-C-002	25	B	McMaster-Carr	7.22 per	Owen, Elliott, Todd, Tom, Michael, Kadja	0.2	0	0.2	0	0	1/16/2013	3/15/2013
	Type 316 SS Pan Head Phillips Machine Screw 4-40 Thread, 3/8" Length	STRU-C-003	50	B	McMaster-Carr	5.15 per	Owen, Elliott, Todd, Tom, Michael, Kadja	0.2	0	0.2	0	0	1/16/2013	3/15/2013
	18-8 Stainless Steel Clinch Captive Nut 4-40 Thread Size, .056" Minimum Panel Thickness	STRU-C-004	50	B	McMaster-Carr	7.48 per	Owen, Elliott, Todd, Tom, Michael, Kadja	0.2	0	0.2	0	0	1/16/2013	3/15/2013
	18-8 SS 82° Deg Flat Head Phillips Machine Screw 4-40 Thread, 3/16" Length, Undercut, MSS1 959-12	STRU-C-005	50	B	McMaster-Carr	7.31 per	Owen, Elliott, Todd, Tom, Michael, Kadja	0.2	0	0.2	0	0	1/16/2013	3/15/2013
	Short Length SS Long-Nose Spring Hunger & 36 Thread, .5-.15 lb Nose Force	STRU-C-006	4	B	McMaster-Carr	4.9	Owen, Elliott, Todd, Tom, Michael, Kadja	0.2	0	0.2	0	0	1/16/2013	3/15/2013
	18-8 SS Female Threaded Round Standoff 14# OD, 7/16" Length & 32 Screw Size	STRU-C-007	4	B	McMaster-Carr	1.59	Owen, Elliott, Todd, Tom, Michael, Kadja	0.2	0	0.2	0	0	1/16/2013	3/15/2013
	MIL Spec Pan Head Phillips Machine Screw 300 Series, 6-32 Thread, 1/4" Length, MS 51957-26	STRU-C-008	100	B	McMaster-Carr	7.00 per	Owen, Elliott, Todd, Tom, Michael, Kadja	0.2	0	0.2	0	0	1/16/2013	3/15/2013
	18-8 SS Flat Undercut Head Phil Machine Screw 4-40 Thread, 3/16" Length	STRU-C-009	100	B	McMaster-Carr	4.16 per	Owen, Elliott, Todd, Tom, Michael, Kadja	0.2	0	0.2	0	0	1/16/2013	3/15/2013
	3X1 Unit Face (3.75" X 12.75" X 0.063" Aluminum sheet 8061) ASH8061/0853 Corner Bracket (0.75" X 1.5" X 14" Aluminum Flat Bar 6061) AF6061/3412	STRU-C-101	4	M	Metal Supermarket	12.48	Owen, Elliott, Todd, Tom, Michael, Kadja	42.7	2	0.2	40	0.5	1/16/2013	3/15/2013
	Top 1X1 Unit Face (0.75" X 4" X 4" Aluminum Flat Bar 6061) AF6061/344 Bottom 1X1 Unit Face (0.75" X 4" X 4" Aluminum Flat Bar 6061) AF6061/344	STRU-C-103	1	M	Metal Supermarket	16.39	Owen, Elliott, Todd, Tom, Michael, Kadja	22.7	2	0.2	20	0.5	1/16/2013	3/15/2013
Payload and Comm Bracket	Flywheel Bracket	STRU-C-104	1	M	Metal Supermarket	14.17	Owen, Elliott, Todd, Tom, Michael, Kadja	22.7	2	0.2	20	0.5	1/16/2013	3/15/2013
	3X1 Unit Fixture Base (0.75" X 6" X 14" Aluminum Flat Bar 6061) AF6061/346 3X1 Unit Fixture Top (0.375" X 6" X 14" Aluminum Flat Bar 6061) AF6061/386 1X1 Unit Fixture Base (0.75" X 4.75" X 4.75" Aluminum Plate 8061) AP8061/750 1X1 Unit Fixture Top (0.25" X 3" X 3" Aluminum Plate 8061) AP8061/250 Corner Bracket Fixture (1.25" X 4" X 20" Aluminum Flat Bar 8061) AF8061/146	STRU-C-105	1	M	Metal Supermarket	39.3	Owen, Elliott, Todd, Tom, Michael, Kadja	12.7	2	0.2	20	0.5	1/16/2013	3/15/2013
	Assembly Tool (1.5" X 6" X 7.5" Aluminum Flat Bar 6061) AF6061/1126	STRU-C-106	1	M	Metal Supermarket	24.92	Owen, Elliott, Todd, Tom, Michael, Kadja	12.7	2	0.2	10	0.5	1/16/2013	3/15/2013
	Subsystem Totals	STRU-C-107	1	M	Metal Supermarket	23.88	Owen, Elliott, Todd, Tom, Michael, Kadja	12.7	2	0.2	10	0.5	1/16/2013	3/15/2013
	STRU-C-108	1	M	Metal Supermarket	12.45	Owen, Elliott, Todd, Tom, Michael, Kadja	12.7	2	0.2	10	0.5	1/16/2013	3/15/2013	
STRU - Cans	Can Body - (6061)	STRU-C-109	1	M	McMaster-Carr	46.59	Owen, Elliott, Michael, Todd, Tom, Kadja	2	2	0.5	5	0.25	1/16/2013	3/15/2013
	Can Lid - (6061)	STRU-C-110	2	M	McMaster-Carr	29.19	Owen, Elliott, Michael, Todd, Tom, Kadja	2	2	0.5	5	0.25	1/16/2013	3/15/2013
	O-Ring (24131191)	STRU-C-111	4	B	McMaster-Carr	8.17	Owen, Elliott, Michael, Todd, Tom, Kadja	2	2	0.5	0	0	1/16/2013	3/15/2013
Electronic Power System (EPS)	Panel for Solar Cells - Aluminum Alloy (6061T1) Solder - General Purpose	EPS-101	4	M	McMaster-Carr	137.65	Paulo, Sam, Russell, Owen, Kadja, Tom, Russell	14	8	0	0	8	3/17/2013	3/20/2013
	Solar Cells - Spectrolab Triangular Advanced Wire	EPS-102	1	B	Lowes	21.79	Owen, Kadja, Tom, Russell	6.1	2	0.1	0.5	2	1/16/2013	3/11/2013
	Solar Panel Assembly	EPS-103	20	cells	Spectrolab	9.98	Paulo, Sam, Russell, Owen, Kadja, Tom, Russell	8	0	0.5	0	0	11/3/2012	3/11/2013
		EPS-104	1	B	McMaster-Carr	0	Paulo, Sam, Russell, Owen, Kadja, Tom, Russell	2	0	0.5	0	0	11/3/2012	3/11/2013
		EPS-1A	4	M		6	Paulo, Sam, Russell, Owen, Kadja, Tom, Russell	0	0	0	0	6	1/16/2013	3/11/2013

Power Board	EPS-201	1 M	Texas Instruments	100	Paulo, Sam, Russell	33	20	3	10	0	1/10/2013	3/15/2013
Step-Down Regulator (Buck type)	TPS54290	EPS-202	Rose Electronics	0	Paulo, Sam, Russell	16	10	2	2	2	1/15/2012	3/15/2013
Battery	EPS-203	2 B	Rose Electronics	50	Paulo, Sam, Russell	6	0	4	0	2	1/15/2012	1/30/2013
Subsystem Totals				189.77		70.1						
Active Attitude Control System (ACCS)												
Precision Flywheel - Aluminum alloy (6061) disk made from 8974k711	AACS-101	1 M	McMaster-Carr	21.81	Michael, Todd, Elliott	15	6	4	5	0	10/1/2012	1/30/2013
Speed Control Board	AACS-102	1 B	RSL	85	Michael, Todd, Elliott	2	0	2	0	0	0/1/2012	1/30/2013
Atomic IMU 6 Degrees of Freedom	AACS-103	1 B	RSL	111.66	Michael, Todd, Elliott	2	0	2	0	0	1/1/2012	1/30/2013
Faulhaber Brushes Flat DC-Motor	AACS-104	1 B	Morono	67.00	Michael, Todd, Elliott	2	0	2	0	0	10/1/2012	1/30/2013
Can Body - Aluminum alloy (6061) tube made from 9056k141 stock	AACS-201	1 M	McMaster-Carr	35.99	Owen, Tom, Kadja, Elliott, Michael, Todd	11	5	1	5	0	1/14/2013	3/1/2013
Can Lid 1 - Aluminum Alloy (6061) rod made from 8974k711 (same as AACS-101)	AACS-202	1 M	McMaster-Carr	16	Owen, Tom, Kadja, Elliott, Michael, Todd	5	1	5	0	1/14/2013	3/1/2013	
Can Lid 2 - Aluminum Alloy (6061) rod made from 8974k711 (same as AACS-101)	AACS-203	1 M	McMaster-Carr	9.88	Michael, Todd, Elliott	5	3	0	3	0	4/19/2013	4/23/2013
Motor Spacer - Delrin rod (8572k25)	AACS-204	1 M	McMaster-Carr	15.78	Michael, Todd, Elliott	6	3	0	3	0	4/19/2013	4/23/2013
Motor Mounting Bracket - Aluminum Alloy (6061) made from 8974k711 (same as AACS-101)	AACS-205	1 M	McMaster-Carr	29.56	Michael, Todd, Elliott	4	0	1	3	0	1/14/2013	1/20/2013
Soft Jaws	AACS-301	1 B	Endo	3.75	Owen, Tom, Kadja, Elliott, Michael, Todd	3	1	1	1	0	4/19/2013	4/23/2013
Soft Collet	AACS-302	1 B	Endo	6.65	Owen, Tom, Kadja, Elliott, Michael, Todd	1	0	1	0	0	1/14/2013	3/1/2013
Can O-Ring (120T141)	AACS-501	2 B	McMaster-Carr	1.39	Michael, Todd, Elliott	1	0	1	0	0	1/14/2013	3/1/2013
M2x10 mm Socket Flat Head Screw (91290A017)	AACS-502	12 B	Jose	0	Michael, Todd, Elliott	0	1	0	1	0	1/14/2013	3/1/2013
M2 Nuts	AACS-503	B	Jose	0	Michael, Todd, Elliott	0	1	0	1	0	1/14/2013	3/1/2013
2-56x0.250" Socket Head Screws (91253A077)	AACS-504	3 B	Shop	0	Michael, Todd, Elliott	1	0	1	0	0	1/14/2013	3/1/2013
M1x3mm Screws	AACS-505	4 B	Mr. Metric - San Jose	2.27	Michael, Todd, Elliott	1	0	1	0	0	1/14/2013	3/1/2013
Flywheel Mechanism Assembly	AACS-501	1 M		20	Michael, Todd, Elliott	94	10	0	10	0	1/14/2013	4/29/2013
Subsystem Totals				390.74								
Communications (COMM) and Distributed Command and Data Handling (dCDH)												
Dallas Master Board	COEN-101	1 O	RSL	40	Zach, Michael, Jake	40	40	0	0	0	1/1/2012	3/1/2013
BCN Antenna	COEN-102	1 B	RSL	100	Zach, Michael, Jake	1	0	1	0	0	1/1/2012	3/1/2013
Transmitter Antenna and Board	COEN-103	1 O	RSL	200	Zach, Michael, Jake	20	20	0	0	0	1/1/2012	3/1/2013
Communications Board	COEN-104	1 O	RSL	40	Zach, Michael, Jake	20	20	0	0	0	1/1/2012	3/1/2013
Subsystem Totals				380		81						
Total				1532.5		476.9						

I Customer Needs Survey Responses

The RSL at SCU is capable of producing a spacecraft with the following specifications:

- Size: 1-6 U
- Schedule: 9-24 months of development
- On-orbit life: 6+ months
- Communications architecture: Microhard S-band and amateur radio (HAM) beacon
- Pointing: passive magnets, perhaps other passive techniques such as a gravity gradient boom, also possibly low-grade active control capable of ± 20 degrees
- Power: body mounted panels with power limited by size of spacecraft
- Propulsion: none
- Payload accommodation: 1-3U; data interfaces such as serial, I2C, Dallas, etc; power on order of 4 [W] continuous for 2U payload (can be duty-cycled to provide higher draw over shortened durations), mass commensurate with volume given CubeSat standards
- Cost to produce: > \$50k apart from customer payload

Please give us your thoughts regarding the following questions:

1. Do you have payloads or projects that could be supported by this type of spacecraft? If so, what type (electronic component test, biological test, technology demonstration, etc.)?
 - (a) Anthony Lee, NASA: Yes, small transponder
 - (b) Brian Custodio, University Space Research Association: N/A
 - (c) Vanessa Kuroda, NASA: Not immediately, but could develop one, most likely an electronic component test or technology demonstration.
 - (d) Elwood Agasid, NASA AMES, SCU contract manager for small satellite technology development contract: yes, this type of satellite/team could certainly support simple electronic package testing for new components of interest to Ames/NASA. This would be very consistent with the cost/risk/schedule profile. And in doing so you would qualify for reduced cost launch options through NASA, perhaps even with NASA paying for the full launch. Some tech demo ideas might also be valuable, particularly some of the technologies that SCU itself produces in the robotics lab with Dr. Kitts. This might include some attitude control experiments, some on-board computing experiments, and/or some automation experiments.

- (e) Chris Kitts, SCU - RSL: Yes, we should be able to "market" simple electronic component testing to several partners (Ames, USAF, Marshall, and perhaps a few others). We could probably use this type of satellite as the basis for grant proposals to the Air Force for technology demonstrations involving multi-satellite applications, and also on-board automation capabilities.
2. Would you be willing to work with a student group to fly a payload on this type of spacecraft given the level of risk involved in these projects?
- (a) AL: Yes, if had something
 - (b) BC: Yes, I believe space exploration is important for the survival of the human race. And thus, despite the risk I would partake.
 - (c) VK: Yes, it would be mutually beneficial for both parties, and a learning experience overall.
 - (d) EA: Absolutely. We have done this before, and our relationship with SCU in particular is outstanding given the mission control work done over the past 8 years. We could easily identify payload options that would make sense given the undergraduate team, cost target, and risk level. SCU has flight proven computing and communication avionics - using that as the backbone for any mission would be essential.
 - (e) CK: It's what I do!
3. What would you require from a student team in terms of tests, processes, and/or benchmarks to make you more comfortable with the risk of working on a student developed spacecraft?
- (a) AL: All the component such as tests for: communications, data, survive all data environments (launch vibrations, thermal environment), control systems, and maintain power.
 - (b) BC: If possible, wind tunnel tests, spin balance tests, drop tests, and shear strength tests should be conducted with model(s) of the spacecraft. The student team could also follow a certain engineering standard (e.g. ANSI)
 - (c) VK: I would probably want a full comprehensive test, including environmental tests (TVAC, shock, vibe, etc) if possible in order to prove it will survive on orbit and for the duration of its mission
 - (d) EA: Well, the more the better, but we understand that there are limits. Showing good teamwork and mature approaches is big. Good use of systems engineering for requirements and trade-offs, and being able to logically explain design choices. Analysis is great - test is even better!
 - (e) CK: Design process, and proof through testing/verification.

4. Given the design profile, what specific subsystem-level capabilities would you need to better support your payload needs? How important are they to you? How much more are you willing to pay for these capabilities?

- (a) AL: Monitor ground station, data handling. Cost: N/A
- (b) BC: N/A
- (c) VK: I would probably need more accurate pointing/control capabilities, which I would probably pay a few thousand more for.
- (d) EA: What you have now would let us start, presuming you can pull it all together and show that it all works in a routine manner. Improving pointing (even reliable +/- 20 deg ADC) and comm bandwidth (which you could get just with the improved ADC) would be great. If you had these capabilities, we could probably routinely pay for your launches and perhaps invest in some parts and students via internships.
- (e) CK: Need to be able to rapidly pull together new spacecraft designs that combine much of what we already have where appropriate with the new design tweaks necessary for any particular payload/mission concept. Need to develop general testing capability. The sweet spot for attracting bigger and better opportunities would be adding things like a little ADC (precision not necessary), perhaps software defined radio, and perhaps structural deployables.

5. To what extent are you or your organization interested in spacecraft education at the university level?

- (a) AL: Very important because technology which means in the future we can collect a lot more data from the space environment. It is needed to have spacecraft education at the university level so in the future we can continue making progress on what is out there and the resources that can benefit us.
- (b) BC: I can't speak for my organization as a whole but I definitely believe they would support spacecraft education at the university level, especially through internships, co-ops, and mentorship programs.
- (c) VK: I am very interested in spacecraft education at the university level, we need the next generation of spacecraft engineers to fill the shoes of the many soon-to-be retirees!
- (d) EA: very very interested - and very interested in continuing to work with Kitts and his students
- (e) CK: It's what we do!